frontiers | Research Topics

TMS application in both health and disease

Edited by
Joao Miguel Castelhano and Sandra Carvalho

Published in
Frontiers in Human Neuroscience

ISSN 1664-8714
ISBN 978-2-83251-349-1
DOI 10.3389/978-2-83251-349-1

About Frontiers

Frontiers is more than just an open access publisher of scholarly articles: it is a pioneering approach to the world of academia, radically improving the way scholarly research is managed. The grand vision of Frontiers is a world where all people have an equal opportunity to seek, share and generate knowledge. Frontiers provides immediate and permanent online open access to all its publications, but this alone is not enough to realize our grand goals.

Frontiers journal series

The Frontiers journal series is a multi-tier and interdisciplinary set of open-access, online journals, promising a paradigm shift from the current review, selection and dissemination processes in academic publishing. All Frontiers journals are driven by researchers for researchers; therefore, they constitute a service to the scholarly community. At the same time, the *Frontiers journal series* operates on a revolutionary invention, the tiered publishing system, initially addressing specific communities of scholars, and gradually climbing up to broader public understanding, thus serving the interests of the lay society, too.

Dedication to quality

Each Frontiers article is a landmark of the highest quality, thanks to genuinely collaborative interactions between authors and review editors, who include some of the world's best academicians. Research must be certified by peers before entering a stream of knowledge that may eventually reach the public - and shape society; therefore, Frontiers only applies the most rigorous and unbiased reviews. Frontiers revolutionizes research publishing by freely delivering the most outstanding research, evaluated with no bias from both the academic and social point of view. By applying the most advanced information technologies, Frontiers is catapulting scholarly publishing into a new generation.

What are Frontiers Research Topics?

Frontiers Research Topics are very popular trademarks of the *Frontiers journals series*: they are collections of at least ten articles, all centered on a particular subject. With their unique mix of varied contributions from Original Research to Review Articles, Frontiers Research Topics unify the most influential researchers, the latest key findings and historical advances in a hot research area.

Find out more on how to host your own Frontiers Research Topic or contribute to one as an author by contacting the Frontiers editorial office: frontiersin.org/about/contact

TMS application in both health and disease

Topic editors
Joao Miguel Castelhano — University of Coimbra, Portugal
Sandra Carvalho — University of Aveiro, Portugal

Topic coordinator
Ana Dionísio — Coimbra Institute for Biomedical Imaging and Translational Research (CIBIT), Portugal

Citation
Castelhano, J. M., Carvalho, S., eds. (2023). *TMS application in both health and disease*. Lausanne: Frontiers Media SA. doi: 10.3389/978-2-83251-349-1

The authors declare that the research was conducted in the absence of any commercial or financial relationships that could be construed as a potential conflict of interest.

Table of contents

frontiers | Frontiers in Human Neuroscience

TYPE Editorial
PUBLISHED 04 January 2023
DOI 10.3389/fnhum.2022.1110274

OPEN ACCESS

EDITED AND REVIEWED BY
Mingzhou Ding,
University of Florida, United States

*CORRESPONDENCE
Joao Castelhano
✉ jmscastelhano@gmail.com

†These authors have contributed equally to this work

SPECIALTY SECTION
This article was submitted to Brain Imaging and Stimulation, a section of the journal Frontiers in Human Neuroscience

RECEIVED 28 November 2022
ACCEPTED 14 December 2022
PUBLISHED 04 January 2023

CITATION
Dionísio A, Carvalho S and Castelhano J (2023) Editorial: TMS application in both health and disease. *Front. Hum. Neurosci.* 16:1110274. doi: 10.3389/fnhum.2022.1110274

Editorial: TMS application in both health and disease

Ana Dionísio[1,2†], Sandra Carvalho[3†] and Joao Castelhano[1,2*†]

[1]Coimbra Institute for Biomedical Imaging and Translational Research, University of Coimbra, Pólo das Ciências da Saúde, Coimbra, Portugal, [2]Institute for Nuclear Sciences Applied to Health, Pólo das Ciências da Saúde, University of Coimbra, Coimbra, Portugal, [3]Translational Neuropsychology Laboratory, Department of Education and Psychology, William James Center for Research, University of Aveiro, Campus Universitário de Santiago, Aveiro, Portugal

KEYWORDS

brain stimulation, therapeutic applications, medical imaging, transcranial magnetic stimulation (TMS), neuronal mechanism

Editorial on the Research Topic
TMS application in both health and disease

Transcranial magnetic stimulation (TMS) can be useful for therapeutic purposes for a variety of clinical conditions. Numerous studies have indicated the potential of this non-invasive brain stimulation technique to recover brain function and to study physiological mechanisms. Following this line, the articles contemplated in this Research Topic show that this field of knowledge is rapidly expanding and considerable advances have been made in the last few years. There are clinical protocols already approved for Depression (and anxiety comorbid with major depressive disorder), Obsessive compulsive Disorder (OCD), migraine headache with aura, and smoking cessation treatment but many studies are concentrating their efforts on extending its application to other diseases, e.g., as a treatment adjuvant. In this Research Topic we have the example of using TMS for pain, post-stroke depression, or smoking cessation, but other diseases/injuries of the central nervous system need attention (e.g., tinnitus or the surprising epilepsy). Further, the potential of TMS in health is being explored, in particular regarding memory enhancement or the mapping of motor control regions, which might also have implications for several diseases.

TMS is a non-invasive brain stimulation technique that can be used for modulating brain activation or to study connectivity between brain regions. It has proven efficacy against neurological and neuropsychiatric illnesses but the response to this stimulation is still highly variable. Research works devoted to studying the response variability to TMS, as well as large-scale studies demonstrating its efficacy in different sub-populations, are therefore of utmost importance. In this editorial, we summarize the main findings and viewpoints detailed within each of the 12 contributing articles using TMS for health and/or disease applications.

The developments in the last two decades have been impressive and as has been shown by Hua et al. a repetitive TMS protocol can have the potential to improve associative memory in health, which can be relevant for many neurological conditions.

In the line of using brain stimulation in healthy volunteers, Ngetich et al., provided evidence for the use of intermittent theta-burst stimulation (iTBS) in visual-spatial working memory enhancement, as well as the safety and effective profile of this technique for investigating the causal role of particular brain areas in specific psychological processes.

Brain stimulation can in fact be used to investigate the neural basis of distinct tasks. Yue and Martin, examined the effects of TMS in working memory (WM) and showed an effect of TMS on task performance, specifically on response time, in a phonological WM recognition task. With their work, they pointed out the relevance of assessing if the memory representations are restricted to local areas or distributed in a network, through studies of functional connectivity or multi-focal brain stimulation (Yue and Martin).

On the other hand, there is the use of TMS in disease, to ameliorate symptoms of e.g., post-stroke depression (PSD). PSD constitutes an important topic of research, given the major prevalence of stroke and its detrimental impact on quality-of-life. Thus, Zhu et al. explored the effects of TMS as an adjuvant to citalopram for post-stroke depression treatment. They found that, TMS in combination with citalopram were able to ameliorate symptoms of depression, as well as the neuropsychological function, in people with PSD. However, the outcome measures or evidence of treatment response of different protocols are still lacking. Strafella et al. provided a systematic review on using EEG markers to that end in major depressive disorder (MDD). They showed that TMS-EEG measures are promising markers to predict response to treatment with brain stimulation, in MDD. Further, these measures may help to non-invasively target cortical regions related to MDD (Strafella et al.).

Repetitive TMS can also be applied as a novel intervention for smoking cessation. Shevorykin et al. studied high-frequency rTMS and delay discounting as a new therapeutic target for smoking cessation. Their preliminary findings supported delay discounting as a possible therapeutic target and suggested that an increase in duration and intensity might lead to greater effect sizes in long-term smoking cessation.

Research on motor related effects of TMS have been also matter of debate and improvement recently. TMS elicits motor-evoked potentials (MEPs), measured by electromyography, but non-MEP points may also affect the estimation of the size and centroid of the excitable area. Jin et al. reported in this Research Topic that the incorporation of non-MEP points can improve the estimate of the active area, suggesting TMS approaches that do not consider the non-MEP points are more likely to overestimate the regions of excitability. Examining motor control of other regions e.g., the lumbopelvic musculature is of high interest to those studying low back pain (LBP). This mapping was done by Jordon et al. utilizing TMS and is also reported in this Research Topic.

The investigation on TMS as a novel type of treatment for several clinical conditions is growing fast due to its safety and non-invasive profile. This has been also the case for pain therapy. However, as reported by the work of Li et al., prospective, multi-center, large-sample, randomized controlled trials would be valuable to assess the effectiveness of TMS parameters in pain.

TMS has great potential to study/interfere with cognitive processes and help disentangle their underlying neuronal networks. Luber et al. took great advantage of TMS to interfere with a deception task and provide spatio-temporal information about the neural activity underlying deception action. In this line, Dong et al. stimulated the cerebellar swallowing cortex with high-frequency rTMS to investigate the effects and possible mechanisms of rTMS on swallowing-related neural networks, with resting-state functional magnetic resonance imaging (rs-fMRI).

TMS applications are really expanding in both health and disease. We summarized here incredible findings related to stroke, depression, pain, smoking, or normal brain function mapping. To finish, we highlight the work by Wang et al., showing that rTMS may also improve the visual function in strabismic amblyopic patients. This is an example of the new meaningful applications that are emerging associated with the broader investigation of this promising therapeutic technique.

Author contributions

All authors listed have made a substantial, direct, and intellectual contribution to the work and approved it for publication.

Acknowledgments

The authors thank their institutions for providing the time to edit this Research Topic and Editorial.

Conflict of interest

The authors declare that the research was conducted in the absence of any commercial or financial relationships that could be construed as a potential conflict of interest.

Publisher's note

frontiers in Human Neuroscience

ORIGINAL RESEARCH
published: 02 March 2022
doi: 10.3389/fnhum.2022.816595

Task-Based Functional Connectivity and Blood-Oxygen-Level-Dependent Activation During Within-Scanner Performance of Lumbopelvic Motor Tasks: A Functional Magnetic Resonance Imaging Study

Max K. Jordon[1], Jill Campbell Stewart[2], Sheri P. Silfies[2,3] and Paul F. Beattie[2]*

[1] Department of Physical Therapy, University of Tennessee at Chattanooga, Chattanooga, TN, United States, [2] Physical Therapy Program, University of South Carolina, Columbia, SC, United States, [3] McCausland Center for Brain Imaging, University of South Carolina, Columbia, SC, United States

OPEN ACCESS

Edited by:
Redha Taiar, Université de Reims Champagne-Ardenne, France

Reviewed by:
JeYoung Jung, University of Nottingham, United Kingdom
Hui He, University of Electronic Science and Technology of China, China

***Correspondence:**
Max K. Jordon
Max-Jordon@utc.edu

Specialty section:
This article was submitted to Motor Neuroscience, a section of the journal Frontiers in Human Neuroscience

Received: *16 November 2021*
Accepted: *10 February 2022*
Published: *02 March 2022*

Citation:
Jordon MK, Stewart JC, Silfies SP and Beattie PF (2022) Task-Based Functional Connectivity and Blood-Oxygen-Level-Dependent Activation During Within-Scanner Performance of Lumbopelvic Motor Tasks: A Functional Magnetic Resonance Imaging Study. Front. Hum. Neurosci. 16:816595. doi: 10.3389/fnhum.2022.816595

There are a limited number of neuroimaging investigations into motor control of the lumbopelvic musculature. Most investigation examining motor control of the lumbopelvic musculature utilize transcranial magnetic stimulation (TMS) and focus primarily on the motor cortex. This has resulted in a dearth of knowledge as it relates to how other regions of the brain activate during lumbopelvic movement. Additionally, task-based functional connectivity during lumbopelvic movements has not been well elucidated. Therefore, we used functional magnetic resonance imaging (fMRI) to examine brain activation and ROI-to-ROI task-based functional connectivity in 19 healthy individuals (12 female, age 29.8 ± 4.5 years) during the performance of three lumbopelvic movements: modified bilateral bridge, left unilateral bridge, and right unilateral bridge. The whole brain analysis found robust, bilateral activation within the motor regions of the brain during the bilateral bridge task, and contralateral activation of the motor regions during unilateral bridging tasks. Furthermore, the ROI-to-ROI analysis demonstrated significant connectivity of a motor network that included the supplemental motor area, bilateral precentral gyrus, and bilateral cerebellum regardless of the motor task performed. These data suggest that while whole brain activation reveals unique patterns of activation across the three tasks, functional connectivity is very similar. As motor control of the lumbopelvic area is of high interest to those studying low back pain (LBP), this study can provide a comparison for future research into potential connectivity changes that occur in individuals with LBP.

Keywords: task-based functional connectivity, lumbopelvic, motor control, spine, movement

INTRODUCTION

Neuroimaging investigations into motor control have typically focused on either upper extremity or distal lower extremity movements (Grefkes et al., 2008; Grooms et al., 2019; Vinehout et al., 2019; Criss et al., 2020). While these investigations have provided great insight into the motor control of the extremities, relatively little is known about brain activation during motor control

for the lumbopelvic region. Investigations into trunk control have either relied on examining non-voluntary, postural corrections to perturbations from the extremities or have used transcranial magnetic stimulation (TMS) (Matthews et al., 2013; Jean-Charles et al., 2017). When used in conjunction with electromyography (EMG), single pulse TMS excites pyramidal neurons within the motor cortex which results in a measurable muscular contraction at the targeted site (Goss et al., 2012). While studies using TMS have provided insight into the neural correlates of lumbopelvic motor control in individuals with and without low back pain (LBP) (Tsao et al., 2008, 2011), this approach is limited for several reasons. First, the presence of pain can alter TMS findings in ways that are unpredictable (Hodges and Tucker, 2011). For example, while there is some evidence demonstrating that motor-evoked potentials (MEPs) increase during local muscle pain (Fadiga et al., 2004), several studies have shown that MEPs can either decrease (Valeriani et al., 1999; Farina et al., 2001; Martin et al., 2008), or stay the same (Romaniello et al., 2000). This variability in findings may be due to the fact that activity within a single muscle can be redistributed in order to protect the body part that is in pain (Hodges and Tucker, 2011). Therefore, findings of either increased or decreased excitability could be influenced simply by slight changes in the placement of the EMG electrode. Second, functional trunk movements require the utilization of multiple muscles working in concert with the sensory feedback. By design, TMS can only assess a single muscle at a time thus limiting its scope in investigating functional movements using multiple synergist muscle groups and sensory feedback to control volitional movements. Lastly, studies assessing motor control using TMS have only assessed the primary motor cortex and not other regions (e.g., those responsible for motor planning or proprioception) of the brain, such as premotor cortices, which might hold important insights into the motor control of the lumbopelvic region.

To better understand the neural control of the trunk, our team developed a protocol which engages the musculature of the lumbopelvic region within the confines of the MRI scanner (Silfies et al., 2020). In a previous preliminary study, modified bilateral and unilateral bridging movements activated numerus trunk muscles including the lumbar multifidus, erector spinae, external obliques, internal obliques, and rectus abdominus; hip muscles were also active (gluteus maximus, hamstrings) with greater activation on the side of movement (e.g., left gluteus and hamstrings during left bridge). During performance of the modified bridging movement, activation was recorded in a bilateral sensorimotor network that included the supplemental motor area (SMA), precentral gyrus (PreCG), postcentral gyrus (PostCG), putamen, parietal operculum, and the superior parietal lobule. During bilateral bridging, brain activation was present in both hemispheres, however, during unilateral bridging, activation was more localized to the hemisphere contralateral to movement. Overall, this previous preliminary study found that it was feasible to collect fMRI data during lumbopelvic motor tasks without excessive head movement. However, functional connectivity during the lumbopelvic tasks was not assessed in that study. A better understanding of the functional connectivity during lumbopelvic tasks could elucidate the functional integration of separate brain regions that might not be observable by looking exclusively at the change in the BOLD signal (Rao et al., 2008). Therefore, the purpose of this study was twofold. First, we aimed to validate the results of the initial feasibility study with a separate larger cohort of participants. Second, we investigated task-based functional connectivity between the sensorimotor regions during bilateral and unilateral bridging. We hypothesized that (1) the whole brain activation patterns of our study would be similar to that of the preliminary paper with bilateral activation for the bilateral bridge and contralateral activation for the unilateral bridging tasks, and (2) functional connectivity would demonstrate unique network connectivity which reflect the different sensorimotor demands of each bridging task.

MATERIALS AND METHODS

Subjects

Twenty-one individuals were recruited to participate in this study. However, one participant was removed due to low-signal amplitude while another participant exhibited abnormal brain morphology and was unable to participate in the study. This left a total of 19 participants [12 female, age 28 $\pm$ 3.9 years, range 21–37 (**Table 1**)] who completed the study. After giving informed consent, participants underwent MRI safety screening to ensure they were safe to participate in the study. Inclusion criteria were: (1) being right-hand dominant; (2) being between the ages of 18–60; (3) no history of activity limiting LBP; (4) no history of inflammatory joint disease or cancer; and (5) no contraindications for undergoing MRI. Handedness was determined by the Edinburgh Handedness Inventory which also assesses for footedness (Oldfield, 1971). All of our participants were right footed. Approval for this study was given by the University of South Carolina Institutional Review Board. This data was collected as part of a larger randomized control trial which was registered with ClinicalTrials.gov (ClinicaTrials.gov ID NCT02828501) prior to the recruitment of the first participant.

Motor Tasks Protocol

Participants were trained in five motor tasks prior to undergoing fMRI. The tasks included a modified bridging movement where participants pushed the back of the left knee (left bridge), right knee (right bridge), or both knees (bilateral bridge) into a firm 22 cm bolster to slightly unweight their hips without lifting them. The reason these tasks were chosen was twofold. First, our previous work demonstrated that they recruited the lumbopelvic musculature without resulting in excessive head movement (Silfies et al., 2020). Second, these tasks resemble exercises that

TABLE 1 | Participant demographics.

N (Female)	Average age	Age range	Weight (Lbs)	Height (in)
19 (12)	28 (3.9)	21–37	158 (40)	68 (5.2)

Numbers in parentheses for average age, age range, weight, and height indicate standard deviation.

engage muscles in areas that are commonly painful and weak in people with LBP. Two tasks, abdominal tightening and ankle plantarflexion, were also performed but were not the focus of this paper. In order to minimize the potential for physiological noise in the Blood-oxygen-level-dependent (BOLD) response, the participants were instructed to keep their head and upper body still, breathe normally, and to just slightly unweight the hips. Training for each task was done both inside and outside the MRI to familiarize the participant with the scanning environment. A block design was utilized where each motor task was performed in random order for 11 s with a 4 s relaxation period following each task. After each task block, there was an 8 s rest block where the participants were instructed to relax. This sequence was repeated six times per run, with each participant completing two runs. This led to a total of 132 s of each task being performed during the study (**Figure 1**).

Functional Magnetic Resonance Imaging Acquisition Parameters

Data were collected on a 3T Siemens Prisma scanner using a 20-channel head coil (502 volumes; 58 axial slices; 2.5 mm thick; TR = 1,000 ms; TE = 37 ms; matrix 64 × 64 voxels; flip angle = 61; 220 mm × 220 mm FOV). A sagittal T1-weight MPRAGE protocol was used to acquire high-resolution structural images (192 slices; 1 mm thick; TR = 2,250 ms; TE = 4.11 ms; matrix = 1 mm × 1 mm × 1 mm; 256 × 256 FOV). The task order was recorded and the instructions were delivered to the participants using EPrime (Psychology Software Tools, Inc., Sharpsburg, PA, United States). Throughout data collection, participants were visually monitored to ensure they were performing the correct task.

Data Pre-processing

All data were processed using SPM 12 (Wellcome Department of Cognitive Neurology, London, United Kingdom) implemented in MATLAB R2017a (Mathworks, Natick, MA, United States). Initially, for each run, every volume was realigned to the first and unwarped. Using the anatomical scan, the mean image for each participant was then normalized to standard Montreal Neurological Institute (MNI) space. Once the normalization was completed, the parameters were applied to each volume in the functional run and data were resampled to 2 mm × 2 mm × 2 mm voxels. Smoothing was then applied using an isotropic Gaussian kernel 8 mm × 8 mm × 8 mm full width at half maximum. Head motion was then assessed for all analyzed data using the Artifact Detection Tool toolbox.[1] The first derivative of the head motion was used to screen for excessive head motion, and all outliers (defined as a greater than 2 mm difference from the previous volume) were de-weighted during the statistical analysis (mean number of outliers per run = 2, ranged from 0 to 8).

Statistical Analysis

Functional Magnetic Resonance Imaging Whole Brain Analysis

First-level analysis was performed using a general linear model for each participant (Friston et al., 1995; Worsley and Friston, 1995). Contrast maps were calculated for each task period vs. rest using the first derivative of head motion for all six directions as a regressor of no interest. The contrast maps for each of the bridging tasks were then moved to a second-level random effects analysis. A group analysis using a factorial design was performed with a factor for condition (left, right, and bilateral bridge). We analyzed the main effect for each condition, the comparison of one condition against another, as well as the combined effect for all bridging tasks. Group-level results were thresholded at a p-value less than 0.05 that was corrected for multiple comparisons using familywise error (FWE).

Functional Connectivity Analysis

We originally planned to select regions of interest (ROI) based on the results of our previous work using the same motor tasks (Silfies et al., 2020). However, the whole brain analysis found no activation peaks within the PostCG and consistent peaks

[1]https://www.nitrc.org/projects/artifact_detect/

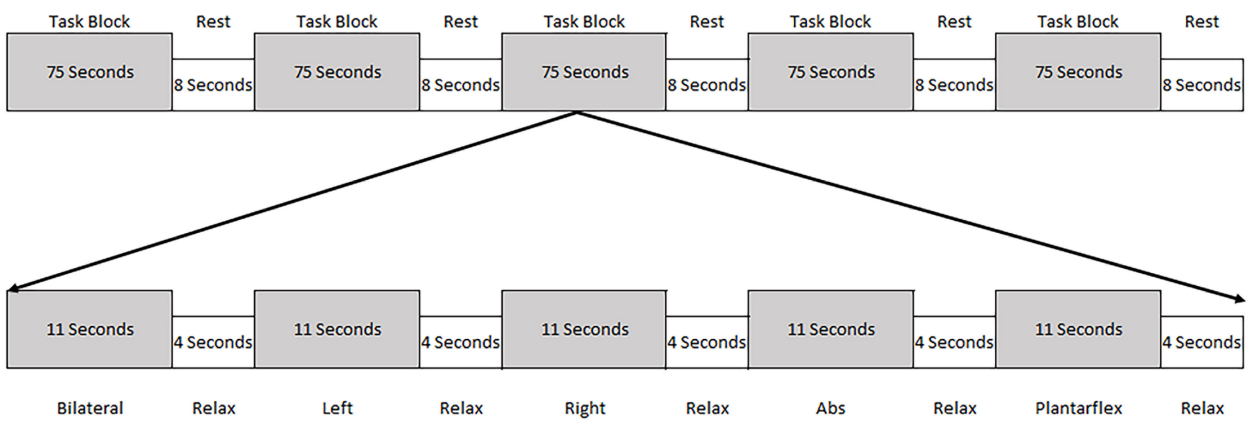

FIGURE 1 | Schematic of the task block. Each task block consisted of the performance of five tasks (each for 11 s) followed by a 4 s relaxation period. The order of the tasks were randomized within the task block. Following each task block the participants were given 8 s of rest.

within the cerebellum. Therefore, we choose the following ROIs to represent a sensorimotor network likely to be utilized during the bridging tasks based on the results of our whole brain analysis: bilateral Precentral Gyrus (PreCG), bilateral Cerebellum, and supplementary motor area (SMA). Using MarsBAR, we created a 5 mm radius sphere centered on the maximum peak of activation found in the group mean bridge analysis. This resulted in ROIs centered on the following MNI coordinates: Left PreCG (−14, −28, 68), Right PreCG (14, −28, 66), Left Cerebellum (−8, −42, −14), Right Cerebellum (6, −42, −16), and SMA (0, −16, 64).

Functional connectivity during movement was analyzed using the CONN toolbox (Whitfield-Gabrieli and Nieto-Castanon, 2012). Each participant's data was imported into the toolbox along with the task onsets and durations. Confounds were then removed *via* CONN's CompCor algorithm for physiological noise to reduce their effect on the functional connectivity values. A GLM approach was used for the ROI-to-ROI connectivity analysis. A bivariate correlation was computed separately on the individual's BOLD time series between each pair of ROIs; correlation coefficients were then transformed to Fisher's *Z* scores to meet the assumptions of normality (Whitfield-Gabrieli and Nieto-Castanon, 2012). The Fisher-Z transformed correlations were then extracted from the first-level analysis using MatLab and imported into SPSS (IBM SPSS Statistics for Windows, Version 25.0). A one-Sample's *t*-test was performed to determine if the correlations between each ROI pair were significantly different from 0 using the Holm's sequential Bonferroni procedure to correct for multiple comparisons (Eichstaedt et al., 2013). Then, an ANOVA with repeated measures (rmANOVA) was used to determine if the correlations between the different ROIs differed based on the task performed. For the rmANOVA, significance was determined using an $\alpha = 0.05$ with a Bonferroni correction.

RESULTS

Activation During Lumbopelvic Motor Task Performance

Brain activation during each motor task is shown in **Figure 2** and **Table 2**. Activation during the bridging tasks included multiple areas in the sensorimotor network consistent with Silfies et al. (2020) and included the PreCG, SMA, Cerebellum, and Putamen. Motor cortex activation was primarily located in the medial regions of the sensorimotor cortex (**Figure 2**) consistent with the somatotopic organization of this region (Asavasopon et al., 2014; Saby et al., 2015). As expected, activation was present in both hemispheres during bilateral bridging task while activation was predominantly located in the contralateral cerebral hemisphere (i.e., right motor regions during left bridge and left motor regions during right bridge) and the ipsilateral cerebellum during unilateral bridging tasks.

Table 3 and **Figure 3** outlines the differences in activation between the tasks. When compared to the left bridging task, the bilateral bridge had greater activation in the left PreCG. Similarly, when compared to the right bridge, the bilateral bridge had greater activation in the right PreCG. When comparing the unilateral bridging tasks against one another, both tasks demonstrated greater activity in the contralateral PreCG and Putamen, as well as greater activity in the ipsilateral Cerebellum. However, when comparing the right bridge to the left bridge, there was significantly greater activation in the left PostCG and Insula.

Connectivity During Task Performance

Figure 4 summarizes the connectivity values within the proposed sensorimotor network during the bridging tasks. The individual *t*-tests demonstrated that the only correlations that were not significant at the $p = 0.05$ level after correction were the connections between the left PreCG and the left cerebellum ($p = 0.415$) and the right PreCG and the left cerebellum ($p = 0.052$) during the bilateral bridging tasks. All other connections were significant. The results of the rmANOVAs revealed some significant differences in the connectivity between the tasks. First, the connectivity between the right PreCG and left PreCG during the bilateral bridging task was significantly higher when compared to the right bridging task ($z = 0.491$ vs. $z = 0.395$; $p = 0.032$). This difference was not observed when comparing the bilateral to the left bridging task. Additionally, the connectivity between the right PreCG and the SMA during the bilateral bridge was significantly higher when compared to the right bridging task ($z = 0.493$ vs. $z = 0.396$; $p = 0.009$).

DISCUSSION

To our knowledge, this is the first study to exam functional connectivity during volitional movements of the lumbopelvic region. The primary aims of this study were to validate the results of a previous investigation (Silfies et al., 2020) and to examine functional connectivity in the sensorimotor network during lumbopelvic motor tasks. Similar to the previous study, robust activation in the medial sensorimotor regions were observed during motor tasks which involved the lumbopelvic musculature. Additionally, during the unilateral bridging tasks activation was shifted toward the contralateral hemisphere, whereas during the bilateral bridging task activation was present in both hemispheres. The functional connectivity analysis demonstrated significant connectivity between each of the ROIs for each of the bridging tasks, with some differences in connectivity exhibited between the right and bilateral bridging tasks.

Sensorimotor Activation During Lumbopelvic Motor Tasks

As hypothesized, during lumbopelvic bridging tasks we found strong activation in the medial motor areas of the brain, consistent with a previous preliminary study (Rao et al., 2008). While the current study utilized tasks which focused on engagement of the lumbopelvic musculature, previous literature investigating cortical activation during other lower limb tasks supports the general activation patterns we found (Mehta et al., 2012). Studies that included unilateral ankle (Debaere et al., 2001; Kapreli et al., 2006, 2007; Cunningham et al., 2013), knee (Fink et al., 1997; Luft et al., 2002; Kapreli et al., 2006, 2007), and toe (Kapreli et al., 2006, 2007) movements have consistently reported

TABLE 2 | Whole brain BOLD response of relative activation compared to rest.

Comparison	Cluster	No. of voxels	P FWE-corr	Peak-*Z*	MNI location, mm			Structural regions
					X	*Y*	*Z*	
Bilateral bridge > Rest	1	200	<0.001	6.04	−10	−40	−16	L Cerebellum
				5.34	6	−42	−16	Vermis
				4.92	16	−38	−20	R Cerebellum
	2	497	<0.001	5.89	0	−16	66	Supplemental motor area
				5.33	14	−28	66	R Precentral Gyrus
				5.28	−12	−30	68	L Precentral Gyrus
	3	37	0.007	5.55	−28	−10	10	L Putamen
Left bridge > Rest	1	230	<0.001	6.6	−8	−42	−16	L Cerebellum
				5.19	−22	−32	−28	L Cerebellum
	2	616	<0.001	6.20	12	−28	70	R Thalamus
				3.05	2	−16	64	R Supplemental motor area
				5.58	6	−32	58	R Precentral Gyrus
	3	25	0.012	4.95	30	−10	6	R Putamen
Right bridge > Rest	1	146	<0.001	6.79	−28	−10	10	L Putamen
				4.75	−24	−22	14	L Thalamus
	2	554	<0.001	6.42	−12	−28	70	L Precentral Gyrus
				5.97	−4	−20	64	L Supplemental motor area
				5.51	−6	−34	58	L Precuneus
	3	238	0.016	6.41	8	−42	−18	R Cerebellum
				5.20	24	−32	−28	R Cerebellum

Comparisons of each task against rest. All clusters were significant at $p < 0.05$ with familywise error correction (FWE-corr) for analysis. In both unilateral bridging tasks, the location of the peak voxel within the somatosensory regions were located in the contralateral hemisphere.
No. of voxels, number of 2 mm^3 voxels in the cluster; Peak-Z, peak Z-value within the cluster; L, Left; R, Right; Rest, rest condition no movement.

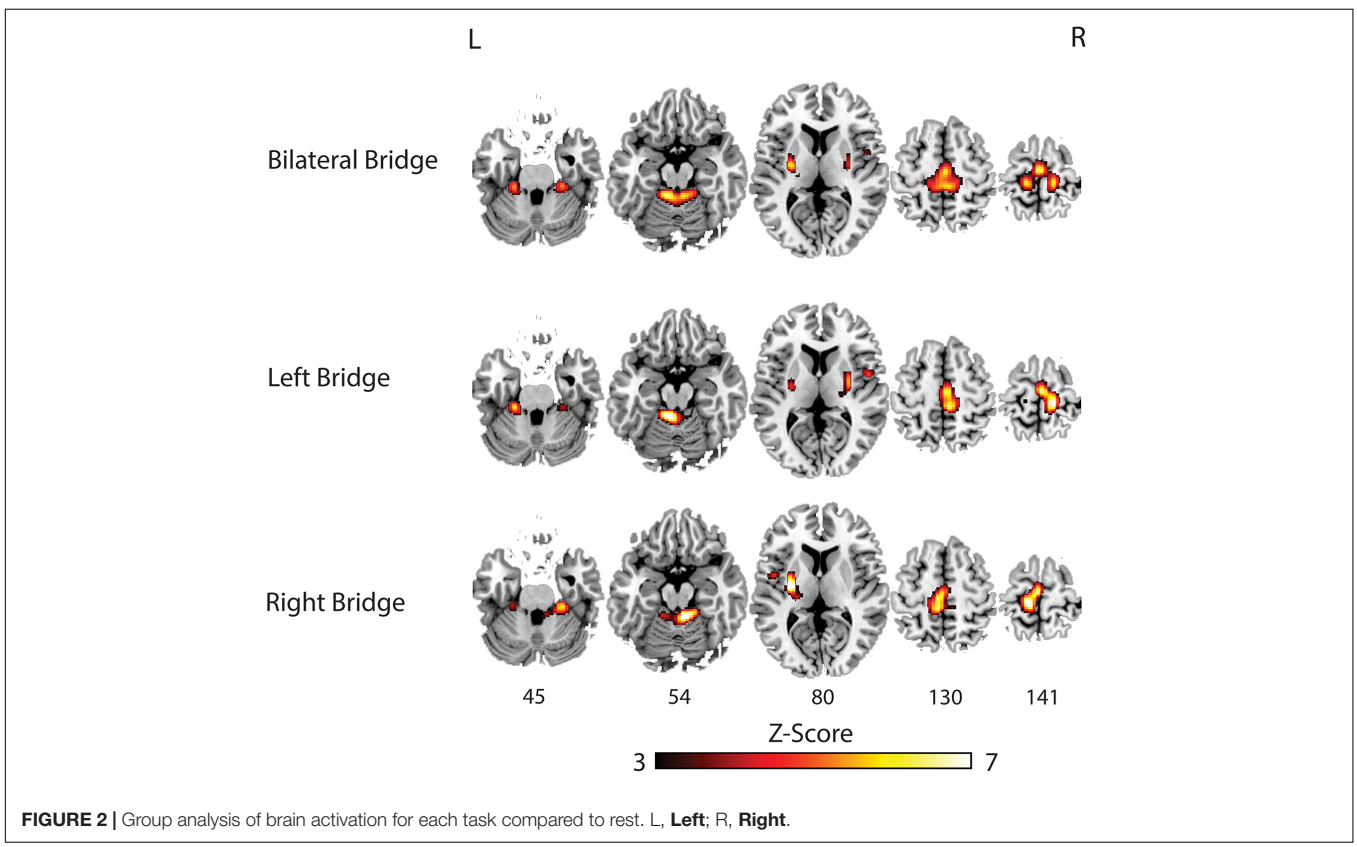

FIGURE 2 | Group analysis of brain activation for each task compared to rest. L, **Left**; R, **Right**.

TABLE 3 | Whole brain BOLD response of comparative bridging tasks.

Comparison	Cluster	No. of voxels	P FWE-corr	Peak-Z	MNI location, mm			Structural regions
					X	*Y*	*Z*	
Bilateral > Left	1	196	<0.001	5.63	−8	−32	70	L Precentral Gyrus
Bilateral > Right	1	474	<0.001	6.41	10	−28	74	R Precentral Gyrus
Left > Right	1	694	<0.001	7.65	10	−28	74	R Precentral Gyrus
	2	93	0.001	8.76	−10	−38	−22	L Cerebellum
	3	51	0.005	5.08	32	−10	6	R Putamen
Right > Left	1	583	<0.001	7.21	−8	−30	70	L Precentral Gyrus
				6.24	−6	−36	62	L Postcentral Gyrus
	2	230	<0.001	5.82	−30	−22	18	L Insular Cortex
				5.48	−28	−8	12	L Putamen
	3	75	0.002	5.69	10	−40	−20	R Cerebellum

Results from comparing each bridging task against one another. All clusters were significant at $p < 0.05$ with familywise error correction (FWE-corr) for analysis. No. of voxels, number of 2 mm^3 voxels in the cluster; Peak-Z, peak Z-value within the cluster; L, Left; R, Right.

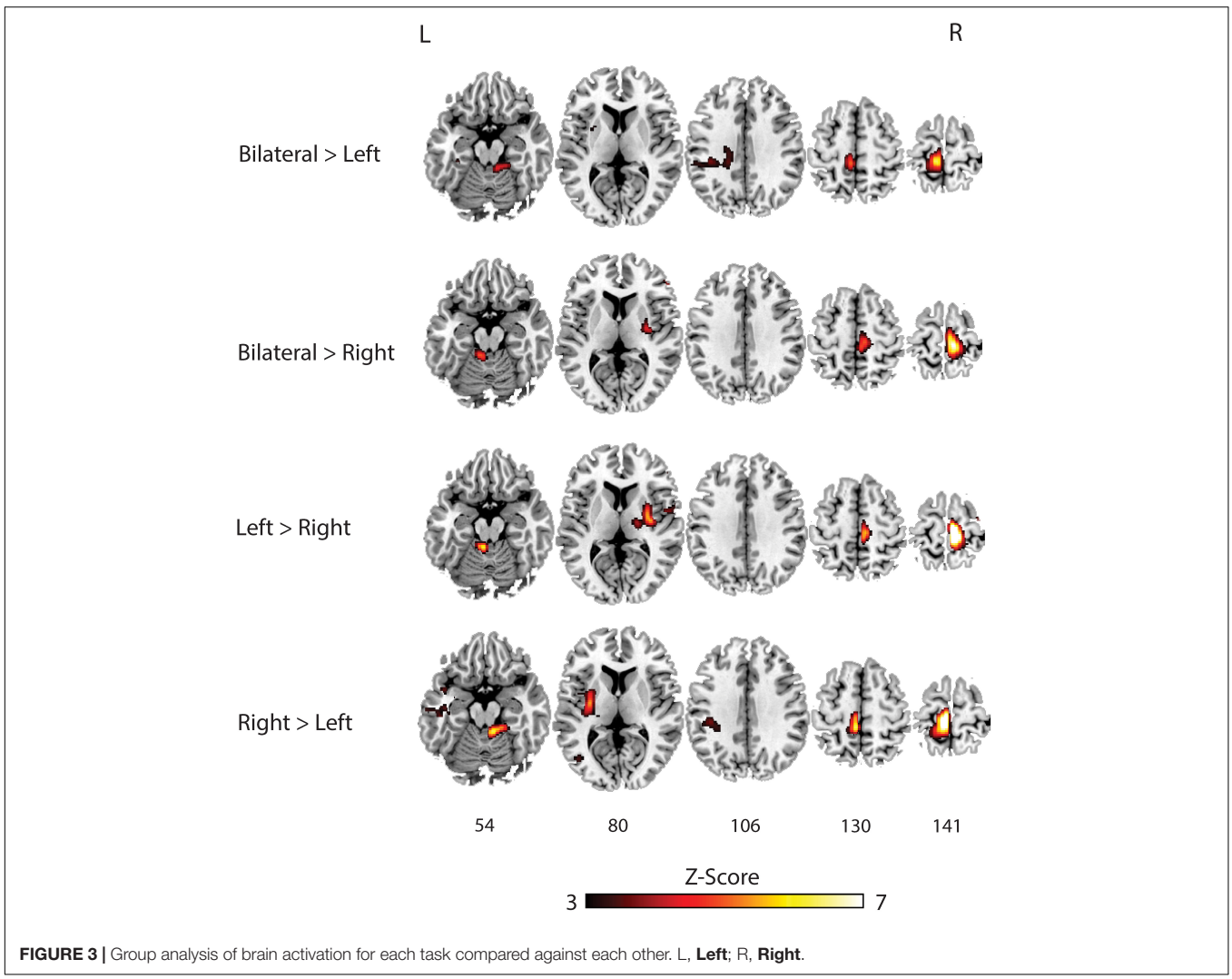

FIGURE 3 | Group analysis of brain activation for each task compared against each other. L, **Left**; R, **Right**.

activation in the SMA, PreCG, and Cerebellum. Furthermore, previous studies have found that the PreCG is somatotopically organized with the feet represented relatively medially and the hands represented relatively laterally (Rao et al., 1995; Kapreli et al., 2007; Plow et al., 2010; Cunningham et al., 2013; Weiss et al., 2013). Overall, the bridging tasks used in the current

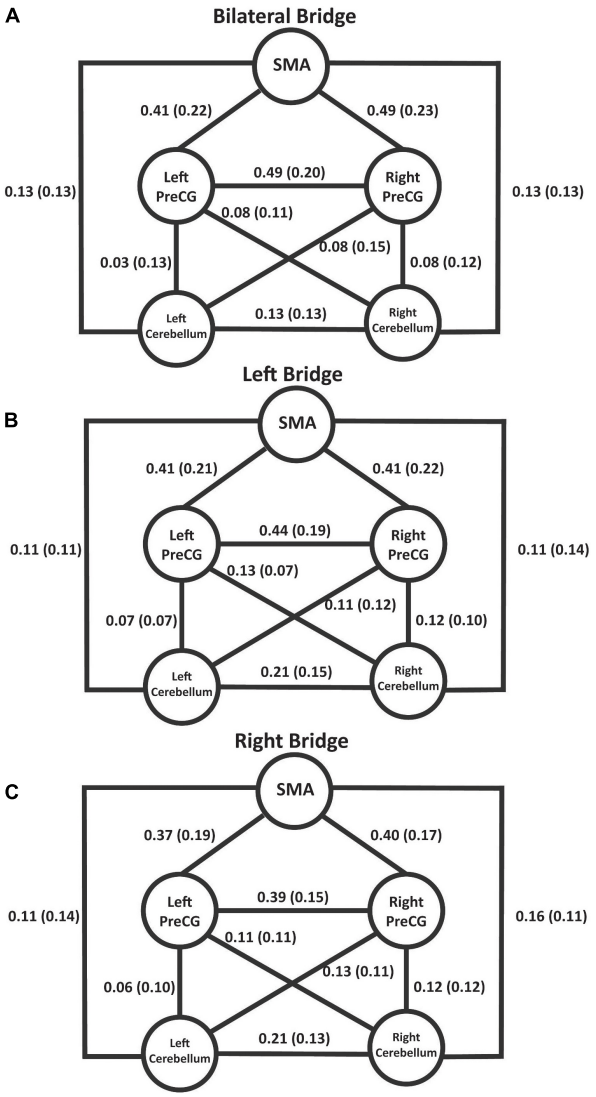

FIGURE 4 | Schematic of the proposed sensorimotor network during the bridging tasks. Values represent Fisher's-Z transformed correlation coefficients with standard deviation in parentheses. With the exception of left and right PreCG to left cerebellum during the bilateral bridge task, all values were significant at $p < 0.05$ after correction using the Holm's sequential Bonferroni procedure (Eichstaedt et al., 2013). **(A)** Connectivity values during the bilateral bridge task. **(B)** Connectivity values during the left bridge task. **(C)** Connectivity values during the right bridge task. SMA, supplemental motor area; PreCG, precentral gyrus.

study activated a medial sensorimotor network, suggesting this protocol provides an approach to examine the neural correlates of lumbopelvic motor control.

One observation that was different for this study compared to our previous one was the amount of lateralization that occurred with the unilateral bridging tasks. Consistent with our previous study, the bilateral bridge resulted in bilateral activation; however, the unilateral bridging tasks in this study resulted in more lateralized activation. Specifically, the unilateral bridging tasks resulted in activation of the contralateral PreCG, SMA, Thalamus, and Putamen, with ipsilateral cerebellar activation. This pattern resembles previous work investigating sensorimotor activation during movement (Grefkes et al., 2008). However, our previous study reported activation occurring across both brain hemispheres during unilateral bridging. One reason for the difference may be due to the slight differences in the task hold time: in our previous study participants held the tasks for 14 s, whereas in our current study they only held the tasks for 11 s. While the difference is small, the extra 3 s might have been enough to necessitate additional recruitment of the trunk musculature in order to prevent fatigue, thus obscuring the distinct hemispheric pattern we observed in the present study. An alternative explanation could be in the total time engaged in each task. In the previous study, the participants performed 84 s of each task, whereas in our current study this was increased to 132 s. This more than 50% increase in task time might have resulted in the more specific activation patterns that were observed. Regardless, this study demonstrated that the lumbopelvic protocol used in the current study is able to delineate different patterns of activation based on the unique demands of the three bridging tasks.

Functional Connectivity During Lumbopelvic Motor Tasks

With limited exceptions, the sensorimotor network we described was significantly connected during the performance of lumbopelvic tasks. Similar to previous work in the upper and lower limb, the bilateral bridging task resulted in interhemispheric connectivity (Grefkes et al., 2008; Vinehout et al., 2019). However, our findings did not fully support our hypothesis. We hypothesized that the unilateral bridging tasks would demonstrate unique connectivity patterns which reflected the specificity of the task. While this was evident in whole brain activation, we found that the pattern of connectivity did not differ between the unilateral bridging tasks, and only minimally so between the bilateral and right bridging tasks. This is inconsistent with previous work investigating differences in unilateral vs. bilateral tasks (Grefkes et al., 2008; Vinehout et al., 2019). For example, Vinehout et al. (2019) examined differences in lower limb task-based functional connectivity in asymptomatic individuals and individuals who had a stroke. They reported that the strength of the functional connections between each of the ROIs was modulated by the tasks. One possible explanation of why our findings were inconsistent with this previous work using extremity movement could be due to the tasks that were used in each study. In the study by Vinehout et al., the bilateral movement was a multi-joint pedaling task that required the coordination of multiple segments; whereas the unilateral task was tapping of the foot, which would require the use of only a single joint. While our tasks incorporated both unilateral and bilateral lumbopelvic movements, all the tasks required the coordination of multiple segments. Therefore, the uniformity of the connectivity values in our study might reflect the complexity of the movement and the higher demands for sensorimotor integration of multi-segmental motor tasks (Vinehout et al., 2019).

This hypothesis is further supported by work that has been done in the upper extremity as well. Prior evidence has shown that unilateral hand opening/closing tasks results in connectivity within the contralateral hemisphere, while bilateral hand opening/closing tasks increases the interhemispheric connectivity (Grefkes et al., 2008). However, Wilkins et al. found that when performing a unilateral hand grasping task, by increasing the complexity of the activity and having the participants coordinate motion between multiple joints of the same limb there was an increase in interhemispheric communication (Wilkins and Yao, 2020). This increase in the interhemispheric communication was absent with a simple hand opening task. Thus, the integration of movement from multiple joints might also explain why there was little difference in interhemispheric connectivity between our bilateral and unilateral lumbopelvic tasks. By utilizing lumbopelvic as opposed to upper or lower limb tasks, our results support the notion that an increase in interhemispheric connectivity is related to the complexity of movement independent of the bilateral or unilateral nature of the task being performed.

One contributing factor to the complexity of the lumbopelvic task could be the bilateral recruitment of the trunk musculature required to stabilize the spine during the modified bridging task (Yoon et al., 2018), whereas no such stabilization is required during foot tapping or performance of simple upper extremity motor tasks. Performing a modified bridge is a complex motor task that requires coordination across the lumbopelvic musculature in order to stiffen the spine and maintain balance while the pelvis is being lifted from the mat (Kim et al., 2013; Czaprowski et al., 2014; Yoon et al., 2018). While the activation patterns in the whole brain analysis were different depending on the task performed, it may be that functional connectivity reflects the coordination and communication required between the bilateral trunk musculature which would be needed regardless of the task (Rao et al., 2008). Thus, while the participants exhibited unique activation patterns during the whole brain analysis, the differences in the functional connectivity could be minimal. Strong structural connections between these regions could also drive the similarity in functional connectivity across the tasks (Ansari et al., 2011). The SMA and PreCG work together to help facilitate movement. The SMA, which is largely devoted to movement planning and early motor preparation has structural connections with the PreCG (Ruddy et al., 2017). Considering the strong structural connections and synergies in function, our results fit well within the established literature.

Implications for Low Back Pain Research

There have been numerous investigations into both the functional connectivity and brain activation during motor tasks involving the hand and upper extremities (Grefkes et al., 2008; Xu et al., 2014; Coombes and Misra, 2016). However, more investigation is needed into the lumbopelvic musculature as this region is implicated in those with chronic low back pain (cLBP). Previous research has demonstrated that cLBP results in specific cortical changes linked to the lumbopelvic region; during both muscle (Tsao et al., 2008, 2011; Schabrun et al., 2015) and cutaneous stimulation (Flor et al., 1997; Hotz-Boendermaker et al., 2016). Furthermore, biomechanical research has suggested deficits in the lumbopelvic motor control in individuals with cLBP (Hodges and Richardson, 1996; Henry et al., 2006; Silfies et al., 2009; Jones et al., 2012; Sung et al., 2015). Therefore, a better understanding of the processes behind the motor control of the lumbopelvic musculature could potentially lead to better therapies in the treatment of those with LBP. By providing functional connectivity data in individuals devoid of pain, the results of this investigation can provide a comparison for future research into potential connectivity changes in individuals with cLBP. Furthermore, this protocol provides researchers another method by which to examine motor control and the effects of different interventions in individuals with cLBP.

Limitations

Unlike previous research using lower extremity tasks, we did not incorporate external stabilization devices to reduce motion artifact and control movement (Debaere et al., 2001; Kapreli et al., 2006, 2007; Newton et al., 2008). While stabilizing the joint may decrease task-related head movement, this isolation may influence the findings. There is an inherent motor variability during movement performance (Balasubramaniam et al., 2000) and the ability to compensate for this variation is vital for optimal feedback control (Todorov and Jordan, 2002). Supplementing joint support during a task may reduce the ability to detect changes in individuals with chronic pain who demonstrate movement impairment (Hodges and Richardson, 1996; Henry et al., 2006; Silfies et al., 2009; Jones et al., 2012; Sung et al., 2015). Stabilizing joint motion appears to improve sensorimotor function as well (Wu et al., 2001; de Vries et al., 2017; Smalley et al., 2018), and may inadvertently diminish differences that may be found between asymptomatic individuals and individuals with musculoskeletal disorders such as cLBP (Tsao et al., 2008, 2011; Schabrun et al., 2015). As such, lumbopelvic motor tasks that are unencumbered by external support may be an important approach for elucidating the cortical changes associated with cLBP. Furthermore, with an average of 2 out of 765 volumes being removed for excessive motion, our task did not seem to create excessive artifact. This in in line with our previous work which found that this specific motor protocol resulted in minimal head movement (Silfies et al., 2020).

Another potential limitation of our study is that the method of analyzing connectivity we chose does not allow for insights into directionality of the network, which could help clarify the modulation of activity between our different ROIs. Future studies could consider the interaction between these regions using an effective connectivity analysis approach.

CONCLUSION

We examined brain activation and functional connectivity during the performance of unsupported bilateral and unilateral

lumbopelvic motor tasks. Robust activation patterns were observed in the motor network and differences were observed depending on the task being performed. Within our constrained motor network of the PreCG, Cerebellum, and SMA we found extensive connectivity between these regions across tasks. This study helps build a foundation for future investigations designed to examine the changes in the neural correlates of movement in individuals with LBP and inform the development of intervention approaches.

DATA AVAILABILITY STATEMENT

The datasets presented in this study can be found in online repositories. The names of the repository/repositories and accession number(s) can be found below: All relevant data are available on Mendeley with the DOI: 10.17632/v9yhyrhhp5.1.

ETHICS STATEMENT

The studies involving human participants were reviewed and approved by the University of South Carolina Institutional Review Board. The patients/participants provided their written informed consent to participate in this study.

AUTHOR CONTRIBUTIONS

MJ: conceptualization, methodology, formal analysis, investigation, writing—original draft, writing—review and editing, and funding acquisition. JS: formal analysis, writing—original draft, and writing—review and editing. SS: conceptualization, methodology, investigation, and writing—review and editing. PB: conceptualization, writing—review and editing, and funding acquisition. All authors contributed to the article and approved the submitted version.

FUNDING

The American Physical Therapy Association (APTA) Orthopedic Section New Investigator Grant supported research reported in this publication.

ACKNOWLEDGMENTS

We would like to thank our colleague Jennifer MC Vendemia, Ph.D. for her valuable and constructive suggestions during the development of the task-based imaging protocol for this project. Furthermore, we extend our gratitude to those who volunteered their time to participate in this study. Without volunteers who readily engage with the scientific community, it is difficult to move science forward.

REFERENCES

Ansari, A. H., Oghabian, M. A., and Hossein-Zadeh, G. A. (2011). "Assessment of functional and structural connectivity between motor cortex and thalamus using fMRI and DWI," in *Annual International Conference of the IEEE Engineering in Medicine and Biology Society IEEE Engineering in Medicine and Biology Society Annual International Conference* (Piscataway: IEEE), 5056–5059. doi: 10.1109/IEMBS.2011.6091252

Asavasopon, S., Rana, M., Kirages, D. J., Yani, M. S., Fisher, B. E., Hwang, D. H., et al. (2014). Cortical activation associated with muscle synergies of the human male pelvic floor. *J. Neurosci.* 34, 13811–13818. doi: 10.1523/JNEUROSCI.2073-14.2014

Balasubramaniam, R., Riley, M. A., and Turvey, M. T. (2000). Specificity of postural sway to the demands of a precision task. *Gait Posture* 11, 12–24.

Coombes, S. A., and Misra, G. (2016). Pain and motor processing in the human cerebellum. *Pain* 157, 117–127. doi: 10.1097/j.pain.0000000000000337

Criss, C. R., Onate, J. A., and Grooms, D. R. (2020). Neural activity for hip-knee control in those with anterior cruciate ligament reconstruction: a task-based functional connectivity analysis. *Neurosci. Lett.* 730:134985. doi: 10.1016/j.neulet.2020.134985

Cunningham, D. A., Machado, A., Yue, G. H., Carey, J. R., and Plow, E. B. (2013). Functional somatotopy revealed across multiple cortical regions using a model of complex motor task. *Brain Res.* 1531, 25–36. doi: 10.1016/j.brainres.2013.07.050

Czaprowski, D., Afeltowicz, A., Gębicka, A., Pawłowska, P., Kędra, A., Barrios, C., et al. (2014). Abdominal muscle EMG-activity during bridge exercises on stable and unstable surfaces. *Phys. Ther. Sport* 15, 162–168. doi: 10.1016/j.ptsp.2013.09.003

de Vries, A. J., van den Akker-Scheek, I., Haak, S. L., Diercks, R. L., van der Worp, H., and Zwerver, J. (2017). Effect of a patellar strap on the joint position sense of the symptomatic knee in athletes with patellar tendinopathy. *J. Sci. Med. Sport* 20, 986–991. doi: 10.1016/j.jsams.2017.04.020

Debaere, F., Swinnen, S. P., Beatse, E., Sunaert, S., Van Hecke, P., and Duysens, J. (2001). Brain areas involved in interlimb coordination: a distributed network. *Neuroimage* 14, 947–958. doi: 10.1006/nimg.2001.0892

Eichstaedt, K. E., Kovatch, K., and Maroof, D. A. (2013). A less conservative method to adjust for familywise error rate in neuropsychological research: the Holm's sequential Bonferroni procedure. *NeuroRehabilitation* 32, 693–696. doi: 10.3233/NRE-130893

Fadiga, L., Craighero, L., Dri, G., Facchin, P., Destro, M. F., and Porro, C. A. (2004). Corticospinal excitability during painful self-stimulation in humans: a transcranial magnetic stimulation study. *Neurosci. Lett.* 361, 250–253. doi: 10.1016/j.neulet.2003.12.016

Farina, S., Valeriani, M., Rosso, T., Aglioti, S., Tamburin, S., Fiaschi, A., et al. (2001). Transient inhibition of the human motor cortex by capsaicin-induced pain. A study with transcranial magnetic stimulation. *Neurosci. Lett.* 314, 97–101. doi: 10.1016/s0304-3940(01)02297-2

Fink, G. R., Frackowiak, R. S., Pietrzyk, U., and Passingham, R. E. (1997). Multiple non-primary motor areas in the human cortex. *J. Neurophysiol.* 77, 2164–2174.

Flor, H., Braun, C., Elbert, T., and Birbaumer, N. (1997). Extensive reorganization of primary somatosensory cortex in chronic back pain patients. *Neurosci. Lett.* 224, 5–8. doi: 10.1016/s0304-3940(97)13441-3

Friston, K. J., Holmes, A. P., Worsley, K. J., Poline, J. P., Frith, C. D., and Frackowiak, R. S. J. (1995). Statistical Parametric Maps in Functional Imaging: a General Linear Approach. *Hum. Brain Mapp.* 2, 189–210. doi: 10.1016/j.neuroimage.2007.01.029

Goss, D. A., Hoffman, R. L., and Clark, B. C. (2012). Utilizing transcranial magnetic stimulation to study the human neuromuscular system. *J. Vis. Exp.* 59:3387. doi: 10.3791/3387

Grefkes, C., Eickhoff, S. B., Nowak, D. A., Dafotakis, M., and Fink, G. R. (2008). Dynamic intra- and interhemispheric interactions during unilateral and bilateral hand movements assessed with fMRI and DCM. *Neuroimage* 41, 1382–1394. doi: 10.1016/j.neuroimage.2008.03.048

Grooms, D. R., Diekfuss, J. A., Ellis, J. D., Yuan, W., Dudley, J., Foss, K. D. B., et al. (2019). A Novel Approach to Evaluate Brain Activation for Lower Extremity Motor Control. *J. Neuroimag.* 29, 580–588. doi: 10.1111/jon.12645

Henry, S. M., Hitt, J. R., Jones, S. L., and Bunn, J. Y. (2006). Decreased limits of stability in response to postural perturbations in subjects with low back pain. *Clin. Biomech.* 21, 881–892. doi: 10.1016/j.clinbiomech.2006.04.016

Hodges, P. W., and Richardson, C. A. (1996). Inefficient muscular stabilization of the lumbar spine associated with low back pain. A motor control evaluation of transversus abdominis. *Spine* 21, 2640–2650. doi: 10.1097/00007632-199611150-00014

Hodges, P. W., and Tucker, K. (2011). Moving differently in pain: a new theory to explain the adaptation to pain. *Pain* 152, S90–S98. doi: 10.1016/j.pain.2010.10.020

Hotz-Boendermaker, S., Marcar, V. L., Meier, M. L., Boendermaker, B., and Humphreys, B. K. (2016). Reorganization in Secondary Somatosensory Cortex in Chronic Low Back Pain Patients. *Spine* 41, E667–E673. doi: 10.1097/BRS.0000000000001348

Jean-Charles, L., Nepveu, J. F., Deffeyes, J. E., Elgbeili, G., Dancause, N., and Barthélemy, D. (2017). Interhemispheric interactions between trunk muscle representations of the primary motor cortex. *J. Neurophysiol.* 118, 1488–1500. doi: 10.1152/jn.00778.2016

Jones, S. L., Henry, S. M., Raasch, C. C., Hitt, J. R., and Bunn, J. Y. (2012). Individuals with non-specific low back pain use a trunk stiffening strategy to maintain upright posture. *J. Electromyogr. Kinesiol.* 22, 13–20. doi: 10.1016/j.jelekin.2011.10.006

Kapreli, E., Athanasopoulos, S., Papathanasiou, M., Van Hecke, P., Kelekis, D., Peeters, R., et al. (2007). Lower Limb Sensorimotor Network: issues of Somatotopy and Overlap. *Cortex* 43, 219–232. doi: 10.1016/s0010-9452(08)70477-5

Kapreli, E., Athanasopoulos, S., Papathanasiou, M., Van Hecke, P., Strimpakos, N., Gouliamos, A., et al. (2006). Lateralization of brain activity during lower limb joints movement. An fMRI study. *Neuroimage* 32, 1709–1721. doi: 10.1016/j.neuroimage.2006.05.043

Kim, M. J., Oh, D. W., and Park, H. J. (2013). Integrating arm movement into bridge exercise: effect on EMG activity of selected trunk muscles. *J. Electromyogr. Kinesiol.* 23, 1119–1123. doi: 10.1016/j.jelekin.2013.07.001

Luft, A. R., Smith, G. V., Forrester, L., Whitall, J., Macko, R. F., Hauser, T. K., et al. (2002). Comparing brain activation associated with isolated upper and lower limb movement across corresponding joints. *Hum. Brain Mapp.* 17, 131–140. doi: 10.1002/hbm.10058

Martin, P. G., Weerakkody, N., Gandevia, S. C., and Taylor, J. L. (2008). Group III and IV muscle afferents differentially affect the motor cortex and motoneurones in humans. *J. Physiol.* 586, 1277–1289. doi: 10.1113/jphysiol.2007.140426

Matthews, D., Murtagh, P., Risso, A., Jones, G., and Alexander, C. M. (2013). Does interhemispheric communication relate to the bilateral function of muscles? A study of scapulothoracic muscles using transcranial magnetic stimulation. *J. Electromyogr. Kinesiol.* 23, 1370–1374. doi: 10.1016/j.jelekin.2013.06.007

Mehta, J. P., Verber, M. D., Wieser, J. A., Schmit, B. D., and Schindler-Ivens, S. M. (2012). The effect of movement rate and complexity on functional magnetic resonance signal change during pedaling. *Mot. Control* 16, 158–175. doi: 10.1123/mcj.16.2.158

Newton, J. M., Dong, Y., Hidler, J., Plummer-D'Amato, P., Marehbian, J., Albistegui-Dubois, R. M., et al. (2008). Reliable assessment of lower limb motor representations with fMRI: use of a novel MR compatible device for real-time monitoring of ankle, knee and hip torques. *Neuroimage* 43, 136–146. doi: 10.1016/j.neuroimage.2008.07.001

Oldfield, R. C. (1971). The assessment and analysis of handedness: the Edinburgh inventory. *Neuropsychologia* 9, 97–113. doi: 10.1016/0028-3932(71)90067-4

Plow, E. B., Arora, P., Pline, M. A., Binenstock, M. T., and Carey, J. R. (2010). Within-limb somatotopy in primary motor cortex–revealed using fMRI. *Cortex* 46, 310–321. doi: 10.1016/j.cortex.2009.02.024

Rao, H., Di, X., Chan, R. C., Ding, Y., Ye, B., and Gao, D. (2008). A regulation role of the prefrontal cortex in the fist-edge-palm task: evidence from functional connectivity analysis. *Neuroimage* 41, 1345–1351. doi: 10.1016/j.neuroimage.2008.04.026

Rao, S. M., Binder, J. R., Hammeke, T. A., Bandettini, P. A., Bobholz, J. A., Frost, J. A., et al. (1995). Somatotopic mapping of the human primary motor cortex with functional magnetic resonance imaging. *Neurology* 45, 919–924. doi: 10.1212/wnl.45.5.919

Romaniello, A., Cruccu, G., McMillan, A. S., Arendt-Nielsen, L., and Svensson, P. (2000). Effect of experimental pain from trigeminal muscle and skin on motor cortex excitability in humans. *Brain Res.* 882, 120–127. doi: 10.1016/s0006-8993(00)02856-0

Ruddy, K. L., Leemans, A., and Carson, R. G. (2017). Transcallosal connectivity of the human cortical motor network. *Brain Struct. Funct.* 222, 1243–1252. doi: 10.1007/s00429-016-1274-1

Saby, J. N., Meltzoff, A. N., and Marshall, P. J. (2015). Neural body maps in human infants: somatotopic responses to tactile stimulation in 7-month-olds. *Neuroimage* 118, 74–78. doi: 10.1016/j.neuroimage.2015.05.097

Schabrun, S. M., Elgueta-Cancino, E. L., and Hodges, P. W. (2015). Smudging of the Motor Cortex Is Related to the Severity of Low Back Pain. *Spine* 42, 1172-1178. doi: 10.1097/BRS.0000000000000938

Silfies, S. P., Beattie, P., Jordon, M., and Vendemia, J. M. C. (2020). Assessing sensorimotor control of the lumbopelvic-hip region using task-based functional MRI. *J. Neurophysiol.* 124, 192–206. doi: 10.1152/jn.00288.2019

Silfies, S. P., Mehta, R., Smith, S. S., and Karduna, A. R. (2009). Differences in feedforward trunk muscle activity in subgroups of patients with mechanical low back pain. *Arch. Phys. Med. Rehabil.* 90, 1159–1169. doi: 10.1016/j.apmr.2008.10.033

Smalley, A., White, S. C., and Burkard, R. (2018). The effect of augmented somatosensory feedback on standing postural sway. *Gait Posture* 60, 76–80. doi: 10.1016/j.gaitpost.2017.11.015

Sung, W., Abraham, M., Plastaras, C., and Silfies, S. P. (2015). Trunk motor control deficits in acute and subacute low back pain are not associated with pain or fear of movement. *Spine J.* 15, 1772–1782. doi: 10.1016/j.spinee.2015.04.010

Todorov, E., and Jordan, M. I. (2002). Optimal feedback control as a theory of motor coordination. *Nat. Neurosci.* 5, 1226–1235. doi: 10.1038/nn963

Tsao, H., Danneels, L. A., and Hodges, P. W. (2011). ISSLS prize winner: smudging the motor brain in young adults with recurrent low back pain. *Spine* 36, 1721–1727. doi: 10.1097/BRS.0b013e31821c4267

Tsao, H., Galea, M. P., and Hodges, P. W. (2008). Reorganization of the motor cortex is associated with postural control deficits in recurrent low back pain. *Brain* 131, 2161–2171. doi: 10.1093/brain/awn154

Valeriani, M., Restuccia, D., Di Lazzaro, V., Oliviero, A., Profice, P., Le Pera, D., et al. (1999). Inhibition of the human primary motor area by painful heat stimulation of the skin. *Clin. Neurophysiol.* 110, 1475–1480. doi: 10.1016/s1388-2457(99)00075-9

Vinehout, K., Schmit, B. D., and Schindler-Ivens, S. (2019). Lower Limb Task-Based Functional Connectivity Is Altered in Stroke. *Brain Connect.* 9, 365–377. doi: 10.1089/brain.2018.0640

Weiss, C., Nettekoven, C., Rehme, A. K., Neuschmelting, V., Eisenbeis, A., Goldbrunner, R., et al. (2013). Mapping the hand, foot and face representations in the primary motor cortex - retest reliability of neuronavigated TMS versus functional MRI. *Neuroimage* 66, 531–542. doi: 10.1016/j.neuroimage.2012.10.046

Whitfield-Gabrieli, S., and Nieto-Castanon, A. (2012). Conn: a functional connectivity toolbox for correlated and anticorrelated brain networks. *Brain Connect.* 2, 125–141. doi: 10.1089/brain.2012.0073

Wilkins, K. B., and Yao, J. (2020). Coordination of multiple joints increases bilateral connectivity with ipsilateral sensorimotor cortices. *Neuroimage* 207:116344. doi: 10.1016/j.neuroimage.2019.116344

Worsley, K. J., and Friston, K. J. (1995). Analysis of fMRI time-series revisited–again. *Neuroimage* 2, 173–181. doi: 10.1006/nimg.1995.1023

Wu, G. K., Ng, G. Y., and Mak, A. F. (2001). Effects of knee bracing on the sensorimotor function of subjects with anterior cruciate ligament reconstruction. *Am. J. Sports Med.* 29, 641–645. doi: 10.1177/03635465010290051801

Xu, L., Zhang, H., Hui, M., Long, Z., Jin, Z., Liu, Y., et al. (2014). Motor execution and motor imagery: a comparison of functional connectivity patterns based on graph theory. *Neuroscience* 261, 184–194. doi: 10.1016/j.neuroscience.2013.12.005

Yoon, J. O., Kang, M. H., Kim, J. S., and Oh, J. S. (2018). Effect of modified bridge exercise on trunk muscle activity in healthy adults: a cross sectional study. *Braz. J. Phys. Ther.* 22, 161–167. doi: 10.1016/j.bjpt.2017.09.005

Conflict of Interest: The authors declare that the research was conducted in the absence of any commercial or financial relationships that could be construed as a potential conflict of interest.

Publisher's Note: All claims expressed in this article are solely those of the authors and do not necessarily represent those of their affiliated organizations, or those of the publisher, the editors and the reviewers. Any product that may be evaluated in this article, or claim that may be made by its manufacturer, is not guaranteed or endorsed by the publisher.

frontiers in Human Neuroscience

ORIGINAL RESEARCH
published: 17 March 2022
doi: 10.3389/fnhum.2022.752519

Enhancing Visuospatial Working Memory Performance Using Intermittent Theta-Burst Stimulation Over the Right Dorsolateral Prefrontal Cortex

Ronald Ngetich, Donggang Jin, Wenjuan Li, Bian Song, Junjun Zhang, Zhenlan Jin and Ling Li**

Ministry of Education (MOE) Key Lab for Neuroinformation, High-Field Magnetic Resonance Brain Imaging Key Laboratory of Sichuan Province, Center for Psychiatry and Psychology, School of Life Sciences and Technology, University of Electronic Science and Technology of China, Chengdu, China

OPEN ACCESS

Edited by:
Mingzhou Ding,
University of Florida, United States

Reviewed by:
Lucas Murrins Marques,
University of São Paulo, Brazil
Nathan S. Rose,
University of Notre Dame, United States

***Correspondence:**
Junjun Zhang
jjzhang@uestc.edu.cn
Ling Li
liling@uestc.edu.cn

Specialty section:
This article was submitted to Brain Imaging and Stimulation, a section of the journal Frontiers in Human Neuroscience

Received: *03 August 2021*
Accepted: *24 February 2022*
Published: *17 March 2022*

Citation:
Ngetich R, Jin D, Li W, Song B, Zhang J, Jin Z and Li L (2022) Enhancing Visuospatial Working Memory Performance Using Intermittent Theta-Burst Stimulation Over the Right Dorsolateral Prefrontal Cortex. Front. Hum. Neurosci. 16:752519. doi: 10.3389/fnhum.2022.752519

Noninvasive brain stimulation provides a promising approach for the treatment of neuropsychiatric conditions. Despite the increasing research on the facilitatory effects of this kind of stimulation on the cognitive processes, the majority of the studies have used the standard stimulation approaches such as the transcranial direct current stimulation and the conventional repetitive transcranial magnetic stimulation (rTMS) which seem to be limited in robustness and the duration of the transient effects. However, a recent specialized type of rTMS, theta-burst stimulation (TBS), patterned to mimic the natural cross-frequency coupling of the human brain, may induce robust and longer-lasting effects on cortical activity. Here, we aimed to investigate the effects of the intermittent TBS (iTBS), a facilitatory form of TBS, over the right DLPFC (rDLPFC), a brain area implicated in higher-order cognitive processes, on visuospatial working memory (VSWM) performance. Therefore, iTBS was applied over either the rDLPFC or the vertex of 24 healthy participants, in two separate sessions. We assessed VSWM performance using 2-back and 4-back visuospatial tasks before iTBS (at the baseline (BL), and after the iTBS. Our results indicate that the iTBS over the rDLPFC significantly enhanced VSWM performance in the 2-back task, as measured by the discriminability index and the reaction time. However, the 4-back task performance was not significantly modulated by iTBS. These findings demonstrate that the rDLPFC plays a critical role in VSWM and that iTBS is a safe and effective approach for investigating the causal role of the specific brain areas.

Keywords: working memory, intermittent theta-burst stimulation (iTBS), right dorsolateral prefrontal cortex (rDLPFC), n-back task, neuroplasticity

INTRODUCTION

Working memory (WM) is a daily used and highly researched cognitive domain. In essence, there is a considerably high demand for WM in complex cognitive task processing, but yet it remains a very limited resource (Baddeley, 2003; Luck and Vogel, 2013; Cowan, 2014; Bruning and Lewis-Peacock, 2020). To contextualize this, we need to remember the questions as we actively endeavor

to answer them, we also need to remember patterns and sequences of events to do maths. Therefore, it is arguable that WM is necessary for us to carry out complex cognitive processes such as problem-solving and decision making. WM has been defined as a limited-capacity cognitive system that involves actively but transiently maintaining and manipulating goal-relevant information (Baddeley, 2010; Cowan, 2014; Wang et al., 2019). While WM is considered a pivot for cognitive processing, the dorsolateral prefrontal cortex (DLPFC) is a major region involved in the regulation of crucial cognitive processes ranging from WM, attention, cognitive control, to decision making (Goldman-Rakic, 1995; Cieslik et al., 2013; Taren et al., 2017).

The modulation of working memory (WM) performance has been consistently used in the study and intervention of psychiatric conditions such as schizophrenia and major depressive disorders (Oliveira et al., 2013; Hoy et al., 2016; Gärtner et al., 2018). Whereby, stimulation such as the intermittent theta-burst stimulation (iTBS) and continuous theta-burst stimulation (cTBS) have been applied often over the implicated WM brain areas including the dorsolateral prefrontal cortex (DLPFC), to enhance or inhibit their neural activity, respectively (Plewnia et al., 2014; Chistyakov et al., 2015; Cheng et al., 2016). We, therefore, targeted DLPFC for enhancement using iTBS. Specifically, we stimulated the right middle frontal gyrus (MFG), corresponding to the rDLPFC. Importantly, the findings of the previous studies indicate a possible hemispheric specialization in the processing of the verbal and visuospatial content. In essence, the processing of the visuospatial information has been primarily linked to the right hemisphere, and this also applies to the VSWM (Jonides et al., 1993; Kessels et al., 2000, 2002). In addition, a previous fMRI study found increased activation in the right ventrolateral and frontopolar prefrontal cortex during the performance of the spatial WM task (Manoach et al., 2004). On the other hand, a recent study applying lower frequency rTMS over the right DLPFC found a deterioration in visual working memory (VWM) (Fried et al., 2014). Furthermore, a previous meta-analytic study observed task-specific activations in the prefrontal cortex (PFC), with the verbal content associated with increased activation in the left PFC, whereas the visuospatial material was linked with increased activation in the right PFC (Owen et al., 2005). These converging evidence indicate the laterality of PFC in verbal WM and VSWM, with an indication of specialization of the left PFC in verbal WM and the right PFC in VSWM.

Moreover, previous studies suggest that applying transcranial magnetic stimulation over the DLPFC affects WM performance. For instance, (Oliveri et al., 2001) found that applying single-pulse TMS over bilateral DLPFC disrupts visual-object and VSWM task performance. Another study found an enhancement in verbal digit span and visuospatial 2-back task when high-frequency repetitive TMS (rTMS) was applied over the left DLPFC (Bagherzadeh et al., 2016). Furthermore, the extant literature suggests that continuous theta-burst stimulation (cTBS) over the left DLPFC decreases verbal WM task performance (Schicktanz et al., 2015; Vékony et al., 2018). While, our previous study using the visuospatial n-back task, found that applying cTBS over the right DLPFC impairs performance in a 2-back task (Ngetich et al., 2021). On the other hand, a study using the verbal WM n-back task indicates that iTBS over the left DLPFC enhances working memory performance (Hoy et al., 2015). Taken together, these studies underscore the importance of DLPFC in WM and the effectiveness of TMS in neuromodulation.

To assess the impact of iTBS on VSWM, we administered pre-and post-stimulation 2-back and 4-back VSWM tasks and measured the effect of stimulation based on the d prime (d') scores and the reaction time (RT). We chose iTBS because of its potentiation effect (Huang et al., 2005; Chung et al., 2018a). An outstanding question, however, is how does iTBS modulate VSWM performance? Here, we aimed to establish whether a similar enhancement effect as that reported in Hoy et al. (2015) could be observed in a visuospatial n-back task following iTBS over the rDLPFC. The findings of the present study would greatly contribute to the growing literature on the cognitive effects of TBS over the focal brain areas. Additionally, the evidence that iTBS is efficacious as a treatment complement to pharmacotherapy in refractory neuropsychiatric disorders such as depression (Plewnia et al., 2014; Cheng et al., 2016; Ngetich et al., 2021), makes this study even more crucial.

It is worth noting that theta-burst stimulation (TBS) is a variant of TMS that uses gamma frequency trains applied in the rhythm of theta (thus mimicking theta-gamma coupling involved in the working and the long-term memory processes) (Chung et al., 2018b; Ngetich et al., 2020). The original study by Huang et al. (2005) indicates that TBS consist of a 50 Hz triplet of pulses interspersed at 5 Hz (repeated every 200 ms), and categorizes TBS into three types based on their stimulation patterns. The first type, which has also been applied in the present study is the iTBS. Under this paradigm, a 2 s TBS train is repeated every 10 s for 190 s to obtain a total of 600 pulses per session. The second type is cTBS, which involves a 40 s sustained application of the TBS train (600 pulses). Finally, the third type, intermediate theta-burst stimulation (imTBS) consists of a 5 s TBS train repeated every 15 s for 110 s to yield 600 pulses per session. According to the aforementioned study which is based on the motor cortex, iTBS led to increased motor evoked potential (MEP), while cTBS decreased the MEP, with no significant effect on MEP after imTBS of the motor cortex (Huang et al., 2005). These findings have considerably influenced the neuromodulation studies and intervention, with TBS currently used to investigate the functional roles of brain areas beyond the motor cortex, and importantly, it has been incorporated into the therapeutic approaches for psychiatric conditions.

Furthermore, the various TBS paradigms, especially iTBS and cTBS are associated with varied effects on neuronal activity. It should be noted that the mammalian brain consists of intricately interconnected neurons and synapses. This intricate but flexible neuronal network can be regulated by the plastic nature of the inter-neuron synaptic transmissions (Li et al., 2019). Importantly, the two main long-term manifestations of synaptic plasticity, long-term potentiation (LTP), and long-term depression (LTD) are instigated by postsynaptic Ca^{2+} changes in concentration (Blitzer et al., 2005). Therefore, it is anticipated that iTBS, which consists of short intermittent trains of bursts, results in excitation

related to a temporary influx of Ca^{2+} and leads to an LTP-like effect. Conversely, cTBS train application facilitates an intensified inter-neuron depression effect through a sustained influx of Ca^{2+}, and in the process, it overpowers the excitatory impact and causes an LTD-like effect (Huang et al., 2011).

However, despite its efficacy in the treatment of neuropsychiatric conditions, a small number of healthy-participant studies including Chung et al. (2018b) have found no significant behavioral impact of iTBS when applied over DLPFC. Interestingly, previous studies have found mixed results, where some studies suggest both iTBS related WM behavioral enhancement alongside the neurophysiological modulation of implicated brain areas (altered inter-regional connectivity) (Hoy et al., 2015). While some studies only demonstrate the neurophysiological effect of iTBS with no significant effect on behavioral performance (Chung et al., 2018b). More studies are thus required to verify whether the iTBS cortical modulation necessarily potentiates behavioral performance. Since most studies indicate that iTBS upregulate cortical activity (Wischnewski and Schutter, 2015; Chung et al., 2017, 2018a,b; Lowe et al., 2018) and DLPFC is implicated in WM (Rottschy et al., 2012; Hoy et al., 2015; Vékony et al., 2018; Ngetich et al., 2021), the present study sought to establish the behavioral impact of iTBS over the rDLPFC on VSWM.

MATERIALS AND METHODS

Participants

Participants were recruited from the undergraduate students of the University of Science and Technology of China (UESTC). To be included in the study, the participants had to be healthy and right-handed [handedness was assessed using Edinburgh Handedness Inventory (Oldfield, 1971)], with normal or corrected to normal eyesight. Exclusion criteria included neurological or psychological illness or history of neuropsychiatric disorders, drug and substance abuse, left-handedness, inability to give informed consent, and having brain ferromagnetic implants. A total of 26 subjects were recruited. However, 2 participants had incomplete data as they could not attend all the sessions due to personal reasons, therefore, they were excluded from the experiment. Ultimately, the data of 24 participants (15 males, M_{age} = 22.25, SD_{age} = 1.6) were included in our analysis. All the experimental procedures adhered to the declaration of Helsinki and were approved by the ethics board of the UESTC.

Procedure

The experiment consisted of 3 sessions, with the second and third sessions separated by a wash-out period of 7 days between them as described in **Figure 1**. All the participants attended all sessions. During the first session, the participants were screened on their eligibility, had their T1-weighted MRI images acquired, and active motor threshold (AMT) estimated. In the second session, the participants performed the baseline (BL) n-back task before receiving iTBS over either the vertex or the rDLPFC. Following the stimulation, the participants performed an n-back task. The third session was conducted a week after the second session, during which the participants received stimulation over the alternate site to that of the second session, and thereafter performed n-back task. In both stimulation sessions (second and third), iTBS was followed by a 5 min break before the behavioral task performance which lasted for approximately 10 min. The order of stimulation was counterbalanced between the subjects. Also, the order of *n*-values for the task was different for each session, i.e., session two could be 4-2-4-2-4-2 and session three could be 2-4-2-4-2-4 but was the same for each participant. The visuospatial n-back task experiment was designed using the E-Prime 2.0 (Psychology Software Tools, Pittsburgh, PA, United States). It consisted of the blue square presented on a black background computer screen with a resolution of 1,024 × 768 and a refresh rate of 60 Hz, at eight different random positions as shown in **Figure 1**.

Moreover, all participants received the same intensity of iTBS, that is, a uniform stimulation of 40% of the maximal machine output (MSO) was administered to either the rDLPFC or the vertex. For this reason, the purpose of measuring the AMT of each participant was to ensure that 40% of MSO did not surpass the individual's stimulation tolerance level and hence enhanced participants' safety. Besides, the application of uniform stimulation intensity is consistent with the previous studies including Ott et al. (2011); Vékony et al. (2018), and our recent cTBS study (Ngetich et al., 2021). All the participants gave written informed consent before they began the experiment and were given monetary compensation at the end of the experiment.

Theta-Burst Stimulation and Neuronavigation

The participants received iTBS to either the rDLPFC or vertex in 2 separate sessions, with the site of stimulation counterbalanced across all the participants. This means 12 participants received stimulation over rDLPFC, and the other half received stimulation over the vertex in the second session. In the third session, participants who were stimulated over the rDLPFC in the second session, received vertex iTBS and vice versa.

TBS was administered using a figure-of-eight magnetic coil with an outer diameter of 70 mm (Magstim Company Ltd., Whitland, Wales, United Kingdom). The iTBS procedure adopted was similar to the one described in Huang et al. (2005), with a 2 s triplet of gamma frequency pulses (50 Hz) applied at a theta rhythm (5 Hz) repeated every 10 s for 190 s to yield a total of 600 pulses. This kind of stimulation design has been found to potentiate the neural activity not only when applied over the motor cortex (Huang et al., 2005) but also over other brain areas including the DLPFC (Hoy et al., 2015). Moreover, a uniform stimulation intensity of 40% of the maximal machine output was used for all participants. This was informed by the limitation in the stimulator's maximal TBS intensity. Nevertheless, applying uniform stimulation intensity has been used previously to study the functional roles of different cortical brain areas (Ott et al., 2011; Kiyonaga et al., 2014; Vékony et al., 2018; Ngetich et al., 2021). The MNI coordinates (x = 43, y = 41, and z = 34) for the rDLPFC were similar to those used by

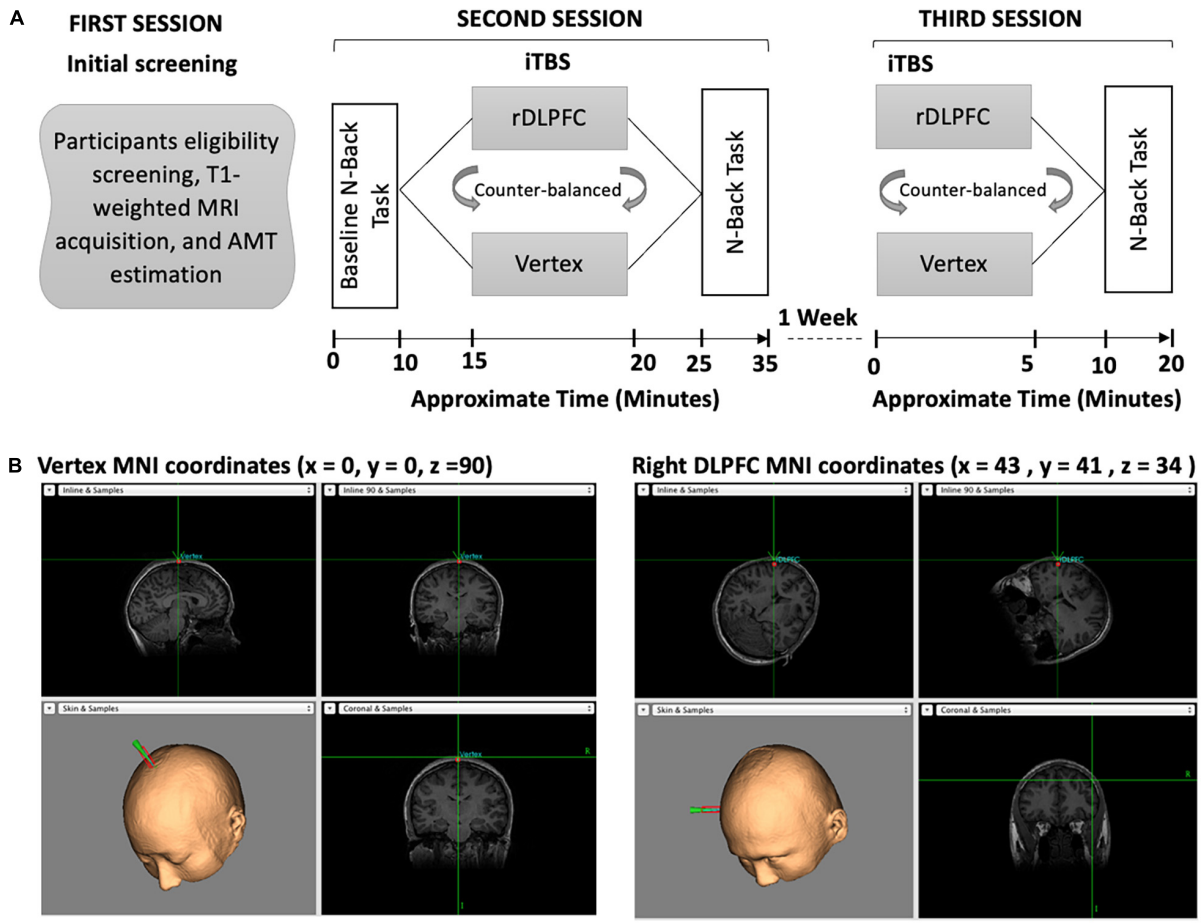

FIGURE 1 | (A) Overview of the experimental paradigm. Our experiment consisted of three separate sessions. During the first session, the participants were screened on eligibility, had their T1-weighted images acquired, and AMT estimated. In the second session, participants performed the baseline n-back task followed by iTBS and then the post-stimulation n-back task. In the third session, the participants received iTBS and performed the post-stimulation n-back task. **(B)** The iTBS target brain areas, the vertex and the Rdlpfc, respectively.

Fried et al. (2014), which correspond to the right middle frontal gyrus (Petrides, 2019). These coordinates were chosen based on the successful modulation of spatial WM task performance using lower intensity rTMS over this specific region in the aforementioned study (Fried et al., 2014).

To control for the iTBS effect over the rDLPFC on VSWM, we used vertex as a control site. The iTBS similar to that of the rDLPFC was applied over the vertex of each participant, located at (x = 0, y = 0, and z = 90) coordinates, corresponding to the midpoint between the inion and nasion. Before applying iTBS, we obtained AMT for each participant to ensure that our stimulation was tolerable and safe for all participants. This was done only in the first session of each participant. The AMT was defined as the minimum most intensity over the right primary motor cortex required to elicit visible movement of the left first index finger in 5 $\geq$ out of 10 probes. During the AMT estimation, the participants were instructed to maintain a steady muscle contraction at 20% of the maximal voluntary contraction. However, some TBS studies have used electromyography (EMG) to determine an individual's motor threshold, a method that has the advantage of providing a quantitative measure of muscle response (Westin et al., 2014). The participants were also instructed to report any discomfort during the stimulation, but there was no report of discomfort from any of them.

To accurately target the stimulation sites, and continuously monitor the position and the orientation of the coil, we used neuronavigation. This was achieved by first co-registering normalized MNI brain to each of the participant's T1-weighted structural magnetic resonance imaging (MRI) using the Brainsight frameless stereotaxic neuronavigation system (Rogue Research, Montreal, QC, Canada). The T1- weighted images were acquired using a 3.0-Tesla GE Sigma scanner with an 8-channel head coil. During the iTBS, the figure-of-eight coil was placed on the specific site over individuals' scalp.

Visuospatial Working Memory Task

In the present study, we used a visuospatial n-back paradigm previously used in our recent cTBS study (Ngetich et al., 2021) and initially modified from the original version of Carlson et al.

(1998). The experimental task consisted of a run of 6 blocks, with 3 blocks each for 2-back and 4-back tasks. Each block had (20+n) trials with six visual targets. The participants were required to respond with a keypress when the position of one of the presented stimuli matched that of the previous nth position presented in the sequence. That is two positions or four positions back for 2-back and 4-back tasks, respectively. For the matched stimuli, the participants were instructed to respond by pressing a key "2" on the numeric keypad of a standard keyboard, and not to react if there was no match. At the beginning of every block, the participants were informed whether the current task is a 2-back or 4-back task. Each session lasted for approximately 10 min and the order of n-values for the task was different for each session, i.e., session one could be 4-2-4-2-4-2 and session two could be 2-4-2-4-2-4 but was the same for each participant. The visuospatial n-back task involved the presentation of blues squares on a black background computer screen with a resolution of 1,024 × 768 and a refresh rate of 60 Hz, at eight different random positions (top, bottom, left, right, top left, top right, bottom left, bottom right, bottom right of the central cross), with each trial lasting for 3 s (stimulus duration of 500 ms, and stimulus interval of 2,500 ms) (for detailed illustration, see **Figure 2**).

Statistical Analyses

The statistical analyses were performed using IBM SPSS 23.0 software. Each Individual's accuracy (ACC) scores and reaction times (RTs) were used to evaluate VSWM performance. Based on findings of the previous WM study (Hoy et al., 2015), and those of a study on the effects of iTBS over the primary motor cortex on motor evoked potentials (MEPs) (Huang et al., 2005), we anticipated that iTBS over the rDLPFC would enhance VSWM performance, relative to vertex stimulation and the baseline. To assess whether the iTBS over rDLPFC affected VSWM performance relative to vertex stimulation, and the baseline (pre-stimulation), we analyzed the participants' accuracy and the reaction times (RTs).

First, to assess accuracy performance, a 2 × 3 within-subject repeated measure ANOVA (RM-ANOVA), with load (2back vs. 4-back) and stimulation condition (BL vs. Vertex vs. rDLPFC) as within-subject factors. The accuracy was measured in terms of discriminability index, d prime (d'). The d' scores were computed from the hit rates (H) and false alarm (FA) rates using the formula: $d' = Z(H) - Z(FA)$, where Z represents the transformation of the two distributions, and therefore, makes it possible to differentiate measures with dissimilar ranges of the absolute values (Haatveit et al., 2010). It should be noted that d' is an effective and efficient measure of WM performance as it is independent of the response bias (John Irwin et al., 2001).

Subsequently, we evaluated the iTBS effect on the accuracy. The iTBS effect on accuracy performance was considered as the difference between the post-stimulation (rDLPFC and vertex), and the pre-stimulation (baseline) d' scores. Therefore, we subtracted an individual's mean baseline from the post-stimulation mean d' scores to get the net effect of iTBS on accuracy (δd' scores). Thereafter, we conducted a 2 × 2 RM-ANOVA with Load (2-back vs. 4-back) and site (vertex vs. rDLPFC) as within-subject factors.

We also conducted a 2 (group: sub vs. supra) * 2 (stimulation: DLPFC vs. vertex) *2 (load: 2 vs. 4-back) ANOVA to ascertain whether the application of lower stimulation (subthreshold) affected VSWM performance differently compared to higher stimulation (suprathreshold). What constitutes sub and suprathreshold in TBS remains indeterminate. While most studies have shown that 80% of AMT is sufficient to modulate cognitive performance when applied over implicated brain areas (Ko et al., 2008; Cho et al., 2010; Ott et al., 2011; Li et al., 2014; Hoy et al., 2015; Mcneill et al., 2018; Pestalozzi et al., 2020), one recent study exploring the efficacy of sub and suprathreshold stimulation in the treatment of Major Depressive Disorder used iTBS of 80% AMT as subthreshold, and 120% AMT as suprathreshold (Lee et al., 2021). However, in the present analysis, we considered stimulation < 80% of AMT as subthreshold, and that > 80% AMT as suprathreshold. Therefore, 10 of the participants were categorized into the subthreshold group and 14 into the suprathreshold group.

Following the accuracy analyses, we compared the individual's RTs under different loads (2-back vs. 4-back), and stimulation conditions (RTs at BL, and after iTBS over the vertex, and the rDLPFC). Similar to the ACC analysis, we conducted a 2 × 3 within-subject RM-ANOVA, with load (2-back vs. 4-back) and stimulation condition (BL vs. vertex vs. rDLPFC) being the within-subject factors. Only the RTs of the correct responses were included in our analysis. We also conducted a correlation analysis to assess whether the BL performance predicted the stimulation effect, both on the d' and the mean RTs. In this analysis, the stimulation effect was considered as the difference between the performance after the rDLPFC and the vertex iTBS (i.e., d'(rDLPFC)—d' (vertex) for d' and mean RTs (rDLPFC)—mean RTs (vertex).

Finally, *post-hoc* paired *t*-test analyses for ACC and the RTs were conducted to identify the source of significant effects (both main and interaction effects). In addition, paired sample *t*-test was conducted to evaluate the effect of counterbalancing on performance. Importantly, Bonferroni correction was applied for multiple comparisons.

RESULTS

Accuracy Performance

Firstly, we performed a two-way repeated measure ANOVA for d' scores to assess the WM performance under different loads and stimulation conditions. As expected, we found a significant main effect of load [$F_{(1,\ 23)} = 93.468$, $p < 0.0001$, $\eta_p^2 = 0.803$], and a significant main effect of stimulation condition [$F_{(2,\ 22)} = 10.641$, $p < 0.001$, $\eta_p^2 = 0.492$]. This suggests that VSWM performance was modulated by both the cognitive load (i.e., 2-back and 4-back), and the stimulation condition (i.e., BL and iTBS over either rDLPFC or vertex). Besides, there was also a significant interaction effect between load and stimulation condition [$F_{(2,\ 22)} = 3.84$, $p = 0.048$, $\eta_p^2 = 0.241$].

To determine the source of the effects, we performed a 2-tailed paired *t*-test *post-hoc* test. Since we were mainly interested in the

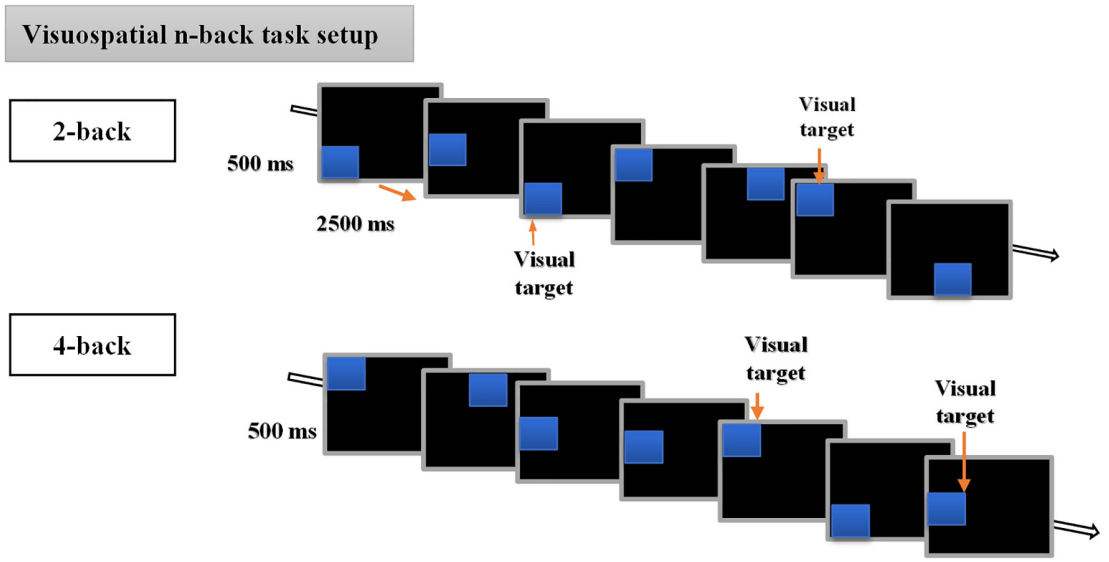

FIGURE 2 | Description of the visuospatial n-back task. The behavioral n-back task consisted of 2-back and 4-back tasks.

effects of iTBS stimulation on VSWM performance, we compared the same load performances between different stimulation conditions (i.e., at BL, and after iTBS over the rDLPFC or the vertex control). Interestingly, VSWM performance was only enhanced in 2-back, and only after iTBS over the rDLPFC. In particular, the 2-back task performance after iTBS over the rDLPFC was significantly better than that at BL [$t_{(23)} = 4.961$, $p < 0.0001$], and after iTBS over the vertex [$t(23) = -2.809$, $p = 0.01$] as illustrated in **Figure 3A**. Unexpectedly, the 2-back performance after the iTBS of the vertex was also significantly better than the BL [$t_{(23)} = -3.046$, $p = 0.006$]. This indicates a possibility of practice effects. However, there was no statistically significant difference in performance in the 4-back task between the BL, and after the stimulation over the rDLPFC [$t_{(23)} = -1.901$, $p = 0.07$], or the vertex [$t_{(23)} = -1.502$, $p = 0.147$]. Similarly, the 4-back task performance did not vary after either the stimulation over the rDLPFC or the vertex [$t_{(23)} = -0.447$, $p = 0.659$]. The lack of improvement in task performance in 4-back may reflect the complexity of non-invasively modulating higher load tasks.

Furthermore, to evaluate the actual effect of the stimulation, we conducted a two-way RM-ANOVA for δd' scores. The δd' scores were obtained by subtracting the BL d' scores from the post-stimulation scores (i.e., d' scores following iTBS over the rDLPFC or the vertex). This was done for both 2-back and 4-back tasks. Our analysis indicated a significant main effect of load [$F_{(1,\ 23)} = 4.216$, $p = 0.05$, $\eta_p^2 = 0.155$], and stimulation site [$F_{(1,\ 23)} = 5.652$, $p = 0.026$, $\eta_p^2 = 0.197$]. However, there was no significant interaction effect between load and site [$F_{(1,\ 23)} = 3.192$, $p = 0.087$, $\eta_p^2 = 0.122$]. Further *post-hoc* analyses showed that the stimulation over the rDLPFC caused a significantly larger effect on 2-back task performance as compared to that over the vertex [$t_{(23)} = -2.809$, $p = 0.01$] as shown in **Figure 3B**. This suggests a causal role of the rDLPFC in VSWM. Conversely, there was no significant difference between the stimulation effect on d' scores after the iTBS over the rDLPFC and the vertex in the 4-back task [$t_{(23)} = -0.45$, $p = 0.66$]. Therefore, it may be deduced that the stimulation did not significantly modulate the higher load task.

Besides, the mixed ANOVA for the participants who received sub and suprathreshold yielded a significant main effect of load [$F_{(1,\ 22)} = 4.927$, $p = 0.037$, $\eta_p^2 = 0.183$] and a main effect of stimulation [$F_{(1,22)} = 4.902$, $p = 0.037$, $\eta_p^2 = 0.182$]. There was no other significant main effect or interaction. *Post hoc* analysis showed a group difference, with better performance in 2-back task following iTBS over vertex in subthreshold group as compared to the suprathreshold group [$t_{(22)} = 3.530$, $p = 0.002$]. There were no other group differences.

Additionally, we conducted a paired sample *t*-test analysis to evaluate the effect of counterbalancing. Our analysis did not find significant difference in d' between the participants who received the iTBS over the right DLPFC in the two separate sessions, either in 2-back [$t_{(11)} = 0.066$, $p = 0.949$] or 4-back [$t_{(11)} = 0.008$, $p = 0.994$]. There was also no significant difference in d' between those who were stimulated over the vertex in separate sessions, both in 2-back [$t_{(11)} = 0.580$, $p = 0.573$] and 4-back [$t_{(11)} = 0.855$, $p = 0.411$].

Reaction Time

We conducted a two-way RM-ANOVA to evaluate the RT performance under different WM loads and stimulation conditions. Our analysis found a significant main effect of load [$F_{(1,\ 23)} = 27.532$, $p < 0.0001$, $\eta_p^2 = 0.545$]. There was also a significant main effect of stimulation condition [$F_{(2,\ 22)} = 6.215$, $p = 0.007$, $\eta_p^2 = 0.361$]. However, there was no significant interaction effect [$F_{(2,\ 22)} = 0.073$, $p = 0.93$, $\eta_p^2 = 0.007$].

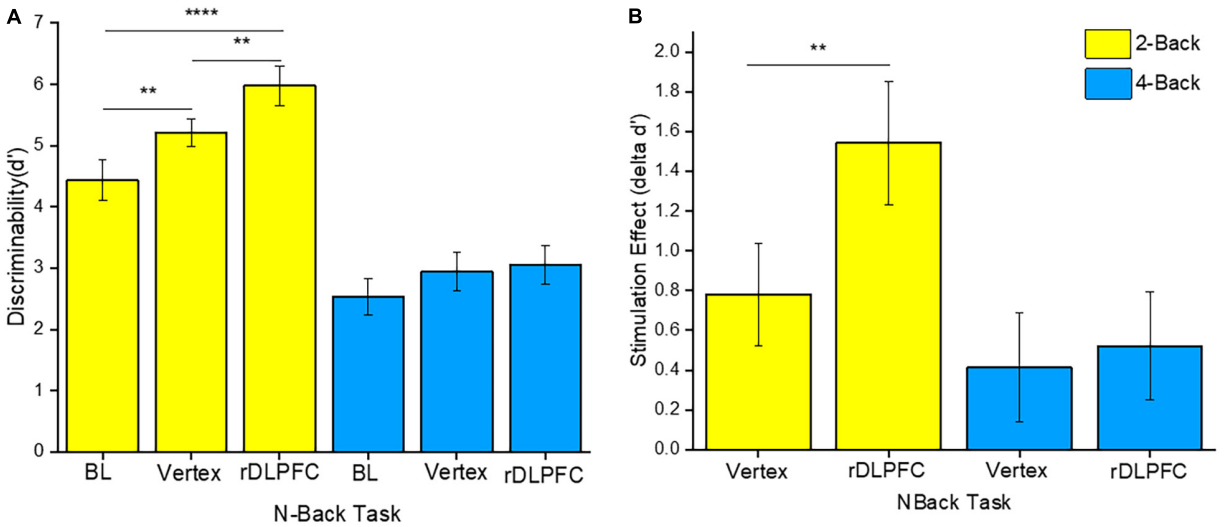

FIGURE 3 | (A) Discriminability index for both 2-back and 4-back tasks under different stimulation conditions, namely: Baseline (BL), iTBS over the vertex, and iTBS over the rDLPFC. **(B)** The stimulation effect (δd' scores). The stimulation effect was obtained by subtracting the BL scores from the post-stimulation scores. The yellow and the blue colors refer to the 2-back and 4-back tasks, respectively. The asterisks indicate the level of significance, with ** indicating $p \leq 0.01$, and **** indicating $p \leq 0.0001$. The errors bars indicate the standard mean error (SME).

To identify the source of the main effects, we performed 2-tailed paired *t*-tests. Similar to the accuracy analysis, we compared the same load n-back task RTs between different stimulation conditions. The *post-hoc* tests indicated that the response speed was significantly faster in the 2-back task after iTBS over the rDLPFC as compared to that at the BL [$t_{(23)} = 3.768$, $p < 0.001$]. Other 2-back tasks mean RTs comparisons did not reach significance, with no significant difference between the RTs at BL and after vertex stimulation [$t_{(23)} = 1.78$, $p = 0.85$], nor between the performance after the stimulation over either vertex or DLPFC [$t_{(23)} = 1.948$, $p = 0.64$]. Moreover, there was no statistically significant difference between the 4-back mean RTs across all the stimulation conditions. The RTs at BL were not significantly different from those after the rDLPFC [$t_{(23)} = 1.942$, $p = 0.061$] and vertex [$t_{(23)} = 1.121$, $p = 0.274$]. While there was also no significant difference following the stimulation over either the vertex or the rDLPFC [$t_{(23)} = 1.443$, $p = 0.163$]. **Figure 4** clearly illustrates the mean RTs performance.

Finally, we performed a Pearson correlation for baseline performance and the effects of iTBS. However, none of the correlations was significant. The Pearson correlation indicated a lack of significant positive association between the baseline and the post-stimulation d' both in 2-back ($r = 0.133$, $p = 0.535$) and 4-back ($r = 0.027$, $p = 0.90$) tasks. Also, there was no positive association between baseline and post-stimulation performance RT, both in 2-back ($r = 0.068$, $p = 0.751$) and 4-back ($r = 0.092$, $p = 0.668$) tasks. Nevertheless, a recent study has shown that BL performance level together with pre-stimulation brain state may influence the behavioral impact of TMS (Silvanto et al., 2018). Therefore, TMS studies should evaluate this factor to clearly understand the TMS effect over a targeted brain area on human behavior.

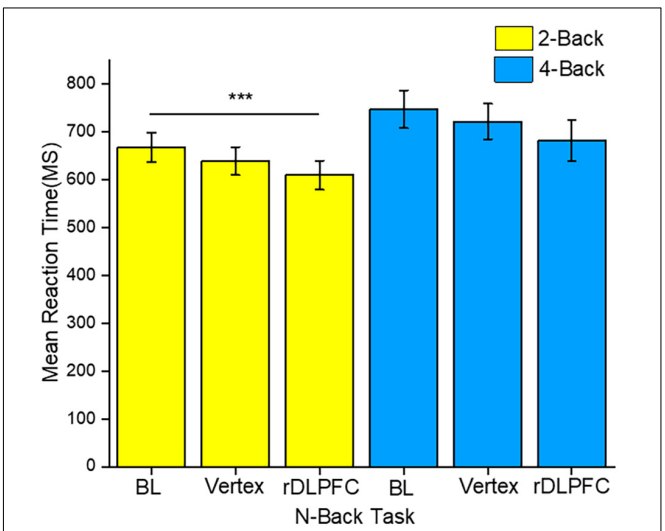

FIGURE 4 | The reaction time (RT) performance for both 2-back and 4-back tasks. The yellow and blue colors indicate 2-back and 4-back tasks, respectively. The asterisks indicate the level of significance, with *** indicating $p \leq 0.001$. The errors bars indicate the standard mean error (SME).

DISCUSSION

In the present study, we investigated the causal role of the rDLPFC on VSWM performance. To achieve this, we applied iTBS over the rDLPFC, and the vertex (control site). The impact of iTBS on VSWM was evaluated by comparing the n-back task performance at the BL with that after the stimulation over either the rDLPFC or the vertex. Notably, the VSWM task consisted of medium (2-back) and higher load (4-back) visuospatial n-back

tasks. Our results indicate that iTBS over the rDLPFC improved visuospatial task performance in 2-back, but not in 4-back tasks. Specifically, iTBS over this target brain area was associated with increased accuracy performance in the medium load task as compared to the performance both at the BL and after the stimulation over the vertex control. However, task performance after the stimulation over the vertex was also significantly better than the BL performance. Indicating a potential practice effect on the accuracy performance. Besides, iTBS over the rDLPFC improved the RT in the 2-back task relative to the BL RT. This notwithstanding, the higher load task performance (both accuracy and RT) was not significantly impacted by the iTBS.

The enhancement of VSWM following iTBS over the rDLPFC was expected, given the importance of DLPFC in WM and the effectiveness of TBS in neuromodulation. Indeed, several studies have established that DLPFC plays a key role in the WM processes (Hoy et al., 2015; Schicktanz et al., 2015; Chung et al., 2018b; Ngetich et al., 2021). In our recent study, we applied cTBS over the same brain area as the present study and observed impairment in the visuospatial 2-back task, which indicates a contrasting effect of cTBS and iTBS when applied over the rDLPFC. Besides, a recent study by Hoy et al. (2015) applied iTBS over the left DLPFC and administered a verbal WM n-back task to assess the stimulation over this area on the WM performance. They found a significantly improved performance in the 2-back task and not in the 3-back task, after the iTBS over the left DLPFC. More importantly, the aforementioned study found that iTBS was associated with an increase in the frontoparietal connectivity, and more so, prominent parietal gamma power relative to the sham stimulation (Hoy et al., 2015).

Furthermore, a recent study investigating inter-and intra-individual iTBS variability, indicates that iTBS induces robust and relatively consistent cortical modulation effects within and between individuals (Hinder et al., 2014). Perhaps this makes it suitable for both research and clinical application. While recent review and meta-analytic studies alongside the earlier reviewed studies indicate that non-invasive brain stimulation over the DLPFC influences WM task performance (Brunoni and Vanderhasselt, 2014; Lowe et al., 2018; Widhalm and Rose, 2019). It is, therefore, interesting to observe that iTBS over the rDLPFC in the present study led to enhancement in VSWM performance. As mentioned earlier, there is evidence suggesting hemispheric specialization in the processing of verbal and visuospatial information. In particular, the right hemisphere has been reported to be involved in the processing of the visuospatial content (Jonides et al., 1993; Kessels et al., 2000), while the processing of the verbal information has been primarily linked to the left hemisphere (Fried et al., 2014). Therefore, the reported effect in our study is in line with the previous studies and supports the role of the right hemisphere, especially the right DLPFC in VSWM.

Moreover, it should be noted that the strength of the frontoparietal network has been positively correlated with the WM performance both in healthy participants (Nee and Brown, 2013) and patients (Figueroa-Vargas et al., 2020). While high gamma power over the peak but not the trough has been found to boost memory performance (Alekseichuk et al., 2016). Despite not collecting electrophysiological or imaging data, it is deducible from the previous studies that perhaps, iTBS over the rDLPFC significantly improved the frontoparietal connectivity and thus enhanced VSWM performance.

The lack of a significant performance enhancement in the 4-back task in the present study can be attributed to some key factors. Firstly, it is likely that the participants were already performing close to or at their highest possible levels. This does not necessarily imply that the VSWM performance itself was already near the maximum possible levels, but perhaps the participants' abilities to perform the higher load task were already stretched to the limits. Therefore, despite the facilitatory effect of iTBS, the significant enhancement in cognitive processing could not modulate the "ceiling performance". Importantly, the extent of facilitation associated with the stimulation, especially in healthy participants, cannot surpass an individual's natural potential (Hoy et al., 2015). Secondly, it is possible that since the cognitive processing resources are directed naturally toward a relatively complex high-load task, iTBS may not significantly potentiate its already optimized performance. Interestingly, high load task is associated with the deactivation of the default mode network (DMN) (Mckiernan et al., 2003; Thomason et al., 2009), increased activation, particularly in the key brain areas such as the frontoparietal (Tomasi et al., 2008), and generally decreased distractibility (Sörqvist et al., 2016). Therefore, it is expected that the aforementioned occurrences may facilitate the reduction of error rate and the realization of the optimal level performance that may not be significantly improved further by the iTBS.

Additionally, the observed iTBS effect only in 2-back and the lack of it in 4-back tasks may also be explained by a phenomenon called stochastic resonance. This phenomenon is characterized by beneficial effects of unpredictable fluctuations such as facilitation of the response to a weak signal by random noise (Stocks, 2000; McDonnell and Abbott, 2009; Romei et al., 2016). Stochastic resonance has been intensely studied and quantified in several physical and biological systems such as neurons (Stocks, 2000; McDonnell and Abbott, 2009). Recently, a study by Silvanto and Cattaneo (2017) established that varying TMS intensities affect neural firing differently. In particular, the aforementioned study suggests that low-intensity TMS enhances early neural firing while higher intensity suppresses it (Silvanto and Cattaneo, 2017). Considering that the AMT varied from one participant to another in the present study, it is likely that administering iTBS at a uniform intensity of 40% of the MSO for all participants might have led to a situation where some participants received sub or suprathreshold stimulation (corresponding to individual's AMT). And since an earlier study (Silvanto et al., 2007) found that TMS reactivated WM for weak representations, it is possible that the subthreshold stimulation preferentially improved the performance in the lower load VSWM tasks (2-back). In particular, despite our analysis finding better performance in 2-back only following vertex stimulation in subthreshold compared to a suprathreshold group, such finding is an important indicator

of the possible stochastic resonance effect, as there were no observable significant differences in 4-back tasks between the two groups. The significant main effect of group is also an important pointer to how performance can be affected differently by sub and suprathreshold stimulation intensities. Therefore, future iTBS studies should use a larger sample size to elucidate the potential impact of this phenomenon on cognitive task performance.

More importantly, our findings demonstrate that iTBS enhances behavioral performance, thus adding to the critical evidence suggesting that the modulatory effects of iTBS extend beyond the motor cortex (Hoy et al., 2015; Chung et al., 2018b). This is especially interesting since our recent study found that cTBS over the rDLPFC impairs VSWM performance (Ngetich et al., 2021), which is opposite to the results of the present study. Also, other studies have consistently found an impairment of verbal WM performance by cTBS of the DLPFC (Schicktanz et al., 2015; Vékony et al., 2018; Ngetich et al., 2021). As we discussed earlier, the original study by Huang et al. (2005) found that iTBS over the primary motor cortex significantly increased motor evoked potentials (MEPs), while cTBS over the same brain area decreased the MEPs.

Therefore, does it necessarily mean that iTBS over the neural cortex enhances cognitive performance while the cTBS decreases it? The evidence suggests otherwise. Apart, from individuals' factors such as age, sex, and endogenous brain oscillations (Ridding and Ziemann, 2010), other specific factors such as (1) the cognitive task, and (2) the functional role of the targeted brain area, influence the direction of behavioral effects associated with TBS (Ngetich et al., 2020). Whereas iTBS generally facilitates neural activity, while cTBS inhibits it (Huang et al., 2005, 2011; Li et al., 2019), the behavioral outcome may vary accordingly. For instance, Kaller et al. (2011) found a functional dissociation between the right and the left DLPFC in planning. In particular, cTBS over the left DLPFC resulted in global acceleration, while that of the right led to global deceleration of the planning processes (Kaller et al., 2011). Therefore, it may be argued that the inhibition of the neural activity of the left DLPFC led to suppression of other competing cognitive processes, and thus enhancement of the cognitive performance. This phenomenon has been termed as addition by subtraction (Luber and Lisanby, 2014). Such behavioral effects that are negatively correlated with the size of the neural activity pose an interesting challenge to the clinical application of the TBS. In essence, it is imperative to understand the cognitive deficiencies associated with specific mental health conditions, and specific neurophysiological modulation occasioned by a particular psychiatric condition. For instance, the hyperactivity and hypoactivity of the right and left DLPFC, respectively, in medication-resistant depression necessitates the application of cTBS over the rDLPFC and iTBS to the left when using a combined cTBS + iTBS treatment protocol (Li et al., 2014). Similarly, findings regarding the brain areas significantly involved in VSWM could be beneficial in the treatment of psychiatric conditions characterized by the deficiency of this cognitive process, like schizophrenia (Cocchi et al., 2009).

Nevertheless, the possible influence of the practice effects in the present study makes it necessary to interpret our findings with caution. Despite our attempt to limit practice effects by using different series of VSWM n-back tasks for different sessions, it still exerted its influence on the performance. Although the accuracy performance in the 2-back task was significantly better after iTBS over the rDLPFC than that at the BL and following iTBS of the vertex, the fact that the performance after vertex stimulation was significantly better than the BL performance, suggests that the practice effects influenced VSWM performance. Interestingly, in our previous cTBS study, the practice effects were not apparent (Ngetich et al., 2021), suggesting that while cTBS may suppress practice effects (Vékony et al., 2018), iTBS may not significantly modulate them. However, the influence of practice effects on cognitive task performance is not generally unexpected. One recent study has shown that a repeated practice with a specific task, even when using different sets of stimuli necessarily results in an enhancement of the subsequent task performance (Dutilh et al., 2011). Furthermore, other related studies have reported the possible influence of practice effects on cognitive task performance (Hoy et al., 2015; Vékony et al., 2018). This notwithstanding, the apparent practice effects did not entirely affect the observation of the impact of iTBS on VSWM.

Moreover, the BL performance was only assessed in the second session, and thus it may not be possible to ascertain the level of BL performance in the third session. Therefore, future studies should consider evaluating BL performance in all stimulation sessions to measure the stimulation effect and to balance the number of tasks across the different sessions. Also, the stimulation was applied at a uniform stimulation intensity of 40% of the MSO. Therefore, since motor thresholds may vary from one individual to another, the stimulation intensity should be adapted to individuals' MTs to ensure uniform stimulation for all participants. Finally, the other limitation of the present study lies in the use of only behavioral tests. This is despite the previous studies including (Polanía et al., 2018) suggesting that it is possible to integrate non-invasive brain stimulation (NIBS) with other techniques such as EEG and fMRI. Thus, future related studies should integrate TBS with EEG or fMRI to determine the most crucial frequency to target and electrophysiological effects of TBS, and to assess the functional connectivity associated with VSWM and the modulation of such connectivity by TBS, respectively. Notably, Romei et al. (2016) suggest that NIBS can be enhanced through rhythmic TMS, which target endogenous neural oscillations via entrainment or phase cancelation.

In conclusion, we have demonstrated that iTBS over the rDLPFC improves VSWM performance. Our findings suggest that the aforementioned brain area plays an important role in VSWM, and that iTBS is a safe and effective technique for investigating the causal role of the specific brain areas. Overall, the present study contributes to the understanding of the modulatory effects of TBS and may have a clinical application, especially in the modeling of the brain stimulation treatment

intervention for neuropsychiatric conditions associated with the deficits in the VSWM.

DATA AVAILABILITY STATEMENT

The raw data supporting the conclusions of this article will be made available by the authors, without undue reservation.

ETHICS STATEMENT

The studies involving human participants were reviewed and approved by the Committee for the Protection of Human Subjects of the University of Electronic Science and Technology of China (UESTC). The patients/participants provided their written informed consent to participate in this study.

AUTHOR CONTRIBUTIONS

RN, JZ, ZJ, and LL conceived and designed the experiments. RN, DJ, and BS performed the experiments. RN and WL analyzed the data. RN wrote the manuscript. All authors reviewed the manuscript.

FUNDING

This work was supported by grants from NSFC (grant nos. 61773092, 61673087, 61773096), the Sichuan Province Science and Technology Support Program (grant no. 2020YFS0230), the Higher Education Discipline Innovation Project (111 project, grant no. B12027), and the Fundamental Research Funds for the Central Universities.

REFERENCES

Alekseichuk, I., Turi, Z., de Lara, G. A., Antal, A., and Paulus, W. (2016). Spatial working memory in humans depends on theta and high gamma synchronization in the prefrontal cortex. *Curr. Biol.* 26, 1513–1521. doi: 10.1016/j.cub.2016.04.035

Baddeley, A. (2003). Working memory: looking back and looking forward. *Nat. Rev. Neurosci.* 4, 829–839. doi: 10.1038/nrn1201

Baddeley, A. (2010). Working memory- A Primer. *Curr. Biol.* 20, 136–140. doi: 10.1016/J.CUB.2009.12.014

Bagherzadeh, Y., Khorrami, A., Zarrindast, M. R., Shariat, S. V., and Pantazis, D. (2016). Repetitive transcranial magnetic stimulation of the dorsolateral prefrontal cortex enhances working memory. *Exp. Brain Res.* 234, 1807–1818. doi: 10.1007/s00221-016-4580-1

Blitzer, R. D., Iyengar, R., and Landau, E. M. (2005). Postsynaptic signaling networks: cellular cogwheels underlying long-term plasticity. *Biol. Psychiatry* 57, 113–119. doi: 10.1016/j.biopsych.2004.02.031

Bruning, A. L., and Lewis-Peacock, J. A. (2020). Long-term memory guides resource allocation in working memory. *Sci. Rep.* 10:22161. doi: 10.1038/s41598-020-79108-1

Brunoni, A. R., and Vanderhasselt, M. A. (2014). Working memory improvement with non-invasive brain stimulation of the dorsolateral prefrontal cortex: a systematic review and meta-analysis. *Brain Cogn.* 86, 1–9. doi: 10.1016/j.bandc.2014.01.008

Carlson, S., Martinkauppi, S., Rämä, P., Salli, E., and Korvenoja, A. (1998). Distribution of cortical activation during visuospatial n -back tasks as revealed by functional magnetic resonance imaging. *Cereb. Cortex (New York, NY: 1991)* 8, 743–752. doi: 10.1093/cercor/8.8.743

Cheng, C., Juan, C., Chen, M., Chang, C., Jie, H., Su, T., et al. (2016). Different forms of prefrontal theta burst stimulation for executive function of medication- resistant depression: evidence from a randomized sham-controlled study. *Prog. Neuropsychopharmacol. Biol. Psychiatry* 66, 35–40. doi: 10.1016/j.pnpbp.2015.11.009

Chistyakov, A. v., Kreinin, B., Marmor, S., Kaplan, B., Khatib, A., Darawsheh, N., et al. (2015). Preliminary assessment of the therapeutic efficacy of continuous theta-burst magnetic stimulation (cTBS) in major depression: a double-blind sham-controlled study. *J. Affect. Disord.* 170, 225–259. doi: 10.1016/j.jad.2014.08.035

Cho, S. S., Ko, H., Pellecchia, G., van Eimeren, T., Cilia, R., and Strafella, P. (2010). Continuous theta burst stimulation of right dorsolateral prefrontal cortex induces changes in impulsivity level. *Brain Stimul.* 3, 170–176. doi: 10.1016/j.brs.2009.10.002

Chung, S. W., Lewis, B. P., Rogasch, N. C., Saeki, T., Thomson, R. H., Hoy, K. E., et al. (2017). Demonstration of short-term plasticity in the dorsolateral prefrontal cortex with theta burst stimulation: a TMS-EEG study. *Clin. Neurophysiol.* 128, 1117–1126. doi: 10.1016/j.clinph.2017.04.005

Chung, S. W., Rogasch, N. C., Hoy, K. E., and Fitzgerald, P. B. (2018a). The effect of single and repeated prefrontal intermittent theta burst stimulation on cortical reactivity and working memory. *Brain Stimul.* 11, 566–574. doi: 10.1016/j.brs.2018.01.002

Chung, S. W., Rogasch, N. C., Hoy, K. E., Sullivan, C. M., Cash, R. F. H., and Fitzgerald, P. B. (2018b). Impact of different intensities of intermittent theta burst stimulation on the cortical properties during TMS-EEG and working memory performance. *Hum. Brain Mapp.* 38, 783–802. doi: 10.1002/hbm.23882

Cieslik, E. C., Zilles, K., Caspers, S., Roski, C., Kellermann, T. S., Jakobs, O., et al. (2013). Is there one DLPFC in cognitive action control? Evidence for heterogeneity from Co-activation-based parcellation. *Cereb. Cortex* 23, 2677–2689. doi: 10.1093/cercor/bhs256

Cocchi, L., Bosisio, F., Carter, O., Wood, S., Berchtold, A., Conus, P., et al. (2009). Visuospatial working memory deficits and visual pursuit impairments are not directly related in schizophrenia. *Aust. N. Z. J. Psychiatry* 43, 766–774. doi: 10.1080/00048670903001901

Cowan, N. (2014). Working memory underpins cognitive development, learning, and education. *Educ. Psychol. Rev.* 26, 197–223. doi: 10.1007/s10648-013-9246-y

Dutilh, G., Krypotos, A. M., and Wagenmakers, E. J. (2011). Task-related versus stimulus-specific practice: a diffusion model account. *Exp. Psychol.* 58, 434–442. doi: 10.1027/1618-3169/a000111

Figueroa-Vargas, A., Cárcamo, C., Henríquez-Ch, R., Zamorano, F., Ciampi, E., Uribe-San-Martin, R., et al. (2020). Frontoparietal connectivity correlates with working memory performance in multiple sclerosis. *Sci. Rep.* 10:9310. doi: 10.1038/s41598-020-66279-0

Fried, P. J., Rushmore, R. J., Moss, M. B., Valero-Cabré, A., and Pascual-Leone, A. (2014). Causal evidence supporting functional dissociation of verbal and spatial working memory in the human dorsolateral prefrontal cortex. *Eur. J. Neurosci.* 39, 1973–1981. doi: 10.1111/ejn.12584

Gärtner, M., Ghisu, M. E., Scheidegger, M., Bönke, L., Fan, Y., Stippl, A., et al. (2018). Aberrant working memory processing in major depression: evidence from multivoxel pattern classification. *Neuropsychopharmacology* 43, 1972–1979. doi: 10.1038/s41386-018-0081-1

Goldman-Rakic, P. S. (1995). Architecture of the prefrontal cortex and the central executive. *Ann. N. Y. Acad. Sci.* 769, 71–83. doi: 10.1111/j.1749-6632.1995.tb38132.x

Haatveit, B. C., Sundet, K., Hugdahl, K., Ueland, T., Melle, I., and Andreassen, O. A. (2010). The validity of d prime as a working memory index: results from the Bergen n-back task. *J. Clin. Exp. Neuropsychol.* 32, 871–880. doi: 10.1080/13803391003596421

Hinder, M. R., Goss, E. L., Fujiyama, H., Canty, A. J., Garry, M. I., Rodger, J., et al. (2014). Inter- and Intra-individual variability following intermittent theta burst stimulation: implications for rehabilitation and recovery. *Brain Stimul.* 7, 365–371. doi: 10.1016/j.brs.2014.01.004

Hoy, K. E., Bailey, N., Michael, M., Fitzgibbon, B., Rogasch, N. C., Saeki, T., et al. (2015). Enhancement of working memory and task-related oscillatory activity following intermittent theta burst stimulation in healthy controls. *Cereb. Cortex* 26, 4563–4573. doi: 10.1093/cercor/bhv193

Hoy, K. E., Whitty, D., Bailey, N., and Fitzgerald, P. B. (2016). Preliminary investigation of the effects of γ-tACS on working memory in schizophrenia. *J. Neural Transm.* 123, 1205–1212. doi: 10.1007/s00702-016-1554-1

Huang, Y. Z., Edwards, M. J., Rounis, E., Bhatia, K. P., and Rothwell, J. C. (2005). Theta burst stimulation of the human motor cortex. *Neuron* 45, 201–206. doi: 10.1016/j.neuron.2004.12.033

Huang, Y., Rothwell, J. C., Chen, R., Lu, C., and Chuang, W. (2011). The theoretical model of theta burst form of repetitive transcranial magnetic stimulation. *Clin. Neurophysiol.* 122, 1011–1018. doi: 10.1016/j.clinph.2010.08.016

John Irwin, R., Hautus, M. J., and Francis, M. A. (2001). Indices of response bias in the same-different experiment. *Percept. Psychophys.* 63, 1091–1100. doi: 10.3758/BF03194527

Jonides, J., Smith, E. E., Koeppe, R. A., Awh, E., Minoshima, S., and Mintun, M. A. (1993). Spatial working memory in humans as revealed by PET. *Nature* 363, 623–625. doi: 10.1038/363623a0

Kaller, C. P., Heinze, K., Frenkel, A., Unterrainer, J. M., Weiller, C., La, C. H., et al. (2011). Differential impact of continuous theta-burst stimulation over left and right DLPFC on planning. *Hum. Brain Mapp.* 36, 36–51. doi: 10.1002/hbm.21423

Kessels, R. P. C., Kappelle, L. J., de Haan, E. H. F., and Postma, A. (2002). Lateralization of spatial-memory processes: evidence on spatial span, maze learning, and memory for object locations. *Neuropsychologia* 40, 1465–1473. doi: 10.1016/s0028-3932(01)00199-3

Kessels, R. P. C., Postma, A., Wijnalda, E. M., and de Haan, E. H. F. (2000). Frontal-lobe involvement in spatial memory: evidence from PET, fMRI, and lesion studies. *Neuropsychology Review* 10, 101–113.

Kiyonaga, A., Korb, F. M., Lucas, J., Soto, D., and Egner, T. (2014). Dissociable causal roles for left and right parietal cortex in controlling attentional biases from the contents of working memory. *NeuroImage* 100, 200–205. doi: 10.1016/j.neuroimage.2014.06.019

Ko, J. H., Monchi, O., Ptito, A., Bloomfield, P., Houle, S., and Strafella, A. P. (2008). Theta burst stimulation-induced inhibition of dorsolateral prefrontal cortex reveals hemispheric asymmetry in striatal dopamine release during a set-shifting task – a TMS –[11 C] raclopride PET study. *Eur. J. Neurosci.* 28, 2147–2155. doi: 10.1111/j.1460-9568.2008.06501.x

Lee, J. C., Corlier, J., Wilson, A. C., Tadayonnejad, R., Marder, K. G., Ngo, D., et al. (2021). Subthreshold stimulation intensity is associated with greater clinical efficacy of intermittent theta-burst stimulation priming for Major Depressive Disorder. *Brain Stimul.* 14, 1015–1021. doi: 10.1016/j.brs.2021.06.008

Li, C. T., Huang, Y. Z., Bai, Y. M., Tsai, S. J., Su, T. P., and Cheng, C. M. (2019). Critical role of glutamatergic and GABAergic neurotransmission in the central mechanisms of theta-burst stimulation. *Hum. Brain Mapp.* 40, 2001–2009. doi: 10.1002/hbm.24485

Li, C., Chen, M., Juan, C., Huang, H., Chen, L., Hsieh, J., et al. (2014). Efficacy of prefrontal theta-burst stimulation in refractory depression: a randomized sham-controlled study. *Brain* 137, 2088–2098. doi: 10.1093/brain/awu109

Lowe, C. J., Manocchio, F., Safati, A. B., and Hall, P. A. (2018). The effects of theta burst stimulation (TBS) targeting the prefrontal cortex on executive functioning: a systematic review and meta-analysis. *Neuropsychologia* 111, 344–359. doi: 10.1016/j.neuropsychologia.2018.02.004

Luber, B., and Lisanby, S. H. (2014). Enhancement of human cognitive performance using transcranial magnetic stimulation (TMS). *NeuroImage* 85, 961–970. doi: 10.1016/j.neuroimage.2013.06.007

Luck, S. J., and Vogel, E. K. (2013). Visual working memory capacity: from psychophysics and neurobiology to individual differences. *Trends Cogn. Sci.* 17, 391–400. doi: 10.1016/j.tics.2013.06.006

Manoach, D. S., White, N. S., Lindgren, K. A., Heckers, S., Coleman, M. J., Dubal, S., et al. (2004). Hemispheric specialization of the lateral prefrontal cortex for strategic processing during spatial and shape working memory. *NeuroImage* 21, 894–903. doi: 10.1016/j.neuroimage.2003.10.025

McDonnell, M. D., and Abbott, D. (2009). What is stochastic resonance? Definitions, misconceptions, debates, and its relevance to biology. *PLoS Comput. Biol.* 5:e1000348. doi: 10.1371/journal.pcbi.1000348

Mckiernan, K. A., Kaufman, J. N., Kucera-thompson, J., and Binder, J. R. (2003). A parametric manipulation of factors affecting task-induced deactivation in fmri. *J. Cogn. Neurosci.* 15, 394–408. doi: 10.1162/089892903321593117

Mcneill, A., Monk, R. L., Qureshi, A. W., Makris, S., and Heim, D. (2018). Continuous theta burst transcranial magnetic stimulation of the right dorsolateral prefrontal cortex impairs inhibitory control and increases alcohol consumption. *Cogn. Affect. Behav. Neurosci.* 18, 1198–1206. doi: 10.3758/s13415-018-0631-3

Nee, D. E., and Brown, J. W. (2013). Dissociable frontal-striatal and frontal-parietal networks involved in updating hierarchical contexts in working memory. *Cereb. Cortex (New York, N.Y.: 1991)* 23, 2146–2158. doi: 10.1093/cercor/bhs194

Ngetich, R., Li, W., Jin, D., Zhang, J., Jin, Z., and Li, L. (2021). Continuous theta-burst stimulation over the right dorsolateral prefrontal cortex impairs visuospatial working memory performance in medium load task. *NeuroReport* 32, 808–814. doi: 10.1097/WNR.0000000000001666

Ngetich, R., Zhou, J., Zhang, J., Jin, Z., and Li, L. (2020). Assessing the effects of continuous theta burst stimulation over the dorsolateral prefrontal cortex on human cognition: a systematic review. *Front. Integr. Neurosci.* 14:35. doi: 10.3389/fnint.2020.00035

Oldfield, R. C. (1971). The assessment and analysis of handedness: the Edinburgh inventory. *Neuropsychologia* 9, 97–113. doi: 10.1016/0028-3932(71)90067-4

Oliveira, J. F., Zanão, T. A., Valiengo, L., Lotufo, P. A., Benseñor, I. M., Fregni, F., et al. (2013). Acute working memory improvement after tDCS in antidepressant-free patients with major depressive disorder. *Neurosci. Lett.* 537, 60–64. doi: 10.1016/j.neulet.2013.01.023

Oliveri, M., Turriziani, P., Carlesimo, G. A., Koch, G., Tomaiuolo, F., Panella, M., et al. (2001). Parieto-frontal interactions in visual-object and visual-spatial working memory: evidence from transcranial magnetic stimulation. *Cereb. Cortex* 11, 606–618. doi: 10.1093/cercor/11.7.606

Ott, D. V. M., Ullsperger, M., Jocham, G., Neumann, J., and Klein, T. A. (2011). Continuous theta-burst stimulation (cTBS) over the lateral prefrontal cortex alters reinforcement learning bias. *NeuroImage* 57, 617–623. doi: 10.1016/j.neuroimage.2011.04.038

Owen, A. M., McMillan, K. M., Laird, A. R., and Bullmore, E. (2005). N-back working memory paradigm: a meta-analysis of normative functional neuroimaging studies. *Hum. Brain Mapp.* 25, 46–59. doi: 10.1002/hbm.20131

Pestalozzi, M. I., Annoni, J. M., Müri, R. M., and Jost, L. B. (2020). Effects of theta burst stimulation over the dorsolateral prefrontal cortex on language switching – A behavioral and ERP study. *Brain Lang.* 205:104775. doi: 10.1016/j.bandl.2020.104775

Petrides, M. (2019). *Atlas of the Morphology of the Human Cerebral Cortex on the Average MNI Brain*, 1st Edn. New York, NY: Academic Press.

Plewnia, C., Pasqualetti, P., Große, S., Schlipf, S., Wasserka, B., Zwissler, B., et al. (2014). Treatment of major depression with bilateral theta burst stimulation: a randomized controlled pilot trial. *J. Affect. Disord.* 156, 219–223. doi: 10.1016/j.jad.2013.12.025

Polanía, R., Nitsche, M. A., and Ruff, C. C. (2018). Studying and modifying brain function with non-invasive brain stimulation. *Nat. Neurosci.* 21, 174–187. doi: 10.1038/s41593-017-0054-4

Ridding, M. C., and Ziemann, U. (2010). Determinants of the induction of cortical plasticity by non-invasive brain stimulation in healthy subjects. *J. Physiol.* 588, 2291–2304. doi: 10.1113/jphysiol.2010.190314

Romei, V., Thut, G., and Silvanto, J. (2016). Information-based approaches of noninvasive transcranial brain stimulation. *Trends Neurosci.* 39, 782–795. doi: 10.1016/j.tins.2016.09.001

Rottschy, C., Langner, R., Dogan, I., Reetz, K., Laird, A. R., and Schulz, J. B. (2012). NeuroImage Modelling neural correlates of working memory: a coordinate-based meta-analysis. *NeuroImage* 60, 830–846. doi: 10.1016/j.neuroimage.2011.11.050

Schicktanz, N., Fastenrath, M., Milnik, A., and Spalek, K. (2015). Continuous theta burst stimulation over the left dorsolateral prefrontal cortex decreases medium load working memory performance in healthy humans. *PLoS One* 10:e0120640. doi: 10.1371/journal.pone.0120640

Silvanto, J., and Cattaneo, Z. (2017). Common framework for "virtual lesion" and state-dependent TMS: the facilitatory/suppressive range model of online TMS effects on behavior. *Brain Cogn.* 119, 32–38. doi: 10.1016/j.bandc.2017.09.007

Silvanto, J., Bona, S., Marelli, M., and Cattaneo, Z. (2018). On the mechanisms of transcranial magnetic stimulation (TMS): how brain state and baseline

performance level determine behavioral effects of TMS. *Front. Psychol.* 9:741. doi: 10.3389/fpsyg.2018.00741

Silvanto, J., Muggleton, N. G., Cowey, A., and Walsh, V. (2007). Neural activation state determines behavioral susceptibility to modified theta burst transcranial magnetic stimulation. *Eur. J. Neurosci.* 26, 523–528. doi: 10.1111/j.1460-9568.2007.05682.x

Sörqvist, P., Dahlström, Ö, Karlsson, T., and Rönnberg, J. (2016). Concentration: the neural underpinnings of how cognitive load shields against distraction. *Front. Hum. Neurosci.* 10:221. doi: 10.3389/fnhum.2016.00221

Stocks, N. G. (2000). Suprathreshold stochastic resonance in multilevel threshold systems. *Rev. Lett.* 84, 2310–2313. doi: 10.1103/PhysRevLett.84.2310

Taren, A. A., Gianaros, P. J., Greco, C. M., Lindsay, E. K., Fairgrieve, A., Brown, K. W., et al. (2017). Mindfulness meditation training and executive control network resting state functional connectivity: a randomized controlled trial. *Psychosom. Med.* 79, 674–683. doi: 10.1097/PSY.0000000000000466

Thomason, M. E., Race, E., Burrows, B., Whitfield-Gabrieli, S., Glover, G. H., and Gabrieli, J. D. E. (2009). Development of spatial and verbal working memory capacity in the human brain. *J. Cogn. Neurosci.* 21, 316–332. doi: 10.1162/jocn.2008.21028

Tomasi, D., Chang, L., Caparelli, E. C., and Ernst, T. (2008). Different activation patterns for working memory load and visual attention load. *Brain Res.* 1132, 158–165. doi: 10.1038/jid.2014.371

Vékony, T., Németh, V. L., Holczer, A., Kocsis, K., Kincses, Z. T., Vécsei, L., et al. (2018). Continuous theta-burst stimulation over the dorsolateral prefrontal cortex inhibits improvement on a working memory task. *Sci. Rep.* 8:14835. doi: 10.1038/s41598-018-33187-3

Wang, H., He, W., Wu, J., Zhang, J., Jin, Z., and Li, L. (2019). A coordinate-based meta-analysis of the n-back working memory paradigm using activation likelihood estimation. *Brain Cogn.* 132, 1–12. doi: 10.1016/j.bandc.2019.01.002

Westin, G. G., Bassi, B. D., Lisanby, S. H., and Luber, B. (2014). Determination of motor threshold using visual observation overestimates transcranial magnetic stimulation dosage: safety implications. *Clin. Neurophysiol.* 125, 142–147. doi: 10.1016/j.clinph.2013.06.187

Widhalm, M. L., and Rose, N. S. (2019). How can transcranial magnetic stimulation be used to causally manipulate memory representations in the human brain? *WIREs Cogn. Sci.* 10:e1469. doi: 10.1002/wcs.1469

Wischnewski, M., and Schutter, D. J. L. G. (2015). Efficacy and time course of theta burst stimulation in healthy humans. *Brain Stimul.* 8, 685–692. doi: 10.1016/j.brs.2015.03.004

Conflict of Interest: The authors declare that the research was conducted in the absence of any commercial or financial relationships that could be construed as a potential conflict of interest.

Publisher's Note: All claims expressed in this article are solely those of the authors and do not necessarily represent those of their affiliated organizations, or those of the publisher, the editors and the reviewers. Any product that may be evaluated in this article, or claim that may be made by its manufacturer, is not guaranteed or endorsed by the publisher.

frontiers | Frontiers in Human Neuroscience

ORIGINAL RESEARCH
published: 08 April 2022
doi: 10.3389/fnhum.2022.790678

Altered Spontaneous Brain Activity Patterns in Children With Strabismic Amblyopia After Low-Frequency Repetitive Transcranial Magnetic Stimulation: A Resting-State Functional Magnetic Resonance Imaging Study

*Yi-Ning Wang†, Yi-Cong Pan†, Hui-Ye Shu, Li-Juan Zhang, Qiu-Yu Li, Qian-Min Ge, Rong-Bin Liang and Yi Shao**

Department of Ophthalmology, The First Affiliated Hospital of Nanchang University, Jiangxi Center of National Ocular Disease Clinical Research Center, Nanchang, China

OPEN ACCESS

Edited by:
Nan-Kuei Chen, University of Arizona, United States

Reviewed by:
Jennifer Kate Evelyn Steeves, York University, Canada
Guanghui Liu, Fujian Provincial People's Hospital, China

***Correspondence:**
Yi Shao
freebee99@163.com

† These authors have contributed equally to this work

Specialty section:
This article was submitted to Brain Imaging and Stimulation, a section of the journal Frontiers in Human Neuroscience

Received: *22 November 2021*
Accepted: *18 March 2022*
Published: *08 April 2022*

Citation:
Wang Y-N, Pan Y-C, Shu H-Y, Zhang L-J, Li Q-Y, Ge Q-M, Liang R-B and Shao Y (2022) Altered Spontaneous Brain Activity Patterns in Children With Strabismic Amblyopia After Low-Frequency Repetitive Transcranial Magnetic Stimulation: A Resting-State Functional Magnetic Resonance Imaging Study. Front. Hum. Neurosci. 16:790678. doi: 10.3389/fnhum.2022.790678

Objective: Previous studies have demonstrated altered brain activity in strabismic amblyopia (SA). In this study, low-frequency repetitive transcranial magnetic stimulation (rTMS) was applied in children with strabismic amblyopia after they had undergone strabismus surgery. The effect of rTMS was investigated by measuring the changes of brain features using the amplitude of low-frequency fluctuation (ALFF).

Materials and Methods: In this study, 21 SA patients (12 males and 9 females) were recruited based on their age (7–13 years old), weight, and sex. They all had SA in their left eyes and they received rTMS treatment one month after strabismus surgery. Their vision before and after surgery were categorized as pre-rTMS (PRT) and post-rTMS (POT). All participants received rTMS treatment, underwent magnetic resonance imaging (MRI), and their data were analyzed using the repeated measures *t*-test. The team used correlation analysis to explore the relationship between logMAR visual acuity and ALFF.

Results: Pre- versus post-rTMS values of ALFF were significantly different within individuals. In the POT group, ALFF values were significantly decreased in the Angular_R (AR), Parietal_Inf_L (PIL), and Cingulum_Mid_R (CMR) while ALFF values were significantly increased in the Fusiform_R (FR) and Frontal_Inf_Orb_L(FIL) compared to the PRT stage.

Conclusion: Our data showed that ALFF recorded from some brain regions was changed significantly after rTMS in strabismic amblyopes. The results may infer the pathological basis of SA and demonstrate that visual function may be improved using rTMS in strabismic amblyopic patients.

Keywords: low-frequency rTMS, strabismic amblyopia, amplitude of low-frequency fluctuation (ALFF), spontaneous brain activity, ophthalmological

INTRODUCTION

Strabismus and amblyopia are two common visual developmental disorders that can occur in infancy and persist into adulthood if treatment is not successful (Tarczy-Hornoch et al., 2013; Chen et al., 2014). Strabismus is an optical manifestation disorder associated with the coordination of the external eye muscles. Different conditions of extraocular muscle incongruity may result in different types of diplopic images (**Figure 1**). Strabismus is generally considered to be associated with maldevelopment of the visual pathways in the brain that mediate eye movement (Min et al., 2018), and inimically affects stereopsis, binocularity, and depth perception (Gunton et al., 2015). Hyperopia, muscle dysfunction, trauma, brain disease, and infection are all important causes of strabismus, and risk factors include premature birth and cerebral palsy. Diagnosis can be made by the observation of light reflected from the anterior eye offset from the center of the pupil. Treatments, including refractive correction and eye alignment surgery, address the impact on vision and are good choices for patients. The incidence rate of adult-onset strabismus is reportedly 54.2 per 100,000 individuals (Mohney et al., 2012), and in adults strabismus is often associated with undiagnosed amblyopia in early childhood and symptoms associated with aging (Chan et al., 2004).

Amblyopia, also known as lazy eye, is a visual disorder with causes which affect cooperation between the eyes and brain (National Eye Institute, 2016). Because the condition is associated with changes in the brain, visual impairment such as ametropia cannot be fully treated after surgery (Schwartz et al., 2002; Levi, 2013). Early detection can improve the rate of successful treatment (Jefferis et al., 2015) and glasses may be an important part of treatment for children (Jefferis et al., 2015; Maconachie and Gottlob, 2015). Many patients with amblyopia, especially mild cases, are unaware of their condition because one eye is affected and the vision of the fellow eye is normal. However, because two eyes are needed for stereo vision (which is usually lacking for the patients), patients with amblyopia may have relatively poor vision, and relatively low sensitivity to contrast and movement in the affected eye (Fazzi and Bianchi, 2016). Amblyopia features reduced stereopsis, visual acuity (VA), visual sensitivity, and impaired spatial vision and binocular summation (Webber and Wood, 2005).

Diplopia refers to the abnormal phenomenon of one object being perceived as two identical but separated images. There are many causes of diplopia, some of which reflect anomalies of the brain (Cerulli Irelli et al., 2021). Diplopia may occur when one or more of the six muscles that control eye movement become inflamed, injured, or neurologically impaired, and the muscles in both eyes do not accurately coordinate (Goseki et al., 2021). Because strabismus causing diplopia and confusion (perceived superposition of two different images) can make the patient feel unwell, the image from the macula of the strabismic eye may be suppressed for a sustained period, and the amblyopia that accompanies this situation is known as strabismic amblyopia (Peña Urbina et al., 2021).

Magnetic resonance imaging (MRI) has been widely used in various pretreatment imaging diagnoses recently. As a non-invasive neuroimaging method, it is mainly used to evaluate the functional and structural changes of the human brain (Brown et al., 2016). Functional Magnetic Resonance Imaging (fMRI) is a technology with precise spatial resolution and is used for the analysis of brain function (Goodyear and Menon, 2001). This imaging method helps to reveal the mechanism underpinning eye diseases (Conner et al., 2007; Wang et al., 2012; Liang et al., 2017). Repetitive transcranial magnetic stimulation (rTMS) mainly achieve excitation or inhibition of local cerebral cortical function by changing the stimulation frequency, with the aim of effective treatment of disease. Thompson's present data show that rTMS of the visual cortex can temporarily improve contrast sensitivity in the adult amblyopic visual cortex (Thompson et al., 2008). Spiegel have shown that a-tDCS to the visual cortex would improve contrast sensitivity in adult patients with amblyopia by enhancing the cortical response to inputs from the amblyopic eye (Spiegel et al., 2013). Rehn found that rTMS could improve the symptoms of patients with obsessive-compulsive disorder (Rehn et al., 2018). Chou demonstrated the effect of rTMS on Alzheimer's disease (Chou et al., 2020). TMS can be used to stimulate the cerebral cortex, such as the visual cortex and somatosensory cortex, to induce local excitatory or inhibitory effects and affect the function of the system. In addition, TMS can also be used in learning, memory, language, and emotional research (Brunoni et al., 2017; Sebastianelli et al., 2017; McClintock et al., 2018; Arns et al., 2019; Yang et al., 2019; Chou et al., 2020; Malkani and Zee, 2020).

Studies suggested the neural networks modulating aspects of emotional behavior to be implicated in the pathophysiology of mood disorders. These networks involve the prefrontal cortex (Rigucci et al., 2010). AhmedA Abdelrahman's findings revealed that HF-rTMS over L-DLPCF for 10 days reduced cigarette consumption, craving, dependence, and improved associated symptoms of anxiety and depression (Abdelrahman et al., 2021). The abnormal activity of dorsolateral prefrontal cortex (DLPFC) is related to the occurrence of anxiety and depression.

MATERIALS AND METHODS

Subjects

Twenty-one patients (12 males and 9 females) were recruited at the First Affiliated Hospital of Nanchang University. Those eligible for participation met the following criteria: (1) Aged between 7 and 13 years old; (2) Their guardian allowed them to receive rTMS treatment within 1 month after strabismus surgery; (3) Clear diagnosis of strabismus. Exclusion criteria were as follows: (1) Patients suffering from other eye diseases, such as cataract, glaucoma, or retinitis pigmentosa; (2) Mental illness. The 21 patients who met the criteria underwent rTMS treatment before and after surgical treatment. The Medical Ethics Committee of the First Affiliated Hospital of Nanchang University approved the research plan. Patients and guardians were informed about the research and potential risks before signing consent forms voluntarily.

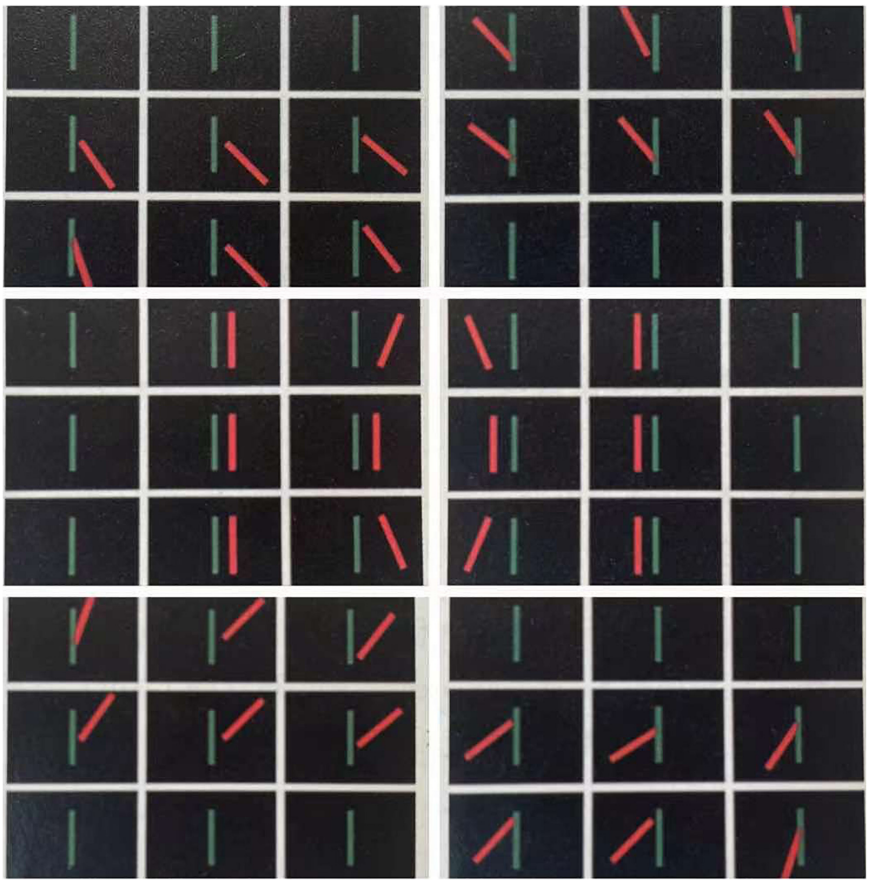

FIGURE 1 | Diplopia in each of the external ocular muscles with paralysis.

This study sought consent from all patients participating in the diagnosis, treatment, and evaluation stages of the study.

Transcranial Magnetic Stimulation

Repetitive transcranial magnetic stimulation (rTMS) was administered by trained researchers using the Magstim Rapid device (Magstim®, Whitland, Wales, United Kingdom) and Magstim d70-mm-air-cooled figure-of-eight coil. Use of stimulus frequency rate of 10Hz, intensity of 100% resting motion threshold, 5s stimulation, pulse 50/5s, the interval was 10s, with 2000 pulses in total, and the treatment lasted for 10min. The stimulation site is DLPFC. Stimulation was performed between baseline measurements and remeasurements. The two rTMS stimulation groups received 30 treatments 5 times a week for 6 weeks.

Magnetic Resonance Imaging Parameters

All patients underwent scanning using 3-TESLA MR scanners (Siemens, Germany) and a gradient-echo echo-planar imaging pulse sequence was used to acquire fMRI values with the following specific parameters: 240 functional images (repetition time = 2,000 ms, echo time = 30 ms, thickness = 4.0 mm, gap = 1.2 mm, acquisition matrix = 64 × 64, flip angle = 90°, field of view = 220 × 220 mm, 29 axial) were obtained. All MRI images were examined for structural abnormalities, and no subject was excluded on this basis.

Functional Magnetic Resonance Imaging Data Processing

The CAT12 toolkit (12.7[1]) from the Statistical Parametric Mapping database (SPM12[2]) was used to analyze the data. All procedures were performed using MATLAB 7.9.0 software (R2009b; The Mathworks, Inc., Natick, MA, United States). Preprocessing included calibration, correction for head movement, image structure and average echo planar imaging alignment, normalization to a standard template, and smoothing using a Gaussian of 8 mm full width at half maximum. The fMRI brain functional images of each subject were co-registered with the T1 brain structure image template of the Montreal Neurological Institute (MNI) space as the reference standard, and the spatial standardization was completed using the Diffeomorphic Anatomical Registration Through Exponentiated

[1]http://www.neuro.uni-jena.de/cat/

[2]https://www.fil.ion.ucl.ac.uk/spm/

TABLE 1 | Demographics and clinical measurements of pre-rTMS (PRT) and post-rTMS (POT).

Condition	PRT	POT	t/x2	P
Male/female	12/9	12/9	N/A	N/A
Age (year)	9.16 ± 2.42	9.16 ± 2.42	N/A	N/A
Weight (Kg)	22.36 ± 7.27	22.36 ± 7.27	N/A	N/A
SE-L (diopter)	3.75 ± 1.35	3.45 ± 1.55	4.431	0.864
SE-R (diopter)	3.15 ± 1.55	3.25 ± 1.35	4.064	0.809
Astigmatism-L (diopter)	1.50 ± 0.50	1.45 ± 0.55	5.873	0.912
Astigmatism-R (diopter)	1.55 ± 0.55	1.35 ± 0.45	5.054	0.846
Esotropia/exotropia	12/9	0/0	NA	NA
Color Vision	Full	Full	NA	NA
Confrontation visual field	Full	Full	NA	NA
log MAR-L(BCVA)	0.68 ± 0.15	0.43 ± 0.25	1.873	0.024
log MAR-R(BCVA)	–0.15 ± 0.05	–0.10 ± 0.05	7.439	0.927

The 2-sample T-test was analyzed between the same patients before and after low frequency (LF) repetitive transcranial magnetic stimulation (rTMS); Data are expressed as mean ± standard deviation.

Lie algebra (DARTEL) method. In addition, the gray matter volumes were normalized and smoothed using a 6-mm full width at half maximum Gaussian kernel.

Correlation Analysis

LogMAR acuity tests were used to assess the patients' visual monocular acuity. The correlations between rTMS and logarithmic MAR values in the AR ($P = 0.0066$), FR ($P < 0.0001$), and CMR ($P = 0.0004$) regions were analyzed using GRAPHIPAD Prism 8. Correlation graphs were produced.

Statistical Analysis

After controlling for age and sex, the repeated measures *t*-test was used to compare the amplitude of low-frequency fluctuation (ALFF) between PRT and POT. The significance level was set at $P < 0.05$, family wise error corrected, voxel level $P < 0.001$, and cluster level $P < 0.05$. A color map was created by overlapping the significant voxels by standardization of 3-dimensional magnetization prepared fast acquisition gradient echo sequences.

RESULTS

Demographics and Visual Measurements

There were no significant differences in age and log MAR-R(BCVA) between the POT and PRT. There were statistically notable differences in the log MAR-L(BCVA) ($P < 0.05$) between the two groups (more details are presented in **Table 1**).

Differences in Amplitude of Low-Frequency Fluctuation

At the PRT stage, the ALFF values were significantly higher in the AR, PIL, and CMR [**Figure 2** (red) and **Table 2**]. and were significantly lower in the FR and FIL compared to the POT stage [**Figure 2** (blue), **3** and **Table 2**]. No significant difference was found in ALFF between PRT and POT in other brain regions ($P > 0.05$).

Correlation Analysis

At the POT stage, significant correlations between ALFF signal value and logMAR acuity were found and were positive at AR ($r^2 = 0.3286$, $P = 0.0066$; **Figure 4A**) and negative at FR ($r^2 = 0.8466$, $P < 0.0001$; **Figure 4B**) and positive at CMR ($r^2 = 0.4940$, $P = 0.0004$; **Figure 4C**). Changes in ALFF values in brain regions are associated with changes in visual acuity and brain activity (**Figures 5, 6**).

Receiver Operating Characteristic Curves

We tested the hypothesis that ALFF may be a potential diagnostic indicator of SA patients at the PRT stage by plotting the average

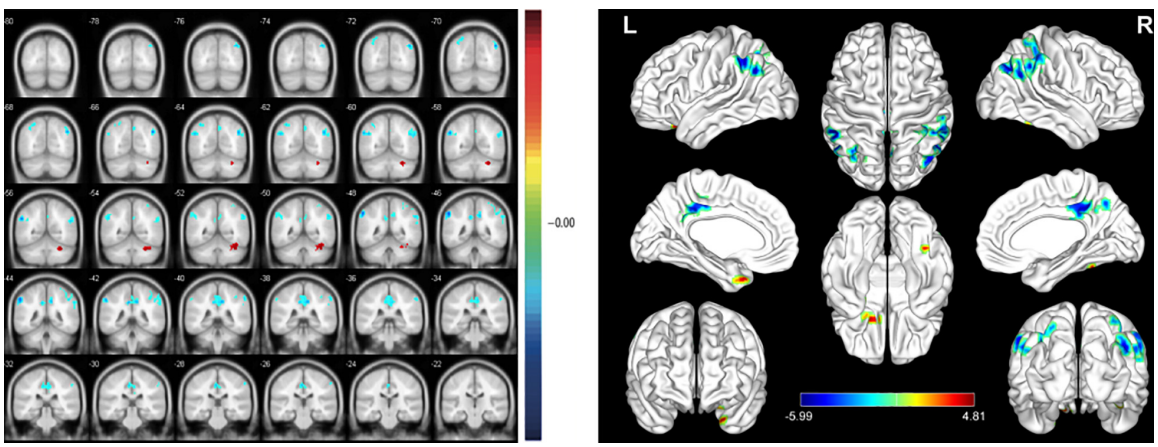

FIGURE 2 | Significant differences in spontaneous brain activity between the pre-rTMS (PRT) and post-rTMS (POT). The sizes of the spots denote the degree of quantitative changes. The different brain regions were observed in the Angular_R (AR), Parietal_Inf_L (PIL), Cingulum_Mid_R (CMR), Fusiform_R (FR) and Frontal_Inf_Orb_L (FIL). The red areas denote that PRT exhibit higher amplitude of low-frequency fluctuation (ALFF) in brain areas than POT and the blue areas denote brain regions with a lower ALFF [$P < 0.001$, cluster > 13 voxels, Alphasim corrected)].

TABLE 2 | Brain areas with significantly different amplitude of low-frequency fluctuation (ALFF) between groups.

Brain areas	MNI coordinates			number of voxels	T value
	X	Y	Z		
PRT < POT					
Fusiform Gyrus (R)	39	–51	–24	61	4.192
Frontal Inf Orb Lobe (L)	–21	21	–27	43	4.8077
PRT > POT					
Angular Gyrus (R)	45	–66	36	240	–5.6255
Cingulum Mid Lobe (R)	9	–39	39	224	–5.0931
Parietal Inf Lobe (L)	–54	–45	45	127	–5.9884

The statistical threshold was set at the voxel level with $P < 0.05$ for multiple comparisons using False Discovery Rate ($Q < 0.01$ and cluster size > 15).
ALFF, amplitude of low-frequency fluctuation; L, left; R, right; MNI, Montreal Neurological Institutet; PRT, pre-rTMS; POT, post-rTMS.

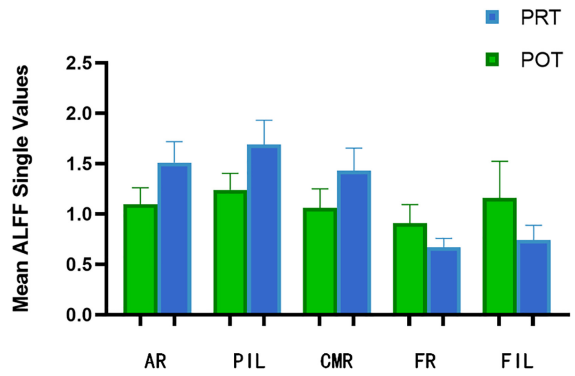

FIGURE 3 | The mean ALFF values between POT and PRT. ALFF, amplitude of low-frequency fluctuation; PRT, pre-rTMS; POT, post-rTMS; L-left; R-right; AR, Angular_R; PIL, Parietal_Inf_L; CMR, Cingulum_Mid_R; FR, Fusiform_R; FIL, Frontal_Inf_Orb_L.

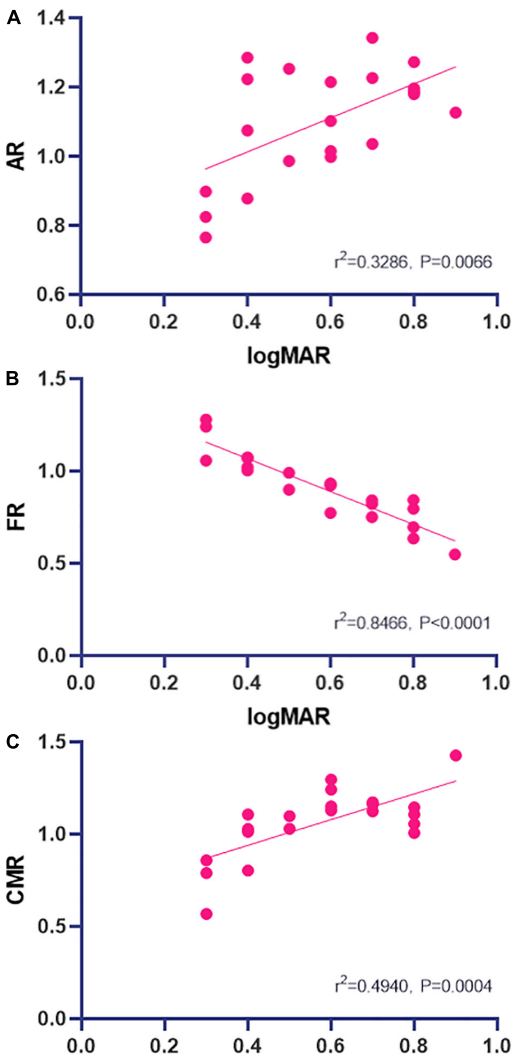

FIGURE 4 | Correlations between mean ALFF signal values and logMAR acuity. The ALFF signal value of AR showed a positive correlation with logMAR [$r^2 = 0.3286$, $P = 0.0066$; **(A)**] and the ALFF signal value of FR showed a negative correlation with logMAR [$r^2 = 0.8466$, $P < 0.0001$; **(B)**]. The logMAR showed a positive correlation with the ALFF signal value of CMR [$r^2 = 0.4940$, $P = 0.0004$; **(C)**] (A lower LogMAR value means better acuity). ALFF, amplitude of low-frequency fluctuation; AR, Angular_R; CMR, Cingulum_Mid_R; FR, Fusiform_R.

ALFF values of each brain region on an ROC curve. Brain regions with significantly different ALFF values showed high accuracy as diagnostic markers (PRT > POT).The AUCs of the ALFF values of the different brain regions were as follows: CMR (0.907, $p < 0.001$), AR (0.961 $p < 0.001$), PIL (0.944, $p < 0.001$), FR (0.874, $p < 0.001$), FIL (0.899, $p < 0.001$) (**Figure 7**).

DISCUSSION

Amplitude of low-frequency fluctuation (ALFF) is a commonly used clinical method which reflects changes in spontaneous brain activity and has been applied in the investigation of several ophthalmological diseases. Amplitude of low-frequency fluctuation is used to measure spontaneous fluctuations in blood oxygen level-dependent fMRI-signal intensity for nervous activity, reflecting the intensity of regional spontaneous brain activity at rest. The increase of ALFF indicated increased blood oxygen dependence level and increased activity in this brain region, on the contrary, activity of the brain area decreased. We used the ALFF sequence to compare the activity of different brain regions in POT and PRT. Our study is the first to determine whether there are ALFF differences in brain regions before and after transcranial magnetic stimulation within SA patients after surgery, and to identify those regions. Functional MRI is one of the most widely used functional brain imaging techniques. ALFF has been applied in ophthalmologic and neurogenic diseases, and in this study (**Table 3**) we demonstrated that the intrinsic patterns of activity in different brain regions of POT were changed after rTMS.

We collected information on the brain regions where ALFF changed after rTMS treatment, including areas unrelated to visual processing (**Table 4**). There were significant differences in ALFF

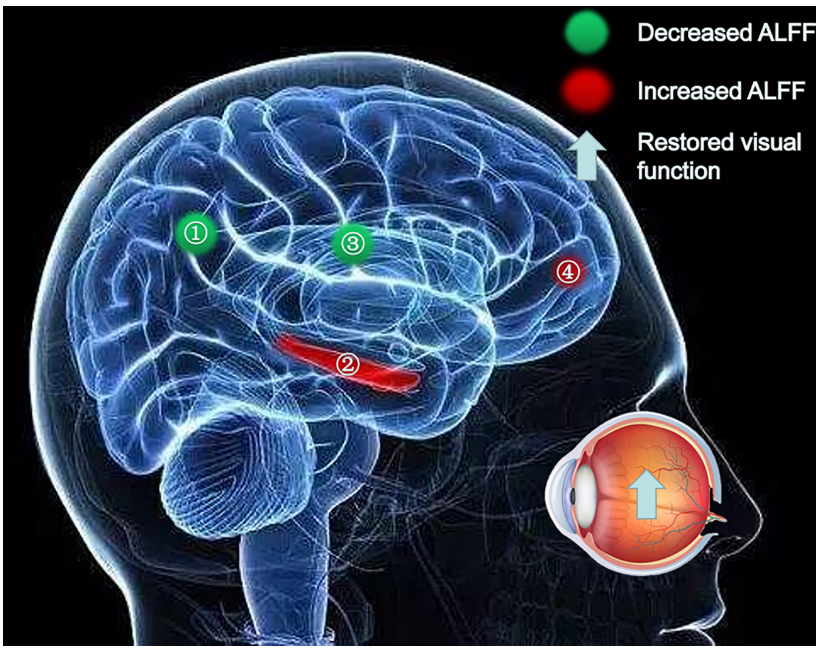

FIGURE 5 | Significant differences in spontaneous brain activity between the PRL and POL stages. Different brain regions that were observed: (1) Angular_R and Parietal_Inf_L; (2) Fusiform_R; (3) Cingulum_Mid_R; (4) Frontal_Inf_Orb_L. The red areas indicate increased ALFF values, and the green areas indicate decreased ALFF values. ALFF, amplitude of low-frequency fluctuation; L, left; R, right.

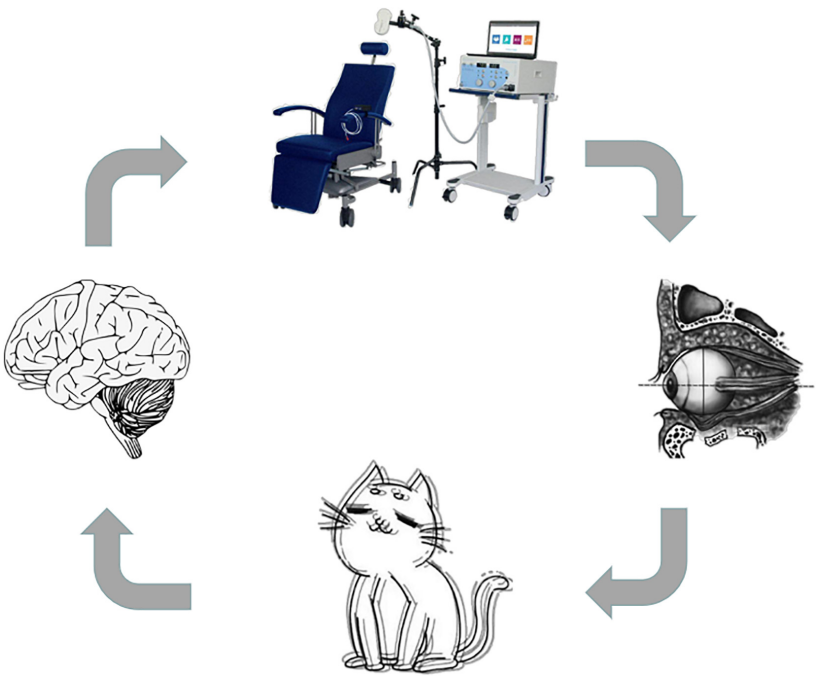

FIGURE 6 | Relationship between rTMS and diplopia. Patients with SA may develop diplopia after surgery. Once diplopia occurs, visual function may be affected, leading to abnormal neural activity in brain regions. SA, oblique amblyopia disease.

values in several brain areas between POT and PRT stages. Values were decreased in the FR and FIL regions, but increased in the AR, PIL, and CMR regions. These results demonstrate bidirectional changes in ALFF values between the POT and PRT stages. The ROC curve shows the clinical diagnostic significance of both the left parietal inferior, right cingulum middle, right

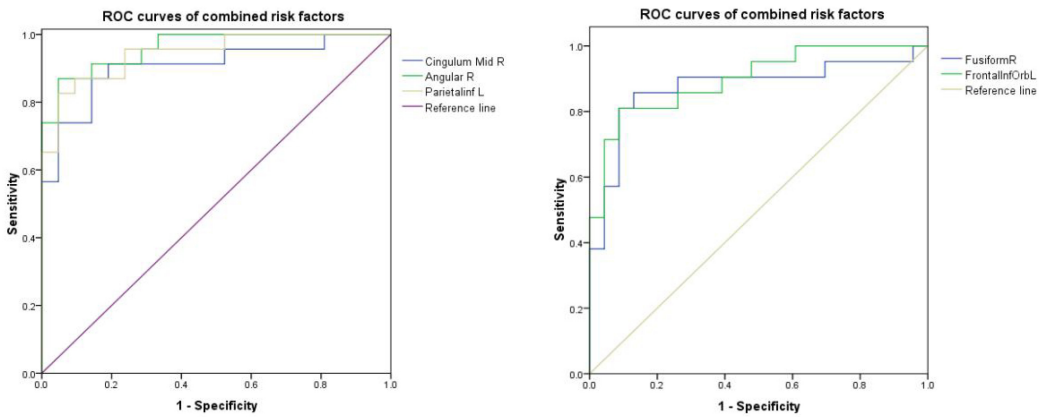

	Cutoff value	Sensitivity	Specificity	AUC	CI	p
Cingulum Mid R	1.173	0.869	0.857	0.907	0.816-0.998	<0.001
Angular R	1.286	0.869	0.952	0.961	0.898-0.942	<0.001
Parietal Inf L	1.512	0.826	0.952	0.944	0.868-0.985	<0.001
Fusiform R	0.735	0.857	0.869	0.874	0.757-0.990	<0.001
Frontal Inf Orb L	0.898	0.809	0.913	0.899	0.807-0.990	<0.001

FIGURE 7 | ROC curve analysis of the mean ALFF values of the affected brain regions in SA patients. ROC, receiver operating characteristic; AUC, area under the curve; CI, confidence interval; ROC, receiver operating characteristic; ALFF, amplitude of low-frequency fluctuation.

angular, right fusiform, and left frontal inferior orb regions. The AUCs of all these brain areas are high, indicating that ALFF may be used in clinical diagnosis of other brain diseases in SA patients after surgery.

Of these areas, the fusiform gyrus is located at the middle inferior part of the visual association cortex. The fusiform gyrus is not only used for face recognition, it is also responsible for the recognition of subcategories of objects (SparkNotes, 2007). In the fusiform face area, most studies have shown that the right hemisphere is more important for face recognition than the left. The face recognition area is located in the right fusiform gyrus, but it is involved in the recognition of a variety of complex stimuli and is a key brain region for acquiring the skills to distinguish similar objects (Tordesillas-Gutierrez et al., 2018). In patients with strabismic amblyopia, rTMS treatment significantly improved the condition of postoperative visual recovery, which may be related to the changes in the activity of the fusiform gyrus.

The angular gyrus, above Wernicke's area, at the parietal-occipital junction, is an important association area in the back of the brain. If the angular gyrus is removed, the visual and auditory perception of words will lose connection, causing dyslexia (a reading and writing disorder) and audio-visual aphasia. In the latter, the sufferer loses the connection between what is seen and what is heard and is unable to understand the meaning of the words (Tordesillas-Gutierrez et al., 2018; Palejwala et al., 2020).

The middle part of the right cingulate is the gyrus between the cingulate sulcus of the medial part of the brain hemisphere and the sulcus of the corpus callosum, belonging to the cortical part of the limbic system (Creel, 2012). This brain region transmits nerve impulses to the anterior cingulate gyrus and striatum and receives output from the amygdala, orbitofrontal gyrus, and medial frontal gyrus (Li et al., 2017). It has long been understood as an important part of the emotional circuit, involved in processes such as emotion and self-evaluation, and is closely associated with depressive symptoms. Audiovisual hallucinations, sensory illusions, and emotional symptoms caused by diplopia onset usually occur after surgery and accompanied by a slow recovery period of 12 months. After rTMS treatment, the condition

TABLE 3 | Amplitude of low-frequency fluctuation (ALFF) method applied in Ophthalmologic and Neurogenic diseases.

	Author	Year	Disease
Ophthalmologic diseases	Hilbert et al., 2019	2016	Optic neuritis
	Wang and Luo, 2004	2018	Comitant strabismus
	Makris et al., 2013	2019	Acute eye pain
	Bocca et al., 2015	2019	SAvanced monocular blindness
	Li et al., 2020	2020	Retinal detachment
Neurogenic diseases	Ferreira et al., 2011	2011	Alzheimer's disease
	Wang et al., 2020	2020	Parkinson's disease
	Suzuki et al., 2020	2020	Huntington's disease

TABLE 4 | Brain areas with altered amplitude of low-frequency fluctuation (ALFF) and potential impacts.

Brain areas	Experimental result	Brain function	Anticipated results
Cingulum Mid R	POT < PRT	Complex somatic and visceral motor function and pain response	Improve monitoring sensation and stereotactic and memory function
Angular R	POT < PRT	The production, expression and reception of language	Improve the ability to identify, explain, or remember words
Parietal inf L	POT < PRT	Ability in mathematics and logic	Improve logical thinking, divergent thinking and other aspects of the ability
Fusiform R	POT > PRT	Responsible for identifying the subcategories of objects	Improved ability to identify similar objects
Frontal Inf Orb L	POT > PRT	Responsible for thinking, calculation, and related to individual needs and emotions	Removal of schizophrenia, major depression and anxiety disorders

PRT, pre-rTMS; POT, post-rTMS; L, left; R, right.

will be greatly reduced (Sasaki et al., 2016; Craciun et al., 2018). Primary epileptic seizures in the cingulate gyrus are mainly complex partial seizures with characteristic automaticity, autonomic nervous dysfunction, affective changes, and urinary incontinence. We speculate that rTMS can effectively control epilepsy in part of the cingulate gyrus brain region. SA may cause abnormalities in cerebral blood flow and metabolism in the brain, resulting in hypofunction, which in turn leads to depression in patients (Craciun et al., 2018).

The lower and upper parietal gyrus contain visual segmentation groups, which can be distinguished according to structural or connection standards, topographic organization, or other functional standards. The conventional view that this brain area is a type of visual sensory area and contains numerous optic motor neurons and parietal visual function focuses on its role in spatial perception, so the lesions in this area will cause abnormalities in the relevant visual field. Therefore, our research showing a decreased ALFF of the left parietal inferior region may manifest as a defect in the visual field, and this pathological change will seriously affect the daily life of the patient (Hilbert et al., 2019).

Previous studies have demonstrated a link between the frontal cortex and emotion. The occurrence and development of the clinical symptoms of schizophrenia, major depression, and anxiety depend on the frontal cortex system. Evidence suggests that affective function, experience, expression, and load information processing have different neural representations in the frontal cortex (Wang and Luo, 2004; Makris et al., 2013; Bocca et al., 2015). Therefore, it is reasonable to infer that the effect of rTMS on the activity of the frontal cortex may be useful for the treatment of patients with schizophrenia, major depression, and anxiety disorders.

We believe that ALFF has clinical significance, it can detect abnormal changes in the brain activity of patients through fMRI in advance of this factor, and provide timely interventions to effectively reduce the sequelae and complications of SA such as diplopia. It is worth noting that the limitations of the current study, including differences in measurement standards and other factors, require further unification of measurement scales in in-depth studies to verify the findings. The clinical features we used in this study were not rigorous. For example, different SA patients have different degrees of visual acuity recovery after surgery, some of which were not significantly different from the preoperative stage. Therefore, attention should be paid to these problems in future studies and the sample size should be expanded to accurately evaluate the changes of brain ALFF indexes in SA patients after surgery. In addition, the control group of patients treated with rTMS after SA surgery was not included in this study, changes in ALFF values generated by longitudinal brain recombination after SA surgery were not measured. As a result, in the results obtained in this study, the difference in ALFF value is not solely affected by rTMS treatment, and part of the difference may be related to longitudinal brain reorganization, the specific differences need to be further studied. Despite these deficiencies, this study revealed specific changes and effects of rTMS on ALFF in the brain regions of SA patients.

CONCLUSION

In summary, we confirmed that within SA patients ALFF changes significantly in some brain regions after rTMS. Changes in ALFF reflect increases or decreases in activity within brain regions and may partly reflect the degree of improvement in visual dysfunction caused by postoperative complications in patients with SA. ALFF may be used for clinical diagnosis and evaluation of postoperative rehabilitation in patients with SA.

DATA AVAILABILITY STATEMENT

The raw data supporting the conclusions of this article will be made available by the authors, without undue reservation.

ETHICS STATEMENT

All research methods were approved by the Committee of the Medical Ethics of the First Affiliated Hospital of Nanchang University and were in accordance with the 1964 Helsinki declaration and its later amendments or comparable ethical standards. All subjects were explained the purpose, method, potential risks and signed an informed consent form. Written informed consent to participate in this study was provided by the participants' legal guardian/next of kin. Written informed consent was obtained from the individual(s), and minor(s)' legal guardian/next of kin, for the publication of any potentially identifiable images or data included in this article.

AUTHOR CONTRIBUTIONS

Y-NW and Y-CP analyzed the data and drafted the manuscript. H-YS, Q-MG, and Y-CP assisted with data interpretation and figure composing. L-JZ, R-BL, and Q-YL collected the data. YS conceived, designed, and directed the study and finally revised and approved the manuscript.

FUNDING

The Central Government Guides Local Science and Technology Development Foundation (No: 20211ZDG02003); Key Research Foundation of Jiangxi Province (Nos: 20181BBG70004 and 20203BBG73059); Excellent Talents Development Project of Jiangxi Province (No: 20192BCBL23020); Natural Science Foundation of Jiangxi Province (No: 20181BAB205034); Grassroots Health Appropriate Technology "Spark Promotion Plan" Project of Jiangxi Province (No: 20188003); Health Development Planning Commission Science Foundation of Jiangxi Province (Nos: 20201032 and 202130210); Health Development Planning Commission Science TCM Foundation of Jiangxi Province (Nos: 2018A060 and 2020A0087); Education Department Foundation of Jiangxi Province (Nos: GJJ200157, GJJ200159, and GJJ200169).

REFERENCES

Abdelrahman, A. A., Noaman, M., Fawzy, M., Moheb, A., Karim, A. A., and Khedr, E. M. (2021). A double-blind randomized clinical trial of high frequency rTMS over the DLPFC on nicotine dependence, anxiety and depression. *Sci. Rep.* 11:1640. doi: 10.1038/s41598-020-80927-5

Arns, M., Bervoets, C., van Eijndhoven, P., Baeken, C., van den Heuvel, O. A., Aleman, A., et al. (2019). Consensusverklaring voor de toepassing van rTMS bij depressie in Nederland en België [Consensus statement on the application of rTMS in depression in the Netherlands and Belgium]. *Tijdschr. Psychiatr.* 61, 411–420.

Bocca, F., Töllner, T., Müller, H. J., and Taylor, P. C. (2015). The right angular gyrus combines perceptual and response-related expectancies in visual search: TMS-EEG evidence. *Brain Stimul.* 8, 816–822. doi: 10.1016/j.brs.2015.02.001

Brown, H. D. H., Woodall, R. L., and Kitching, R. E. (2016). Using magnetic resonance imaging to assess visual deficits: a review. *Ophthalmic Physiol. Opt.* 36, 240–265. doi: 10.1111/opo.12293

Brunoni, A. R., Chaimani, A., Moffa, A. H., Razza, L. B., Gattaz, W. F., Daskalakis, Z. J., et al. (2017). Repetitive Transcranial Magnetic Stimulation for the Acute Treatment of Major Depressive Episodes: A Systematic Review With Network Meta-analysis. *JAMA Psychiatry* 74, 143–152. doi: 10.1001/jamapsychiatry.2016.3644

Cerulli Irelli, E., Di Pietro, G., Fisco, G., Orlando, B., Asci, F., Salamone, E. M., et al. (2021). Acute-onset binocular diplopia in neurological unit: aetiological factors and diagnostic assessment. *Acta Neurol. Scand.* 144, 92–98. doi: 10.1111/ane.13425

Chan, S. T., Tang, K. W., Lam, K. C., Chan, L. K., Mendola, J. D., and Kwong, K. K. (2004). Neuroanatomy of adult strabismus: a voxel-based morphometric analysis of magnetic resonance structural scans. *Neuroimage* 22, 986–994. doi: 10.1016/j.neuroimage.2004.02.021

Chen, X., Fu, Z., Yu, J., Ding, H., Bai, J., Chen, J., et al. (2014). Prevalence of amblyopia and strabismus in Eastern China: results from screening of preschool children aged 36–72 months. *Br. J. Ophthalmol.* 100, 515–519. doi: 10.1136/bjophthalmol-2015-306999

Chou, Y. H., Ton That, V., and Sundman, M. (2020). A systematic review and meta-analysis of rTMS effects on cognitive enhancement in mild cognitive impairment and Alzheimer's disease. *Neurobiol. Aging* 86, 1–10. doi: 10.1016/j.neurobiolaging.2019.08.020

Conner, I. P., Odom, J. V., Schwartz, T. L., and Mendola, J. D. (2007). Monocular activation of V1 and V2 in amblyopic adults measured with functional magnetic resonance imaging. *J. AAPOS.* 11, 341–350. doi: 10.1016/j.jaapos.2007.01.119

Craciun, L., Taussig, D., Ferrand-Sorbets, S., Pasqualini, E., Biraben, A., Delalande, O., et al. (2018). Investigation of paediatric occipital epilepsy using stereo-EEG reveals a better surgical outcome than in adults, especially when the supracalcarine area is affected. *Epileptic Disord.* 20, 346–363. doi: 10.1684/epd.2018.1000

Creel, D. J. (2012). *Visually Evoked Potentials—Webvision—NCBI Bookshelf*. Salt Lake City: University of Utah Health Sciences Center.

Fazzi, D. E., and Bianchi, P. E. (2016). "Visual development in childhood," in *Visual Impairments and Developmental Disorders: From diagnosis to rehabilitation*, ed. L. John (London: Mariani Foundation Paediatric Neurology).

Ferreira, L. K., Diniz, B. S., Forlenza, O. V., Busatto, G. F., and Zanetti, M. V. (2011). Neurostructural predictors of Alzheimer's disease: a meta-analysis of VBM studies. *Neurobiol Aging* 32, 1733–1741. doi: 10.1016/j.neurobiolaging.2009.11.008

Goodyear, B. G., and Menon, R. S. (2001). Brief visual stimulation allows mapping of ocular dominance in visual cortex using fMRI. *Hum. Brain Mapp.* 14, 210–217. doi: 10.1002/hbm.1053

Goseki, T., Suh, S. Y., Robbins, L., Pineles, S. L., Demer, J. L., and Velez, F. G. (2021). Reply to: comment on Prevalence of Sagging Eye Syndrome in Adults with Binocular Diplopia. *Am. J. Ophthalmol.* 221, 324–325. doi: 10.1016/j.ajo.2020.08.010

Gunton, K. B., Wasserman, B. N., and Debenedictis, C. (2015). Strabismus. *Prim. Care* 42, 393–407.

Hilbert, S., McAssey, M., Bühner, M., Schwaferts, P., Gruber, M., Goerigk, S., et al. (2019). Right hemisphere occipital rTMS impairs working memory in visualizers but not in verbalizers. *Sci. Rep.* 9:6307. doi: 10.1038/s41598-019-42733-6

Jefferis, J. M., Connor, A. J., and Clarke, M. P. (2015). Amblyopia. *BMJ* 351:h5811. doi: 10.1136/bmj.h5811

Levi, D. (2013). Linking assumptions in amblyopia. *Vis. Neurosci.* 30, 277–287. doi: 10.1017/S0952523813000023

Li, B., Liu, Y. X., Li, H. J., Yuan, Q., Zhu, P. W., Ye, L., et al. (2020). Reduced gray matter volume in patients with retinal detachment: evidence from a voxel-based morphometry study. *Acta Radiol.* 61, 395–403. doi: 10.1177/0284185119861898

Li, D., Zhang, H., Jia, W., Zhang, L., Zhang, J., Liu, W., et al. (2017). Significance of the Tentorial Alignment in Protecting the Occipital Lobe with the Poppen Approach for Tentorial or Pineal Area Meningiomas. *World Neurosurg.* 108, 453–459. doi: 10.1016/j.wneu.2017.08.013

Liang, M., Xie, B., Yang, H., Yin, X., Wang, H., Yu, L., et al. (2017). Altered interhemispheric functional connectivity in patients with anisometropic and strabismic amblyopia: a resting-state fMRI study. *Neuroradiology* 59, 517–524. doi: 10.1007/s00234-017-1824-0

Maconachie, G. D., and Gottlob, I. (2015). The challenges of amblyopia treatment. *Biomed. J.* 38, 510–516. doi: 10.1016/j.bj.2015.06.001

Makris, N., Preti, M. G., Wassermann, D., Rathi, Y., Papadimitriou, G. M., Yergatian, C., et al. (2013). Human middle longitudinal fascicle: segregation and behavioral-clinical implications of two distinct fiber connections linking temporal pole and superior temporal gyrus with the angular gyrus or superior parietal lobule using multi-tensor tractography. *Brain Imag. Behav.* 7, 335–352. doi: 10.1007/s11682-013-9235-2

Malkani, R. G., and Zee, P. C. (2020). Brain Stimulation for Improving Sleep and Memory. *Sleep Med. Clin.* 15, 101–115. doi: 10.1016/j.jsmc.2019.11.002

McClintock, S. M., Reti, I. M., Carpenter, L. L., McDonald, W. M., Dubin, M., Taylor, S. F., et al. (2018). Consensus Recommendations for the Clinical Application of Repetitive Transcranial Magnetic Stimulation (rTMS) in the Treatment of Depression. *J. Clin. Psychiatry* 79:16cs10905. doi: 10.4088/JCP.16cs10905

Min, Y. L., Su, T., Shu, Y. Q., Liu, W. F., Chen, L. L., Shi, W. Q., et al. (2018). Altered spontaneous brain activity patterns in strabismus with amblyopia patients using amplitude of low-frequency fluctuation: a resting-state fMRI study. *Neuropsychiatr. Dis. Treatment* 14, 2351–2359. doi: 10.2147/NDT.S171462

Mohney, B. G., Martinez, J. M., Holmes, J. M., and Diehl, N. N. (2012). Incidence of strabismus in an adult population. *J. AAPOS.* 16:e23. doi: 10.1016/j.jaapos.2011.12.089

National Eye Institute (2016). *Facts About Amblyopia*. Bethesda: National Eye Institute.

Palejwala, A. H., O'Connor, K. P., Pelargos, P., Briggs, R. G., Milton, C. K., Conner, A. K., et al. (2020). Anatomy and white matter connections of the lateral occipital cortex. *Surg. Radiol. Anat.* 42, 315–328. doi: 10.1007/s00276-019-02371-z

Peña Urbina, P., Hernández García, E., Gómez de Liaño Sánchez, R., and Domingo Gordo, B. (2021). Restrictive strabismus and diplopia after conjunctivodacryocystorhinostomy with Jones tube. *J. Fr. Ophtalmol.* 44, e187–e190. doi: 10.1016/j.jfo.2020.08.005

Rehn, S., Eslick, G. D., and Brakoulias, V. (2018). A Meta-Analysis of the Effectiveness of Different Cortical Targets Used in Repetitive Transcranial Magnetic Stimulation (rTMS) for the Treatment of Obsessive-Compulsive Disorder (OCD). *Psychiatry Q.* 89, 645–665. doi: 10.1007/s11126-018-9566-7

Rigucci, S., Serafini, G., Pompili, M., Kotzalidis, G. D., and Tatarelli, R. (2010). Anatomical and functional correlates in major depressive disorder: the contribution of neuroimaging studies. *World J. Biol. Psychiatry* 11, 165–180. doi: 10.1080/15622970903131571

Sasaki, F., Kawajiri, S., Nakajima, S., Yamaguchi, A., Tomizawa, Y., Noda, K., et al. (2016). Occipital lobe seizures and subcortical T2 and T2* hypointensity associated with nonketotic hyperglycemia: a case report. *J. Med. Case Rep.* 10:228. doi: 10.1186/s13256-016-1010-8

Schwartz, M. W., Bell, L. M., Bingham, P. M., Chung, E. K., Cohen, M. I., Friedman, D. F., et al. (2002). *The 5-minute Pediatric Consult*, 3rd Edn. Philadelphia: Lippincott Williams & Wilkins.

Sebastianelli, L., Versace, V., Martignago, S., Brigo, F., Trinka, E., Saltuari, L., et al. (2017). Low-frequency rTMS of the unaffected hemisphere in stroke patients: A systematic review. *Acta Neurol. Scand.* 136, 585–605. doi: 10.1111/ane.12773

SparkNotes. (2007). *Brain Anatomy: Parietal and Occipital Lobes*. New York: SparkNotes.

Spiegel, D. P., Byblow, W. D., Hess, R. F., and Thompson, B. (2013). Anodal transcranial direct current stimulation transiently improves contrast sensitivity and normalizes visual cortex activation in individuals with amblyopia. *Neurorehabilit. Neural Repair* 27, 760–769. doi: 10.1177/1545968313491006

Suzuki, F., Sato, N., Ota, M., Sugiyama, A., Shigemoto, Y., Morimoto, E., et al. (2020). Discriminating chorea-acanthocytosis from Huntington's disease with single-case voxel-based morphometry analysis. *J. Neurol. Sci.* 408:116545. doi: 10.1016/j.jns.2019.116545

Tarczy-Hornoch, K., Cotter, S. A., Borchert, M., McKean-Cowdin, R., Lin, J., Wen, G., et al. (2013). Prevalence and causes of visual impairment in Asian and non-Hispanic white preschool children: multiethnic pediatric eye disease study. *Ophthalmology* 120, 1220–1226. doi: 10.1016/j.ophtha.2012.12.029

Thompson, B., Mansouri, B., Koski, L., and Hess, R. F. (2008). Brain plasticity in the adult: modulation of function in amblyopia with rTMS. *Curr. Biol.* 18, 1067–1071. doi: 10.1016/j.cub.2008.06.052

Tordesillas-Gutierrez, D., Ayesa-Arriola, R., Delgado-Alvarado, M., Robinson, J. L., Lopez-Morinigo, J., Pujol, J., et al. (2018). The right occipital lobe and poor insight in first-episode psychosis. *PLoS One* 13:e0197715. doi: 10.1371/journal.pone.0197715

Wang, N. Y., and Luo, Y. J. (2004). Emotional abnormalities in patients with prefrontal cortex damage. *Adv. Psychol. Sci.* 2, 161–167.

Wang, X., Cui, D., Zheng, L., Yang, X., Yang, H., and Zeng, J. (2012). Combination of blood oxygen level-dependent functional magnetic resonance imaging and visual evoked potential recordings for abnormal visual cortex in two types of amblyopia. *Mol. Vis.* 18, 909–919.

Wang, Z., Liu, Y., Ruan, X., Li, Y., Li, E., Zhang, G., et al. (2020). Aberrant amplitude of low-frequency fluctuations in different frequency bands in patients with Parkinson's disease. *Front. Aging Neurosci.* 12:576682. doi: 10.3389/fnagi.2020.576682

Webber, A. L., and Wood, J. (2005). Amblyopia: prevalence, natural history, functional effects and treatment. *Clin. Exp. Optometr.* 88, 365–375. doi: 10.1111/j.1444-0938.2005.tb05102.x

Yang, L. L., Zhao, D., Kong, L. L., Sun, Y. Q., Wang, Z. Y., Gao, Y. Y., et al. (2019). High-frequency repetitive transcranial magnetic stimulation (rTMS) improves neurocognitive function in bipolar disorder. *J. Affect. Disord.* 246, 851–856. doi: 10.1016/j.jad.2018.12.102

Conflict of Interest: The authors declare that the research was conducted in the absence of any commercial or financial relationships that could be construed as a potential conflict of interest.

Publisher's Note: All claims expressed in this article are solely those of the authors and do not necessarily represent those of their affiliated organizations, or those of the publisher, the editors and the reviewers. Any product that may be evaluated in this article, or claim that may be made by its manufacturer, is not guaranteed or endorsed by the publisher.

frontiers | Frontiers in Human Neuroscience

ORIGINAL RESEARCH
published: 27 April 2022
doi: 10.3389/fnhum.2022.802996

The Effect of Repetitive Transcranial Magnetic Stimulation of Cerebellar Swallowing Cortex on Brain Neural Activities: A Resting-State fMRI Study

Linghui Dong[1†], *Wenshuai Ma*[2†], *Qiang Wang*[1], *Xiaona Pan*[1], *Yuyang Wang*[1], *Chao Han*[1] *and Pingping Meng*[1*]

[1] *Department of Rehabilitation Medicine, Affiliated Hospital of Qingdao University, Qingdao, China,* [2] *Department of Radiology, Affiliated Hospital of Qingdao University, Qingdao, China*

OPEN ACCESS

Edited by:
Filippo Brighina, University of Palermo, Italy

Reviewed by:
Bülent Cengiz, Gazi University, Turkey
Satoshi Maesawa, Nagoya University Graduate School of Medicine, Japan

***Correspondence:**
Pingping Meng
neuroreh_meng@163.com

[†] *These authors share first authorship*

Specialty section:
This article was submitted to Brain Imaging and Stimulation, a section of the journal Frontiers in Human Neuroscience

Received: *08 December 2021*
Accepted: *22 March 2022*
Published: *27 April 2022*

Citation:
Dong L, Ma W, Wang Q, Pan X, Wang Y, Han C and Meng P (2022) The Effect of Repetitive Transcranial Magnetic Stimulation of Cerebellar Swallowing Cortex on Brain Neural Activities: A Resting-State fMRI Study. Front. Hum. Neurosci. 16:802996. doi: 10.3389/fnhum.2022.802996

Objective: The effects and possible mechanisms of cerebellar high-frequency repetitive transcranial magnetic stimulation (rTMS) on swallowing-related neural networks were studied using resting-state functional magnetic resonance imaging (rs-fMRI).

Method: A total of 23 healthy volunteers were recruited, and 19 healthy volunteers were finally included for the statistical analysis. Before stimulation, the cerebellar hemisphere dominant for swallowing was determined by the single-pulse TMS. The cerebellar representation of the suprahyoid muscles of this hemisphere was selected as the target for stimulation with 10 Hz rTMS, 100% resting motor threshold (rMT), and 250 pulses, with every 1 s of stimulation followed by an interval of 9 s. The motor evoked potential (MEP) amplitude of the suprahyoid muscles in the bilateral cerebral cortex was measured before and after stimulation to evaluate the cortical excitability. Forty-eight hours after elution, rTMS was reapplied on the dominant cerebellar representation of the suprahyoid muscles with the same stimulation parameters. Rs-fMRI was performed before and after stimulation to observe the changes in amplitude of low-frequency fluctuation (ALFF) and regional homology (ReHo) at 0.01–0.08 Hz, 0.01–0.027 Hz, and 0.027–0.073 Hz.

Results: After cerebellar high-frequency rTMS, MEP recorded from swallowing-related bilateral cerebral cortex was increased. The results of rs-fMRI showed that at 0.01–0.08 Hz, ALFF was increased at the pons, right cerebellum, and medulla and decreased at the left temporal lobe, and ReHo was decreased at the left insular lobe, right temporal lobe, and corpus callosum. At 0.01–0.027 Hz, ALFF was decreased at the left temporal lobe, and ReHo was decreased at the right temporal lobe, left putamen, and left supplementary motor area.

Conclusion: Repetitive transcranial magnetic stimulation of the swallowing cortex in the dominant cerebellar hemisphere increased the bilateral cerebral swallowing cortex

excitability and enhanced pontine, bulbar, and cerebellar spontaneous neural activity, suggesting that unilateral high-frequency stimulation of the cerebellum can excite both brainstem and cortical swallowing centers. These findings all provide favorable support for the application of cerebellar rTMS in the clinical practice.

Keywords: swallowing, repetitive transcranial magnetic stimulation (rTMS), motor evoked potentials (MEP), cerebellum, resting-state functional magnetic resonance imaging (rs-fMRI)

INTRODUCTION

Dysphagia is a common complication after stroke, and it has been documented that more than half of stroke patients have swallowing problems (Singh and Hamdy, 2006; Geeganage et al., 2012). Dysphagia may lead to various complications such as malnutrition, dehydration, pneumonia, prolonged hospitalization cycle, and even death (Bonilha et al., 2014; Cohen et al., 2016). The traditional rehabilitation methods for post-stroke dysphagia (PSD) include tongue muscle training, levator laryngeal muscle training, sensory stimulation training, dietary modification, and others, but these methods have poor efficacy (Martino and Mcculloch, 2016; Guillén-Solà et al., 2017). In order to accelerate the recovery speed and recovery rate of PSD patients, researchers are constantly exploring new treatment methods (Fisicaro et al., 2019).

Repetitive transcranial magnetic stimulation (rTMS) is a noninvasive brain stimulation technique, which can increase cortical excitability of the target area at high frequency (>1 Hz) and decrease it at low frequency (≤1 Hz) (Iglesias, 2020). Several studies have shown that recovery of swallowing function in PSD is associated with regulated excitability of the swallowing-related cortex and that rTMS treatment has a positive effect in patients with PSD (Khedr et al., 2009; Khedr and Abo-Elfetoh, 2010; Kim et al., 2011; Du et al., 2016; Cheng et al., 2017; Zhang et al., 2019). At present, the targets of rTMS treatment for PSD patients are mainly located in the cerebral cortex, but some patients have problems such as suboptimal efficacy and limited application, which promote clinicians to constantly search for new therapeutic targets.

As cerebellar function continues to be explored, multiple studies on healthy volunteers have shown that cerebellar rTMS may have a positive effect on swallowing function (Jayasekeran et al., 2011; Vasant et al., 2015; Sasegbon et al., 2019, 2020). This implies that the cerebellum has the potential to be a novel therapeutic target for PSD. Jayasekeran first demonstrated in 2011 that motor evoked potentials (MEPs) similar to those of pharyngeal constrictors can be generated in healthy humans by cerebellar single TMS. These findings suggested that cerebellar stimulation could induce swallowing movements in humans (Jayasekeran et al., 2011). Subsequently, sustained, high-frequency (5, 10, and 20 Hz) rTMS of unilateral hemispherical cerebellum showed significantly increased MEP amplitude at the swallowing-related cortex of both cerebral hemispheres, with maximum effect maintained for at least 30 min at 250 pulses (Vasant et al., 2015).

In order to verify whether the excitatory cortical effect produced by cerebellar rTMS can improve PSD, Sasegbon (Sasegbon et al., 2019, 2020) simulated post-stroke swallowing disorder in healthy volunteers using a total of 600 low-frequency pulses for 10-min inhibitory stimulation in the cortical region representative of pharyngeal constrictor muscle. Following this, rTMS (10 Hz, 250 pulses) was performed on the cerebellum, and results indicated that unilateral or bilateral stimulation could completely reverse simulated dysphagia and improve the excitability of the cortex related to bilateral cerebral swallowing, with bilateral stimulation more effective than unilateral stimulation. However, the above studies using electrophysiology show changes in the excitability of swallowing-related cortex but not the mechanism by which cerebellar rTMS affects this cortical region, or whether cerebellar stimulation affects other swallowing-related networks. Before cerebellar rTMS can be applied clinically, its effects on brain function need to be explored.

Recently, resting-state functional magnetic resonance imaging (rs-fMRI) has played an important role in studying brain functional activity as a safe, noninvasive technique, which reflects neural activity *via* blood oxygen level-dependent (BOLD) signals (Mosier et al., 1999; Mosier and Bereznaya, 2001; Suzuki et al., 2003; Zhang et al., 2020; Ma et al., 2021). Amplitude of low-frequency fluctuations (ALFF) and regional homogeneity (ReHo) are two classic local indices of rs-fMRI, which are widely used due to good stability (Qiu et al., 2019; Wu et al., 2020). ALFF has been calculated as the mean amplitude of the BOLD signal deviating from baseline over a short period of time, reflecting the strength of the spontaneous neural activity in voxels (Zang et al., 2007). ReHo can indirectly reflect the synchrony of neural activity in local brain regions by calculating the time series consistency between the response at each voxel and its neighbors (Zang et al., 2004). Increased ReHo indicates that neural activity in local brain regions is synchronized. Reduced ReHo indicates a consistent reduction in neural activity.

Most of the current research on rs-fMRI focuses on low-frequency oscillatory signals in the classical frequency band (0.01–0.08 Hz), which are considered most relevant to neural activity. However, it has also been found that sensitivity to oscillatory signals in different frequency bands varies with brain regions and that sensitivity to wider frequency bands is reduced in some brain regions, leading to reduced detection of brain activity in those regions. Therefore, ALFF and ReHo are assessed in response to several different frequency bands, such as the slow-4 band (0.027–0.073 Hz) and the slow-5 band (0.01–0.027 Hz), for more targeted investigation of brain functional activity (Zuo et al., 2010).

In this study, we used the multifrequency ALFF and ReHo methods to observe regional changes in brain function after

high-frequency rTMS of the cerebellum. The study aimed to explore the effects and mechanisms of cerebellar rTMS on swallowing-related neural networks and ultimately to facilitate its clinical application.

MATERIALS AND METHODS

Participants

This study included 23 healthy volunteers recruited at the Department of Rehabilitation, the Affiliated Hospital of Qingdao University, from September 2020 to February 2021. The study was reviewed by the ethics committee of the Affiliated Hospital of Qingdao University (ethics approval number: qyfy wzll 26154), and all volunteers provided a signed declaration of informed consent for participation. All volunteers received unilateral (dominant side) cerebellar hemisphere 10 Hz, 250 pulse rTMS stimulation.

Inclusion Criteria

1). Age $\geq$ 18 years.
2). No history of diseases, such as Parkinson's disease or stroke, which may cause dysphagia.
3). No contraindications to the use of rTMS or to fMRI (history of seizures, intracorporeal implantation of pacemaker or drug pump, cranial metal implant, claustrophobia, and others).
4). Normal cognitive function and ability to cooperate with the study procedures.

Exclusion Criteria

1). Current use of drugs affecting the central nervous system.
2). Current pregnancy, late-stage malignancy, history of brain surgery, or central nervous system disease.
3). Mandibular skin breakdown, infection, and other effects of surface electrode sheet placement.
4). Combined heart, lung, liver, kidney, and other important organ diseases, and if the condition is critical.

Experimental Procedure

One group of healthy volunteers was included. Single-pulse TMS was used to stimulate bilateral cerebellar hot-pot of suprahyoid muscles, observing and comparing the bilateral resting motor threshold (rMT) and MEP. The dominant cerebellar hemisphere was defined as that with lower rMT, or if rMT was symmetrical, higher MEP was observed in the hemisphere. The dominant cerebellar representation of suprahyoid muscles was stimulated with 10 Hz rTMS, 100% rMT, and 250 pulses, with every 1 s of stimulation followed by an interval of 9 s. Before and after stimulation, the MEP amplitude of bilateral cerebral representation of suprahyoid muscles was measured to evaluate the excitability of swallowing-related cerebral cortex.

Forty-eight hours after elution, rTMS was repeated using the same parameters. Rs-fMRI was performed before and after stimulation to observe changes in ALFF and ReHo at 0.01–0.08 Hz, 0.01–0.027 Hz, and 0.027–0.073 Hz. **Figure 1** shows the study design and flow chart.

TMS and Electromyography

A circular coil (outer ring diameter: 70 mm) connected to CCY-IA TMS (Yiruide CCY-IA, Wuhan, China) was used, with a maximum stimulator output of 3.0 Tesla. Volunteers were seated, and alcohol was used to cleanse the neck skin and increase electrode conductivity. The circular coil was positioned at 45° tangential to the skull, and suprahyoid muscles electromyography was recorded *via* surface electrodes. The recording electrode was placed 2 cm left and right at the midpoint of the line connecting the mandible to the middle of the hyoid bone, and the reference electrode was affixed to the angle of the mandible. Coil movements were made in a region of 2–4 cm anterior and 4–6 cm lateral to the vertex of the skull, using 80% output, to obtain the maximal MEP at the location of suprahyoid muscles' motor representation of the cerebral cortex. Similarly, to find the cerebellar representation of suprahyoid muscles, the coil was moved around 1 cm lateral to and below the occipital external carina.

Resting MT

Resting MT was defined as the lowest TMS intensity that can evoke MEP amplitude greater than 50 μV in five out of ten trials, expressed as a percentage of the stimulator's maximum output intensity.

The MEP Amplitude

The MEP amplitude used for comparison was measured in the bilateral cerebral motor representation of the suprahyoid muscles, with 100% rMT as the stimulation intensity, measured for five times, and the average value was taken.

Image Data Acquisition

A Signa HDX 3.0T (GE Healthcare, USA) nuclear magnetic resonance instrument was used to collect fMRI data. Volunteers were in the supine position with their head position fixed bilaterally using foam pads, eyes closed using an eye mask, and earplugs to protect hearing. Volunteers were instructed to relax, slow their breathing, and refrain from falling asleep during the scanning procedure. The fMRI scanning procedure began with a 3PL localizer scan, followed by an assessment calibration, and a subsequent blood signal scan. A total of 128 volumes were acquired using an echo-planar imaging sequence (30 axial slices, repetition time = 3,000 ms, echo time = 40 ms, flip angle = 90°, matrix = 128 × 128, in-plane resolution of 1.875 mm × 1.875 mm, thickness/gap = 5/0 mm). Subsequently, 3D T1-weighted anatomical images were acquired (248 sagittal slices, repetition time = 5.5 s, echo time =1.7 ms, matrix = 256 × 256, voxel size 1 mm × 1 mm × 1.2 mm).

Image Data Preprocessing

Based on the Matlab 2018a software platform, preprocessing was performed using RESTplus v1.24. The image of the left dominant side was flipped to the right before statistical analysis, using a new version of RESTplus_v1.25.

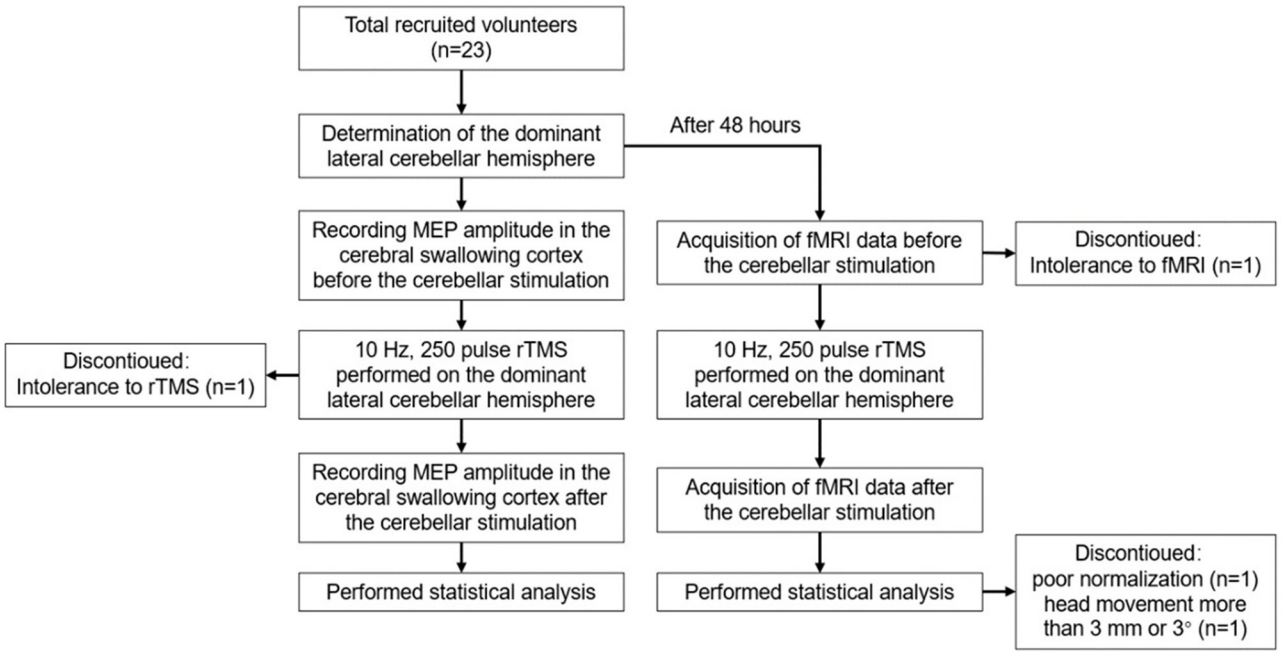

FIGURE 1 | The study design and flowchart.

Image Preprocessing

Image preprocessing was conducted using REST plus v1.24 as follows: (1) Data conversion from DICOM to Neuroimaging Informatics Technology Initiative format; (2) Removal of the first 10 time points; (3) Slice timing; (4) Image realignment; (5) Image normalization; (6) Image detrending; (7) Nuisance covariates regression: Friction 24, white matter signal, and cerebrospinal fluid signal; (8) ALFF and ReHo were calculated at three filtered bands: 0.01–0.08 (classical frequency band), 0.01 – 0.027 (slow-5), and 0.027–0.073 (slow-4); and (9) Data exclusion due to poor normalization or head movement more than 3 mm or 3°.

The global mean ALFF (mALFF) maps and mean fractional ALFF (mfALFF) maps at three bands were calculated for each subject using RESTplus v1.82 software in MATLAB prior to statistical analysis.

Smoothing

The mALFF and mean ReHo (mReHo) in the above frequency bands were smoothed using a 4 x 4 x 4 kernel in SPM software version 12.

Flip

Subjects turning to the right in response to the left side of the stimulus used the software package RESTplus v1.25.

Statistical Analysis

SPSS version 22.0 was used to conduct paired samples *t*-tests comparing the MEP amplitude before and after stimulation.

Resting-state fMRI analysis was conducted using paired *t*-tests and FD_Power taut regression as a covariate in the Matlab 2018a software platform and the DPABI V5.1 software package. The resulting T-maps were Gaussian random field corrected, voxel $p < 0.05$, cluster $p < 0.05$, two-tailed test, default corner connected, default cluster size adopted, and finally output reported.

RESULTS

Participants

Of a total of 23 healthy volunteers recruited for this study, two withdrew due to poor compliance or tolerance of the rTMS and fMRI procedures, and data from another two were excluded from preprocessing due to movement exceeding 3 mm or 3°, or poor registration. Therefore, data from 19 participants were included (thirteen female and six male participants, mean age 25.53 ± 4.29 years). In six out of the 19 participants, the dominant cerebellar hemisphere was on the right, while in others, it was on the left.

MEP Amplitude Changes in Cerebral Swallowing Cortex

We found that the MEP amplitude in the swallowing-related cortex was significantly elevated in both ipsilateral and contralateral hemispheres after stimulation ($p < 0.05$; **Figure 2**), indicating that high-frequency rTMS stimulation of the dominant lateral cerebellum can induce bilateral elevation of the swallowing cortex excitability.

Rs-fMRI Analyses Under Different Frequency Bands

Resting-State fMRI Results Based on the ALFF Method

After cerebellar stimulation, in the classical frequency band we found that ALFF was significantly elevated at the pons, right cerebellum, and medulla and significantly

reduced at the left temporal lobe ($p < 0.05$; **Figure 3** and **Table 1**), indicating that unilateral cerebellar stimulation can produce increased spontaneous neural activity in the cerebellum and brainstem and suppress activity at the contralateral temporal lobe. In addition, we found that ALFF at the left temporal lobe was also decreased in the slow-4 band and slow-5 band ($p < 0.05$; **Figures 4**, **5** and **Table 1**).

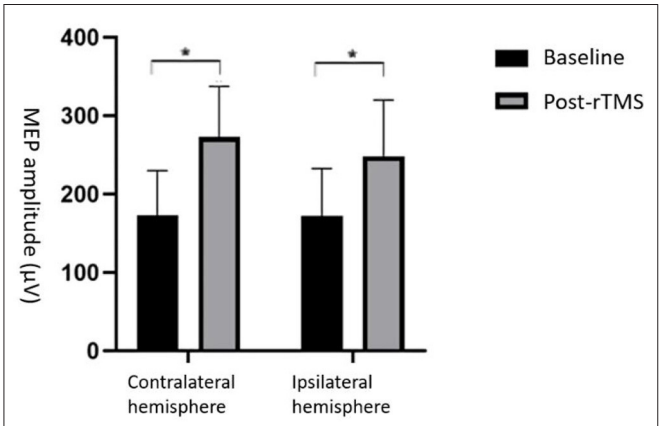

FIGURE 2 | Comparison of MEP amplitude between rTMS and baseline. MEP amplitude increased in both cerebral hemispheres *$p < 0.05$.

TABLE 1 | Brain regions with alteration of ALFF after cerebellar rTMS.

Brain region	Cluster size (voxel)	Coordinates (x, y, z)	Peak *t*-value
Classical frequency band (0.01–0.08 Hz)			
Brainstem	149	12, −42, −39	3.972
Pons	67		
Cerebellum_9_R (aal)	21		
Medulla	19		
Temporal_Sup_L (aal)	260	−51, 3, −9	−4.6805
Slow-4 band (0.027–0.073 Hz)			
Temporal_Sup_L (aal)	175	−60, 6, −9	−4.2171
Slow-5 band (0.01–0.027 Hz)			
Temporal_Pole_Sup_L (aal)	292	−57, 9, 6	−6.1004

aal, anatomical automatic labeling; L, left; R, right; T, statistical value of peak voxel showing ALFF changes pre- and post-rTMS (negative values: ALFF decreased after rTMS; positive values: ALFF increased after rTMS).

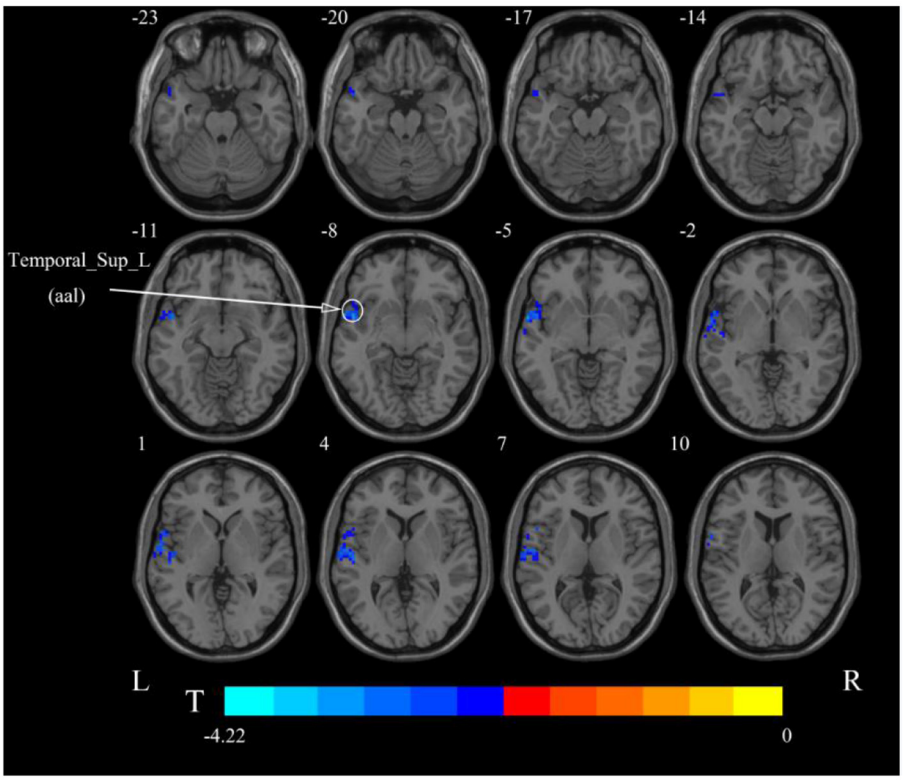

FIGURE 3 | Statistical maps showing ALFF change pre- and post-rTMS in the classical frequency band. Warm colors showing ALFF increased and cool colors showing ALFF decreased after rTMS $p < 0.05$.

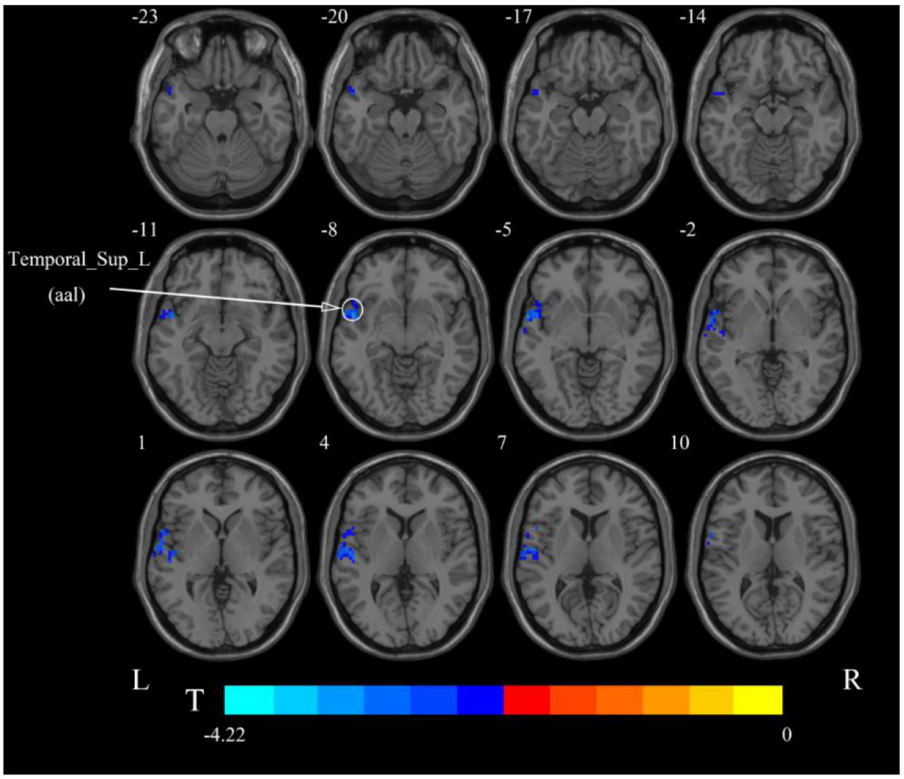

FIGURE 4 | Statistical maps showing ALFF change pre- and post-rTMS in the slow-4 band. Cool colors showing ALFF decreased after rTMS $p < 0.05$.

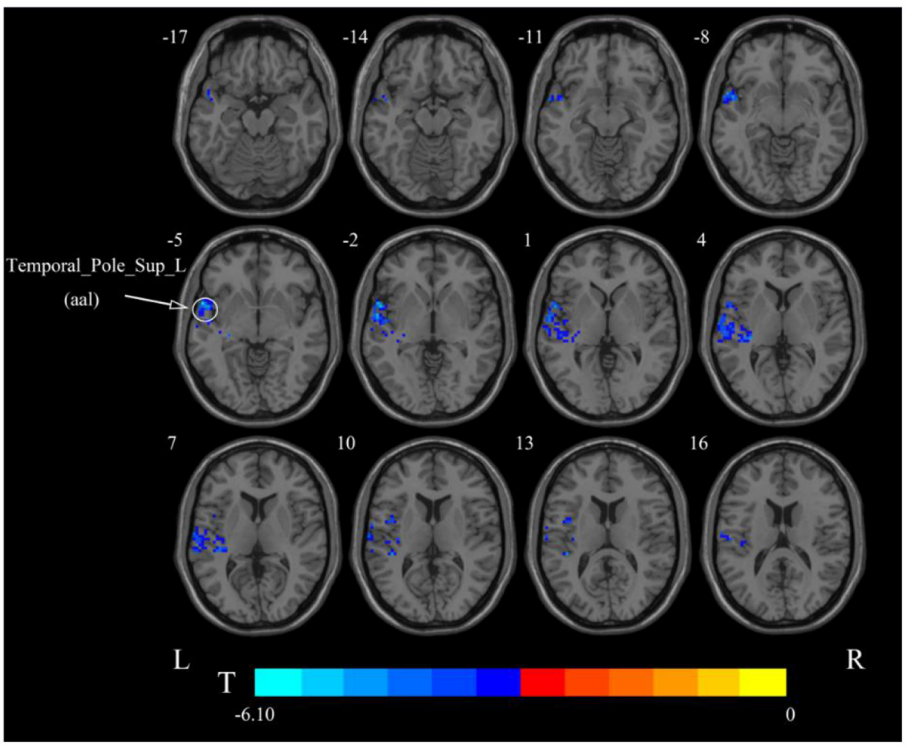

FIGURE 5 | Statistical maps showing ALFF change pre- and post-rTMS in the slow-5 band. Cool colors showing ALFF decreased after rTMS $p < 0.05$.

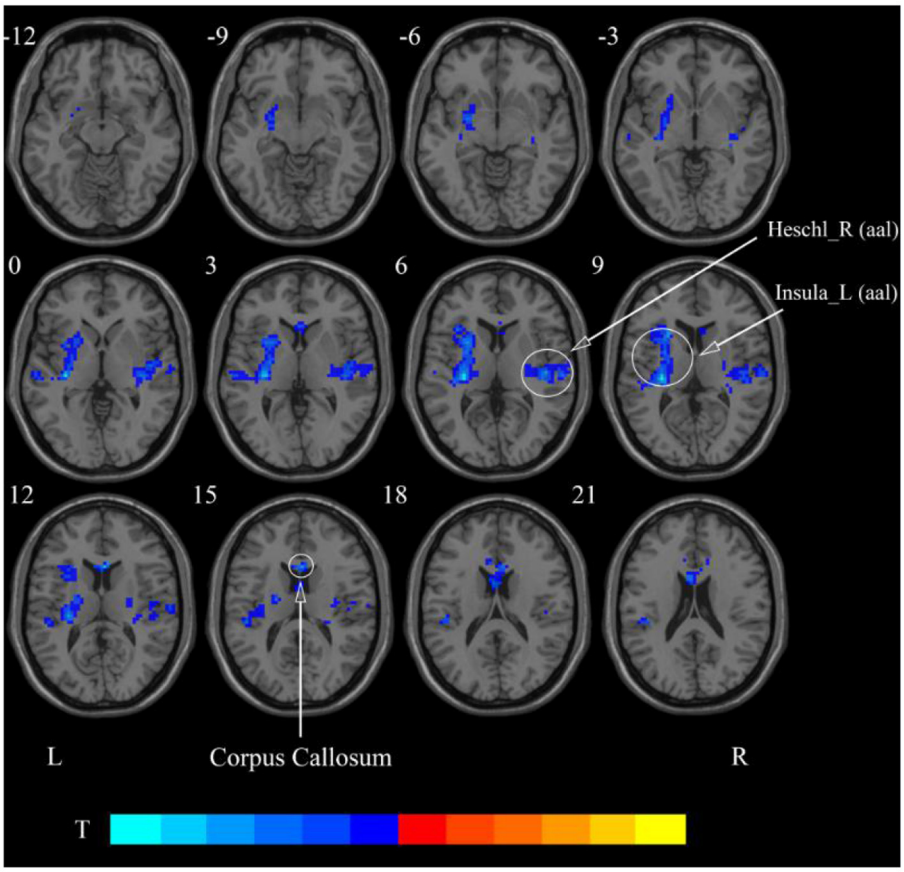

FIGURE 6 | Statistical maps showing ReHo change pre- and post-rTMS in the classical frequency band. Cool colors showing ReHo decreased after rTMS $p < 0.05$.

TABLE 2 | Brain regions with alteration of ReHo after cerebellar rTMS.

Brain region	Cluster size (voxel)	Coordinates (x, y, z)	Peak *t*-value
Classical frequency band (0.01–0.08 Hz)			
Insula_L (aal)	506	−30, −24, 9	−5.9848
Heschl_R (aal)	253	45, −18, 6	−4.0475
Corpus Callosum	109	3, 21, 12	−5.4896
Slow-4 band (0.027–0.073 Hz)			
Insula_L (aal)	274	−30, 21, 9	−4.4308
Corpus callosum	8		
Slow-5 band (0.01–0.027 Hz)			
Temporal_Sup_R (aal)	312	45, −18, 3	−4.8464
Putamen_L (aal)	354	−30, −18, 6	−5.1193
Supp_Motor_Area_L (aal)	367	−6, −15, 54	−6.0648

aal, anatomical automatic labeling; L, left; R, right; T, statistical value of peak voxel showing ReHo changes pre- and post-rTMS (negative values: ReHo decreased after rTMS).

The Results of rs-fMRI Based on ReHo Method

After cerebellar stimulation, in the classical frequency band we found significantly decreased ReHo at the left insula, right temporal lobe, and corpus callosum ($p < 0.05$; **Figure 6** and **Table 2**). In addition, a decrease in ReHo was also found at the left insula and corpus callosum in the slow-4 band and at the right temporal lobe, left putamen, and left motor accessory area in the slow-5 band ($p < 0.05$; **Figures 7**, **8** and **Table 2**).

DISCUSSION

By examining neuroimaging and electrophysiological changes after rTMS, this study demonstrated that cerebellar rTMS may improve swallowing function. The electrophysiological findings are consistent with those of previous studies, showing that MEP amplitude at swallowing-related areas of bilateral cerebral hemispheres increased after unilateral cerebellar high-frequency stimulation (Vasant et al., 2015; Sasegbon et al., 2019, 2020). This means that high-frequency rTMS stimulation of the unilateral cerebellum can have a positive effect on the swallowing-related cortex of bilateral cerebral hemispheres. In addition to this, rs-fMRI results based on the ALFF method showed that neural activity in the pons and medulla was significantly enhanced after stimulation, providing the first validation that high-frequency stimulation of the cerebellar dominant hemisphere can produce excitatory brainstem effects. These findings provide supportive evidence

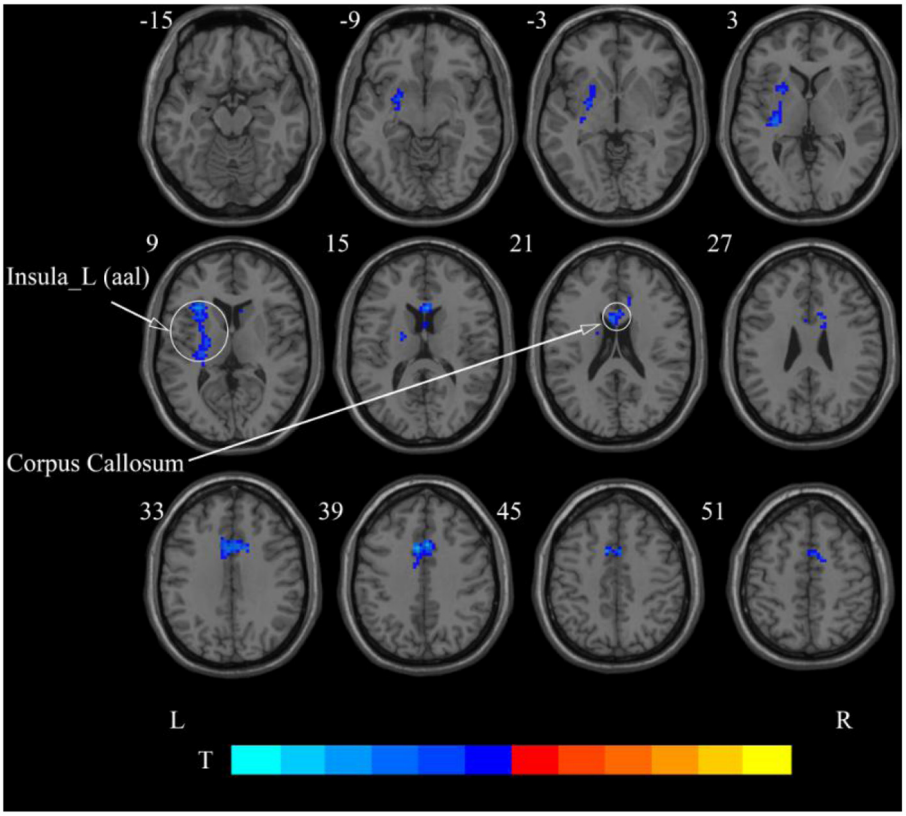

FIGURE 7 | Statistical maps showing ReHo change pre- and post-rTMS in the slow-4 band. Cool colors showing ReHo decreased after rTMS $p < 0.05$.

for the application of cerebellar rTMS in the treatment of PSD.

ALFF Results in Different Frequency Bands

In the classical frequency band, ALFF of posterior pons and medulla oblongata after cerebellar rTMS increased after stimulation, suggesting that brainstem spontaneous neural activity may be enhanced by high-frequency rTMS stimulation in the dominant cerebellar hemisphere. The generation of physiological swallowing activity requires oropharyngeal sensory stimulation afferent to the swallowing control center of the brainstem. This process is mainly mediated by the brainstem, whereas cortical higher-order centers act to initiate and regulate voluntary swallowing (Torii et al., 2012). The brainstem swallowing center, also called the central pattern generator (CPG), is located dorsolaterally in the medulla oblongata and is responsible for controlling and modulating the swallowing reflex. The CPG includes two bilaterally symmetrical regions, namely, the dorsal region comprising the nucleus tractus solitarius and its reticular formation; and the ventral region comprising the nucleus ambiguus and its reticular formation (Jean, 2001). Under physiological conditions, there is bilateral synergy between the two CPG regions, and their nerve fibers cross the midline in the brainstem to induce contraction of swallowing-related muscle groups bilaterally (Aydogdu et al., 2001). As a swallowing center, the brainstem is crucial in the swallowing process, and elevated ALFF values at the pons and medulla imply that high-frequency rTMS of the cerebellar dominant hemisphere may play a positive role on the efferent process of swallowing movements.

We also observed elevated ALFF in the cerebellum in the classical band. The cerebellum is a major site for the coordination of fine limb movements (Glickstein et al., 2009; Stoodley and Schmahmann, 2009). Several studies have previously shown that the cerebellum similarly plays an important role in swallowing movements. For example, fMRI research shows significant activation of the cerebellum during the oral phase of swallowing movements and coordinated orofacial and labial lingual movements (Onozuka et al., 2002). In addition, the accuracy of swallowing can be improved by cerebellar rTMS as measured using challenging swallow response tasks (Mistry et al., 2007; Sasegbon et al., 2019), and this finding may reflect the cerebellum increasing its role in modulating fine motor activity, thereby increasing movement accuracy.

In addition, we also found decreased ALFF in the contralateral temporal lobe after cerebellar rTMS, suggesting a possible inhibitory effect of cerebellar rTMS on the contralateral temporal lobe. Previous studies have shown that swallowing is governed by multiple parts of the cerebral cortex, such as the sensory/motor cortex, prefrontal areas, anterior cingulate, insula, parietal and

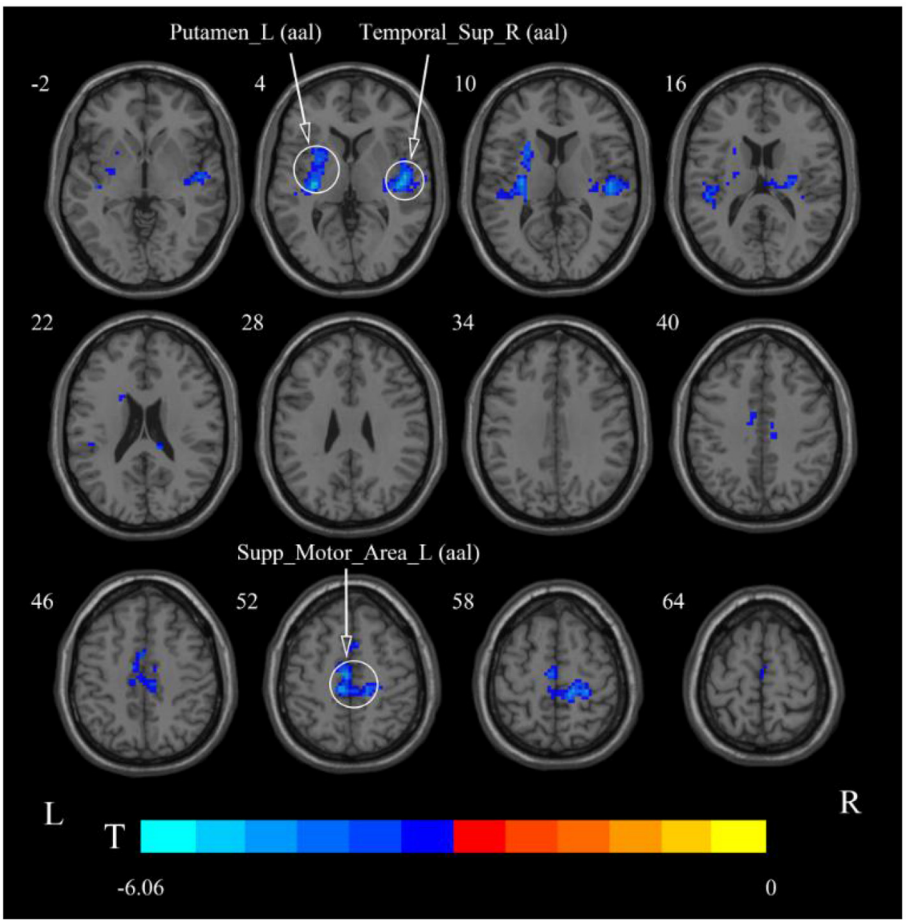

FIGURE 8 | Statistical maps showing ReHo change pre- and post-rTMS in the slow-5 band. Cool colors showing ReHo decreased after rTMS $p < 0.05$.

temporal lobes (Hamdy et al., 1999; Martin et al., 2001; Suzuki et al., 2003; Babaei et al., 2012, 2013; Ushioda et al., 2012). The temporal lobe is thought to be involved in taste recognition during swallowing (Small et al., 1999). Since the swallowing action directly induced by cerebellar rTMS skips taste recognition, the temporary lobe suppression may be related to the negative feedback between cerebellum and temporal lobe. The cortical ALFF results showed an inhibitory effect of cerebellar rTMS on the contralateral temporal lobe in both the slow-4 and slow-5 frequency bands. However, unlike the classical band, no functional changes in the pons, medulla oblongata, or cerebellum were found in either frequency band. This suggests that the activity of these regions may be manifested in the entire classical frequency band rather than in some part of it.

ReHo Results in Different Frequency Bands

In the classical frequency band, we observed that functional changes in the cerebral cortex were induced after rTMS stimulation in the cerebellum. The ReHo was decreased after stimulation in the left insula and right temporal lobe. The insula and temporal lobe function, similar to their involvement in swallowing, are jointly involved in taste recognition (Ertekin and Aydogdu, 2003). In addition to taste, the insula processes information such as food touch in the mouth and plays an important role in oral motility (Ushioda et al., 2012). We observed reduced ReHo in the temporal lobe, putamen, and motor supplementary area at slow-5, which may be more sensitive at slow-5. The supplementary motor area is involved in the planning of swallowing movements and has a role in coordinating bilateral movements (Welniarz et al., 2019; Sadler et al., 2021). The cerebral cortex plays a role in the initiation and regulation of voluntary swallowing (Suzuki et al., 2003). After stimulation of the cerebellum, the spontaneous neural activity of the stimulated lateral cerebellum and brainstem was enhanced, while multiple regions of the cerebral cortex were negatively affected. Swallowing movements induced by cerebellar rTMS probably require neither the planning of the cerebral cortex nor the afferents of the orofacial sensation. This external stimulation may cause decreased ReHo in the cingulate gyrus, insula, temporal lobe, and supplementary motor areas. In addition, negative feedback regulation occurs between higher cortical

centers and subcortical centers such as the brainstem. The elevated brainstem function after rTMS in the cerebellum may contribute to the suppression of generalized cortical function (Mosier and Bereznaya, 2001).

Our study also revealed reduced ReHo in the corpus callosum, the largest commissural connection between the cerebral hemispheres, after cerebellar rTMS. It has been suggested that the bilateral cerebral hemispheres are under interactive inhibition and that the inhibition of unilateral hand motor areas by low-frequency rTMS is beneficial by elevating contralateral hand innervation (Bajwa et al., 2008). Similarly, bilateral innervation *via* the corpus callosum may exert excitatory contralateral modulation of swallowing (Mistry et al., 2012). The findings of this study suggest that while performing bilaterally controlled swallowing movements, the inhibitory effect of the corpus callosum may be reduced.

As we all know, swallowing is divided into oral, pharyngeal, and esophageal phases. The oral phase mainly involves the formation and transport of food boluses, which are regulated autonomously by the cerebral cortex. The main activity of the pharyngeal phase is to swallow food to the esophagus, which is a reflex action, and is controlled by the CPG of the medulla oblongata (Torii et al., 2012). Our results suggest that cerebellar rTMS may not only regulate swallowing during the oral phase by inhibiting the cerebral cortex but also directly improve the performance of swallowing during the pharyngeal phase by enhancing the descending efferent pathways of the brainstem.

CONCLUSION

In this study, we found that rTMS of the swallowing cortex in the dominant cerebellar hemisphere increased the bilateral cerebral swallowing cortex excitability and enhanced pontine, bulbar, and cerebellar spontaneous neural activity, suggesting that unilateral high-frequency stimulation of the cerebellum can excite both brainstem and cortical swallowing centers. Furthermore, we found reduced ReHo in the corpus callosum, which may facilitate the execution of this bilaterally innervated action of swallowing. These findings all provide favorable support for the application of cerebellar rTMS in the clinical practice.

LIMITATIONS

Our study has some limitations. First, unlike previous clinical studies that have simulated stroke damage, we stimulated and observed healthy volunteers. This does not directly mimic the recovery process of swallowing function in stroke patients. Second, because of the higher acquisition and analysis costs of rs-fMRI, we studied a limited number of volunteers, and studies with larger samples are still needed to further confirm these conclusions.

DATA AVAILABILITY STATEMENT

The raw data supporting the conclusions of this article will be made available by the authors, without undue reservation.

ETHICS STATEMENT

The studies involving human participants were reviewed and approved by the Ethics Committee of the Affiliated Hospital of Qingdao University. The patients/participants provided their written informed consent to participate in this study.

AUTHOR CONTRIBUTIONS

LD, PM, and QW contributed to conception and design of the study. WM and conducted data collection. YW and XP performed the statistical analysis. LD wrote the first draft of the manuscript. PM, QW, CH, and LD wrote sections of the manuscript. All authors contributed to manuscript revision, read, and approved the submitted version.

FUNDING

This work was supported by the Key Research and Development Projects of Shandong Province (grant no. 2019GSF108262).

ACKNOWLEDGMENTS

The authors thank the Radiology Department of the Affiliated Hospital of Qingdao University for the fMRI data acquisition and all volunteers who participated in this study.

REFERENCES

Aydogdu, I., Ertekin, C., Tarlaci, S., Turman, B., Kiylioglu, N., and Secil, Y. (2001). Dysphagia in lateral medullary infarction (Wallenberg's syndrome): an acute disconnection syndrome in premotor neurons related to swallowing activity? *Stroke* 32, 2081–2087. doi: 10.1161/hs0901.094278

Babaei, A., Siwiec, R. M., Kern, M., Douglas-Ward, B., Li, S. J., and Shaker, R. (2013). Intrinsic functional connectivity of the brain swallowing network during subliminal esophageal acid stimulation. *Neurogastroenterol. Motil.* 25, 992–e779. doi: 10.1111/nmo.12238

Babaei, A., Ward, B. D., Ahmad, S., Patel, A., Nencka, A., Li, S. J., et al. (2012). Reproducibility of swallow-induced cortical BOLD positive and negative fMRI activity. *Am. J. Physiol. Gastrointest. Liver Physiol.* 303, G600–G609. doi: 10.1152/ajpgi.00167.2012

Bajwa, S., Bermpohl, F., Rigonatti, S. P., Pascual-Leone, A., Boggio, P. S., and Fregni, F. (2008). Impaired interhemispheric interactions in patients with major depression. *J. Nerv. Ment. Dis.* 196, 671–677. doi: 10.1097/NMD.0b013e318183f86f

Bonilha, H. S., Simpson, A. N., Ellis, C., Mauldin, P., Martin-Harris, B., and Simpson, K. (2014). The one-year attributable cost of post-stroke dysphagia. *Dysphagia* 29, 545–552. doi: 10.1007/s00455-014-9543-8

Cheng, I. K. Y., Chan, K. M. K., Wong, C. S., Li, L. S. W., Chiu, K. M. Y., Cheung, R. T. F., et al. (2017). Neuronavigated high-frequency repetitive transcranial magnetic stimulation for chronic post-stroke dysphagia: a randomized controlled study. *J. Rehabil. Med.* 49, 475–481. doi: 10.2340/16501977-2235

Cohen, D. L., Roffe, C., Beavan, J., Blackett, B., Fairfield, C. A., Hamdy, S., et al. (2016). Post-stroke dysphagia: a review and design considerations

for future trials. *Int. J. Stroke* 11, 399–411. doi: 10.1177/1747493016639057

Du, J., Yang, F., Liu, L., Hu, J., Cai, B., Liu, W., et al. (2016). Repetitive Transcranial magnetic stimulation for rehabilitation of poststroke dysphagia: a randomized, double-blind clinical trial. *Clin. Neurophysiol.* 127, 1907–1913. doi: 10.1016/j.clinph.2015.11.045

Ertekin, C., and Aydogdu, I. (2003). Neurophysiology of swallowing. *Clin. Neurophysiol.* 114, 2226–2244. doi: 10.1016/S1388-2457(03)00237-2

Fisicaro, F., Lanza, G., Grasso, A. A., Pennisi, G., Bella, R., Paulus, W., et al. (2019). Repetitive transcranial magnetic stimulation in stroke rehabilitation: review of the current evidence and pitfalls. *Ther. Adv. Neurol. Disord.* 12, 1756286419878317. doi: 10.1177/1756286419878317

Geeganage, C., Beavan, J., Ellender, S., and Bath, P. M. (2012). Interventions for dysphagia and nutritional support in acute and subacute stroke. *Cochrane Database Syst. Rev.* 10, CD000323. doi: 10.1002/14651858.CD000323.pub2

Glickstein, M., Strata, P., and Voogd, J. (2009). Cerebellum: history. *Neuroscience* 162, 549–559. doi: 10.1016/j.neuroscience.2009.02.054

Guillén-Solà, A., Messagi Sartor, M., Bofill Soler, N., Duarte, E., Barrera, M. C., and Marco, E. (2017). Respiratory muscle strength training and neuromuscular electrical stimulation in subacute dysphagic stroke patients: a randomized controlled trial. *Clin. Rehabil.* 31, 761–771. doi: 10.1177/0269215516652446

Hamdy, S., Mikulis, D. J., Crawley, A., Xue, S., Lau, H., Henry, S., et al. (1999). Cortical activation during human volitional swallowing: an event-related fMRI study. *Am. J. Physiol.* 277, G219–G225. doi: 10.1152/ajpgi.1999.277.1.G219

Iglesias, A. H. (2020). Transcranial magnetic stimulation as treatment in multiple neurologic conditions. *Curr. Neurol. Neurosci. Rep.* 20, 1. doi: 10.1007/s11910-020-1021-0

Jayasekeran, V., Rothwell, J., and Hamdy, S. (2011). Non-invasive magnetic stimulation of the human cerebellum facilitates cortico-bulbar projections in the swallowing motor system. *Neurogastroenterol. Motil.* 23, 831–e341. doi: 10.1111/j.1365-2982.2011.01747.x

Jean, A. (2001). Brain stem control of swallowing: neuronal network and cellular mechanisms. *Physiol. Rev.* 81, 929–969. doi: 10.1152/physrev.2001.81.2.929

Khedr, E. M., and Abo-Elfetoh, N. (2010). Therapeutic role of rTMS on recovery of dysphagia in patients with lateral medullary syndrome and brainstem infarction. *J. Neurol. Neurosurg. Psychiatry.* 81, 495–499. doi: 10.1136/jnnp.2009.188482

Khedr, E. M., Abo-Elfetoh, N., and Rothwell, J. C. (2009). Treatment of post-stroke dysphagia with repetitive transcranial magnetic stimulation. *Acta Neurol. Scand.* 119, 155–161. doi: 10.1111/j.1600-0404.2008.01093.x

Kim, L., Chun, M. H., Kim, B. R., and Lee, S. J. (2011). Effect of repetitive transcranial magnetic stimulation on patients with brain injury and dysphagia. *Ann. Rehabil. Med.* 35, 765–771. doi: 10.5535/arm.2011.35.6.765

Ma, J. D., Wang, C. H., Huang, P., Wang, X., Shi, L. J., Li, H. F., et al. (2021). Effects of short-term cognitive-coping therapy on resting-state brain function in obsessive-compulsive disorder. *Brain Behav.* 11, e02059. doi: 10.1002/brb3.2059

Martin, R. E., Goodyear, B. G., Gati, J. S., and Menon, R. S. (2001). Cerebral cortical representation of automatic and volitional swallowing in humans. *J. Neurophysiol.* 85, 938–950. doi: 10.1152/jn.2001.85.2.938

Martino, R., and Mcculloch, T. (2016). Therapeutic intervention in oropharyngeal dysphagia. *Nat. Rev. Gastroenterol. Hepatol.* 13, 665–679 doi: 10.1038/nrgastro.2016.127

Mistry, S., Michou, E., Rothwell, J., and Hamdy, S. (2012). Remote effects of intermittent theta burst stimulation of the human pharyngeal motor system. *Eur. J. Neurosci.* 36, 2493–2499. doi: 10.1111/j.1460-9568.2012.08157.x

Mistry, S., Verin, E., Singh, S., Jefferson, S., Rothwell, J. C., and Thompson, D. G. (2007). Unilateral suppression of pharyngeal motor cortex to repetitive transcranial magnetic stimulation reveals functional asymmetry in the hemispheric projections to human swallowing. *J. Physiol.* 585, 525–538. doi: 10.1113/jphysiol.2007.144592

Mosier, K., and Bereznaya, I. (2001). Parallel cortical networks for volitional control of swallowing in humans. *Exp. Brain Res.* 140, 280–289. doi: 10.1007/s002210100813

Mosier, K. M., Liu, W. C., Maldjian, J. A., Shah, R., and Modi, B. (1999). Lateralization of cortical function in swallowing: a functional mr imaging study. *AJNR Am. J. Neuroradiol.* 20, 1520–1526.

Onozuka, M., Fujita, M., Watanabe, K., Hirano, Y., Niwa, M., Nishiyama, K., et al. (2002). Mapping brain region activity during chewing: a functional magnetic resonance imaging study. *Dent. Res.* 81, 743–746. doi: 10.1177/0810743

Qiu, H., Li, X., Luo, Q., Li, Y., Zhou, X., Cao, H., et al. (2019). Alterations in patients with major depressive disorder before and after electroconvulsive therapy measured by fractional amplitude of low-frequency fluctuations(fALFF). *Affect. Disord.* 244, 92–99. doi: 10.1016/j.jad.2018.10.099

Sadler, C. M., Kami, A. T., Nantel, J., and Carlsen, A. N. (2021). Transcranial direct current stimulation of supplementary motor area improves upper limb kinematics in parkinson's disease. *Clin. Neurophysiol.* 132, 2907–2915. doi: 10.1016/j.clinph.2021.06.031

Sasegbon, A., Smith, C. J., Bath, P., Rothwell, J., and Hamdy, S. (2020). The Effects of unilateral and bilateral cerebellar rTMS on human pharyngeal motor cortical activity and swallowing behavior. *Exp. Brain Res.* 238, 1719–1733 doi: 10.1007/s00221-020-05787-x

Sasegbon, A., Watanabe, M., Simons, A., Michou, E., Vasant, D. H., Magara, J., et al. (2019). Cerebellar repetitive transcranial magnetic stimulation restores pharyngeal brain activity and swallowing behaviour after disruption by a cortical virtual lesion. *J. Physiol.* 5, 597–599. doi: 10.1113/JP277545

Singh, S., and Hamdy, S. (2006). Dysphagia in stroke patients. *Postgrad. Med.* 82, 383–391. doi: 10.1136/pgmj.2005.043281

Small, D. M., Zald, D. H., Jones-Gotman, M., Zatorre, R. J., Pardo, J. V., Frey, S., et al. (1999). Human cortical gustatory areas: a review of functional neuroimaging data. *Neuroreport* 10,7–14. doi: 10.1097/00001756-199901180-00002

Stoodley, C., and Schmahmann, J. (2009). Functional topography in the human cerebellum: a meta-analysis of neuroimaging studies. *Neuroimage* 44, 489–501. doi: 10.1016/j.neuroimage.2008.08.039

Suzuki, M., Asada, Y., Ito, J., Hayashi, K., Inoue, H., and Kitano, H. (2003). Activation of cerebellum and basal ganglia on volitional swallowing detected by functional magnetic resonance imaging. *Dysphagia* 18, 71–77. doi: 10.1007/s00455-002-0088-x

Torii, T., Sato, A., Nakahara, Y., Iwahashi, M., Itoh, Y., and Iramina, K. (2012). Frequency-dependent effects of repetitive transcranial magnetic stimulation on the human brain. *Neuroreport* 23, 1065–1070. doi: 10.1097/WNR.0b013e32835afaf0

Ushioda, T., Watanabe, Y., Sanjo, Y., Yamane, G. Y., Abe, S., Tsuji, Y., et al. (2012). Visual and auditory stimuli associated with swallowing activate mirror neurons: a magnetoencephalography study. *Dysphagia* 27, 504–513. doi: 10.1007/s00455-012-9399-8

Vasant, D. H., Michou, E., Mistry, S., Rothwell, J. C., and Hamdy, S. (2015). High-frequency focal repetitive cerebellar stimulation induces prolonged increases in human pharyngeal motor cortex excitability. *J. Physiol.* 593, 4963–4977. doi: 10.1113/JP270817

Welniarz, Q., Gallea, C., Lamy, J. C., Méneret, A., Popa, T., Valabregue, R., et al. (2019). The supplementary motor area modulates interhemispheric interactions during movement preparation. *Hum. Brain Mapp.* 40, 2125–2142. doi: 10.1002/hbm.24512

Wu, Z., Luo, Q., Wu, H., Wu, Z., Zheng, Y., Yang, Y., et al. (2020). Amplitude of low-frequency oscillations in major depressive disorder with childhood trauma. *Front. Psychiatry* 11, 596337. doi: 10.3389/fpsyt.2020.596337

Zang, Y. F., He, Y., Zhu, C. Z., Cao, Q. J., Sui, M. Q., Liang, M., et al. (2007). Altered baseline brain activity in children with ADHD revealed by resting-state functional MRI. *Brain Dev.* 29, 83–91. doi: 10.1016/j.braindev.2006.07.002

Zang, Y. F., Jiang, T. Z., Lu, Y. L., He, Y., and Tian, L. X. (2004). Regional homogeneity approach to fMRI data analysis. *Neuroimage* 22, 394–400. doi: 10.1016/j.neuroimage.2003.12.030

Zhang, C. L., Zheng, X. Q., Lu, R. L., Yun, W. W., Yun, H. F., and Zhou, X. J. (2019). Repetitive transcranial magnetic stimulation in combination with neuromuscular electrical stimulation for treatment of post-stroke

dysphagia. *Int. Med. Res.* 47, 662–672. doi: 10.1177/03000605188 07340

Zhang, Z., Bo, Q., Li, F., Zhao, L., Wang, Y., Liu, R., et al. (2020). Increased ALFF and functional connectivity of the right striatum in bipolar disorder patients. *Prog. Neuropsychopharmacol. Biol. Psychiatry* 111, 110140. doi: 10.1016/j.pnpbp.2020.110140

Zuo, X. N., Di-Martino, A., Kelly, C., Shehzad, Z. E., Gee, D. G., Klein, D. F., et al. (2010). The Oscillating brain: complex and reliable. *Neuroimage* 49, 1432–1445. doi: 10.1016/j.neuroimage.2009. 09.037

Conflict of Interest: The authors declare that the research was conducted in the absence of any commercial or financial relationships that could be construed as a potential conflict of interest.

Publisher's Note: All claims expressed in this article are solely those of the authors and do not necessarily represent those of their affiliated organizations, or those of the publisher, the editors and the reviewers. Any product that may be evaluated in this article, or claim that may be made by its manufacturer, is not guaranteed or endorsed by the publisher.

frontiers | Frontiers in Human Neuroscience

ORIGINAL RESEARCH
published: 20 June 2022
doi: 10.3389/fnhum.2022.883337

Effects of Online Single Pulse Transcranial Magnetic Stimulation on Prefrontal and Parietal Cortices in Deceptive Processing: A Preliminary Study

Bruce Luber[1*†], *Lysianne Beynel*[1†], *Timothy Spellman*[2], *Hannah Gura*[1], *Markus Ploesser*[3,4], *Kate Termini*[5] *and Sarah H. Lisanby*[1]

[1] *Noninvasive Neuromodulation Unit, Experimental Therapeutics and Pathophysiology Branch, National Institute of Mental Health, Bethesda, MD, United States,* [2] *Department of Neuroscience, University of Connecticut School of Medicine, Farmington, CT, United States,* [3] *Department of Psychiatry and Neurosciences, University of California, Riverside, Riverside, CA, United States,* [4] *Forensic Psychiatry, Department of Psychiatry, Faculty of Medicine, The University of British Columbia, Vancouver, BC, Canada,* [5] *Clinical and Forensic Psychology, Fifth Avenue Forensics, New York, NY, United States*

OPEN ACCESS

Edited by:
Joshua Oon Soo Goh, National Taiwan University, Taiwan

Reviewed by:
Elisa Kallioniemi, University of Texas Southwestern Medical Center, United States
Teodóra Vékony, Université Claude Bernard Lyon 1, France

***Correspondence:**
Bruce Luber
bruce.luber@nih.gov

[†] These authors have contributed equally to this work and share first authorship

Specialty section:
This article was submitted to Cognitive Neuroscience, a section of the journal Frontiers in Human Neuroscience

Received: *24 February 2022*
Accepted: *26 May 2022*
Published: *20 June 2022*

Citation:
Luber B, Beynel L, Spellman T, Gura H, Ploesser M, Termini K and Lisanby SH (2022) Effects of Online Single Pulse Transcranial Magnetic Stimulation on Prefrontal and Parietal Cortices in Deceptive Processing: A Preliminary Study. Front. Hum. Neurosci. 16:883337. doi: 10.3389/fnhum.2022.883337

Transcranial magnetic stimulation (TMS) was used to test the functional role of parietal and prefrontal cortical regions activated during a playing card Guilty Knowledge Task (GKT). Single-pulse TMS was applied to 15 healthy volunteers at each of three target sites: left and right dorsolateral prefrontal cortex and midline parietal cortex. TMS pulses were applied at each of five latencies (from 0 to 480 ms) after the onset of a card stimulus. TMS applied to the parietal cortex exerted a latency-specific increase in inverse efficiency score and in reaction time when subjects were instructed to lie relative to when asked to respond with the truth, and this effect was specific to when TMS was applied at 240 ms after stimulus onset. No effects of TMS were detected at left or right DLPFC sites. This manipulation with TMS of performance in a deception task appears to support a critical role for the parietal cortex in intentional false responding, particularly in stimulus selection processes needed to execute a deceptive response in the context of a GKT. However, this interpretation is only preliminary, as further experiments are needed to compare performance within and outside of a deceptive context to clarify the effects of deceptive intent.

Keywords: TMS, deception, parietal cortex, fronto-parietal network, guilty knowledge task (GKT)

INTRODUCTION

Deception is an active cognitive process by which the deceiver must inhibit truth-telling while generating false information (Mitchell, 1986). Due to its negative social consequences, there has long been a keen interest in an objective method of detecting deception in the fields of law and security, given for example the inaccuracy of juries and judges in assessing veracity (Appelbaum, 2007). Such objective measures could also aid in the understanding and treatment of psychiatric disorders in which the ability to deceive is impaired (e.g., autism: Sodian and Frith, 1992) or is a symptomatic component (e.g., antisocial personality disorders: Ford et al., 1988). In the early 20th century, the polygraph, relying on peripheral, anxiety-induced autonomic indicators,

was proposed as a tool to study lie detection (Larson and Haney, 1932). However, the ability of individuals to defeat these methods by learning to manipulate physiological measures such as skin conductance and heart rate (Honts et al., 1985, 1996), as well as their intrinsic variability (Saxe et al., 1985), has suggested that an objective technology of deception detection requires a greater understanding of the brain processes underlying deception itself. Thus, attention has since turned toward direct measures of brain activity involved with deception utilizing electrophysiological and functional magnetic resonance imaging (fMRI) techniques.

Research on deception using electrophysiology dates back three decades and indicates that scalp electrical potential measures are sensitive to deceptive contexts. There has been a great deal of work focusing on the relationship of deception and event-related potentials (ERPs) with a later onset latency, especially P300s (e.g., Farwell and Donchin, 1991; Johnson et al., 2005). The literature suggests that deceiving requires a higher cognitive workload than truth-telling and that this difference is reflected by changes in the magnitude and latency of specific ERPs (Czigler et al., 2002). However, ERPs with latencies much earlier than P300s are also influenced by deception manipulations, suggesting that deception can influence processing in earlier stages as well. For example, for tasks using visual stimuli, a negative component appearing around 80–180 ms post-stimulus onset, the N1, with greatest amplitudes in the occipital area, is more negative when deception is required, probably due to greater use of early attentive processes (Hu et al., 2011). From about 180–325 ms post-stimulus, an N2 waveform is prominent in frontal and central regions and its change found with deception has been proposed to reflect the mental task of categorizing a stimulus to be lied about and preparing that response (Wu et al., 2009; Hu et al., 2011, Leng et al., 2019).

Neuroimaging has also been shown to be sensitive to experimental manipulation of deception, with studies finding regional activation differences when subjects are practicing deception vs. truth-telling. A recent meta-analysis (Delgado-Herrera et al., 2021) demonstrated substantial involvement of the fronto-parietal network in deception (see also Christ et al., 2009; Lisofsky et al., 2014; Yu et al., 2019), with frontal activations associated with executive functions required to deceive, such as working memory, inhibition, and task switching (Christ et al., 2009); and parietal activations linked to the recruitment of additional resources such as socio-cognitive processes when the task involves social or virtual interactions (Lisofsky et al., 2014); or additional attentional resources when instances requiring deception arise (Christ et al., 2009). However, the ability to use neuroimaging for the detection of deception is hampered by the sheer number and complexity of processes involved in deception such as the cognitive and emotional processes necessary to generate the rationale, intent, and strategies for deception within a given context, as well as those needed to execute a response which is incompatible with the truth (Johnson et al., 2003). Acts of deliberation over deception include weighing risks and benefits, the mind of the other(s) to be lied to, the content and context of the lie, and the recognition of the truth and its inhibition, all governed by many overlapping cognitive processes most likely having a great degree of individual variability (Keckler, 2005). Even the most general taxonomy of the processes involved in deception is complex, grouping them under four sets of cognitive resources: information management, risk management, impression management, and reputation management (Sip et al., 2008). This processing complexity, and the concomitant complexity of its neural underpinnings, has been acknowledged (e.g., Nuñez et al., 2005), and some studies have attempted to differentiate component executive processes used in the deceptive act with manipulations of working memory load (Ganis et al., 2003) or memory content (Nuñez et al., 2005). Nevertheless, the correlative nature of imaging studies, especially when several neural processes are involved, has made interpretation difficult.

Several groups have attempted to use non-invasive brain stimulation such as transcranial magnetic stimulation (TMS) and transcranial direct current stimulation (tDCS) as a more direct approach to detection of deception than imaging. By using results found in electrophysiological and imaging studies to target cortical regions involved with specific aspects of deception, stimulation holds the attractive potential to directly interfere with brain processes involved with producing a deceptive response to produce a measurable difference in performance when being truthful or deceptive (Luber et al., 2009). TMS and tDCS have already been shown to affect behavioral performance in deceptive contexts. Two early studies applied TMS over the motor cortex and found greater cortico-spinal excitability while subjects responded with lies compared to truth (Lo et al., 2003; Kelly et al., 2009). Five studies focused on stimulation of prefrontal cortex (PFC), and while one of them did not show any differences between truth conditions caused by TMS (Verschuere et al., 2012), a series of four other experiments conducted by the same group demonstrated significant TMS effects on deception processes (Karton and Bachmann, 2011, 2017; Karton et al., 2014a,b). Indeed, using both online and offline TMS, Karton and associates found hemispheric differences between truth and lie conditions, with a lower number of deceptive responses with stimulation to left PFC compared to right, as well as an abolishment of the difference seen between truth conditions in the electrical P300 evoked response.

There have also been several studies of deception using tDCS. Two studies stimulated the right temporo-parietal junction and found decreased deceptive responding in a social context (Tang et al., 2017; Noguchi and Oizumi, 2018), while most have focused on PFC stimulation (Priori et al., 2008; Karim et al., 2010; Mameli et al., 2010; Fecteau et al., 2013; Maréchal et al., 2017; Sánchez et al., 2020). Priori et al. found bilateral stimulation increased reaction time in deceitful responses compared to truth, while Mameli et al., Karim et al., and Fecteau et al. found faster RT in lie conditions. Marechal et al. found tDCS to right DLPFC decreased the number of lie responses, and Sanchez et al. found right ventrolateral PFC tDCS disrupted truth-telling, with no effects on lies. Overall, while these TMS and tDCS studies vary in their specific findings, they do indicate that brain stimulation can be effective in producing behavioral differences which depend on deceptive intent. However, most

of these studies used offline stimulation—i.e., they evaluated performance changes before and after stimulation. While the offline approach provides important information about the role of specific brain regions in deception, results may be contaminated by the cumulative effects of stimulation that can spread to other brain regions transsynaptically (Beynel et al., 2020). Moving toward a paradigm of direct, online stimulation which can affect behavioral performance on a trial-by-trial basis in specific contexts could afford a means of disrupting deceptive processes on an individual basis with temporal and spatial precision. In addition, these cited studies used trains of rTMS or continuous tDCS which, while effective, cannot provide precise temporal information of the neural mechanisms involved in deception. Single pulses of TMS provide a much more fine-grained time-resolution and allow the experimenter to precisely dissect network activity in time as well as space. This approach was first used by Amassian et al. (1989) to disrupt letter identification, and has successfully been used by our group and others to disrupt complex object recognition in higher visual areas (Luber et al., 2020), self-related episodic memory and self-judgments (Lou et al., 2004; Lou et al., 2010; Luber et al., 2012), numerical cognition (Garcia-Sanz et al., 2022) or cognitive functions assessed via the stop signal task (Bashir et al., 2020), suggesting that single pulse TMS can provide important information regarding the chronometry of complex cognitive functions. The present study attempted to target processes involved with the execution of deceptive responses in a simplified behavioral context as a proof-of-concept for this paradigm.

Disrupting deception with non-invasive brain stimulation, however, is not straightforward. There is no "deception region" of cortex, no "deception network." Correspondingly, cognitively there is no process central to deception. Deception describes a family of behaviors, all intended to instill a false belief in another person's mind. A particular deceptive action chosen from this family of behaviors is generated from a set of general cognitive processes (e.g., risk processing, Theory of Mind, attention, working memory, etc.). Therefore, studying deception using TMS involves the careful dissection of cognitive processes called on within a deceptive context, which can only be done over a series of experiments. In our preliminary experiment, to focus the application of TMS on the output stages of a deceptive act, we chose a validated deception task, the Guilty Knowledge task (GKT) (Lykken, 1960; MacLaren, 2001). The GKT, in its original form, posed questions concerning a "crime scene" with multiple answer options. The correct answers involved details that only the "criminal" would know. The examiner used physiological indicators during the GKT to look for differences in responses to true and false alternatives (Lykken, 1960; MacLaren, 2001). A simplified analogous playing card version of the GKT was developed for imaging studies using a computer monitor instead of a human examiner (e.g., Langleben et al., 2002). In this type of GKT, subjects are given playing cards, divided into those the subject is instructed to tell the truth about and those they are instructed to deny having. This version of the GKT is arguably the most simplified model of the act of deception. We expected the playing card GKT to minimize the deliberative aspects of deception related to cognitive and emotional processes used in generating a lie since the experimenter controlled what to lie about and when to lie. As Sip et al. (2008) observed, the greatest advantage of using the GKT is that it does not address deception in its totality, but only focuses on a limited set of processes, primarily those involving response selection and inhibition: "if deception is a goal, the most basic scenario requires inhibition of prepotent truth responses to make others believe what we want them to believe," which is the focus of the GKT. TMS was applied to dorsolateral prefrontal cortex (DLPFC) and medial parietal cortex, two nodes of the fronto-parietal network (FPN) involved with executive processing of the type used in the GKT. The two most important roles of the executive system in the present task were to select the response category (lie/truth), and to inhibit the prepotent truth response related to the lie category. We expected the DLPFC to be involved primarily with truthful response inhibition, and the medial parietal cortex to be involved with response selection given its large role in the mapping of salient stimuli to the proper response category. Both have been shown to be activated in imaging studies of deception (DLPFC: Spence et al., 2001; Lee et al., 2002; Ganis et al., 2003; Kozel et al., 2004; Nuñez et al., 2005; Phan et al., 2005; Feredoes et al., 2011; Ito et al., 2011; medial parietal cortex: Lee et al., 2002; Ganis et al., 2003; Langleben et al., 2005; Mohamed et al., 2006; Sip et al., 2010; Hu et al., 2011; Ito et al., 2011). Executive functions relevant to the GKT such as working memory have long been shown to be affected by TMS to DLPFC (Pascual-Leone et al., 1994), including situations in which the task involved handling of relevant and irrelevant stimuli (Feredoes et al., 2011). The medial parietal cortex was chosen as a target over lateral parietal cortex given that TMS to medial parietal cortex has been shown to modulate executive processing (Lou et al., 2004; Luber et al., 2007); working memory, especially in cases where the number of items to be remembered was high (Luber et al., 2007, 2008); and to disrupt selection of salient stimuli (Mevorach et al., 2006). Past imaging work found a strong network node in midline parietal cortex when subjects used working memory to manipulate items in memory, as opposed to just maintaining them over a delay period (Davis et al., 2018). This involvement of midline parietal cortex during item manipulation, high-capacity item maintenance, and categorization suggested this region's involvement in processing related to the GKT task used here.

The high temporal resolution of TMS also allows not just spatial targeting of deceptive processes of selection and inhibition, but temporal targeting as well. We were able to test whether single pulse TMS, applied at various latencies in relation to onset of test playing cards (0, 80, 160, 240, and 480 ms after stimulus onset), reduced performance during the accuracy of deceptive responses. We based our range of pulse times on the N2 complex of ERP components of visual response, which are observed over a range 150–350 ms after stimulus onset, and whose elements associated with executive processing in the FPN peak between 200 and 300 ms (Folstein and van Petten, 2008; Pires et al., 2014). We expected only the pulses in the middle of this range of times (240 and possibly 160 ms) to disrupt performance in deception conditions.

METHODS

Subjects

Fifteen healthy subjects (8 females) with a mean age of 30.5 ± 6.7 (SD) years were recruited and signed written informed consent to participate in this 3-day study, approved by the New York State Psychiatric Institute IRB. Seven subjects were Caucasian, three were African American, three were Hispanic, and two were Asian. Subjects were required to have normal or corrected-to-normal vision. All subjects were screened with psychiatric, physical, and neurological examinations, urine drug screens, and pregnancy tests for women of childbearing capacity. Potential subjects were excluded if they had a history of current or past Axis I psychiatric disorders (including substance abuse/dependence) as determined by the Structured Clinical Interview for DSM-IV Axis I Disorders (SCID-NP), a history of neurological disease, or seizure risk factors. The SCID for Axis II personality disorders was also administered, and any potential subject with a history of antisocial personality disorder was excluded.

Guilty Knowledge Task

Deception studies using GKTs require subjects to answer a series of yes/no questions about stimuli with instructions to answer some questions truthfully and other questions untruthfully (Lykken, 1960; MacLaren, 2001). In a playing card GKT (e.g., Langleben et al., 2002, 2005), subjects are "dealt" a hand and are then shown a playing card on a monitor, along with the question, "Do you have this card?". They are to respond "no" to designated cards in their hands (those that were to be lied about) and to respond truthfully with a "yes" response to the other cards in their hand or to other cards in the deck. In our design, the GKT is repeated over three sessions and subjects are asked to perform six blocks of 60 trials each in each session (see task procedure). The subjects were "dealt" six cards: three to be lied about and three to be responded to truthfully, and 34 "other" cards not in hand (i.e., all non-face cards in an ordinary deck of playing cards were used). Beyond the large number of card stimuli used, the identity of the six cards in hand was changed every block of trials. This continual change in the identity of the lie and truth cards prevented subjects from learning automatic responses based on a constant stimulus-response mapping, and instead forced them to continue to use the executive processes used by the FPN. By using this variable mapping procedure (e.g., Shiffrin and Schneider, 1977), we expected to keep controlled processing in play: executive processes to continually maintain Lie and Truth categories. Similar information management processes must be used in everyday deceptive behavior, when one must remember what was said to whom while weighing what truth or lies will be told (Sip et al., 2008). The variable mapping procedure also mimicked what happens in a card game, where the cards that might be lied about fluctuate with each new hand.

We also attempted to increase the difficulty for control processes to maintain the Lie and Truth categories by preceding each "Deception" block of trials in which the subject was to attempt to deceive the computer or to say the truth, by an "All-Truth" block using the same hand of cards in both blocks, in which subjects were asked to always respond truthfully (i.e., respond "yes" if the displayed card was in hand, and "no" if it was not). It was expected that in the deception block, in a "Lie" trial, subjects would need to inhibit a more prepotent truthful "yes" response temporarily established by stimulus-response mappings generated in the previous block, thus making the control process involved more vulnerable to TMS disruption.

Further, we attempted to maintain a personal context of being deceptive on the part of the subjects by creating a virtual "Other" they would be deceiving. Subjects were told that the computer would use their responses during a block of trials to guess which cards they had in their hand and that the computer's guess would be displayed at the end of the block. They were told that this guessing program was a work in progress, that they were there to test it by actively trying to fool the computer by lying about some of their cards, and that they succeeded if the computer's guess was wrong. This manipulation was performed to increase subject's incentive to deceive convincingly throughout a session. Moreover, such continued virtual interactions have been shown to elicit strong parietal activations in imaging studies (Lisofsky et al., 2014), leading to an expectation that parietal stimulation might affect the processing associated with that interaction and virtual interaction processes that would elicit stronger parietal activations. The order of card presentation in a block of trials was designed to reinforce the perception that the computer was gradually homing in on the cards in the subject's hand by presenting the subject's cards more and more frequently over the course of the block. One indication that this had been effective came during subject debriefing after their last session. All subjects were surprised to find out that the computer was not trying to guess their cards, and that their efforts to fool it were unnecessary.

Task Procedure

Subjects were seated in a cushioned chair in the middle of the testing room, facing a computer monitor 100 cm away, with their heads resting on a chin rest. In each session, subjects were asked to perform six blocks of 60 trials. In each block, they were dealt a "hand" of six physical playing cards, displayed along the bottom of the monitor to allow for continuous viewing of the cards throughout the trial. Cards were chosen randomly by a computer before the session, with the only constraint being that the hand contained a mixture of suits.

The blocks alternated between "All-Truth" blocks, in which subject had to answer truthfully to all trials; and "Deception" blocks, in which they had to either: deny having three of the cards ("Lie" cards: 20 trials), answer truthfully about three others ("Truth" cards: 20 trials), or answer truthfully about not-in-hand cards ("Other" cards: 20 trials) (**Figure 1A**). Before this second block, they were told that the computer would use their responses to guess which cards they had in their hand. The computer's "guess" of the subject's hand appeared at the end of the block of trials. The trial type for each trial was randomly chosen with two constraints: first, that there were twenty of each of the three trial types over the 60-trial block, and second, that as trial number increased, the probability of an "Other" trial decreased. For a given trial, a number between 1 and 60 was randomly chosen by the computer. If the number was less than the trial number + 6, the card would be chosen from the "in hand" cards (+6 was

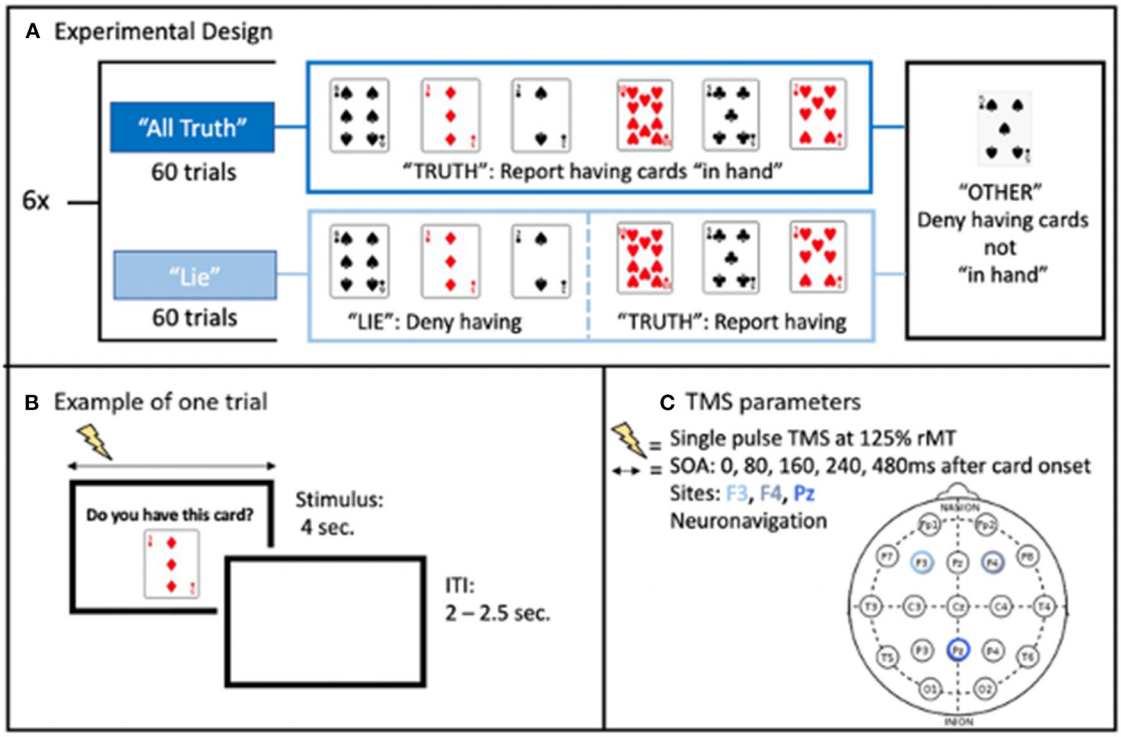

FIGURE 1 | (A) Illustration of the experimental design. **(B)** Example of one trial with each card presented for 4 s, during which single pulse TMS was applied, and separated from each other by a random inter-trial interval. **(C)** Stimulation parameters with randomized stimulus onset asynchrony (SOA) relative to the card presentation onset.

arrived at empirically to lead to more in hand cards earlier in the block). This resulted in an increased frequency of "in hand" cards over the block of trials. On each trial, a digital image of a playing card was displayed on the monitor for 4 s, with a randomized 2.0–2.5 s interval between displays (**Figure 1B**). Only numbered cards and aces were used (a forty card "deck"). The display of a card was the cue to respond as to whether it was in their hand or not. Subjects were instructed to confirm or deny their possession of a given card by making a speeded response by button press.

TMS Application

Single pulse TMS were applied using a figure 8 coil (9 cm diameter) powered by a Magstim 200 stimulator (Magstim Co., Whitland, Southwest Wales, UK). Stimulation intensity was set at 125% of resting motor threshold of the left hemisphere. Resting motor threshold was defined as the lowest intensity needed to evoke motor potentials of at least 50 μV recorded via EMG from the right first dorsal interosseus muscle (FDI) in at least 5 out of 10 stimulations (Rossini et al., 1994). Stimulation was applied over the left DLPFC, right DLPFC, and medial parietal cortex on three different days, with the order counterbalanced across subjects. These three areas are associated with deception (see Introduction) and were targeted using the International 10–20 EEG system (F3, F4, Pz, respectively). Monophasic TMS pulses were used, with the TMS-induced electric field going in the posterior-anterior direction. Without electric field modeling or participant's anatomical MRI to serve as a guide, the coil was positioned perpendicularly to the midline for the frontal targets with the handle pointing down for the left and the right DLPFC. For the medial parietal cortex, the coil handle was parallel to the midline and pointing downward. The coil was positioned and continuously monitored during each session using a computerized frameless stereotaxic system (Brainsight, Rogue Research, Montreal, Canada) based upon a standard brain (MNI). In each trial, single pulse TMS was delivered with a stimulus onset asynchrony (SOA) between card presentation and the TMS pulse of either 0 (Control condition), 80, 160, 240, or 480 ms (**Figure 1C**). The SOA in each trial was randomized, with the constraint that there were four trials of each SOAs for each of the three trial types (truth, lie, other) in each 60-trial block. This resulted in 24 trials per SOA per trial type over a given scalp location. There were three sessions per subject, each session lasted ∼3 h. At the end of the third session, the subject was debriefed as to the purpose of the study and the real nature of the stimulus presentation program.

Performance was assessed by measuring response accuracy and reaction time (RT), as well as a score that combines accuracy and RT into a composite score called the inverse efficiency score (IES = RT/Accuracy: Townsend and Ashby, 1978). We included the IES as it is a robust predictor in detecting deception from truth telling (Monaro et al., 2021). We expected single pulse TMS to disrupt deception processes specific to executive control of

stimulus/response selection and inhibition, as reflected by lower accuracy, slower RT and/or higher IES, only for "Lie" cards for stimulation applied over the parietal cortex and the DLPFC; and only for stimulation applied at 240 ms (and possibly 160 ms), when these specific processes are critically active, as reflected by the peak activity of N2 ERP components. We did not expect any changes for stimulation applied at 0 ms, when these executive processes had not yet been called into play. While the "extra" processing required to select a deceptive response was expected to make performance in the Lie category vulnerable to TMS, we did not expect any changes in reaction time, accuracy, or IES when "truth" or "other" cards are presented, as response selection can occur according to the truthful well-learned default.

Analysis

Omnibus repeated measure ANOVAs were run for median reaction time (RT), mean accuracy (% correct), and inverse efficiency score (IES) calculated as the ratio between RT and accuracy. The All-Truth Blocks were not included in the analysis since they were only used as a primer to make the inhibition of truthful answers more challenging in the subsequent Deception Blocks. Analyses were performed only on the Deception Blocks with the following within-subjects factors: Site (Left DLPFC, Right DLPFC and medial parietal), Card Conditions (Truth, Lie, and Other), and SOA (0, 80, 160, 240, 480 ms).

RESULTS

Fifteen subjects were enrolled. Data from one subject was excluded due to excessively long reaction times which were greater than two standard deviations above the group mean in all conditions (our *a priori* defined criterion for drop-out). All data are reported as mean ± standard deviation.

Accuracy Performance in the GKT Task

There were no effects on performance accuracy caused by TMS or by deception. The repeated measures ANOVA revealed a main effect of Card Condition [$F_{(2,26)} = 3.85$, $p = 0.03$, $\eta^2 = 0.031$] on accuracy. *Post-hoc* Bonferroni comparisons showed that, while no differences were found between "Lie" (95.18 ± 5.99%) and "Other" cards (97.43 ± 4.14%) [$t_{(13)} = -2.05$, $p = 0.15$] or between "Lie" and "Truth" cards (94.52 ± 5.91%), [$t_{(13)} = 0.59$, $p > 0.05$], a significant difference was found between "Truth" cards and "Other" cards (97.43 ± 4.14%) [$t_{(13)} = 2.64$, $p = 0.04$], suggesting that participants were more accurate when responding truthfully about the cards that were not in their hand compared to the cards that were. Results also revealed a main effect of SOA [$F_{(4,52)} = 3.20$, $p = 0.02$, $\eta^2 = 0.003$] but Bonferroni corrections did not reveal any significant differences between each pairwise comparisons ($p > 0.05$ for all, see **Table 1**). There was no main effect of Site [$F_{(2,26)} = 0.686$, $p = 0.51$] and no interaction was found between Site and Card Condition, Site and SOA, or Card Type and SOA ($F < 1$ for the three interactions), nor was the two-way interaction between the three factors significant [$F_{(16,208)} = 1.25$, $p = 0.23$].

Reaction Time Performance in the GKT Task

The repeated measures ANOVA did not reveal a main effect of Card Condition [$F_{(2,26)} = 1.27$, $p = 0.30$], Site [$F_{(2,26)} = 0.49$, $p = 0.62$], or SOA [$F_{(4,52)} = 2.45$, $p = 0.06$] (see **Table 1**). However, a significant interaction was found between Site and SOA [$F_{(8,104)} = 2.26$, $p = 0.03$, $\eta^2 = 0.010$], suggesting that TMS had location and latency specific effects on RT. *Post-hoc* Bonferroni comparisons, performed to decompose this interaction revealed a significant difference between stimulation applied at 240 ms SOA at the parietal site (1,080 ± 330 ms) compared to TMS applied at 0 ms SOA (980 ± 240 ms) [$t_{(13)} = 3.97$, $p = 0.01$] (see **Figure 2**). No other comparison reached statistical difference threshold. This suggests that applying TMS at 240 ms after stimulus onset slowed participants' performance compared to our control condition. Another interaction was found between Stimulation Site and Card Type [$F_{(4,52)} = 3.05$, $p = 0.03$, $\eta^2 = 0.013$], and Bonferroni corrected *post-hoc* comparisons revealed a trend toward significance between parietal stimulation when subjects were instructed to lie (1,080 ± 330 ms) vs. when responding to "Other" cards (990 ± 0.210 ms) [$t_{(13)} = 3.20$, $p = 0.07$]. Subjects tended to take longer to lie than to respond neutrally when the parietal region was stimulated.

Inverse Efficiency Score in the GKT Task

The repeated measures ANOVA performed on the IES, a composite measure that integrates reaction time and accuracy and to be a good indicator of deception, found no main effect of Site [$F_{(2,26)} = 0.39$, $p = 0.68$], SOA [$F_{(4,52)} = 1.64$, $p = 0.18$], or Card Type [$F_{(2,26)} = 2.78$, $p = 0.08$]. The interactions

TABLE 1 | Mean percent accuracy and reaction time (in seconds) and their standard deviation for each SOA, card condition, and site.

SOA	**0 ms**	**80 ms**	**160 ms**	**240 ms**	**480 ms**
Accuracy	95.38 (5.28)	95.37 (5.30)	95.92 (4.97)	95.47 (4.77)	96.42 (4.29)
Reaction time	1.00 (0.21)	1.03 (0.22)	1.03 (0.23)	1.04 (0.24)	1.04 (0.20)
Card condition	**Lie**	**Other**	**Truth**		
Accuracy	95.18 (5.99)	97.43 (4.14)	94.52 (5.91)		
Reaction time	1.04 (0.24)	1.01 (0.22)	1.03 (0.20)		
Site	**Left**	**Right**	**Parietal**		
Accuracy	96.51 (4.40)	96.23 (6.89)	94.37 (7.69)		
Reaction time	1.06 (0.31)	1.03 (0.25)	1.00 (0.19)		

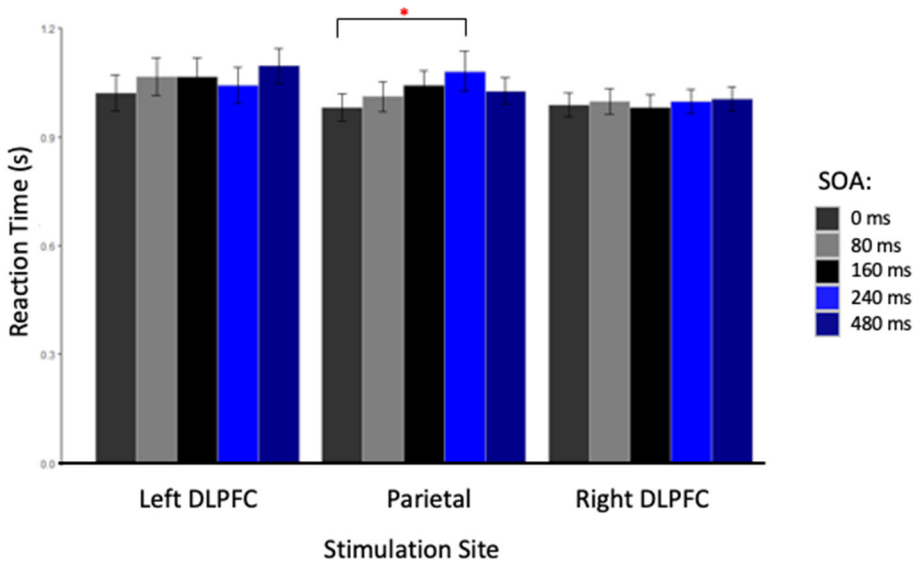

FIGURE 2 | Reaction Time in seconds for each stimulation site at each stimulus onset asynchrony (SOA). The red star indicated a significant difference between reaction times for TMS applied at 0 and 240 ms, only when the parietal cortex was stimulated.

between Card Type and SOA, and Site and SOA were not significant [$F_{(8,104)} = 0.84$, $p = 0.57$; and $F_{(8,104)} = 1.52$, $p = 0.16$, respectively]. However, the interaction between Card Type and Site was significant [$F_{(4,52)} = 2.67$, $p = 0.04$, $\eta^2 = 0.019$]. *Post-hoc* Bonferroni-corrected *t*-tests showed that only when the parietal cortex was stimulated, participants were less efficient in responding with a lie about the cards in their hands than with the truth about the cards that they did not have in their hands ("Lie" cards = 0.011 ± 0.003 ms vs. "Other" cards = 0.010 ± 0.003 ms, $p = 0.02$). Finally, the two-way interaction between the three factors was close to significance [$F_{(16,208)} = 1.63$, $p = 0.06$, $\eta^2 = 0.021$], and the decomposition of this interaction with Bonferroni correction showed that applying TMS over the parietal cortex at 240 ms made participants significantly less efficient when asked to lie (0.013 ± 0.005 ms) than when stimulation was applied at 0 ms (0.011 ± 0.002 ms, $p = 0.05$), mirroring the effect seen with RT alone. Moreover, participants were less efficient at lying when TMS was applied at 240 ms compared to responding with the truth about "Other" cards at every SOA (0 ms = 0.009 ± 0.002 ms, $p < 0.01$; 80 ms = 0.010 ± 0.002 ms, $p = 0.012$; 160 ms = 0.010 ± 0.002 ms, $p = 0.03$; 240 ms = 0.010 ± 0.003 ms, $p = 0.02$; and 480 ms = 0.010 ± 0.002 ms, $p = 0.016$, see **Figure 3**). In contrast with these TMS effects related to the deception condition found with parietal stimulation, no differences were found in IES with TMS applied over right or left DLPFC.

When considering the effect of TMS on IES at the individual level, and focusing on the Lie condition, where the TMS effects were found, some influential interindividual variability can be seen, with some participants less efficient than others (**Figure 4**). However, this is specific to some of our conditions, for example, participants with high IES in parietal cortex stimulation do not display high IES for left DLPFC stimulation, suggesting that stimulation effects are different at the parietal site. Therefore, future studies might want to reproduce this experiment with larger sample size to understand why some participants show stronger TMS effects than others.

DISCUSSION

In this preliminary study, we tested whether applying single pulse TMS at specific time points over three nodes of the fronto-parietal network while participants performed a playing card guilty knowledge task could disrupt behavioral performance conditional on deception instructions. Our results demonstrated a site- and latency-specific effect of TMS, since performance to "Lie" cards was disrupted only when the parietal cortex was stimulated 240 ms after stimulus onset, therefore supporting a functional role for the midline parietal cortex processes supporting deception.

Parietal Cortex Involvement in Processes Supporting Deception

The disruption of processes used for deception, as reflected by an increase in reaction time and IES when TMS was applied over the parietal cortex at 240 ms after the stimulus onset, is in keeping with the expanding knowledge of the role of parietal cortex in control of task processing as part of the fronto-parietal executive network. While parietal association cortex has traditionally been associated with sensorimotor control (e.g., grasping with hands, or eye movements toward, salient visual objects; e.g., Rafal, 2006), research over the last few decades has expanded the role of posterior parietal cortex to include more processing preparatory to such actions: identifying objects within a visual scene according to their salience in relation to goals (Buschman and Miller, 2007; Egner et al., 2008) and their affordances (i.e., understanding objects by the actions they

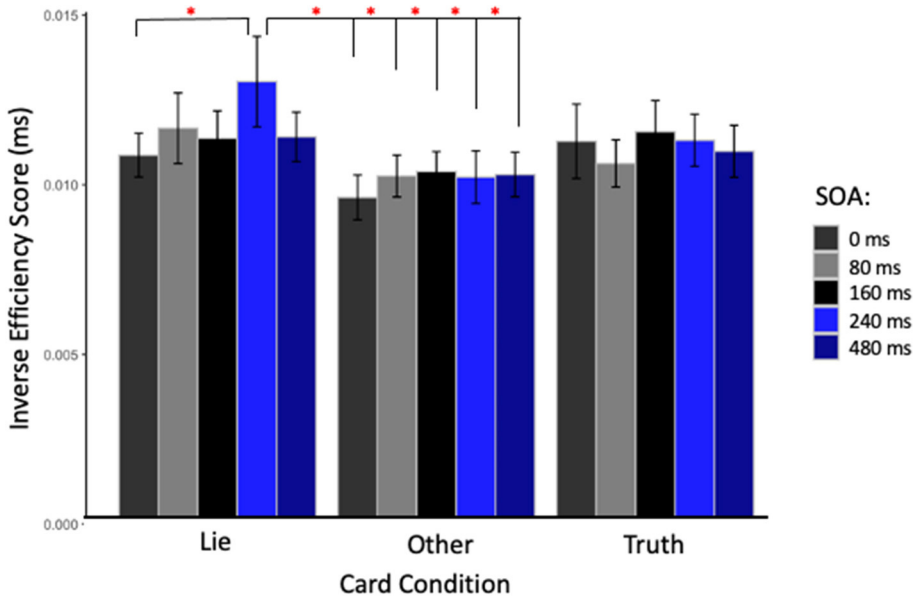

FIGURE 3 | Inverse efficiency score (IES) in milliseconds for TMS applied over the parietal cortex at each SOA and for each card type. Red stars indicate significant IES difference when stimulation was applied at 240 ms after the stimulus onset and subjects were asked to lie, compared to when stimulation was applied at 0 ms in the same condition; or to any other timing when subjects were asked to being truthful about cards not in hand.

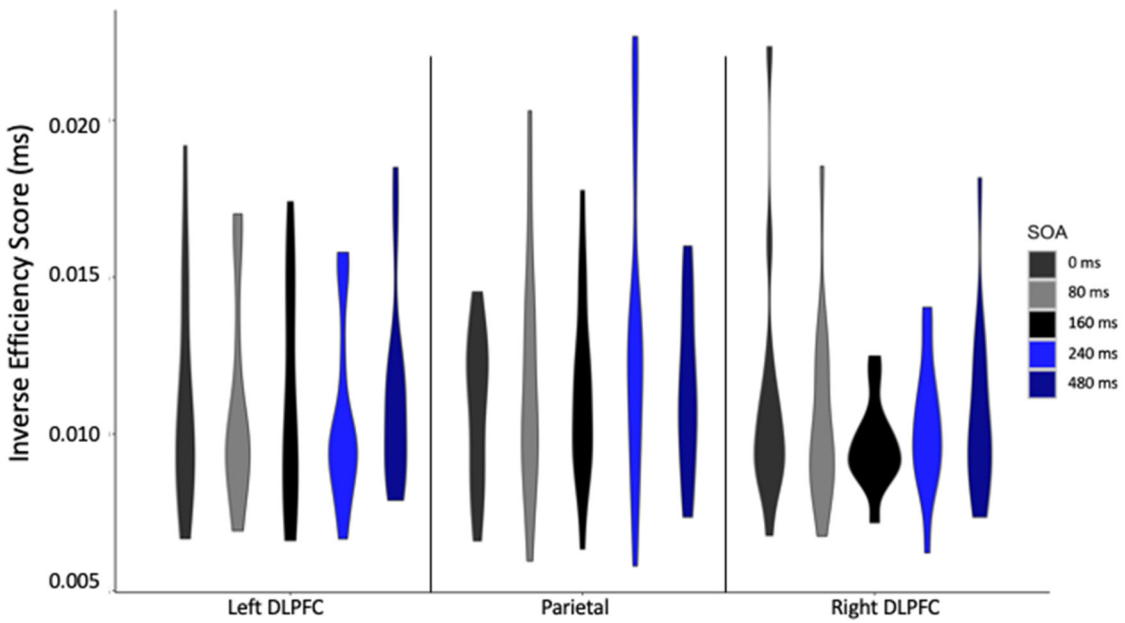

FIGURE 4 | Inverse efficiency score (IES) in milliseconds for each stimulation site, at each stimulus onset asynchrony (SOA) for Lie cards only.

afford; Binkofski and Buccino, 2018). Such mapping is done laying out relational inferences between objects and categories structurally in a scene (Summerfield et al., 2020) with object representations formed in relation to their action affordance and task salience but independent of action planning (Kastner et al., 2017). This independence from action allows for the involvement of working memory on object representations (Marois and Todd, 2004; Davis et al., 2018; Papagno, 2018; using TMS Luber et al., 2007), although ultimately all is in the service of visuomotor transformation based on task-related salience and object affordance (Binkofski and Buccino, 2018). In the present study the choice of the GKT removed many of the

processes associated with deception such as risk management, impression management, and reputation management (Sip et al., 2008). Instead, it focused on information management processes requiring involvement of the fronto-parietal network to carry out a deceptive response, primarily those involving response selection and inhibition of prepotent truth. In particular, the categorization of Truth and Lie cards by spatial position, the concurrent placement of the test card in the visual field with the cards in hand, and the complexity of the individual stimuli (six cards in hand, thirty-two other cards, all varied across blocks of trials) would be expected to require the mapping-for-action processes the posterior parietal cortex specializes in. Moreover, it has become clear that the dorsal visual processing stream flowing through the parietal cortex (Mishkin and Ungerleider, 1982) is itself divided into multiple processing streams, with a ventro-dorsal pathway that handles more constant object properties, and a more medial dorso-dorsal stream handling more variable visual context (Sakreida et al., 2016). Given the continued variation in card stimuli, it is not surprising that TMS to the medial parietal cortex could disrupt performance in the present study which would be dependent on this latter pathway, although that remains to be tested by comparing TMS to the two paths.

The finding that the performance disruption only occurred in the Lie condition provides evidence that the added requirement to suppress a prepotent truth and respond with a no places an extra processing burden on the parietal visuomotor transformation mechanisms. The timing of the TMS generating the parietal performance disruption at 240 ms post visual stimulus onset also lines up with event-related potential (ERP) findings: namely, the N2B and N2C components, which occur between 200 and 300 ms post stimulus onset, and which are associated with executive processing in the fronto-parietal control network and with task-related stimulus classification in posterior cortex (Folstein and van Petten, 2008; Pires et al., 2014).

Beyond its involvement in goal-related representation, visuomotor transformation, and executive functions, the parietal cortex is also known to be highly involved in theory of mind and social cognition, and this leads to a second possible mechanism behind the effect on performance in a deceptive context with parietal TMS. The location of the stimulating coil was near the precuneus, which is involved in self-processing (Cavanna and Trimble, 2006; in TMS: Lou et al., 2004) and which has been activated in tasks involving deception in imaging studies (Lisofsky et al., 2014). In our modified version of the GKT, a game-playing context was created in which subjects were trying to fool a device that was trying to guess their cards by trying to "read" their responses. At the same time, the computer appeared to be narrowing in on the cards in their hands by querying about them with a greater and greater frequency, although it did not always guess them correctly at the end of a block. According to debriefings, subjects were generally convinced that this back-and-forth game with the computer was real, and that the computer was getting closer and closer to knowing what cards were in their hands, even though they were lying about half of them. Thinking about their active deceptive role while moving progressively closer to being "caught" may have resulted in precuneus self-related processing in our subjects which contributed toward the Lie response, which TMS to this site could disrupt. However, given our current design, it is difficult to dissociate those two cognitive vs. socio-cognitive potential explanations, and will require future studies to better answer this question.

Lack of Prefrontal Effect on Deceptive Performance

As major nodes in the fronto-parietal network, right and left DLPFC were chosen as TMS sites, given that, as with the parietal cortex, we expected they could be active during the GKT task, where the sorts of controlled processing performed by DLPFC might be needed to execute the deception task. This expectation has been supported by several electrophysiologic, neuroimaging and brain stimulation studies with TMS and tDCS all demonstrating significant involvement of the DLPFC in processing during deception tasks. However, our results failed to show an effect of our deception manipulation. Several factors could have been responsible for this.

First, using the present version of the playing card GKT, DLPFC processing might not be essential to performance, a possibility supported by the present results. It is possible that the parietal part of the FPN network alone was sufficient to perform the task, as the DLPFC tends to be activated with added task complexity (e.g., Feredoes et al., 2011). Given that the GKT used here has arguably the simplest form a deception task can take, with a framework of simple categorization using well-known stimuli, this may well be the case. The addition of a working memory component to the deception task (e.g., Ganis et al., 2003), or a greater number of categories, such as a "yes" lie condition, or a more complicated decision rule about which cards to lie about, could be expected to promote the involvement of DLPFC and give TMS applied there something to disrupt.

Second, the site of TMS application may not have been optimal, both within the DLPFC, or more generally, within prefrontal cortex. Supporting the latter case, some previous imaging studies using GKT found deception-related activations in ventrolateral PFC rather than DLPFC (Langleben et al., 2005; Spence et al., 2008). Future TMS research investigating GKT and deception processing should utilize targeting using individualized fMRI (Beynel et al., 2020)—a limitation of the present study (see below). Along the lines of choice of stimulation site, both imaging and stimulation studies of deception have noted more lateral, and bilateral, prefrontal involvement (e.g., Priori et al., 2008; Sandrini et al., 2008). Interhemispheric compensation could have prevented a TMS effect, especially in response to single pulse TMS. Future studies might be designed to explore this possibility by using bilateral stimulation of the DLPFC concurrently using two stimulation coils (Santarnecchi et al., 2018).

A third potential reason for the lack of a PFC-based disruption could have been the timing of the TMS pulses. The range of SOAs for TMS (0–480 ms) was centered on the time period between 150 and 300 ms, when visual processing involved with

task-relevant classification that we hoped to affect primarily occurs, as reflected in the activity (and frontal and posterior distribution) of the N200 complex of ERP components. However, TMS pulsed at later SOAs beyond the range used here may have affected frontal processing also associated with deception, as indicated by later frontally distributed ERP components that have been shown to be involved with deception (e.g., Johnson et al., 2008). Future studies might want to more closely coordinate ERPs, as proxies for the dynamics of processing, with the timing of TMS pulses: for example, using a closed loop TMS approach by sending pulses when changes in ERP magnitude are detected, therefore replicating, and extending Karton and Bachmann (2017).

A fourth potential reason is more general: while a single pulse at 240 ms SOA might work to disrupt the kind of processing occurring in parietal cortex when deception is required, the stimulus parameters used in this study may have not been appropriate to do so in DLPFC. For example, while a single pulse might not be effective, a short train of pulses might be, or single pulses at a higher intensity than used here.

Lack of Difference in Truth and Lie Performance

An interesting result in this study was the absence of difference between Truth and Lie conditions, in contrast to the observed worsening of performance in the Lie condition compared to the "Other" card condition. It is worthy of consideration that in many deception tasks, RT in lie conditions is observed to be slowed relative to truth conditions (e.g., Seymour et al., 2000; Spence et al., 2001; Ganis et al., 2003), and that this is offered as evidence that the act of deception requires additional, time-consuming executive processing beyond what is required for truthful responses. While this is often the case, there have been other studies in which there was no difference in RT between lie and truth (Kozel et al., 2005; Abe et al., 2006), or in which truth response was actually slower (Langleben et al., 2005). As these studies indicate, RT differences in lie vs. truth conditions are task dependent. Relative increases in the lie condition in some deception tasks may have to do with increased executive processing as responses are produced which conflict with prepotent responses to the truth. Production of a deceptive response in our playing card GKT may have relied less upon these processes, as what is to be lied about has been clearly demarcated well ahead of response production. Here, deception may rely upon keeping lie and truth categories clear in working memory, as a visual search matching the test card and cards in hand proceeds, while this was not the case in responding to "Other" cards.

Conclusions and Limitations of the Study

While TMS offers a means to interfere with cortical processing associated with deception, there are many challenges due to the large number of processes contributing to deceptive acts, including: deciding who to lie to, when to lie in a given context, and what to lie about, assessing the social consequences of lying, monitoring the success of the lie and keeping track of what was lied about, as well as the immediate processing involved with performing an act of deception, categorizing the perceptual stimuli in the context of the lie and suppressing the default of telling the truth in response to a query. In this study, we deliberately limited the set of processes needed for deceptive performance to the latter group needed for immediate response selection and inhibition, to establish an initial proof-of-concept for this TMS paradigm to explore the underlying neural mechanisms of deception. Single pulse TMS applied to medial parietal cortex at 240 ms after visual stimulus onset significantly slowed response and decreased performance efficiency when stimuli were presented to be lied about, while no effects of TMS on performance were observed with stimuli to be responded to truthfully. This result provides evidence that TMS can be used to target specific processes and network nodes involved with producing deceptive actions in the GKT, and that medial parietal cortex is such a node. However, TMS to DLPFC, a prefrontal region implicated in deception across many imaging, electrophysiological and brain stimulation studies, did not produce any change in deceptive performance in our specific implementation of the GKT. A number of reasons for this lack of frontal effects were suggested, involving the choices of GKT task, target site and method, and TMS timing and other parameters, and a number of future directions for future TMS research were pointed out.

Two other limitations should be pointed out. First, the sample size was relatively small, such that although significant and interpretable effects were found they cannot be generalized, and more subjects would be required to reduce interindividual variability and conduct more powerful and meaningful statistical analyses. Second, the targeting approach represents another limitation since the 10–20 EEG approach was used to target the DLPFC and the parietal cortex. While this method offers easy and cheap technique it has been found to often miss the desired target (e.g., Herwig et al., 2003). Spatial targeting could be improved by first obtaining functional brain images specific to this version of the GKT with fMRI, and then using the individual brain images to guide the selection of TMS targets on an individual subject basis, which has been found to be the most effective TMS targeting approach (Beynel et al., 2020). In addition to allowing for finer positioning of the coil, using anatomical MRI could also increase TMS efficacy with an optimal coil orientation, defined by maximizing the strength of the electric field perpendicularly to the closest sulcus (Janssen et al., 2015). Finally, the use of a playing card GKT provided information on the dynamics and neural substrates necessary for the execution of a simple deceptive response, corresponding most directly to bluffing or deceiving in a card game. Future TMS studies are needed to test whether these results generalize to other tasks in which the substance of the deception is not based on simple, arbitrary categories. A more ecologically valid approach might examine deception using real-world knowledge, both autobiographical and more general. Using more complex knowledge representations could illuminate more prefrontal processes of interference and conflict resolution, response inhibition, and higher-level cognitive control that may be more central to understanding and manipulating real-world deception.

To summarize, we demonstrated that single pulse TMS can interfere with ongoing processes used in a deceptive action, providing spatial and temporal information about the neural activity underlying them, and providing an initial step toward using brain stimulation to work out the complex interplay of neural processing required for deception. The utility of such research is broad and could be developed, for instance, as an objective method of detecting deception in the fields of psychiatry and of law and security. In carrying out our paradigm, we succeeded in what must be the first order of business in any study of deception- maintaining a continuous context of deception for the participants throughout their performance of the task- as supported by the fact that each believed they were working against a computer that was actively trying to guess their cards, and were surprised to find out that this was not so. However, these preliminary results cannot clarify whether the TMS affected processes of category selection and inhibition of prepotent response while they were specifically employed under a deceptive intent, or whether the TMS would have had similar performance effects under different (non-deceptive) intent. This requires further studies manipulating deceptive context, for instance by adding a control condition using the same experimental design in which participants would be asked to inhibit the predominant response for certain cards but without being asked to lie. This would be a next step in a series of future studies using TMS needed to explore the neural basis for deceptive actions by examining the component general processes used, both within and outside of a deceptive context, for which the present study provides an initial first step.

DATA AVAILABILITY STATEMENT

The datasets presented in this study can be found in online repositories. The names of the repository/repositories and accession number(s) can be found below: Open Science Framework: https://osf.io/u2npy/.

ETHICS STATEMENT

The studies involving human participants were reviewed and approved by New York State Psychiatric Institute IRB. The patients/participants provided their written informed consent to participate in this study.

AUTHOR CONTRIBUTIONS

BL and SL: conceptualization, funding acquisition, investigation, methodology, project administration, and supervision. TS, MP, and KT: data curation. BL, LB, and HG: formal analysis. LB and HG: visualization. BL, LB, HG, TS, MP, KT, and SL: writing–review and editing. All authors have read and agreed to the published version of the manuscript.

FUNDING

This research was supported by a grant from the Defense Advanced Research Projects Agency (DARPA).

REFERENCES

Abe, N., Suzuki, M., Tsukiura, T., Mori, E., Yamaguchi, K., Itoh, M., et al. (2006). Dissociable roles of prefrontal and anterior cingulate cortices in deception. *Cerebral Cortex* 16, 192–199. doi: 10.1093/cercor/bhi097

Amassian, V. E., Cracco, R. Q., Maccabee, P. J., Cracco, J. B., Rudell, A., and Eberle, L. (1989). Suppression of visual perception by magnetic coil stimulation of human occipital cortex. *Electroencephalogr. Clin. Neurophysiol. Evoked Potentials* 74, 458–462. doi: 10.1016/0168-5597(89)90036-1

Appelbaum, P. S. (2007). Law & psychiatry: the new lie detectors: neuroscience, deception, and the courts. *Psychiatr. Ser.* 58, 460–462. doi: 10.1176/ps.2007.58.4.460

Bashir, S., Al-Hussain, F., Hamza, A., Shareefi, G. F., Abualait, T., and Yoo, W. K. (2020). Role of single low pulse intensity of transcranial magnetic stimulation over the frontal cortex for cognitive function. *Front. Hum. Neurosci.* 14, 1–6. doi: 10.3389/fnhum.2020.00205

Beynel, L., Powers, J. P., and Appelbaum, L. G. (2020). Effects of repetitive transcranial magnetic stimulation on resting-state connectivity: a systematic review. *NeuroImage* 211, 116596. doi: 10.1016/j.neuroimage.2020.116596

Binkofski, F., and Buccino, G. (2018). "The role of the parietal cortex in sensorimotor transformations and action coding," in *Handbook of Clinical Neurology*. 1st Edn. Vol. 151 (Elsevier B.V.), 467–479. doi: 10.1016/B978-0-444-63622-5.00024-3

Buschman, T. J., and Miller, E. K. (2007). Top-down versus bottom-up control of attention in the prefrontal and posterior parietal cortices. *Science* 315, 1860–1864. doi: 10.1126/science.1138071

Cavanna, A. E., and Trimble, M. R. (2006). The precuneus: a review of its functional anatomy and behavioural correlates. *Brain* 129, 564–583. doi: 10.1093/brain/awl004

Christ, S. E., Van Essen, D. C., Watson, J. M., Brubaker, L. E., and McDermott, K. B. (2009). The contributions of prefrontal cortex and executive control to deception: EVIDENCE from activation likelihood estimate meta-analyses. *Cerebral Cortex* 19, 1557–1566. doi: 10.1093/cercor/bhn189

Czigler, I., Balázs, L., and Winkler, I. (2002). Memory-based detection of task-irrelevant visual changes. *Psychophysiology* 39, 869–873. doi: 10.1111/1469-8986.3960869

Davis, S. W., Crowell, C. A., Beynel, L., Deng, L., Lakhlani, D., Hilbig, S. A., et al. (2018). Complementary topology of maintenance and manipulation brain networks in working memory. *Sci. Rep.* 8, 1–14. doi: 10.1038/s41598-018-35887-2

Delgado-Herrera, M., Reyes-Aguilar, A., and Giordano, M. (2021). What deception tasks used in the lab really do: systematic review and meta-analysis of ecological validity of fMRI deception tasks. *Neuroscience* 468, 88–109. doi: 10.1016/j.neuroscience.2021.06.005

Egner, T., Monti, J. M. P., Trittschuh, E. H., Wieneke, C. A., Hirsch, J., and Mesulam, M. M. (2008). Neural integration of top-down spatial and feature-based information in visual search. *J. Neurosci.* 28, 6141–6151. doi: 10.1523/JNEUROSCI.1262-08.2008

Farwell, L. A., and Donchin, E. (1991). The truth will out: interrogative polygraphy ("lie detection") with event-related brain potentials. *Psychophysiology* 28, 531–547. doi: 10.1111/j.1469-8986.1991.tb01990.x

Fecteau, S., Boggio, P., Fregni, F., and Pascual-Leone, A. (2013). Modulation of untruthful responses with non-invasive brain stimulation. *Front. Psychiatry* 3, 97. doi: 10.3389/fpsyt.2012.00097

Feredoes, E., Heinen, K., Weiskopf, N., Ruff, C., and Driver, J. (2011). Causal evidence for frontal involvement in memory target maintenance by posterior brain areas during distracter interference of visual working memory. *Proc. Natl. Acad. Sci. U. S. A.* 108, 17510–17515. doi: 10.1073/pnas.1106439108

Folstein, J. R., and van Petten, C. (2008). Influence of cognitive control and mismatch on the N2 component of the ERP: a review. *Psychophysiology* 45, 152–170. doi: 10.1111/j.1469-8986.2007.00602.x

Ford, C. V., King, B. H., and Hollender, M. H. (1988). Lies and liars: psychiatric aspects of prevarication. *Am. J. Psychiatry* 145, 554–562). doi: 10.1176/ajp.145.5.554

Ganis, G., Kosslyn, S. M., Stose, S., Thompson, W. L., and Yurgelun-Todd, D. A. (2003). Neural correlates of different types of deception: an fMRI investigation. *Cerebral Cortex* 13, 830–836. doi: 10.1093/cercor/13.8.830

Garcia-Sanz, S., Ghotme, K. A., Hedmont, D., Arévalo-Jaimes, M. Y., Cohen Kadosh, R., Serra-Grabulosa, J. M., et al. (2022). Use of transcranial magnetic stimulation for studying the neural basis of numerical cognition: A systematic review. *J. Neurosci. Methods.* 369, 109485. doi: 10.1016/J.JNEUMETH.2022.109485

Herwig, U., Abler, B., Schönfeldt-Lecuona, C., Wunderlich, A., Grothe, J., Spitzer, M., et al. (2003). Verbal storage in a premotor-parietal network: Evidence from fMRI-guided magnetic stimulation. *NeuroImage* 20, 1032–1041. doi: 10.1016/S1053-8119(03)00368-9

Honts, C. R., Devitt, M. K., Winbush, M., and Kircher, J. C. (1996). Mental and physical countermeasures reduce the accuracy of the concealed knowledge test. *Psychophysiology* 33, 84–92. doi: 10.1111/j.1469-8986.1996.tb02111.x

Honts, C. R., Hodes, R. L., and Raskin, D. C. (1985). Effects of physical countermeasures on the physiological detection of deception. *J. Appl. Psychol.* 70, 177–187. doi: 10.1037/0021-9010.70.1.177

Hu, X., Wu, H., and Fu, G. (2011). Temporal course of executive control when lying about self- and other-referential information: an ERP study. *Brain Res.* 1369, 149–157. doi: 10.1016/j.brainres.2010.10.106

Ito, A., Abe, N., Fujii, T., Ueno, A., Koseki, Y., Hashimoto, R., et al. (2011). The role of the dorsolateral prefrontal cortex in deception when remembering neutral and emotional events. *Neurosci. Res.* 69, 121–128. doi: 10.1016/j.neures.2010.11.001

Janssen, A. M., Oostendorp, T. F., and Stegeman, D. F. (2015). The coil orientation dependency of the electric field induced by TMS for M1 and other brain areas. *J. Neuroeng. Rehabil.* 12, 1–13. doi: 10.1186/s12984-015-0036-2

Johnson, R., Barnhardt, J., and Zhu, J. (2003). The deceptive response: effects of response conflict and strategic monitoring on the late positive component and episodic memory-related brain activity. *Biol. Psychol.* 64, 217–253. doi: 10.1016/j.biopsycho.2003.07.006

Johnson, R., Barnhardt, J., and Zhu, J. (2005). Differential effects of practice on the executive processes used for truthful and deceptive responses: An event-related brain potential study. *Cognitive Brain Res.* 24, 386–404. doi: 10.1016/j.cogbrainres.2005.02.011

Johnson, R., Henkell, H., Simon, E., and Zhu, J. (2008). The self in conflict: the role of executive processes during truthful and deceptive responses about attitudes. *NeuroImage* 39, 469–482. doi: 10.1016/j.neuroimage.2007.08.032

Karim, A. A., Schneider, M., Lotze, M., Veit, R., Sauseng, P., Braun, C., et al. (2010). The truth about lying: inhibition of the anterior prefrontal cortex improves deceptive behavior. *Cerebral Cortex* 20, 205–213. doi: 10.1093/cercor/bhp090

Karton, I., and Bachmann, T. (2011). Effect of prefrontal transcranial magnetic stimulation on spontaneous truth-telling. *Behav. Brain Res.* 225, 209–214. doi: 10.1016/j.bbr.2011.07.028

Karton, I., and Bachmann, T. (2017). Disrupting dorsolateral prefrontal cortex by rTMS reduces the P300 based marker of deception. *Brain Behav.* 7, 1–8. doi: 10.1002/brb3.656

Karton, I., Palu, A., Jõks, K., and Bachmann, T. (2014a). Deception rate in a "lying game": different effects of excitatory repetitive transcranial magnetic stimulation of right and left dorsolateral prefrontal cortex not found with inhibitory stimulation. *Neurosci. Lett.* 583, 21–25. doi: 10.1016/j.neulet.2014.09.020

Karton, I., Rinne, J. M., and Bachmann, T. (2014b). Facilitating the right but not left DLPFC by TMS decreases truthfulness of object-naming responses. *Behav. Brain Res.* 271, 89–93. doi: 10.1016/j.bbr.2014.05.059

Kastner, S., Chen, Q., Jeong, S. K., and Mruczek, R. E. B. (2017). A brief comparative review of primate posterior parietal cortex: a novel hypothesis on the human toolmaker. *Neuropsychologia* 105, 123–134. doi: 10.1016/j.neuropsychologia.2017.01.034

Keckler, C. N. W. (2005). Cross-examining the brain: a legal analysis of neural imaging for credibility impeachment. *Hastings Law J.* 57, 509. doi: 10.2139/ssrn.667601

Kelly, K. J., Murray, E., Barrios, V., Gorman, J., Ganis, G., and Keenan, J. P. (2009). The effect of deception on motor cortex excitability. *Soc. Neurosci.* 4, 570–574. doi: 10.1080/17470910802424445

Kozel, F. A., Johnson, K. A., Mu, Q., Grenesko, E. L., Laken, S. J., and George, M. S. (2005). Detecting deception using functional magnetic resonance imaging. *Biol. Psychiatry* 58, 605–613. doi: 10.1016/j.biopsych.2005.07.040

Kozel, F. A., Padgett, T. M., and George, M. S. (2004). A replication study of the neural correlates of deception. *Behav. Neurosci.* 118, 852–856. doi: 10.1037/0735-7044.118.4.852

Langleben, D. D., Loughead, J. W., Bilker, W. B., Ruparel, K., Childress, A. R., Busch, S. I., et al. (2005). Telling truth from lie in individual subjects with fast event-related fMRI. *Hum. Brain Map.* 26, 262–272. doi: 10.1002/hbm.20191

Langleben, D. D., Schroeder, L., Maldjian, J. A., Gur, R. C., Mcdonald, S., Ragland, J. D., et al. (2002). Brain activity during simulated deception : an event-related functional magnetic resonance study. *NeuroImage* 732, 727–732. doi: 10.1006/nimg.2001.1003

Larson, J. A., and Haney, G. W. (1932). Cardio-respiratory variations in personality studies. *Am. J. Psychiatry* 88, 1035–1081. doi: 10.1176/ajp.88.6.1035

Lee, T. M. C., Liu, H.-L., Tan, L.-H., Chan, C. C. H., Mahankali, S., Feng, C.-M., et al. (2002). Lie detection by functional magnetic resonance imaging. *Hum. Brain Map.* 15, 157–164. doi: 10.1002/hbm.10020

Leng, H., Wang, Y., Li, Q., Yang, L., and Sun, Y. (2019). Sophisticated deception in junior middle school students: an ERP study. *Front. Psychol.* 9, 2675. doi: 10.3389/fpsyg.2018.02675

Lisofsky, N., Kazzer, P., Heekeren, H. R., and Prehn, K. (2014). Investigating socio-cognitive processes in deception: a quantitative meta-analysis of neuroimaging studies. *Neuropsychologia* 61, 113–122. doi: 10.1016/j.neuropsychologia.2014.06.001

Lo, Y. L., Fook-Chong, S., and Tan, E. K. (2003). Increased cortical excitability in human deception. *NeuroReport* 14, 1021–1024. doi: 10.1097/00001756-200305230-00023

Lou, H. C., Luber, B., Crupain, M., Keenan, J. P., Nowak, M., Kjaer, T. W., et al. (2004). Parietal cortex and representation of the mental Self. *Proc. Natl. Acad. Sci.* 101, 6827–6832. doi: 10.1073/pnas.0400049101

Lou, H. C., Luber, B., Stanford, A., and Lisanby, S. H. (2010). Self-specific processing in the default network: a single-pulse TMS study. *Exp. Brain Res.* 207, 27–38.

Luber, B., Fisher, C., Appelbaum, P. S., Ploesser, M., and Lisandy, S. H. (2009). Non-invasive brain stimulation in the detection of deception: Scientific challenges and ethical consequences. *Behav. Sci. Law* 27, 191–208. doi: 10.1002/bsl.860

Luber, B., Jangraw, D. C., Appelbaum, G., Harrison, A., Hilbig, S., Beynel, L., et al. (2020). Using transcranial magnetic stimulation to test a network model of perceptual decision making in the human brain. *Front. Hum. Neurosci.* 14, 4. doi: 10.3389/fnhum.2020.00004

Luber, B., Kinnunen, L. H., Rakitin, B. C., Ellsasser, R., Stern, Y., and Lisanby, S. H. (2007). Facilitation of performance in a working memory task with rTMS stimulation of the precuneus: frequency- and time-dependent effects. *Brain Res.* 1128, 120–129. doi: 10.1016/j.brainres.2006.10.011

Luber, B., Lou, H. C., Keenan, J. P., and Lisanby, S. H. (2012). Self-enhancement processing in the default network: a single-pulse TMS study. *Exp. Brain Res.* 223, 177–187. doi: 10.1007/s00221-012-3249-7

Luber, B., Stanford, A. D., Bulow, P., Nguyen, T., Rakitin, B. C., Habeck, C., et al. (2008). Remediation of sleep-deprivation-induced working memory impairment with fMRI-guided transcranial magnetic stimulation. *Cerebral Cortex* 18, 2077–2085. doi: 10.1093/cercor/bhm231

Lykken, D. T. (1960). The validity of the guilty knowledge technique: the effects of faking. *J. Appl. Psychol.* 44, 258–262. doi: 10.1037/h0044413

MacLaren, V. V. (2001). A quantitative review of the guilty knowledge test. *J. Appl. Psychol.* 86, 674. doi: 10.1037/0021-9010.86.4.674

Mameli, F., Mrakic-Sposta, S., Vergari, M., Fumagalli, M., Macis, M., Ferrucci, R., et al. (2010). Dorsolateral prefrontal cortex specifically processes general – but not personal – knowledge deception: multiple brain networks for lying. *Behav. Brain Res.* 211, 164–168. doi: 10.1016/j.bbr.2010.03.024

Maréchal, M. A., Cohn, A., Ugazio, G., and Ruff, C. C. (2017). Increasing honesty in humans with noninvasive brain stimulation. *Proc. Natl. Acad. Sci. U. S. A.* 114, 4360–4364. doi: 10.1073/pnas.1614912114

Marois, R., and Todd, J. J. (2004). Capacity limit of visual short-term memory in human posterior parietal cortex. *Nature* 428, 751−754. doi: 10.1038/nature02466

Mevorach, C., Humphreys, G. W., and Shalev, L. (2006). Opposite biases in salience-based selection for the left and right posterior parietal cortex. *Nat. Neurosci.* 9, 740–742. doi: 10.1038/nn1709

Mishkin, M., and Ungerleider, L. G. (1982). Contribution of striate inputs to the visuospatial functions of parieto-preoccipital cortex in monkeys. *Behav. Brain Res.* 6, 57–77. doi: 10.1016/0166-4328(82)90081-X

Mitchell, R. W. (1986). "A framework for discussing deception," in *Deception: Perspectives on Human and Nonhuman Deceit*, eds R. W. Mitchell and N. S. Thompson (Albany, NY: State University of New York Press), 3–40.

Mohamed, F. B., Faro, S. H., Gordon, N. J., Platek, S. M., Ahmad, H., and Williams, J. M. (2006). Brain mapping of deception and truth telling about an ecologically valid situation: functional MR imaging and polygraph investigation—initial experience. *Radiology* 238, 679–688. doi: 10.1148/radiol.2382050237

Monaro, M., Zampieri, I., Sartori, G., Pietrini, P., and Orr,ù, G. (2021). The detection of faked identity using unexpected questions and choice reaction times. *Psychol. Res.* 85, 2474–2482. doi: 10.1007/s00426-020-01410-4

Noguchi, Y., and Oizumi, R. (2018). Electric stimulation of the right temporo-parietal junction induces a task-specific effect in deceptive behaviors. *Neurosci. Res.* 128, 33–39. doi: 10.1016/j.neures.2017.07.004

Nuñez, J. M., Casey, B. J., Egner, T., Hare, T., and Hirsch, J. (2005). Intentional false responding shares neural substrates with response conflict and cognitive control. *Neuroimage* 25, 267–277. doi: 10.1016/j.neuroimage.2004.10.041

Papagno, C. (2018). "Memory deficits," in *Handbook of Clinical Neurology*, 1st Edn. Vol. 151. (Elsevier B.V.), 377–393. doi: 10.1016/B978-0-444-63622-5.00019-X

Pascual-Leone, A., Pascual-Leone, A., and Hallett, M. (1994). Induction of errors in a delayed response task by repetitive transcranial magnetic stimulation of the dorsolateral prefrontal cortex. *Neuroreport* 5, 2517–2520. doi: 10.1097/00001756-199412000-00028

Phan, K. L., Magalhaes, A., Ziemlewicz, T. J., Fitzgerald, D. A., Green, C., and Smith, W. (2005). Neural correlates of telling lies: a functional magnetic resonance imaging study at 4 Tesla. *Acad. Radiol.* 12, 164–172. doi: 10.1016/j.acra.2004.11.023

Pires, L., Leitão, J., Guerrini, C., and Simões, M. R. (2014). Event-related brain potentials in the study of inhibition: cognitive control, source localization and age-related modulations. *Neuropsychol. Rev.* 24, 461–490. doi: 10.1007/s11065-014-9275-4

Priori, A., Mameli, F., Cogiamanian, F., Marceglia, S., Tiriticco, M., Mrakic-Sposta, S., et al. (2008). Lie-specific involvement of dorsolateral prefrontal cortex in deception. *Cerebral Cortex* 18, 451–455. doi: 10.1093/cercor/bhm088

Rafal, R. D. (2006). Oculomotor functions of the parietal lobe: effects of chronic lesions in humans. *Cortex* 42, 730–739. doi: 10.1016/S0010-9452(08)70411-8

Rossini, P. M., Barker, A. T., Berardelli, A., Caramia, M. D., Caruso, G., Cracco, R. Q., et al. (1994). Non-invasive electrical and magnetic stimulation of the brain, spinal cord and roots: basic principles and procedures for routine clinical application. Report of an IFCN committee. *Electroencephalogr. Clin. Neurophysiol.* 91, 79–92. doi: 10.1016/0013-4694(94)90029-9

Sakreida, K., Effnert, I., Thill, S., Menz, M. M., Jirak, D., Eickhoff, C. R., et al. (2016). Affordance processing in segregated parieto-frontal dorsal stream sub-pathways. *Neurosci. Biobehav. Rev.* 69, 89–112. doi: 10.1016/j.neubiorev.2016.07.032

Sánchez, N., Masip, J., and Gómez-Ariza, C. J. (2020). Both high cognitive load and transcranial direct current stimulation over the right inferior frontal cortex make truth and lie responses more similar. *Front. Psychol.* 11, 1–14. doi: 10.3389/fpsyg.2020.00776

Sandrini, M., Rossini, P. M., and Miniussi, C. (2008). Lateralized contribution of prefrontal cortex in controlling task-irrelevant information during verbal and spatial working memory tasks: rTMS evidence. *Neuropsychologia* 46, 2056–2063. doi: 10.1016/j.neuropsychologia.2008.02.003

Santarnecchi, E., Momi, D., Sprugnoli, G., Neri, F., Pascual-Leone, A., Rossi, A., et al. (2018). Modulation of network-to-network connectivity via spike-timing-dependent noninvasive brain stimulation. *Hum. Brain Mapp.* 39, 4870–4883. doi: 10.1002/hbm.24329

Saxe, L., Dougherty, D., and Cross, T. (1985). The validity of polygraph testing: scientific analysis and public controversy. *Am. Psychol.* 40, 355–366. doi: 10.1037/0003-066X.40.3.355

Seymour, T. L., Seifert, C. M., Shafto, M. G., and Mosmann, A. L. (2000). Using response time measures to assess "guilty knowledge." *J. Appl. Psychol.* 85, 30–37. doi: 10.1037/0021-9010.85.1.30

Shiffrin, R. M., and Schneider, W. (1977). Controlled and automatic human information processing: II. Perceptual learning, automatic attending and a general theory. *Psychol. Rev.* 84, 127–190. doi: 10.1037/0033-295X.84.2.127

Sip, K. E., Lynge, M., Wallentin, M., McGregor, W. B., Frith, C. D., and Roepstorff, A. (2010). The production and detection of deception in an interactive game. *Neuropsychologia* 48, 3619–3626. doi: 10.1016/j.neuropsychologia.2010.08.013

Sip, K. E., Roepstorff, A., McGregor, W., and Frith, C. D. (2008). Detecting deception: the scope and limits. *Trends Cogn. Sci.* 12, 48–53. doi: 10.1016/j.tics.2007.11.008

Sodian, B., and Frith, U. (1992). Deception and sabotage in autistic, retarded and normal children. *J. Child Psychol. Psychiatry* 33, 591–605. doi: 10.1111/j.1469-7610.1992.tb00893.x

Spence, S. A., Farrow, T. F. D., Herford, A. E., Wilkinson, I. D., Zheng, Y., and Woodruff, P. W. R. (2001). Behavioural and functional anatomical correlates of deception in humans. *Neuroreport* 12, 2849–2853. doi: 10.1097/00001756-200109170-00019

Spence, S. A., Kaylor-Hughes, C., Farrow, T. F. D., and Wilkinson, I. D. (2008). Speaking of secrets and lies: the contribution of ventrolateral prefrontal cortex to vocal deception. *Neuroimage* 40, 1411–1418. doi: 10.1016/j.neuroimage.2008.01.035

Summerfield, C., Luyckx, F., and Sheahan, H. (2020). Structure learning and the posterior parietal cortex. *Progress Neurobiol.* 184, 101717. doi: 10.1016/j.pneurobio.2019.101717

Tang, H., Ye, P., Wang, S., Zhu, R., Su, S., Tong, L., et al. (2017). Stimulating the right temporoparietal junction with tDCS decreases deception in moral hypocrisy and unfairness. *Front. Psychol.* 8, 2033. doi: 10.3389/fpsyg.2017.02033

Townsend, J. T., and Ashby, F. G. (1978). "Methods of modeling capacity in simple processing systems," in *Cognitive Theory*, eds N. J. Castellan and F. Restle, 1st Edn (Psychology Press), 199–239.

Verschuere, B., Schuhmann, T., and Sack, A. T. (2012). Does the inferior frontal sulcus play a functional role in deception? A neuronavigated theta-burst transcranial magnetic stimulation study. *Front. Hum. Neurosci.* 6, 284. doi: 10.3389/fnhum.2012.00284

Wu, H., Hu, X., and Fu, G. (2009). Does willingness affect the N2-P3 effect of deceptive and honest responses? *Neurosci. Lett.* 467, 63–66. doi: 10.1016/j.neulet.2009.10.002

Yu, J., Tao, Q., Zhang, R., Chan, C. C. H., and Lee, T. M. C. (2019). Can fMRI discriminate between deception and false memory? A meta-analytic comparison between deception and false memory studies. *Neurosci. Biobehav. Rev.* 104, 43–55. doi: 10.1016/j.neubiorev.2019.06.027

Author Disclaimer: The opinions expressed in this article are the author's own and do not reflect the views of the National Institutes of Health, the Department of Health and Human Services, or the United States government.

Conflict of Interest: BL, LB, HG, and SL were supported by the NIMH Intramural Research Program (ZIAMH002955). This work was done while BL and SL were at Columbia University, prior to their NIMH employment. SL is an inventor on a patent on TMS technology assigned to Columbia University. SL has received grant support from the Brain and Behavior Research Foundation, the Stanley Medical Research Foundation, Neosync, Nexstim, NIH, and Brainsway.

The remaining authors declare that the research was conducted in the absence of any commercial or financial relationships that could be construed as a potential conflict of interest.

Publisher's Note: All claims expressed in this article are solely those of the authors and do not necessarily represent those of their affiliated organizations, or those of the publisher, the editors and the reviewers. Any product that may be evaluated in this article, or claim that may be made by its manufacturer, is not guaranteed or endorsed by the publisher.

frontiers | Frontiers in Human Neuroscience

ORIGINAL RESEARCH
published: 21 June 2022
doi: 10.3389/fnhum.2022.887246

Research Hotspots and Effectiveness of Transcranial Magnetic Stimulation in Pain: A Bibliometric Analysis

*Chong Li[1], Mingyu Sun[1] and Shiliu Tian[1,2,3,4]**

[1] School of Kinesiology, Shanghai University of Sport, Shanghai, China, [2] Key Laboratory of Exercise and Health Science of Ministry of Education, Shanghai University of Sport, Shanghai, China, [3] Shanghai Frontiers Science Research Base of Exercise and Metabolic Health, Shanghai, China, [4] Fujian Sports Vocational Education and Technical College, Fuzhou, China

Transcranial magnetic stimulation, as a relatively new type of treatment, is a safe and non-invasive method for pain therapy. Here, we used CiteSpace software to visually analyze 440 studies concerning transcranial magnetic stimulation in pain research from 2010 to 2021, indexed by Web of Science, to clarify the research hotspots in different periods and characterize the process of discovery in this field. The United States ranked first in this field. Lefaucheur JP, Fregni F, and Andrade ACD made great contributions to this field of study. The most prolific institution was University of São Paulo. The four main hot keywords were neuropathic pain, motor cortex, connectivity, and non-invasive brain stimulation. There were three main points that were generally accepted: (1) definite analgesic effect of high-frequency rTMS of M1 contralateral to pain side in neuropathic pain; (2) there are inconclusive recommendations regarding rTMS of the dorsolateral prefrontal cortex (DLPFC) in fibromyalgia and neuropathic pain; (3) there is low-quality evidence that single doses of high-frequency rTMS of the motor cortex may have short-term effects on chronic pain. This bibliometric analysis indicated that prospective, multi-center, large-sample, randomized controlled trials are still needed to further verify the effectiveness of various transcranial magnetic stimulation parameters in pain research.

Keywords: transcranial magnetic stimulation, pain, citation burst, Web of Science, CiteSpace

OPEN ACCESS

Edited by:
Marina De Tommaso,
University of Bari Aldo Moro, Italy

Reviewed by:
Joaquim Pereira Brasil-Neto,
Unieuro, Brazil
Kun Xiong,
Independent Researcher,
Changsha, China

***Correspondence:**
Shiliu Tian
tianshiliu@sus.edu.cn

Specialty section:
This article was submitted to Brain Imaging and Stimulation, a section of the journal Frontiers in Human Neuroscience

Received: *01 March 2022*
Accepted: *25 May 2022*
Published: *21 June 2022*

Citation:
Li C, Sun M and Tian S (2022) Research Hotspots and Effectiveness of Transcranial Magnetic Stimulation in Pain: A Bibliometric Analysis. Front. Hum. Neurosci. 16:887246. doi: 10.3389/fnhum.2022.887246

INTRODUCTION

Pain is termed as an unpleasant sensory and emotional experience associated with, or resembling that associated with, actual or potential tissue damage (Raja et al., 2020). Pain is a subjective emotional experience, and there are few effective treatments. At present, application of analgesic drugs is the main way to relieve pain (Klit et al., 2009; Alles and Smith, 2018). However, long-term use of analgesic drugs is not only prone to addiction, but also has many side effects (Koob, 2021). Transcranial magnetic stimulation (TMS) is considered to be a safe and non-invasive treatment method that has been extensively used in pain therapy (Leung et al., 2009; de Andrade et al., 2011; O'Connell et al., 2014). Different frequencies of TMS can achieve different therapeutic purposes.

Studies of the motor cortex indicate that high frequencies (>1 Hz) mainly produce excitatory effects, while low-frequency stimulation (≤ 1Hz) produces inhibitory effects (Hallett, 2007; Pitcher et al., 2021). TMS can affect local nerves by altering neural function at multiple sites through the connectivity and interactions between neural networks (Nurmikko et al., 2016; Li et al., 2021). Thus, TMS may have therapeutic effects on pain intensity resulted from various diseases.

Visualization analysis is to use of relevant visualization software to import and convert a large amount of literature data into a visual atlas, so that readers can have a more intuitive and clear understanding of the data contained in the literature through the atlas (Chen, 2004). Based on co-citation analysis theory and pathfinding network algorithm, CiteSpace software can analyze literature of specific disciplines or fields from multiple perspectives and draw visual maps, so as to explore the critical paths, research hotspots, and frontiers of the evolution of this discipline or field (Chen and Song, 2019). In recent years, using CiteSpace software combined with relevant authoritative databases to analyze the literature visualization of a certain discipline or field has become a hot research topic for scholars all over the world (Chen et al., 2012; Ugolini et al., 2013; Xu and Sun, 2020; Wang et al., 2021).

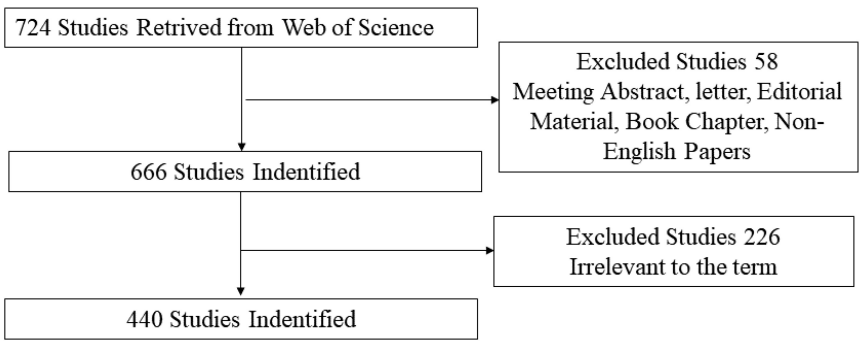

FIGURE 1 | Flow chart of studies inclusion.

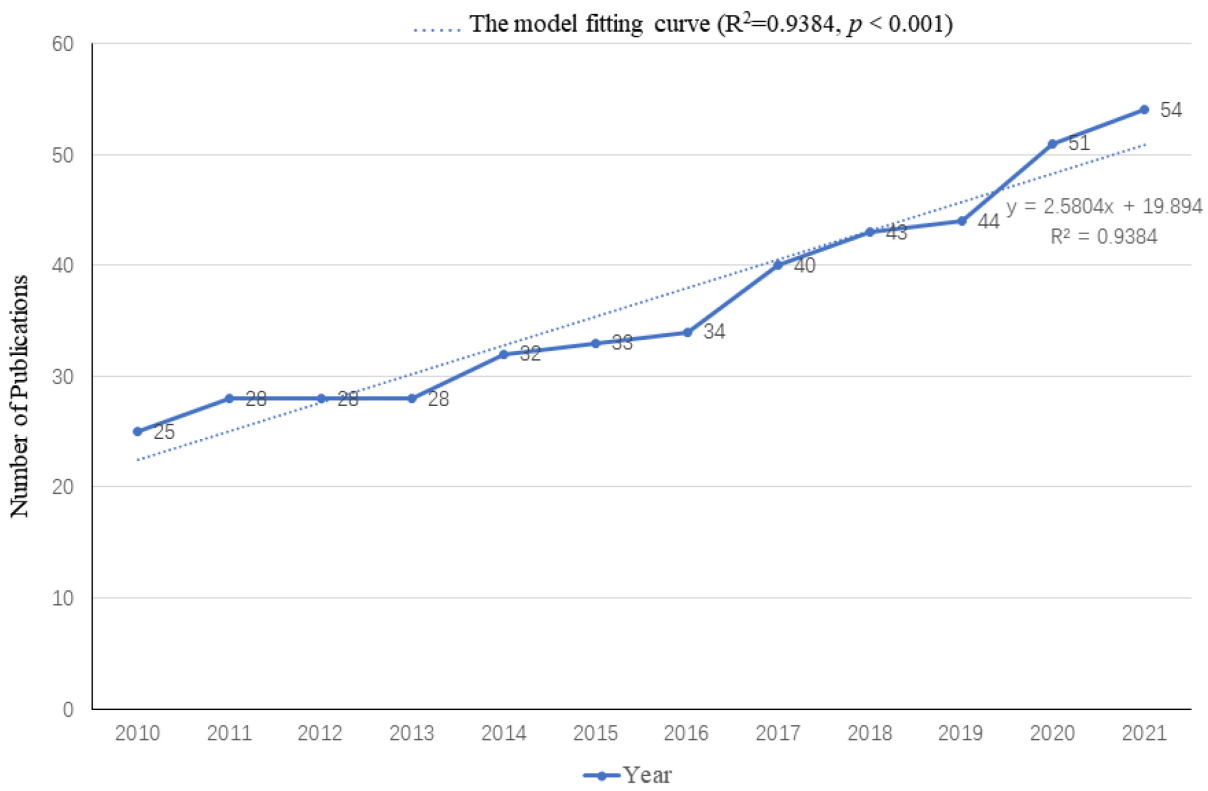

FIGURE 2 | Annual publication outputs and the model fitting curve of the time trend of transcranial magnetic stimulation (TMS) in pain research.

The aim of this study was two-folded: (1) perform a visual analysis of TMS in pain studies using CiteSpace software, and (2) objectively clarify the time changes of research hotspots and dynamic frontiers in this field.

MATERIALS AND METHODS

Data Source and Search Strategy

Published papers were retrieved via a topic search of Web of Science (WOS) Core Collection Database. The search terms were as follows: (((((TS = (transcranial magnetic stimulation)) OR TS = (TMS)) OR TS = (rTMS)) OR TS = (iTBS)) OR TS = (cTBS)) AND TS = (pain). Time span were retrieved from January 01, 2010 to December 31, 2021.

Inclusion Criteria

Studies related to the application of TMS in pain research were selected after reading the title and abstract. Only articles and reviews were included. Other document types, such as letters, commentaries, and meeting abstracts, were excluded. In addition, the publication language was restricted to English. The flow chart of the inclusion is shown in **Figure 1**. Finally, 440 records (344 articles, 96 reviews) were used in the final analysis.

Analytic Methods

Software Parameter Settings

CiteSpace is a bibliometric analysis visualization software developed by Prof. Chen Chaomei (Drexel University, United States) for bibliometric analysis. We used CiteSpace 5.8.R3 to analyze the final records. The "Time Sliding" value was set to 1 year and the type of Node was selected according to the purpose of analysis.

Interpretation of Main Parameters in Visualization Map

Citation Tree Rings

The citation tree ring represents the citation history of a paper. The color of a citation ring denotes the time of the corresponding citation, and the thickness of an annual ring

Cited Journals	Year	Strength	Begin	End	2010 - 2021
CNS SPECTRUMS	2010	6.19	2010	2012	
ARCH NEUROL-CHICAGO	2010	4.58	2010	2014	
COGNITIVE BRAIN RES	2010	3.97	2010	2011	
NEUROSURGERY	2010	4.75	2011	2012	
OTOLARYNG HEAD NECK	2010	3.49	2011	2014	
EXP NEUROL	2010	3.41	2011	2015	
EUR J PHYS REHAB MED	2010	4.37	2012	2014	
WORLD J BIOL PSYCHIA	2010	4.72	2014	2017	
INT J NEUROPSYCHOPH	2010	3.52	2014	2018	
PAIN PHYSICIAN	2010	4.17	2016	2021	
SPINE	2010	3.48	2016	2019	
FRONT NEUROSCI-SWITZ	2010	7.45	2018	2021	
DEPRESS ANXIETY	2010	4.44	2018	2021	
RHEUMATOLOGY	2010	3.96	2018	2019	
CLIN REHABIL	2010	3.91	2018	2021	
TRIALS	2010	3.52	2018	2021	
SCI REP-UK	2010	8.27	2019	2021	
NEURAL PLAST	2010	7.39	2019	2021	
J PAIN RES	2010	7.25	2019	2021	
NEUROSCI BIOBEHAV R	2010	6.83	2019	2021	
ARTHRIT CARE RES	2010	5.63	2019	2021	
FRONT PSYCHOL	2010	5.54	2019	2021	
FRONT HUM NEUROSCI	2010	5.28	2019	2021	
PAIN REP	2010	4.43	2019	2021	
BMC MUSCULOSKEL DIS	2010	4.15	2019	2021	

FIGURE 3 | Top 25 cited journals with the strongest citation burst.

is directly proportional to the number of citations in the corresponding time sliding.

Node Circle and the Link Between Nodes

The radius of a node circle indicates the number of papers published in the author or institutional co-authorship network, and also indicates the frequency of keywords in the co-occurrence network. A link indicates the presence of co-authorship or a co-occurrence relationship. The node colors range from cold to warm to represent the chance of time, blue for earlier years, and red for recent years.

Betweenness Centrality

Betweenness centrality is an index that measures the importance of nodes in the network. CiteSpace uses this index to discover and measure the importance of studies and highlights such studies with purple circles.

Cluster View and Burst Detection

Cluster view is carried out on the generated map, and each cluster is labeled by citing the title, keywords, and subject headings in the abstract of the citing reference. The function of Burst detection is to detect the situation where there is a great change in the number of citations in a certain period. Thus it can be used to find the decline or rise of keywords.

Dual-Map Overlaps

Dual-map overlaps are a new method to display the distribution and citation trajectory of papers in various disciplines. As a result, there is a distribution of citing journals on the left side and a distribution of cited journals on the right side. The curve is the citation line, which completely shows the context of the citation.

RESULTS

Publication Outputs

A total of 440 publications were included in the analysis. **Figure 2** shows the distribution of the annual publication of TMS in pain research from 2010 to 2021. The overall trend is positive and the time trend of publications indicated a significant correlation ($R^2 = 0.9384$, $p < 0.001$) between the annual publication outputs and the years in the last 11 years.

Journal Co-citation Analysis

Journal co-citation analyses of reference from 2010 to 2021 cited by 440 publications found that among the earliest journals, *CNS SPECTRUMS*, *ARCH NEUROL-CHICAGO*, and *COGNITIVE BRAIN RES* had the earliest hotspots in 2010, and *PAIN PHYSICIAN* had hotspots for the longest period and also had recent frontier hotspot from 2016 to

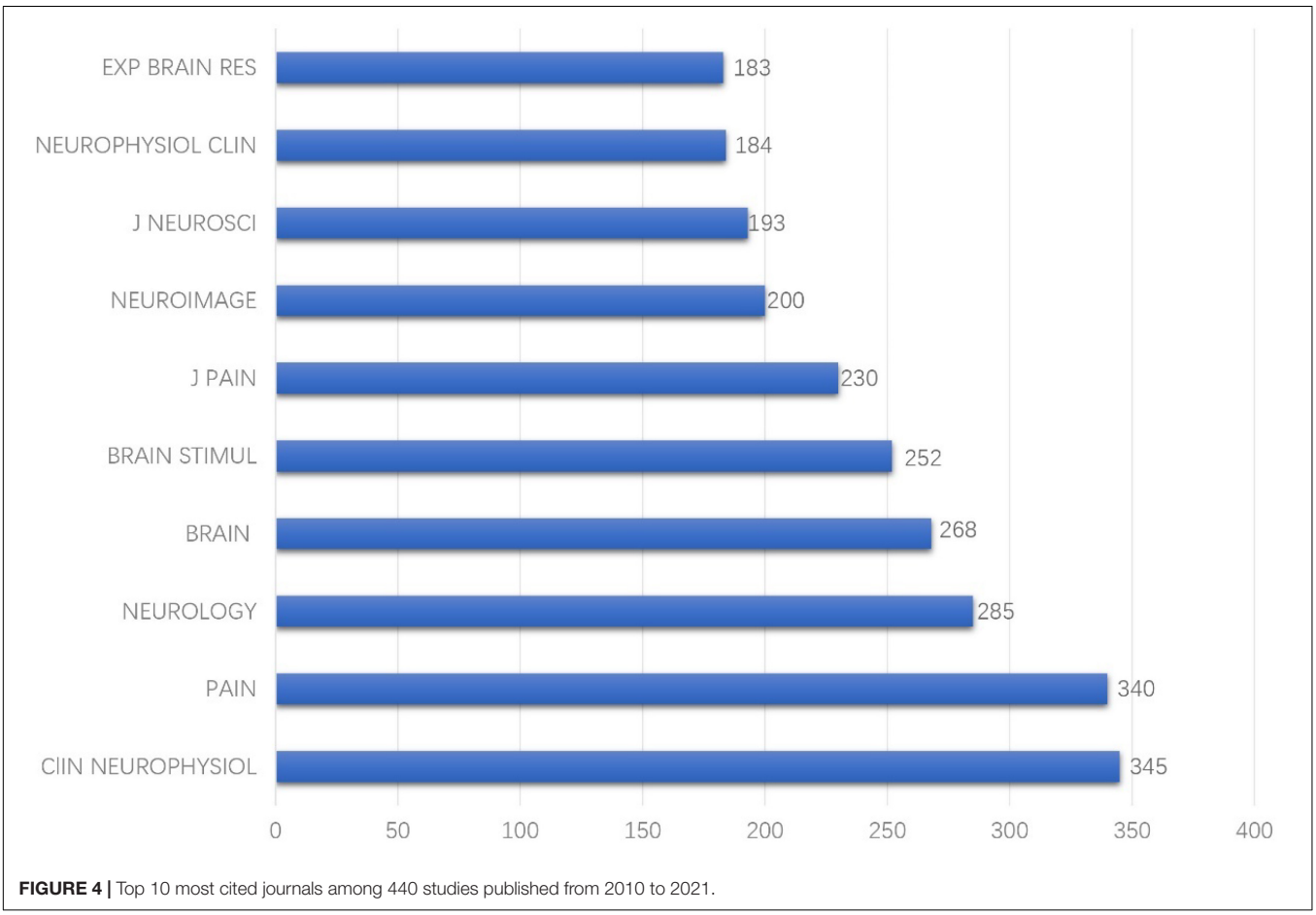

FIGURE 4 | Top 10 most cited journals among 440 studies published from 2010 to 2021.

2021 (**Figure 3**). Among the top 10 cited journals, *CLIN NEUROPHYSIOL* was the most frequently cited, which was cited 345 times, followed by *PAIN* (340 times) and *NEUROLOGY* (285 times) (**Figure 4**).

Based on the Blondel algorithm, dual-map overlaps of journals are displayed in **Figure 5**. The citing journals of 440 studies were mainly from the fields of MEDICINE, MEDICAL, NEUROLOGY, and SPORTS. The cited journals were mainly from the fields of HEALTH, MEDICINE, SPORTS, and REHABILITATION. As shown in the center of the circle on the right, rehabilitation medicine was the most concentrated one in the cited journals. While in the center of the circle on the left, neurology medicine was the hotspot of current research on TMS in pain research.

Reference Co-citation Analysis

The clustered research categories of reference co-citation analysis were divided into 14 groups (#0-13). The timeline view of clusters was shown in **Figure 6**, which presents the characteristics of the time-span citation information for the cluster domains. The cluster category with the largest time span for the cited references was #1 migraine from 2006 to 2015, which was also the most frequently cited category. Moreover, there were a series of important landmark achievements

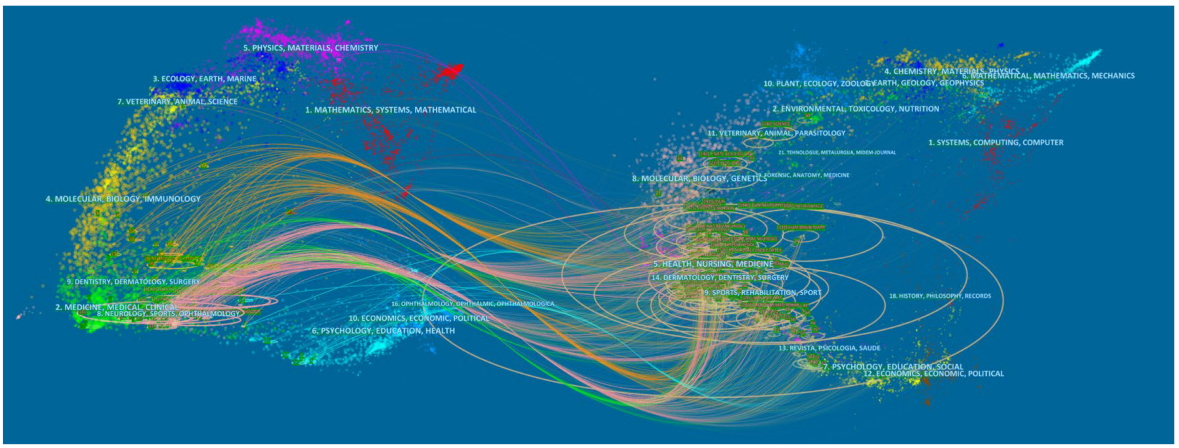

FIGURE 5 | Visualization of dual-map overlays of citing journals and cited journals of 440 studies published from 2010 to 2021. The colored curve indicates the path of citation, which originates from 11 fields of the citing journals on the left and points to 14 fields of the cited journals on the right.

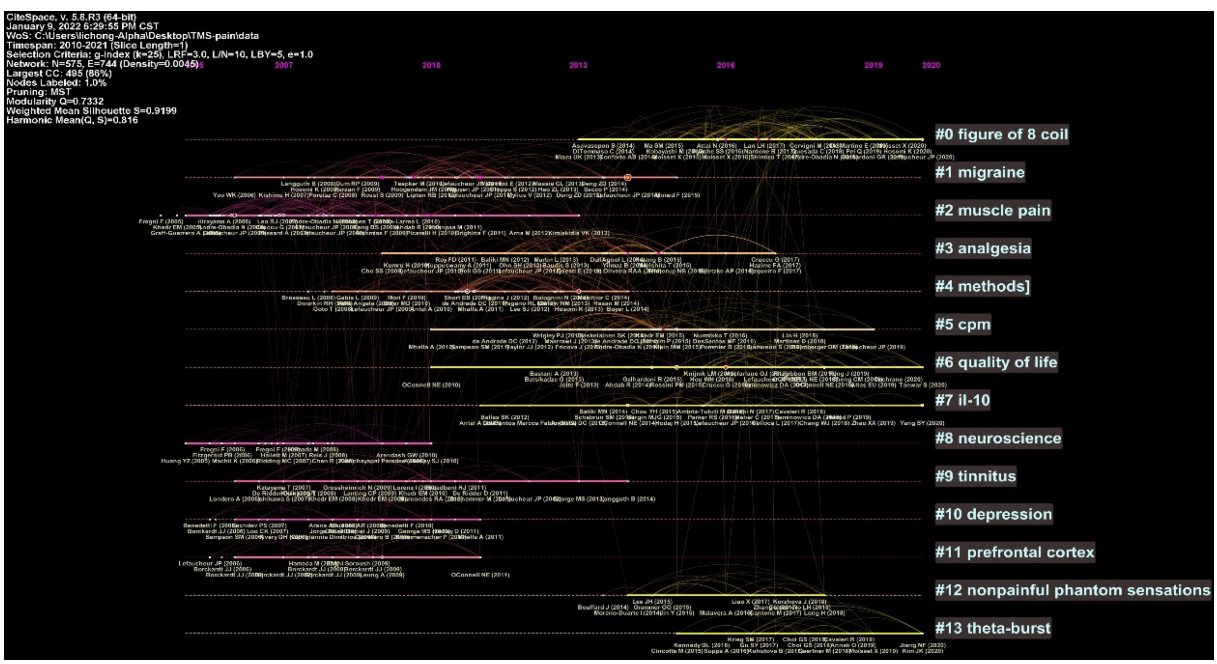

FIGURE 6 | Timeline view of reference co-citation analysis.

TABLE 1 | Ten representative studies of transcranial magnetic stimulation (TMS) in pain research among the cited references of the included 440 studies.

Study	Citation counts	Journal	Study type	Sample	Intervention	Outcomes	Highlights
Lefaucheur et al., 2014	67	Clin Neurophysiol	Guidelines	\	\	\	Recommendation: definite analgesic effect of HF rTMS of M1 contralateral to pain side in neuropathic pain (Level A)
Mhalla et al., 2011	38	Pain	Randomized controlled trial	40	40 fibromyalgia patients were randomized to receive active or sham rTMS of the left primary motor cortex.	Self-reported average pain intensity with the numerical scale.	TMS may be a valuable and safe new therapeutic option in patients with fibromyalgia.
Rossini et al., 2015	35	Clin Neurophysiol	An updated report	\	\	\	Further research is still needed to compare the respective value of various cortical targets, depending on the side and frequency of stimulation and the clinical presentation, with respect to the location and the respective sensory-discriminant and affective-emotional components of pain.
Hosomi et al., 2013	31	Pain	A randomized, multicenter, double-blind, crossover, sham-controlled trial.	70	A series of 10 daily 5-Hz rTMS (500 pulses/session) of primary motor cortex (M1) or sham stimulation was applied to each patient with a follow-up of 17 days.	McGill pain questionnaire.	Daily high-frequency rTMS of M1 is tolerable and transiently provides modest pain relief in neuropathic pain patients.
de Andrade et al., 2011	29	Pain	A randomized, double-blind crossover design.	12	Three groups of 12 volunteers were selected at random and given active stimulation (frequency 10Hz, at 80% motor threshold intensity, 1500 pulses per session) of the right M1, active stimulation of the right DLPFC, or sham stimulation, during two experimental sessions 2 weeks apart.	Cold pain thresholds and the intensity of pain.	Endogenous opioids are shown to be involved in the analgesic effects of repetitive transcranial magnetic stimulation of the motor cortex.
Klein et al., 2015	28	Pain	Guidelines	\	\	\	The suffering and disability associated with uncontrolled chronic pain, the common and serious adverse effects associated with pain medications, and the preliminary evidence of efficacy and safety of TMS for treating some types of pain mandate greater investment in developing this therapy.
Rossi et al., 2009	26	Clin Neurophysiol	Guidelines	\	\	\	The present updated guidelines review issues of risk and safety of TMS in clinical practice and research.
Moisset et al., 2016	26	European Journal of Pain	Review	\	\	\	LTP-like mechanisms, dependence on endogenous opioids and increase in concentration of neurotransmitters (monoamines, GABA) have all been implicated in its analgesic effects.
Leung et al., 2009	26	The Journal of Pain	A meta-analysis	\	\	\	rTMS appears to be more effective in suppressing centrally than peripherally originated neuropathic pain states.
O'Connell et al., 2014	25	The Cochrane database of systematic reviews	An updated review	\	\	\	The available evidence suggests that low-frequency rTMS, rTMS applied to the pre-frontal cortex, CES and tDCS are not effective in the treatment of chronic pain.

in this cluster. Rossi et al. (2009) released guidelines for the use of TMS in clinical practice and research. Lipton and Pearlman (2010) published a review of TMS in the treatment of migraine. Lefaucheur et al. (2011) assessed the value of rTMS in the prediction of the efficacy of epidural motor cortex stimulation to treat neuropathic pain. Lefaucheur et al. (2014) released evidence-based guidelines on the therapeutic use of rTMS.

The top 10 cited reference information of the 440 included studies are summarized in **Table 1**. The studies by Lefaucheur et al. (2014), Klein et al. (2015), Rossini et al. (2015) were guidelines for the efficacy and safety of TMS in clinical research. A study by Mhalla et al. (2011) focused on the long-term maintenance of the analgesic effects of TMS in fibromyalgia. A study by Hosomi et al. (2013) was a randomized crossover sham-controlled trial focusing on the effect of daily rTMS of primary motor cortex for neuropathic pain. A study by de Andrade et al. (2011) investigated the role of endogenous opioid systems in the analgesic effects induced by rTMS. A study by Leung et al. (2009) was a meta-analysis of rTMS for suppressing neuropathic pain.

Innovative Reference Analysis

The Sigma value can be used to identify innovative references. Five innovative references are summarized in **Table 2**. A study by Lefaucheur et al. (2011) was a retrospective study that assess the value of rTMS to predict the efficacy of epidural motor cortex stimulation to treat neuropathic pain. A study by de Oliveira et al. (2014) found that rTMS of the premotor cortex/dorsolateral prefrontal cortex was not effective in relieving central poststroke pain. A study by Lindholm et al. (2015) found that the right S2 cortex is a promising new target for the treatment of neuropathic orofacial pain with high-frequency rTMS. Kang et al. (2009) found that the therapeutic efficacy of rTMS was not demonstrated when rTMS was applied to the hand motor cortical area in patients with chronic

TABLE 2 | Five innovative studies about TMS in pain research among the cited references of the included 440 studies.

Study	Sigma*	Journal	Study type	Sample	Intervention	Outcomes	Highlights
Lefaucheur et al., 2011	0.14	Journal of Pain	Retrospective study	59	Patients were treated by epidural motor cortex stimulation for more than 1 year and in whom active and sham 10 Hz rTMS sessions were performed targeted over the cortical representation of the painful area.	The visual analog scale	Neuropathic pain can be significantly relieved by motor cortex rTMS.
de Oliveira et al., 2014	0.13	Journal of Pain	Prospective, double-blind, placebo-controlled study	23	Active rTMS and sham rTMS, and were treated with 10 daily sessions of rTMS over the left PMC/DLPFC (10 Hz, 1,250 pulses/d).	The visual analog scale	rTMS of the PMC/DLPFC is not effective in relieving CPSP.
Lindholm et al., 2015	0.13	Pain	Randomized, placebo-controlled, crossover study	16	Navigated high-frequency rTMS was given to the sensorimotor (S1/M1) and the right secondary somatosensory (S2) cortices.	The numerical rating scale	The right S2 cortex is a promising new target for the treatment of neuropathic orofacial pain with high-frequency rTMS.
Kang et al., 2009	0.13	Archives of Physical Medicine and Rehabilitation	Blinded, randomized crossover study	11	rTMS was applied on the hand motor cortical area using a figure-of-eight coil. One thousand stimuli were applied daily on 5 consecutive days. Real and sham rTMS were separated by 12 weeks.	Numeric rating scale, the Brief Pain Inventory	The therapeutic efficacy of rTMS was not demonstrated when rTMS was applied to the hand motor cortical area in patients with chronic neuropathic pain at multiple sites in the body, including the lower limbs, trunk, and pelvis.
Picarelli et al., 2010	0.11	Journal of Pain	Double-blind, placebo-controlled, randomized trial	23	Patients were treated with the best medical treatment (analgesics and adjuvant medications, physical therapy) plus 10 daily sessions of either real or sham 10 Hz rTMS to the motor cortex (M1).	The visual analog scale	Repetitive sessions of high-frequency rTMS shows efficacy as an add-on therapy to refractory CRPS type I patients.

**Sigma = (centrality+1)burstness (burstness on the index) to identify innovative reference.*

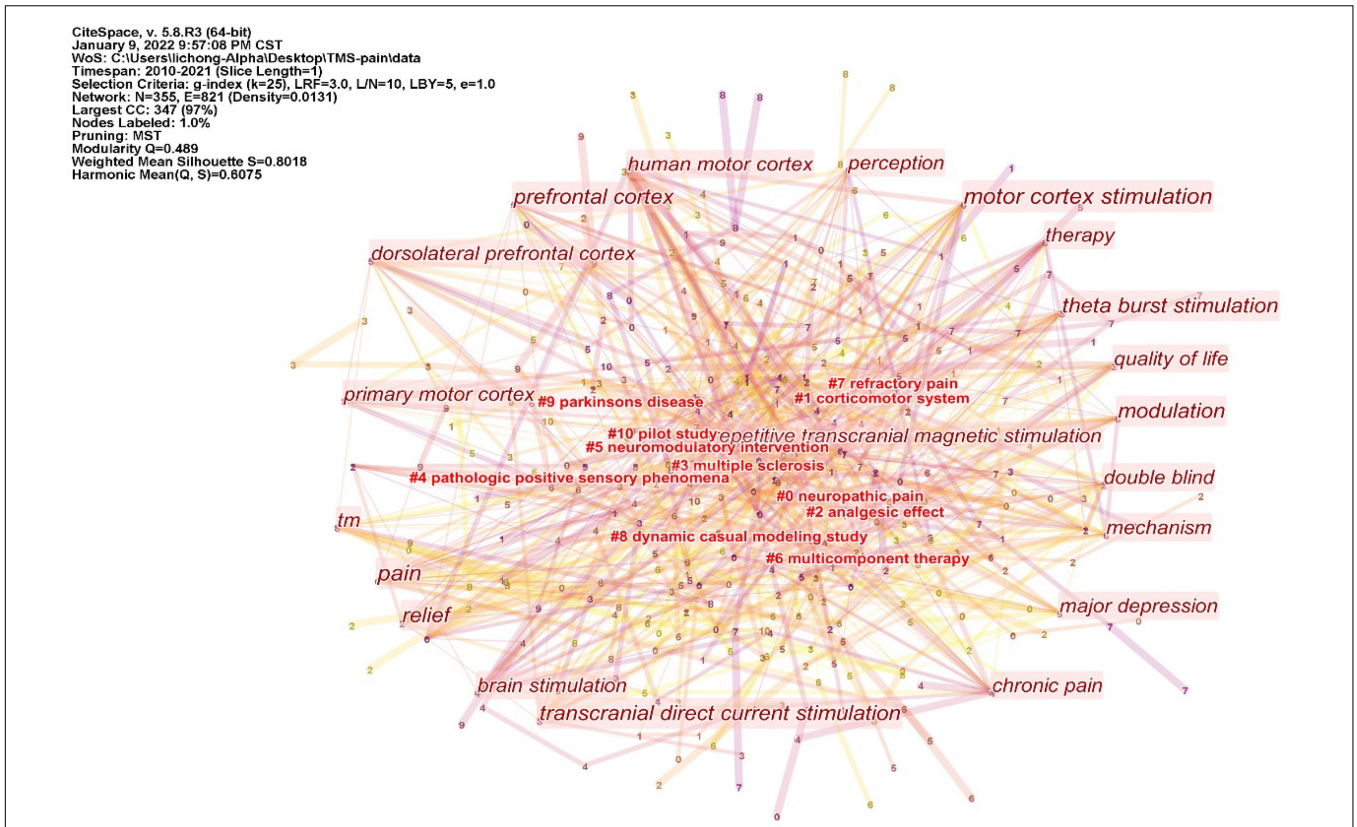

FIGURE 7 | Cluster of keywords from 440 inclusion studies. The keyword clusters (LLR algorithm) were divided into 11 categories (#0-10). Those without # are high-frequency keywords.

neuropathic pain at multiple sites in the body. A study by Picarelli et al. (2010) was a controlled randomized trial that highlighted an add-on therapy of high-frequency rTMS for refractory CRPS type I patients.

Analysis of Keywords

The keywords co-occurrence analysis in the 440 included studies revealed 355 keyword nodes and 821 connection lines. The keyword clusters were divided into 11 categories (#0-10) (**Figure 7**). The largest cluster (#0) has 53 members and a silhouette value of 0.847. It is labeled as *neuropathic pain* by LLR. The most relevant citer to the cluster is "Motor cortex stimulation for deafferentation pain" (Hussein et al., 2018). The second-largest cluster (#1) labeled as *corticomotor system* has 49 members and a silhouette value of 0.752. The most relevant citer to the cluster is "Paired associative electroacupuncture and transcranial magnetic stimulation in humans" (Huang et al., 2019). The third-largest cluster (#2) labeled as *analgesic effect* has 43 members and a silhouette value of 0.763. The most relevant citer is "Neural correlates of the antinociceptive effects of repetitive transcranial magnetic stimulation on central pain after stroke" (Ohn et al., 2012).

The ten representative keywords of TMS in pain research from 440 included studies are shown in **Table 3**. Studies of TMS in pain have focused on stimulating the motor cortex and dorsolateral prefrontal cortex. Existing studies have focused on pain including neuropathic pain, chronic pain, intractable deafferentation pain, and pain related to spinal cord injury. At present, more attention is paid to theta-burst stimulation.

TABLE 3 | Ten representative keywords of TMS in pain research from 440 included studies.

Rank	Keyword	Year	Count	Centrality
1	Neuropathic pain	2010	110	0.06
2	Motor cortex	2010	102	0.05
3	Brain	2010	56	0.03
4	Modulation	2012	42	0.12
5	Theta-burst stimulation	2010	39	0.14
6	Excitability	2011	38	0.04
7	Chronic pain	2010	35	0.09
8	Dorsolateral prefrontal cortex	2010	34	0.09
9	Intractable deafferentation pain	2010	29	0.04
10	Spinal cord injury	2013	29	0.04

Figure 8 shows the years when hot keywords began to appear and end. The hot keywords indicated three main points. (1) In the first stage, chronic neuropathic pain (2010−2013) was the first hot keyword. (2) In the second stage, intractable deafferentation pain (2012−2013), spinal cord injury

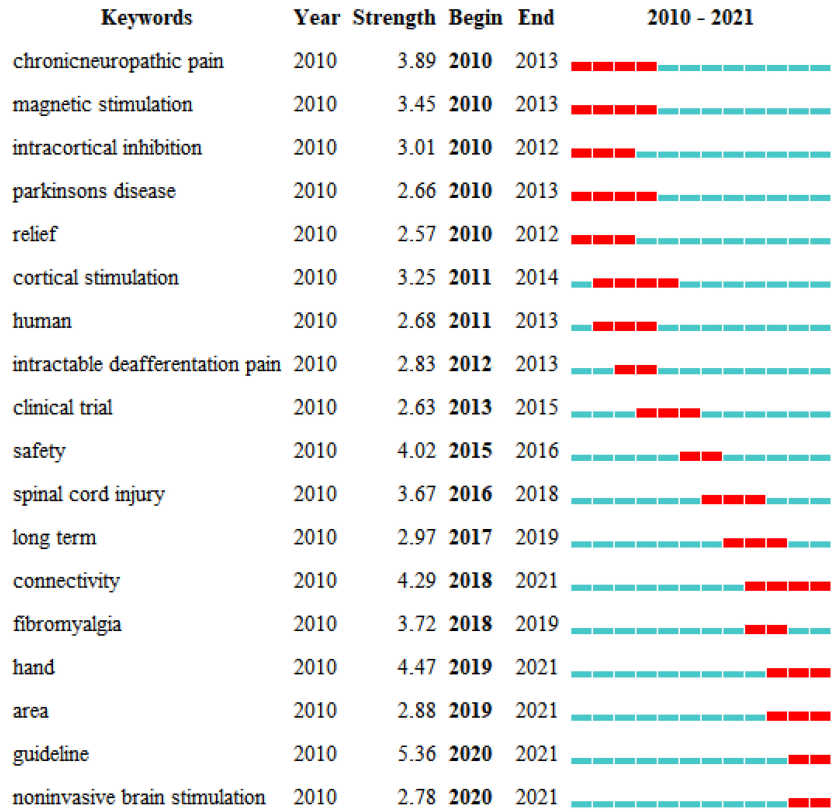

FIGURE 8 | Top 18 keywords with the strongest citation bursts of the 440 included studies from 2010 to 2021.

TABLE 4 | The top 10 authors and co-cited authors in TMS research in pain.

Rank	Author	Count	Co-cited author	Count
1	Jeanpascal lefaucheur	19	Lefaucheur	284
2	Felipe fregni	19	Khedr em	136
3	Daniel ciampi de andrade	11	Rossi s	126
4	Youichi asitoh	9	Andre-obadia n	122
5	Jeffrey j borckardt	8	Fregni f	100
6	Alvaro pascualleone	8	Oconnell ne	99
7	Mark s george	7	Garcia-larrea l	96
8	Alaa mhalla	7	Rossini pm	96
9	Albert leung	7	Borckardt jj	96
10	Wolnei caumo	7	Mhalla a	93

(2016–2018), and fibromyalgia (2018–2019) were the keywords, mainly describing the effects of TMS in different pain types. (3) In the third stage, connectivity (2018–2021) and area (2019–2021) were the keywords, indicating that studies are increasingly focusing on brain mechanisms in the area of TMS in pain.

Authoritative Authors Analysis

Authoritative authors analysis is presented in **Table 4**. In terms of publications number, Jeanpascal Lefaucheur and Felipe Fregni both published 19 papers separately, followed by author Daniel Ciampi De Andrade (11 publications) and Youichi Asitoh (9 publications). In terms of co-citation counts, Lefaucheur (284 citations) ranked first as the most co-cited author, followed by author Khedr EM (136 citations), Rossi S (126 citations).

Co-country and Co-institution Analysis

Collaboration networks of authoritative countries and institutions were presented in **Figure 9**. Amongst the 440 publications included in this study, the top-ranked country by citation counts was the United States (111 publications). The second one was France with citation counts of 67 and the third was Italy with citation counts of 40. In terms of authoritative institutions, Univ São Paulo (22) ranked first in the number of publications, followed by Harvard Univ (19) and Hop Henri Mondor (14), as presented in **Table 5**.

DISCUSSION

General Trends of Transcranial Magnetic Stimulation in Pain Research

From 2010 to 2021, TMS has received great attention, and research related to pain has been increasingly performed. It is reasonable to expect a promising future for TMS in pain research based on analyzing the time trend of annual publication outputs.

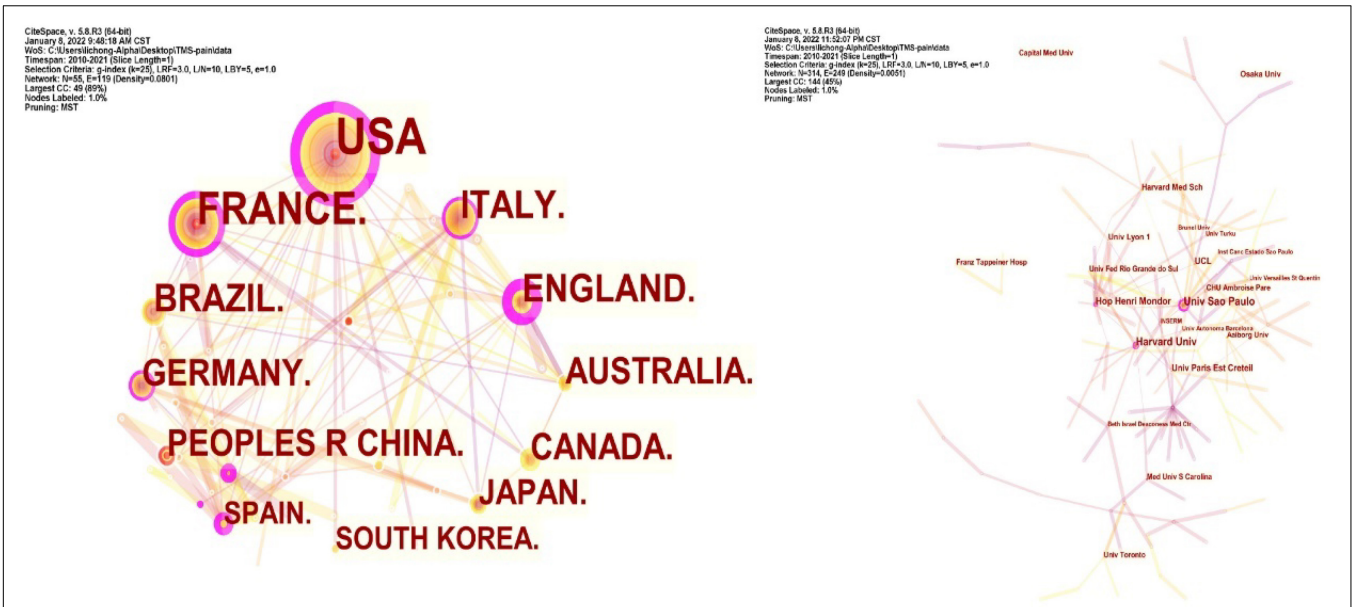

FIGURE 9 | Network map of countries and institutions in TMS in pain research.

Among the 10 top-performing journals, *Brain* (IF, 2021 = 13.501) had IF score > 10, and six journals, namely, *Pain* (IF, 2021 = 6.961), *Neurology* (IF, 2021 = 9.91), *Brain Stimulation* (IF, 2021 = 8.955), *Journal of Pain* (IF, 2021 = 5.828), *Neuroimage* (IF, 2021 = 6.556), *Journal of Neuroscience* (IF, 2021 = 6.167) had IF scores between 5, 000 and 10, 000. Amongst the top 10 countries, eight are developed countries and only Brazil and China are developing countries. From this perspective, there was still a wide gap between developed and developing countries in this field. The United States ranked first in terms of publication count (111) and is the leading country in terms of the over influence in this area. Among the 10 top institutions, University of São Paulo ranked first in terms of publication count (22) but it lacks international cooperation. Amongst authoritative authors, Jeanpascal Lefaucheur and Felipe Fregni both ranked first in terms of publication count (19). Jeanpascal Lefaucheur is a doctor in Henri Mondor Hospital from France and Felipe Fregni is a researcher in Harvard Medical School from the United States.

Emerging Trends of Transcranial Magnetic Stimulation in Pain Research

The evolution of a knowledge domain can be reflected by keywords. Therefore, keywords analysis can reveal emerging trends and provide directions for future research.

(I) Neuropathic pain: Neuropathic pain refers to pain initiated or caused by a primary lesion or dysfunction in the somatosensory system (Finnerup et al., 2021). Neuropathic pain is thought to be associated with peripheral nerve problems such as diabetes, but injuries to the brain or spinal cord can also lead to chronic neuropathic pain (Cohen and Mao, 2014). As a non-invasive brain stimulation, TMS now has become a treatment for neuropathic pain. However, it is difficult to determine which specific parameters are best for clinical use. The effectiveness of TMS depends on the type of neuropathic pain, and significant results have been reported when employing rTMS at 20 Hz (Aamir et al., 2020; Attia et al., 2021). Therefore, multi-centers, large sample sizes, randomized controlled trials are needed to carry out.

TABLE 5 | The top 10 countries or institution among 440 studies.

Rank	Country	Count	Centrality	Bursts
1	United states	111	0.49	2.68
2	France	67	0.29	2.89
3	Italy	40	0.13	\
4	Brazil	37	0.06	\
5	England	37	0.40	\
6	Australia	33	0.13	\
7	Canada	33	0.06	\
8	Peoples r china	29	0.07	4.47
9	Japan	28	0.00	\
10	Spain	24	0.02	\
	Institution			
1	Univ sao paulo	22	0.23	\
2	Harvard univ	19	0.18	2.99
3	Hop henri mondor	14	0.11	\
4	Ucl	12	0.09	\
5	Univ pris est creteil	10	0.09	\
6	Harvard med sch	9	0.04	\
7	Univ lyon 1	9	0.03	\
8	Osaka univ	9	0.00	\
9	Univ toronto	8	0.02	\
10	Med univ s carolina	8	0.07	3.69

(II) Motor Cortex: The most commonly targeted area of TMS in pain research is represented by the M1 contralateral to the position corresponding to the somatotopic location of the pain source (O'Connell et al., 2018). With further research, the secondary somatosensory cortex (S2) and supplementary motor area (SMA) show as promising targeted areas for pain research (Lockwood et al., 2013; Rao et al., 2020).

(III) Connectivity: The pain caused by central nervous system injury may be caused by the lack of connectivity between various parts of the brain caused by neuron damage. Regardless of the etiology and pain model, chronic pain may trigger various forms of maladaptive structural connection. TMS can strengthen the plasticity of neuronal connections. Locally, within one hemisphere, increased EEG activity can be seen in several neighboring electrodes, suggesting the spread of TMS-evoked activity to anatomically interconnected cortical areas (Martin et al., 2013; Weissman-Fogel and Granovsky, 2019).

(IV) Non-invasive brain stimulation: In addition to TMS, transcranial direct current stimulation (tDCS) is also a common non-invasive brain stimulation technique for pain treatment (O'Connell et al., 2018; Lloyd et al., 2020; Pacheco-Barrios et al., 2020). tDCS is a non-invasive technology that uses a weak current (1−2 mA) to regulate the activity of neurons in the cerebral cortex. Existing studies have proved that both TMS and tDCS can effectively treat pain caused by different diseases (O'Connell et al., 2018). However, the comparative study of the two technologies is still lacking. Further research is needed to prove the difference and connection between the two technologies in the field of pain.

Generally Accepted Conclusion Regarding Transcranial Magnetic Stimulation in Pain Research

(1) Definite analgesic effect of high-frequency rTMS of M1 contralateral to pain side in neuropathic pain (Level A). Low-frequency rTMS of M1 to pain side is probably ineffective in neuropathic pain (Level B). Possible analgesic effect of high-frequency rTMS of M1 contralateral to pain in complex regional pain syndrome type I (level C) (Lefaucheur et al., 2014). (2) There are inconclusive recommendations regarding rTMS of the dorsolateral prefrontal cortex (DLPFC) in fibromyalgia and neuropathic pain (Cruccu et al., 2016). (3) There is low-quality evidence that single doses of high-frequency rTMS of the motor cortex may have short-term effects on chronic pain (O'Connell et al., 2014).

Future Research Trends

At present, TMS is still in the development stage of pain treatment, and future research can be carried out from the following aspects. First, it is necessary to explore the influencing factors of TMS in the treatment of pain. Second, we need to explore the mechanism of TMS in treating pain. Third, it is necessary to explore the clinical therapeutic effects of potential therapeutic targets.

Limitations of This Study

To the best of our knowledge, this study is the first to access the trends of TMS in pain research based on literature published from 2010 to 2021 through a bibliometric approach. Nevertheless, this work has some limitations. Because of a limitation of the CiteSpace software, we only analyzed references in the WOS database. Some papers could inevitably have been missed. In addition, large-sample randomized controlled data are lacking.

CONCLUSION

This study may help investigators discover the publication patterns and emerging trends of TMS on pain research from 2010 to 2021. The most influential author, institutions, journals, and countries were Jeanpascal Lefaucheur, University of São Paulo, *Clinical Neurophysiology*, and the United States. The visual map shows the hot research directions of TMS on pain research in recent years, such as TMS on neuropathic pain, motor cortex, and connectivity. Our bibliometrics analysis of 420 studies using CiteSpace software is in line with current clinical studies of TMS on pain research, indicating that the methodology is valid. In the future, large sample, randomized controlled trials are needed to carry out for TMS in the pain area.

DATA AVAILABILITY STATEMENT

The raw data supporting the conclusions of this article will be made available by the authors, without undue reservation.

AUTHOR CONTRIBUTIONS

ST contributed to the conception of the study. CL and MS performed the data analyses and wrote the manuscript. All authors contributed to the article and approved the submitted version.

REFERENCES

Aamir, A., Girach, A., Sarrigiannis, P. G., Hadjivassiliou, M., Paladini, A. (2020). Repetitive magnetic stimulation for the management of peripheral neuropathic pain: a systematic review. *Adv. Ther.* 37, 998–1012. doi: 10.1007/s12325-020-01231-2

Alles, S., and Smith, P. A. (2018). Etiology and pharmacology of neuropathic pain. *Pharmacol. Rev.* 70, 315–347. doi: 10.1124/pr.117.014399

Attia, M., McCarthy, D., and Abdelghani, M. (2021). Repetitive transcranial magnetic stimulation for treating chronic neuropathic pain: a systematic review. *Curr. Pain Headache Rep.* 25:48. doi: 10.1007/s11916-021-00960-5

Chen, C. (2004). Searching for intellectual turning points: progressive knowledge domain visualization. *Proc. Natl. Acad. Sci. U S A* 101(Suppl. 1), 5303–5310. doi: 10.1073/pnas.0307513100

Chen, C., Hu, Z., Liu, S., and Tseng, H. (2012). Emerging trends in regenerative medicine: a scientometric analysis in CiteSpace. *Expert Opin. Biol. Ther.* 12, 593–608. doi: 10.1517/14712598.2012.674507

Chen, C., and Song, M. (2019). Visualizing a field of research: a methodology of systematic scientometric reviews. *PLoS One* 14:e223994. doi: 10.1371/journal.pone.0223994

Cohen, S. P., and Mao, J. (2014). Neuropathic pain: mechanisms and their clinical implications. *Bmj* 348:f7656. doi: 10.1136/bmj.f7656

Cruccu, G., Garcia-Larrea, L., Hansson, P., Keindl, M., Lefaucheur, J. P. (2016). EAN guidelines on central neurostimulation therapy in chronic pain conditions. *Eur. J. Neurol.* 23, 1489–1499. doi: 10.1111/ene.13103

de Andrade, D. C., Mhalla, A., Adam, F., Texeira, M. J., and Bouhassira, D. (2011). Neuropharmacological basis of rTMS-induced analgesia: the role of endogenous opioids. *Pain* 152, 320–326. doi: 10.1016/j.pain.2010.10.032

de Oliveira, R. A., de Andrade, D. C., Mendonça, M., Barros, R., Luvisoto, T. (2014). Repetitive transcranial magnetic stimulation of the left premotor/dorsolateral prefrontal cortex does not have analgesic effect on central poststroke pain. *J. Pain* 15, 1271–1281. doi: 10.1016/j.jpain.2014.09.009

Finnerup, N. B., Kuner, R., and Jensen, T. S. (2021). Neuropathic pain: from mechanisms to treatment. *Physiol. Rev.* 101, 259–301. doi: 10.1152/physrev.00045.2019

Hallett, M. (2007). Transcranial magnetic stimulation: a primer. *Neuron* 55, 187–199. doi: 10.1016/j.neuron.2007.06.026

Hosomi, K., Shimokawa, T., Ikoma, K., Nakamura, Y., Sugiyama, K. (2013). Daily repetitive transcranial magnetic stimulation of primary motor cortex for neuropathic pain: a randomized, multicenter, double-blind, crossover, sham-controlled trial. *Pain* 154, 1065–1072. doi: 10.1016/j.pain.2013.03.016

Huang, Y., Chen, J. C., Chen, C. M., Tsai, C. H., and Lu, M. K. (2019). Paired associative electroacupuncture and transcranial magnetic stimulation in humans. *Front. Hum. Neurosci.* 13:49. doi: 10.3389/fnhum.2019.00049

Hussein, A. E., Esfahani, D. R., Moisak, G. I., Rzaev, J. A., and Slavin, K. V. (2018). Motor cortex stimulation for deafferentation pain. *Curr. Pain Headache Rep.* 22:45. doi: 10.1007/s11916-018-0697-1

Kang, B. S., Shin, H. I., and Bang, M. S. (2009). Effect of repetitive transcranial magnetic stimulation over the hand motor cortical area on central pain after spinal cord injury. *Arch. Phys. Med. Rehabil.* 90, 1766–1771. doi: 10.1016/j.apmr.2009.04.008

Klein, M. M., Treister, R., Raij, T., Pascual-Leone, A., Park, L. (2015). Transcranial magnetic stimulation of the brain: guidelines for pain treatment research. *Pain* 156, 1601–1614. doi: 10.1097/j.pain.0000000000000210

Klit, H., Finnerup, N. B., and Jensen, T. S. (2009). Central post-stroke pain: clinical characteristics, pathophysiology, and management. *Lancet Neurol.* 8, 857–868. doi: 10.1016/S1474-4422(09)70176-0

Koob, G. F. (2021). Drug addiction: hyperkatifeia/Negative reinforcement as a framework for medications development. *Pharmacol. Rev.* 73, 163–201. doi: 10.1124/pharmrev.120.000083

Lefaucheur, J. P., André-Obadia, N., Antal, A., Ayache, S. S., Baeken, C. (2014). Evidence-based guidelines on the therapeutic use of repetitive transcranial magnetic stimulation (rTMS). *Clin. Neurophysiol.* 125, 2150–2206. doi: 10.1016/j.clinph.2014.05.021

Lefaucheur, J. P., Ménard-Lefaucheur, I., Goujon, C., Keravel, Y., and Nguyen, J. P. (2011). Predictive value of rTMS in the identification of responders to epidural motor cortex stimulation therapy for pain. *J. Pain* 12, 1102–1111. doi: 10.1016/j.jpain.2011.05.004

Leung, A., Donohue, M., Xu, R., Lee, R., Lefaucheur, J. P. (2009). RTMS for suppressing neuropathic pain: a meta-analysis. *J. Pain* 10, 1205–1216. doi: 10.1016/j.jpain.2009.03.010

Li, Y., Li, W., Zhang, T., Zhang, J., Jin, Z. (2021). Probing the role of the right inferior frontal gyrus during Pain-Related empathy processing: evidence from fMRI and TMS. *Hum. Brain Mapp.* 42, 1518–1531. doi: 10.1002/hbm.25310

Lindholm, P., Lamusuo, S., Taiminen, T., Pesonen, U., Lahti, A. (2015). Right secondary somatosensory cortex-a promising novel target for the treatment of drug-resistant neuropathic orofacial pain with repetitive transcranial magnetic stimulation. *Pain* 156, 1276–1283. doi: 10.1097/j.pain.0000000000000175

Lipton, R. B., and Pearlman, S. H. (2010). Transcranial magnetic simulation in the treatment of migraine. *Neurotherapeutics* 7, 204–212. doi: 10.1016/j.nurt.2010.03.002

Lloyd, D. M., Wittkopf, P. G., Arendsen, L. J., and Jones, A. (2020). Is transcranial direct current stimulation (tDCS) effective for the treatment of pain in fibromyalgia? *A systematic review and Meta-Analysis. J. Pain* 21, 1085–1100. doi: 10.1016/j.jpain.2020.01.003

Lockwood, P. L., Iannetti, G. D., and Haggard, P. (2013). Transcranial magnetic stimulation over human secondary somatosensory cortex disrupts perception of pain intensity. *Cortex* 49, 2201–2209. doi: 10.1016/j.cortex.2012.10.006

Martin, L., Borckardt, J. J., Reeves, S. T., Frohman, H., Beam, W. (2013). A pilot functional MRI study of the effects of prefrontal rTMS on pain perception. *Pain Med.* 14, 999–1009. doi: 10.1111/pme.12129

Mhalla, A., Baudic, S., de Andrade, D. C., Gautron, M., Perrot, S. (2011). Long-term maintenance of the analgesic effects of transcranial magnetic stimulation in fibromyalgia. *Pain* 152, 1478–1485. doi: 10.1016/j.pain.2011.01.034

Moisset, X., de Andrade, D. C., and Bouhassira, D. (2016). From pulses to pain relief: an update on the mechanisms of rTMS-induced analgesic effects. *Eur. J. Pain* 20, 689–700. doi: 10.1002/ejp.811

Nurmikko, T., MacIver, K., Bresnahan, R., Hird, E., Nelson, A. (2016). Motor cortex reorganization and repetitive transcranial magnetic stimulation for Pain-A methodological study. *Neuromodulation* 19, 669–678. doi: 10.1111/ner.12444

O'Connell, N. E., Marston, L., Spencer, S., DeSouza, L. H., and Wand, B. M. (2018). Non-invasive brain stimulation techniques for chronic pain. *Cochrane Database Syst. Rev.* 4:D8208. doi: 10.1002/14651858.CD008208.pub5

O'Connell, N. E., Wand, B. M., Marston, L., Spencer, S., and Desouza, L. H. (2014). Non-invasive brain stimulation techniques for chronic pain. *Cochrane Database Syst. Rev.* 9:CD00820. doi: 10.1002/14651858.CD008208.pub3

Ohn, S. H., Chang, W. H., Park, C. H., Kim, S. T., Lee, J. I. (2012). Neural correlates of the antinociceptive effects of repetitive transcranial magnetic stimulation on central pain after stroke. *Neurorehabil. Neural Repair* 26, 344–352. doi: 10.1177/1545968311423110

Pacheco-Barrios, K., Cardenas-Rojas, A., Thibaut, A., Costa, B., Ferreira, I. (2020). Methods and strategies of tDCS for the treatment of pain: current status and future directions. *Expert Rev. Med. Devices* 17, 879–898. doi: 10.1080/17434440.2020.1816168

Picarelli, H., Teixeira, M. J., de Andrade, D. C., Myczkowski, M. L., Luvisotto, T. B. (2010). Repetitive transcranial magnetic stimulation is efficacious as an add-on to pharmacological therapy in complex regional pain syndrome (CRPS) type I. *J. Pain* 11, 1203–1210. doi: 10.1016/j.jpain.2010.02.006

Pitcher, D., Parkin, B., and Walsh, V. (2021). Transcranial magnetic stimulation and the understanding of behavior. *Annu. Rev. Psychol.* 72, 97–121. doi: 10.1146/annurev-psych-081120-013144

Raja, S. N., Carr, D. B., Cohen, M., Finnerup, N. B., Flor, H. (2020). The revised International Association for the Study of Pain definition of pain: concepts, challenges, and compromises. *Pain* 161, 1976–1982. doi: 10.1097/j.pain.0000000000001939

Rao, N., Chen, Y. T., Ramirez, R., Tran, J., Li, S. (2020). Time-course of pain threshold after continuous theta burst stimulation of primary somatosensory cortex in pain-free subjects. *Neurosci. Lett.* 722:134760. doi: 10.1016/j.neulet.2020.134760

Rossi, S., Hallett, M., Rossini, P. M., and Pascual-Leone, A. (2009). Safety, ethical considerations, and application guidelines for the use of transcranial magnetic stimulation in clinical practice and research. *Clin. Neurophysiol.* 120, 2008–2039. doi: 10.1016/j.clinph.2009.08.016

Rossini, P. M., Burke, D., Chen, R., Cohen, L. G., Daskalakis, Z.,. (2015). Non-invasive electrical and magnetic stimulation of the brain, spinal cord, roots and peripheral nerves: basic principles and procedures for routine clinical and research application. *An updated report from an I.F.C.N. Committee. Clin. Neurophysiol.* 126, 1071–1107. doi: 10.1016/j.clinph.2015.02.001

Ugolini, D., Neri, M., Cesario, A., Marazzi, G., Milazzo, D. (2013). Bibliometric analysis of literature in cerebrovascular and cardiovascular diseases rehabilitation: growing numbers, reducing impact factor. *Arch. Phys. Med. Rehabil.* 94, 324–331. doi: 10.1016/j.apmr.2012.08.205

Wang, Y. Z., Wu, C. C., and Wang, X. Q. (2021). Bibliometric Study of Pain after Spinal Cord Injury. *Neural Plast.* 2021:6634644. doi: 10.1155/2021/6634644

Weissman-Fogel, I., and Granovsky, Y. (2019). The "virtual lesion" approach to transcranial magnetic stimulation: studying the brain-behavioral relationships in experimental pain. *Pain Rep*. 4:e760. doi: 10.1097/PR9.0000000000000760

Xu, A. H., and Sun, Y. X. (2020). Research hotspots and effectiveness of repetitive transcranial magnetic stimulation in stroke rehabilitation. *Neural Regen. Res.* 15, 2089–2097. doi: 10.4103/1673-5374.282269

Conflict of Interest: The authors declare that the research was conducted in the absence of any commercial or financial relationships that could be construed as a potential conflict of interest.

Publisher's Note: All claims expressed in this article are solely those of the authors and do not necessarily represent those of their affiliated organizations, or those of the publisher, the editors and the reviewers. Any product that may be evaluated in this article, or claim that may be made by its manufacturer, is not guaranteed or endorsed by the publisher.

frontiers | Frontiers in Human Neuroscience

ORIGINAL RESEARCH
published: 23 June 2022
doi: 10.3389/fnhum.2022.890483

Phonological Working Memory Representations in the Left Inferior Parietal Lobe in the Face of Distraction and Neural Stimulation

Qiuhai Yue[1,2]* *and Randi C. Martin*[1]*

[1]Department of Psychological Sciences, Rice University, Houston, TX, United States, [2]Department of Psychology, Vanderbilt University, Nashville, TN, United States

The neural basis of phonological working memory (WM) was investigated through an examination of the effects of irrelevant speech distractors and disruptive neural stimulation from transcranial magnetic stimulation (TMS). Embedded processes models argue that the same regions involved in speech perception are used to support phonological WM whereas buffer models assume that a region separate from speech perception regions is used to support WM. Thus, according to the embedded processes approach but not the buffer approach, irrelevant speech and TMS to the speech perception region should disrupt the decoding of phonological WM representations. According to the buffer account, decoding of WM items should be possible in the buffer region despite distraction and should be disrupted with TMS to this region. Experiment 1 used fMRI and representational similarity analyses (RSA) with a delayed recognition memory paradigm using nonword stimuli. Results showed that decoding of memory items in the speech perception regions (superior temporal gyrus, STG) was possible in the absence of distractors. However, the decoding evidence in the left STG was susceptible to interference from distractors presented during the delay period whereas decoding in the proposed buffer region (supramarginal gyrus, SMG) persisted. Experiment 2 examined the causal roles of the speech processing region and the buffer region in phonological WM performance using TMS. TMS to the SMG during the early delay period caused a disruption in recognition performance for the memory nonwords, whereas stimulations at the STG and an occipital control region did not affect WM performance. Taken together, results from the two experiments are consistent with predictions of a buffer model of phonological WM, pointing to a critical role of the left SMG in maintaining phonological representations.

Keywords: phonological working memory, supramarginal gyrus, buffer, functional magnetic resonance imaging, representational similarity analysis, distractor, transcranial magnetic stimulation

OPEN ACCESS

Edited by:
Carol Seger,
Colorado State University,
United States

Reviewed by:
Rongjuan Zhu,
Shaanxi Normal University, China
Benjamin Kowialiewski,
University of Zurich, Switzerland
Steven Christian Schwering,
University of Wisconsin-Madison,
United States

***Correspondence:**
Qiuhai Yue
yueqiuhai@gmail.com
Randi C. Martin
rmartin@rice.edu

Specialty section:
This article was submitted to Cognitive Neuroscience, a section of the journal Frontiers in Human Neuroscience

Received: *06 March 2022*
Accepted: *30 May 2022*
Published: *23 June 2022*

Citation:
Yue Q and Martin RC (2022) Phonological Working Memory Representations in the Left Inferior Parietal Lobe in the Face of Distraction and Neural Stimulation. Front. Hum. Neurosci. 16:890483. doi: 10.3389/fnhum.2022.890483

INTRODUCTION

Verbal working memory (WM) storage (also known as short-term memory, STM) refers to the capacity of maintaining verbal information in an accessible format to support cognitive operations and the planning of behavioral responses. A failure of maintaining verbal WM representations (e.g., due to damaged neural substrates of verbal WM) would impair subsequent behavioral performance

(e.g., reducing recall of memory items). Thus, an important property of the verbal WM store is to prevent memory representations from being degraded by task-irrelevant interference coming from internal or external sources. To date, the theoretical basis and neural loci of verbal WM storage are still under debate.

At a theoretical level, embedded processes models claim that WM consists of the activated portion of long-term memory (LTM; Oberauer and Lange, 2009; Cowan et al., 2021); thus, WM is assumed to recruit the same brain regions which are involved in processing a specific type of information (Jonides et al., 2005; Postle, 2006). The lateral superior temporal gyrus (STG; particularly on the left) is involved in the processing of speech through which low-level acoustic representations are mapped onto long-term memory representations for phonological features (Turkeltaub and Coslett, 2010; Price, 2012; Yi et al., 2019). According to the embedded processes models, such temporarily activated phonological representations in the left STG constitute verbal WM. If the left STG serves as the sole neural substrate of short-term maintenance of phonological information, the disruption of memory representations maintained in this region (e.g., by either task-irrelevant verbal distractors or external neural stimulation) would cause a reduction in verbal WM performance. If successful WM performance is achieved despite this interference, such would suggest a separate module other than the processing system that is capable of temporarily housing WM representations while the speech processing system continues to process up-coming stimuli that are irrelevant to WM performance. Such a module has been conceptualized in multi-component buffer models of WM. These models propose dedicated temporary stores (i.e., buffers) for different types of information (e.g., visual-spatial vs. phonological), and these stores are different from long-term memory (LTM) or processing systems (e.g., visual and speech perception systems) in that domain (Baddeley et al., 2021; Martin et al., 2021a; Purcell et al., 2021). According to buffer accounts, once representations have been transferred into the buffer, the processing of distractors in perceptual regions would not disrupt WM performance (Xu, 2017, 2018), and interference would occur only if the representations held in a buffer were disturbed (e.g., by external neural stimulation). A way of addressing these claims is to test the causal role of the speech processing region and the buffer region in verbal WM. Neuropsychological studies with brain-damaged patients have provided evidence bearing on this issue, showing that an impairment of the left inferior parietal lobe (particularly the ventral part of the left supramarginal gyrus, SMG) was associated with deficits in verbal WM (Baldo and Dronkers, 2006; Paulesu et al., 2017; Martin et al., 2021b; Purcell et al., 2021). This inferior parietal lobe region is different from the speech perception region in the STG[1] and has been proposed as the neural substrate of a phonological buffer (Martin, 2005). However, some studies using lesion-symptom mapping approaches have reported an association between the degree of damage in the left STG and phonological WM performance, suggesting that the left STG serves as the neural substrate of phonological WM (e.g., Leff et al., 2009; Baldo et al., 2012), but these studies have limitations. For example, in Leff et al. (2009) study, performance on a nonword repetition task was partialled out in the lesion-behavior correlational analyses. Nonword repetition has been argued to reflect an important component of phonological WM (Gupta, 2003; Majerus, 2013). In Baldo et al. (2012) study, speech perception abilities were not controlled for. In a recent study in our lab, when these issues were addressed, the lesions associated with impaired phonological WM capacity were primarily localized in the left SMG (Martin et al., 2021b). Neuroimaging work with healthy subjects also found mixed evidence regarding the neural substrate of phonological WM. Some studies found that the speech processing regions showed neural evidence for phonological WM (e.g., Ravizza et al., 2011; also see Buchsbaum and D'Esposito, 2008), though in those studies the speech processing region in the left STG was not well defined. In a recent study, using an independent localizer task involving syllable discrimination, we defined the phonological processing region in the left STG but did not find significant neural evidence for phonological WM in this region. Instead, consistent evidence for a phonological WM buffer in the left SMG was found (Yue et al., 2019). One means of providing converging evidence with healthy subjects is to apply neural stimulation (e.g., transcranial magnetic stimulation, TMS) to the SMG to temporarily disturb neural activity at this putative buffer region (Cohen et al., 1997; Pascual-Leone et al., 1999) and determine how behavioral performance is affected. TMS is a noninvasive technique of brain stimulation which uses an electromagnetic coil that is placed on the scalp to induce electric current applied to a specific brain region *via* electromagnetic induction. The induced current has been assumed to produce either excitatory or inhibitory effects on the neuronal activity of the stimulated area, depending on its intensity and frequency (Hallett, 2007; Valero-Cabré et al., 2017; Pitcher et al., 2021). Previous studies using either single-pulse, triple-pulse, or repetitive TMS procedures have been shown to disrupt WM functions (e.g., Oliveri et al., 2001; Desmond et al., 2005; also see a detailed discussion in the introduction to the TMS experiment). Thus, testing distractor and neural stimulation interference effects and examining their neural loci provides a means of evaluating the theoretical debate of embedded processes vs. buffer accounts of verbal WM by determining whether it is the processing region or the buffer region that plays an essential role in WM storage.

In the current study, we carried out two experiments with neuroimaging and brain stimulation approaches to examine the neural locus for phonological WM storage and test its resistance to inference. The first was an fMRI experiment in which we used a representational similarity analysis (RSA) approach

[1]It should be noted that what we refer to as phonological processing in the current study involves those processes that map acoustic input to phonological long-term units (e.g., phonemes, syllables, words), but not some other general processes (from a broad perspective) that are involved in a task which relies on phonological retention. However, that is not to say that the role of the left SMG is exclusively as a phonological buffer. It may also be involved in other complex functions related to phonology (e.g., Jacquemot et al., 2003; Stoeckel et al., 2009; Church et al., 2011), but we focus on phonological maintenance in the current study.

which explicitly modeled phonological WM representations for individual items (Yue and Martin, 2021) during the delay period of a recognition memory task. The task included a distractor manipulation with distractors presented during the delay period to enable us to assess the resistance of neural representations in phonological WM to the distracting information. In a second experiment, with the same group of participants, we used TMS to directly test the causal role of the speech processing region (i.e., the left STG) and the putative buffer region (i.e., the left SMG) in phonological WM. The region that is crucial to maintaining phonological WM representations would be disturbed by TMS applied during the delay period of the phonological WM task and hence behavioral performance would be affected.

EXPERIMENT 1: fMRI OF DISTRACTOR EFFECTS ON WM

In early behavioral studies in the verbal domain, the Brown-Peterson task paradigm (Brown, 1958; Peterson and Peterson, 1959) was used to explore the effects of interpolated tasks on STM performance (e.g., recall; Crowder, 1976). In this paradigm, a short list of memory items (e.g., letters) is presented to subjects, followed by a short delay period filled with some distracting activity (e.g., reading aloud numbers during the delay or counting backward). Then the memory list items are recalled. Many studies have investigated the effects of the interpolated material on performance (Posner and Rossman, 1965; Crowder, 1967; Dillon and Reid, 1969). For example, Posner and Rossman (1965) found that a difficult interpolated task (e.g., judging if the sum of a pair of digits is odd or even) interfered more with memory performance than did an easy task (e.g., simply reading a pair of digits). One component of the interference from the interpolated tasks has been postulated to be a diversion of subjects' attention from rehearsal of the memory stimuli, thus reducing recall of the memory list items (Peterson, 1969). Both buffer and embedded processes models include an attentional component [e.g., central executive in Baddeley et al. (2021) model; focus of attention in Cowan et al. (2021)], and thus an effect of diversion of attention is accommodated by both approaches. However, the effects of distractors cannot be accounted for solely on such grounds, as the degree of interference depended on the properties of the task-irrelevant materials *per se* (Wickelgren, 1965; Corman and Wickens, 1968; Landauer, 1974), specifically, the phonological similarity of the distractor items to the memory list items. For instance, Wickelgren (1965) found that recall of letters decreased as the number of phonologically similar interfering letters increased when subjects were required to write down the interfering items presented between the memory list and recall. Interference from the content of interpolated materials has been explained as overwriting of the memory items by the distracting items (Nairne, 1990). Such overwriting is assumed to be greater as the degree of similarity increases. In these studies, however, subjects were required to carry out a secondary task with the interpolated materials, and thus it is hard to attribute the interference solely to the interpolated materials automatically engaging WM due to perceptual processing of the stimuli, as the need to perform a task on the interfering material would necessitate that the information entered WM (Barrouillet et al., 2004). However, according to an embedded processes account, the interfering material should have an effect even if no task is required as that information should be processed in the perception region, causing interference with neural representations of the list items being maintained in that region. Another behavioral paradigm has examined the effects of irrelevant background speech on verbal WM performance, with detrimental effects on recall even though the irrelevant speech is to be ignored (see Neath, 2000 for a review). Unlike the effects of performing a task on interpolated material, the decrement from irrelevant speech does not depend on the phonological similarity of the background to the memory items and can be observed even with tonal stimuli (Jones and Macken, 1993). Also, the effect is typically demonstrated by presenting the irrelevant speech at the same time as the memory list items (which may be presented visually or auditorily), with effects of distractors presented after the set of memory items only occurring under certain conditions. The findings have thus led some to propose that the effect is an attentional one, rather than one due to a disruption of phonological storage (e.g., Jones and Macken, 1995). Recent behavioral studies continue to find mixed evidence regarding the explanation of the irrelevant speech effect in verbal WM, with some supporting the feature overwriting account (e.g., Oberauer and Lange, 2008) whereas others show that overwriting cannot explain a proactive interference effect in a memory list (i.e., earlier encoded items impact the recall of newly presented items which share features with those early items; e.g., Roodenrys et al., 2022).

More recently, neuroimaging approaches have been directed at assessing the effects of distractors on WM and the neural locus of such effects. Recent studies with multivariate approaches (e.g., multivariate pattern analysis, MVPA) have provided a way to assess the cortical response to distractors in the visual domain (Bettencourt and Xu, 2016; Lorenc et al., 2018; for a review see Lorenc et al., 2021). As compared to the traditional univariate neuroimaging approach, MVPA determines activation patterns associated with a few stimulus conditions or different features of items and has been regarded to be more sensitive in detecting WM storage representations (Sreenivasan et al., 2014; Sreenivasan and D'Esposito, 2019; though see Naselaris and Kay, 2015). For instance, Bettencourt and Xu (2016) found that while visual WM representations for grating patterns could be decoded in both the visual processing cortex and a proposed visual buffer region in the parietal lobe (e.g., superior intra-parietal sulcus) during a delay period when no distracting stimuli were presented, such decoding was only possible in the parietal lobe but not sensory cortex when distraction from various types of irrelevant visual items was present during the delay. In addition, in-scanner behavioral performance was not affected by the presence of distractors. Based on these findings, the authors suggested that since sensory regions need to be available to process other incoming stimuli (e.g., distractors), storage in the parietal lobe is needed to maintain a representation during distraction in order to achieve successful WM performance. The results are more consistent with a buffer model, suggesting a central role of the

parietal lobe as a neural substrate for a buffer in maintaining visual WM representations.

In the present fMRI experiment, we employed an RSA approach (Yue and Martin, 2021) and included a distractor manipulation analogous to that of Bettencourt and Xu (2016). As compared to MVPA, which associates a few stimulus conditions to neural activation patterns, RSA can be used to evaluate the representational correspondence between the neural activation patterns and theoretical predictions based on the phonological similarity of stimulus items, thus providing a more sensitive approach to determining the nature of maintained representations (Naselaris and Kay, 2015). We manipulated whether there were distractors during the delay period or not and used nonwords as both memory items and distractor items to avoid an influence from semantics (Yue et al., 2019). In a prior study (Yue et al., 2019), we found converging MVPA evidence for phonological WM during the delay period in a proposed buffer region (e.g., the left supramarginal gyrus, SMG), as well as some MVPA evidence in a speech processing area (e.g., the left superior temporal gyrus, STG). Although the evidence in the SMG was stronger than that for the STG, the nature of MVPA decoding evidence is still vague. For instance, in the Yue et al. (2019) study, the MVPA decoding assessed whether speech vs. nonspeech could be discriminated but could not determine the basis of this discrimination. More recently, using an RSA approach, Yue and Martin (2021) further examined the phonological WM codes maintained in the left SMG and confirmed that the decoding evidence was attributed to phonological representations. In the present experiment, using RSA with the nonword stimuli allowed us to test whether phonological decoding was possible and whether such evidence was affected by distractors. We focused on the effects of distraction on decoding from the left SMG and the left STG. According to the embedded processes account, if the left STG serves as the neural substrate for phonological WM storage, RSA decoding evidence would be observed during the delay period in this region. In addition, to achieve successful recognition performance, the presence of distractors during the delay period would have no effect on the neural representations in the left STG if this region was the sole neural substrate for phonological WM storage, or the neural representations in the left STG would be reduced by the presence of distractors though they are still decodable. In contrast, according to the buffer account, the neural representations during the delay in the left STG (if any) would be affected by the presence of distractors (e.g., being wiped out by the distractors), whereas the left SMG should maintain memory representations, to achieve the undisrupted memory performance, even if distractors were presented.

fMRI Experiment: Materials and Methods

Participants

Ten subjects (18–22 years old, mean: 19.7 years old, six females) recruited from Rice University participated in this experiment. All subjects were native speakers and reported no hearing, neurological, or psychiatric disorder. Subjects signed consent forms according to procedures approved by the Rice University Institutional Review Board to participate in the fMRI experiment and received monetary compensation or credit toward course requirements for their participation.

Materials and Procedure

A set of 16 one-syllable nonwords were used as the target memory items in the fMRI experiment in both the no-distractor condition and the distractor condition, allowing us to assess the effect of distractors on the phonological WM representations of the target nonwords. The 16 nonwords were created using online text-to-speech software[2] mimicking a female speaker of standard American English and recorded at a sampling rate of 22.05 Hz. All nonwords were matched for the average sound amplitude by using the software Praat[3]. The average duration of the nonwords was 648 ms.

A delayed recognition task was used (**Figure 1**). Each trial began with a fixation cross being presented for 500 ms in the center of a gray background screen. Then a spoken memory nonword was played to the subjects with a maximum duration of 1.5 s, followed by a 9-s delay period. Subjects were instructed to maintain this nonword over the delay period. Then a probe nonword was presented, and subjects were instructed to judge whether the probe nonword matched the memory nonword by pressing the left button if the probe matched the memory nonwords or the right button if not. There were two delay-period conditions. In the no-distractor condition, there were no other stimuli during the delay. In the distractor condition, the trial procedure was the same except that during the 9-s delay, a set of six distracting nonwords were presented at a rate of 1.5 s per each nonword. Subjects were instructed to remember the target nonword as their memory for that would be tested, but not for the delay period distractor stimuli. Thus, subjects just passively listened to the distracting nonwords without any explicit task. To reduce the potential confusion between the distracting stimuli and the memory items, the distracting nonwords were produced by a male speaker using the same software as for the memory nonwords. Previous studies have shown that speaker identities and phonemes are separately and independently represented in the human cortex (Formisano et al., 2008; Bonte et al., 2014), thus speaker identity information should not confound the ability to detect phonological representations (if any) of the memory nonwords which were of interest in this experiment.

For both the no-distractor and the distractor conditions, half of the probes were matching trials and half non-matching. The non-matching probes differed in a single distinctive feature of one phoneme from the target memory nonwords (e.g., sirb vs. sirp). For each trial, the distractor nonwords had no overlapping phonemes with the target memory nonword.

fMRI Procedure and Data Acquisition

In the fMRI experiment, the task was administered to subjects *via* E-prime 2.0 software (Psychology Software Tools[4]). The auditory nonwords were played binaurally *via* MRI-compatible earphones, and foam canal tips were used to reduce scanning noise. To ensure that subjects could clearly hear the nonwords

[2]http://www.fromtexttospeech.com
[3]http://www.fon.hum.uva.nl/praat/
[4]https://pstnet.com/

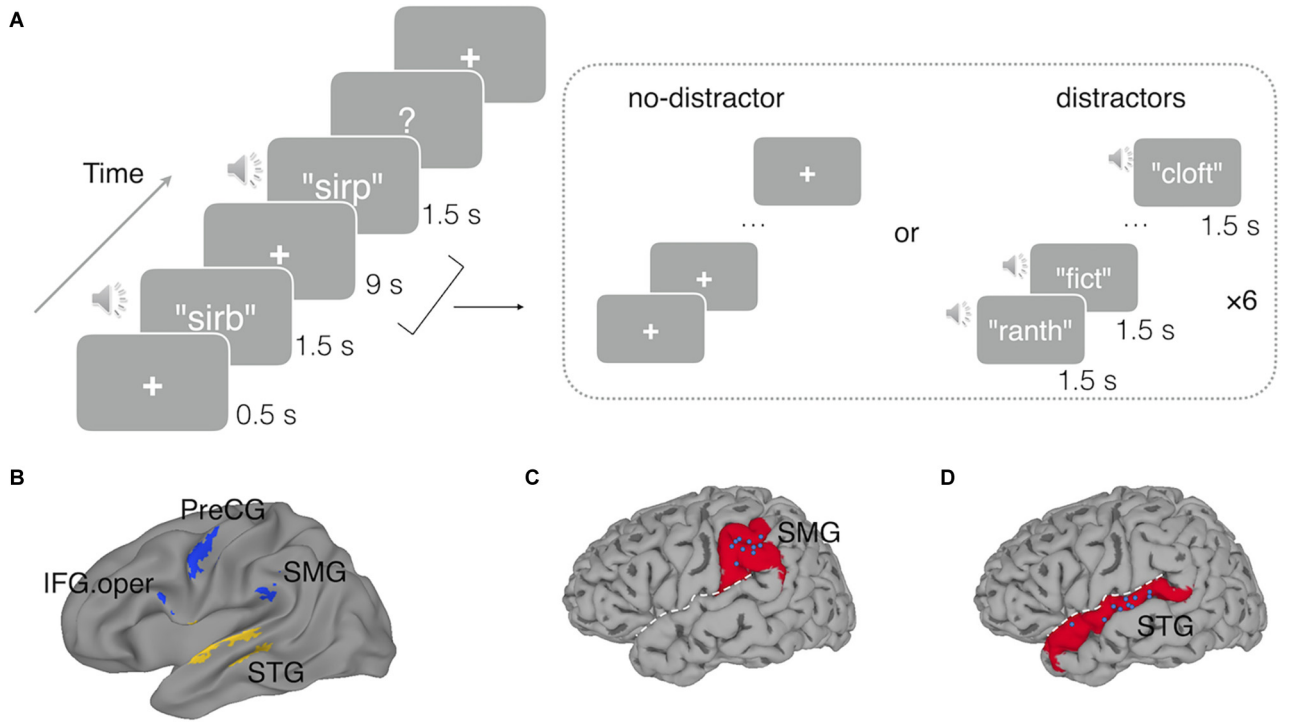

FIGURE 1 | (A) An example trial with a non-matching probe in the delayed recognition task in the fMRI experiment. In the no-distractor condition, the delay period was silent with a fixation cross; in the distractor condition, the delay period was filled with six auditory distracting nonwords, presenting at a rate of 1.5 s per each. In the TMS Experiment, a similar delayed nonword recognition task was used except that a short duration of the delay period (3 s) was used. The memory nonword was presented for 700 ms, and triple-pulse TMS stimulation was triggered at either 700 ms (early) or 1,300 ms (late) after the onset of the memory nonword. **(B)** Functional regions of interest used in Experiment 1 derived from a prior study (Yue et al., 2019): the left superior temporal gyrus (STG), the left supramarginal gyrus (SMG), the opercular part of the left inferior frontal gyrus (IFG.oper), and the left precentral gyrus (PreCG). **(C)** The blue dots indicate the target sites stimulated by TMS in the left SMG and in **(D)** the left STG, with each dot representing a subject. White dashed line represents the Sylvain fissure. The underlying red regions mark the anatomical parcellations of the left SMG and left STG for reference.

and were aware of variation of phonetic features against the scanning noise, a short scanning session including 10 speech perception trials (i.e., discriminating pairs of nonwords which differ a single distinctive feature, "ba"-"pa") was administered to each subject before the experimental functional scanning. The sound volume was adjusted to a comfortable level for each subject.

Each functional scan run contained trials from only one condition (either no-distractor condition or distractor condition), and in each scan, all unique 16 memory nonwords were played to subjects randomly with the inter-trial interval jittered at 4.5 s, 6 s, and 7.5 s. The average duration for each trial (stimuli presentation and post-trial interval) was 18 s. There were 9-s rest periods at the beginning of each scan, to allow equilibrium of the magnetic field, and at the end, to accommodate the hemodynamic delay of the last trial. The total duration for each functional scan was 306 s (5 min 6 s). There were six no-distractor runs and six distractor runs, with two types of runs being presented alternatively, and the order of two types of runs was counterbalanced across all subjects. There were 192 trials in total across the whole fMRI experiment for each subject, with 96 trials in the no-distractor condition and 96 in the distractor condition. Although the same memory nonwords were represented six times (across six runs) in both no-distractor and distractor conditions, the same memory nonword was never repeated within a run, and across six runs, the probe nonwords were never repeated. In other words, each time the subjects heard the same memory nonword, they encountered a new probe nonword.

The fMRI experiment was performed at the Core for Advanced Magnetic Resonance Imaging (CAMRI) at the Baylor College of Medicine. Images were obtained on a 3-Tesla Siemens Magnetom Tim Trio scanner (Prisma) equipped with a 64-channel head coil. Foam pads were used to keep subjects' heads stabilized during the scanning. Functional scans were acquired by using a modified Massachusetts General Hospital Simultaneous Multi-Slice (SMS) EPI sequence which featured both high spatial and high temporal resolutions for the RSA approach with the following parameters: TR = 1.5 s, TE = 30 ms, FA = 72°, matrix size = 100 × 100, FoV = 200 mm, voxel size = 2 × 2 mm^2. Each scan had 204 volumes and for each volume 69 2-mm thickness slices were acquired along the axial direction to cover the whole brain, with an SMS factor of 3. After the functional scans, an anatomical scan was also obtained with MPRAGE sequence: TR = 2,600 ms, TE = 3.03 ms, FA = 8°, matrix size = 256 × 256, voxel size = 1 × 1 × 1 mm^3.

Data Analyses

Preprocessing

fMRI data preprocessing, general linear modeling and univariate group-level analysis were performed using AFNI software (version: AFNI_18.0.00; Cox, 1996). Preprocessing includes de-spiking of large fluctuation for some time points, slice timing, and head motion correction. The functional images were aligned to that individual's anatomical image. The images were kept in the native space for the RSA approach and no spatial smoothing was applied to the data in order to preserve the spatial information across neighboring voxels. Spatial smoothing with a 4-mm full width half-maximum Gaussian kernel was applied to the functional data only for univariate activation analyses. A whole brain mask was generated and applied to the functional data, and voxel-wise signal scaling was calculated for each run. The resolution of functional data was kept in the native space with a voxel size of $2 \times 2 \times 2$ mm^3. For univariate voxel-wise group level testing, each subject's data were warped to the Talairach standard space (Talairach and Tournoux, 1988) and registered to the TT_N27 template in AFNI.

General Linear Model

A general linear model was applied to the preprocessed time series to estimate the regression coefficients (i.e., beta values) for the no-distractor condition and the distractor condition respectively. For the RSA approach, a regressor was modeled for each individual memory nonword, with six repetitions across six runs for that nonword. Thus, 16 regressors of interest for 16 nonwords were included in the regression model. For the univariate analyses, a single regressor was modeled across all nonwords and all runs. A multiple parameter shape-free hemodynamic response function model (i.e., "TENT" function in AFNI) was used for each regressor to estimate the amplitude of signal change at each time point across the whole period for a trial (i.e., from the onset to 21 s later). The correct and incorrect trials were modeled separately, and all the following analyses were based on correct trials. Besides the experimental regressors, some nuisance regressors, including third-order polynomial baseline trends, six head motion correction parameters, and six temporal derivatives of head motion parameters, were also modeled. To reduce the influence of potential outliers, censoring was applied in the general linear model to the time points in which head motion exceeded a distance (i.e., Euclidean norm) of 0.3 mm with respect to the preceding time point or in which more than 10% of whole brain voxels were regarded as outliers by AFNI 3dToutcount. According to our calculation, on average across subjects, there were only 5.3 volumes (i.e., TRs; out of 2,448 across 12 runs, 0.22%) detected by 3dToutcount as outliers and censored out, indicating only a small proportion of outliers in the data.

Univariate Activation Analysis

For the group-level univariate analyses, the average amplitude of responses at the third and the fourth TRs (4.5 s and 6 s) after the onset of memory nonword was used as the signal change for the encoding period, and the average amplitude of responses across the sixth and the seventh TRs (9 s and 10.5 s) after the onset of memory nonword was calculated as the signal change for the delay period. Paired t-tests were performed on the signal changes to compare the distractor and no-distractor conditions, as well as the single condition vs. fixation baseline, during the encoding and the delay periods, respectively. Multiple comparison correction was conducted to estimate the cluster size threshold based on a permutation approach with a voxel-wise p-value of 0.001 and then corrected at the cluster-wise α value of 0.05. This simulation approach has been shown to effectively control the false positive rate under 5% (Cox et al., 2017).

Representation Dissimilarity Matrix

The phonological representation dissimilarity matrix (RDM) was constructed using the same procedure as in Yue and Martin (2021). The RDM represents the pairwise distances among 16 memory nonwords. Specifically, pronunciations of sixteen nonwords were obtained from the Carnegie Mellon University Pronouncing Dictionary[5] and phonological transcriptions were coded with a set of phoneme symbols (ARPAbet; Shoup, 1980). Then, we used Phonological Corpus Tools[6] to estimate the phonological distance for each pair of nonwords. To do this, phonological transcriptions were first aligned so as to minimize the number of different phonemes between two strings. All phoneme segments were mapped into a phonetic feature space (Hayes, 2008), and the distance between two phoneme segments was calculated as the distance between their phoneme feature values (Allen and Becker, 2015)—that is, the distance between two identical feature values is 0, while the distance of two opposite feature values (e.g., voiced/unvoiced) is 1, and the distance between two feature values in case one of them is unspecified is set to 0.25. Then, the phonological distance between two nonwords was calculated by adding up distances between all phoneme segment pairs.

ROI-Based RSA

Two regions of interest (ROI) were chosen from a recent study on testing the buffer vs. the embedded processes accounts of phonological WM (Yue et al., 2019): one region in the left STG (Talairach coordinates: $x = -57$, $y = -15$, $z = 2$) which was involved in speech processing and the other one in the left SMG (Talairach coordinates: $x = -53$, $y = -33$, $z = 24$). Converging evidence from neuroimaging studies (Paulesu et al., 1993; Salmon et al., 1996; Yue et al., 2019) and brain damaged patient data (Martin, 2005; Paulesu et al., 2017) had suggested the left SMG as a phonological buffer with phonological representations being maintained in this region. Besides the left STG and the left SMG, we also conducted an exploratory analysis in another two ROIs uncovered in Yue et al. (2019): the opercular part of the left inferior frontal gyrus (IFG.oper; Talairach coordinates: $x = -59$, $y = 5$, $z = 20$) and the left precentral gyrus (PreCG; Talairach coordinates: $x = -49$, $y = -7$, $z = 40$), as these two regions, particularly the inferior frontal gyrus, have been suggested to play a role in articulatory rehearsal in phonological WM (Paulesu et al., 1993; Chein and Fiez, 2001).

ROI-based RSA was performed by using CoSMoMVPA toolbox (Oosterhof et al., 2016) in Matlab (R2018a, The

[5]http://www.speech.cs.cmu.edu/cgi-bin/cmudict
[6]http://phonologicalcorpustools.github.io/CorpusTools/

MathWorks, Inc., USA). Masks of prior ROIs were obtained for each subject by using an inverse transformation from the standard space to each individual's native space. The RSA procedure was conducted during the delay period for the no-distractor condition and distractor condition respectively. In each ROI, we estimated neural RDM by calculating the Pearson correlation distance (Haxby et al., 2001; Kriegeskorte et al., 2008) on the neural activation patterns across all voxels in that ROI for all pairs of nonwords. Before calculating the pair-wise neural distances, the data were centered across all conditions (i.e., subtracting the mean activation pattern of all nonwords; Diedrichsen and Kriegeskorte, 2017). Then, the neural RDM was compared with the theoretical RDM by computing Spearman's rank correlation (Kriegeskorte et al., 2008). For group-level inference, Fisher r-to-z transformation was applied to the Spearman correlation coefficient, and one-sample one-tailed *t*-tests were conducted to test the average similarity index against zero for a single condition. In addition, paired-sample *t*-tests were performed to determine if the difference between the no-distractor condition and the distractor condition (i.e., the distractor effect) was significant.

Results: fMRI Experiment

fMRI In-Scanner Behavioral Results

As shown in **Figure 2**, distractors presented during the delay period did not decrease the recognition of the memory nonword (Accuracy: 92.2% for no-distractor condition and 94.1% for distractor condition). In fact, the presence of distractors marginally improved STM performance as compared to the no-distractor condition ($t_{(9)} = 2.21$, $p = 0.054$, Cohen's $d = 0.7$, paired-sample *t*-test). Distractors had no effect on response times (1,576 ms for no-distractor condition and 1,587 ms for distractor condition, $t_{(9)} = 0.49$, $p = 0.63$, Cohen's $d = 0.15$, paired-sample *t*-test). To correct for potential accuracy-RT trade-off effects and provide a better measure combining both RT and accuracy, we calculated an inverse efficiency (IE) score (i.e., the mean RT on the correct trials divided by accuracy; Townsend and Ashby, 1983). There was no significant difference in the IE scores between the no-distractor condition (mean: 1,717) and the distractor condition (mean: 1,693; $t_{(9)} = 0.71$, $p = 0.49$, Cohen's $d = 0.22$). According to Nairne (1990) feature model of STM, a memory trace is susceptible to interference by an external list, with a feature in the memory trace being overwritten by a similar feature presented in the distracting list. It is possible that the lack of an interference effect resulted because of two factors: (1) no task was required for the distracting items; and (2) the distracting list had no overlapping phonemes with the memory nonword. The absence of distractor interference effect on behavioral performance suggested that features of the memory trace were preserved in the face of these unrelated distracting sounds.

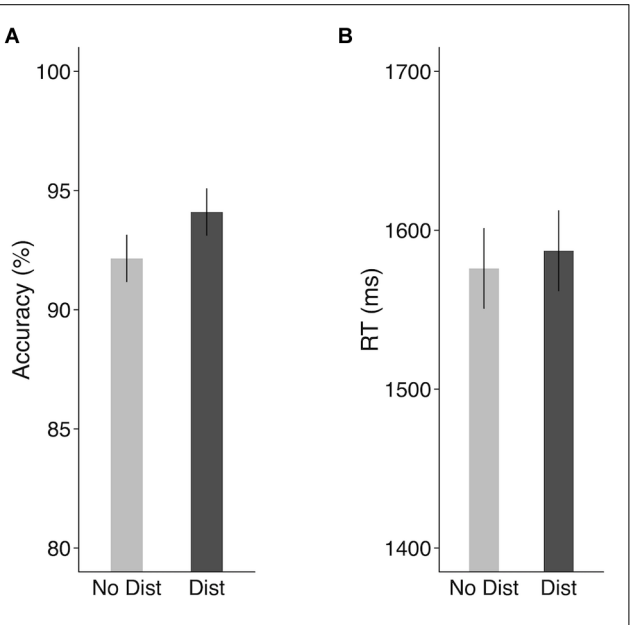

FIGURE 2 | Behavioral results in the scanner in the fMRI experiment. **(A)** Accuracy and **(B)** response times. Error bars represent 95% within-subjects confidence intervals around the mean. No Dist, no-distractor condition; Dist, distractor condition.

Univariate Activation Results

Univariate activation analyses showed that, during the encoding period, the target memory nonwords similarly activated bilateral STG as compared to the fixation baseline in the no-distractor condition (**Figure 3A**) and distractor condition (**Figure 3B**). Because task activation was compared to a fixation baseline condition, it was unsurprising that the activated regions for perceiving nonwords included bilateral Heschl's gyri (i.e., primary auditory cortex) and a large cluster in the right STG. The activated regions for the target nonwords also included the left supplementary motor area, the right superior occipital gyrus, bilateral cerebellum, and bilateral visual occipital gyri for both the distractor and no-distractor conditions (for all regions activated in the no-distractor and distractor conditions, see **Supplementary Table S1** in **Supplementary Materials**). A contrast of distractor vs. no-distractor conditions during the encoding period showed that bilateral Heschl's gyri and STG regions beyond Heschl's gyri were activated more for the distractor condition than the no-distractor condition, suggesting that the distractors presented immediately after the memory nonword activated the primary and associated auditory cortex (**Figure 3C**). Given there was no jittering of the delay between the target nonword and distractors, it was not possible to strictly separate target and distractor activation.

During the delay period, no greater activity for the no-distractor condition relative to the fixation baseline was observed in the temporal lobe (**Figure 3D**). This is consistent with the univariate results from Yue et al. (2019) where no activation was uncovered in superior temporal regions during the delay period of a phonological STM task. Only a few clusters were observed in the right occipital lobes showing activity for the no-distractor condition relative to the baseline. In the distractor condition, during the delay period, greater activity relative to the fixation baseline was observed in bilateral STG, as well as in bilateral superior occipital gyri and bilateral lingual gyri (**Figure 3E**; for all regions activated

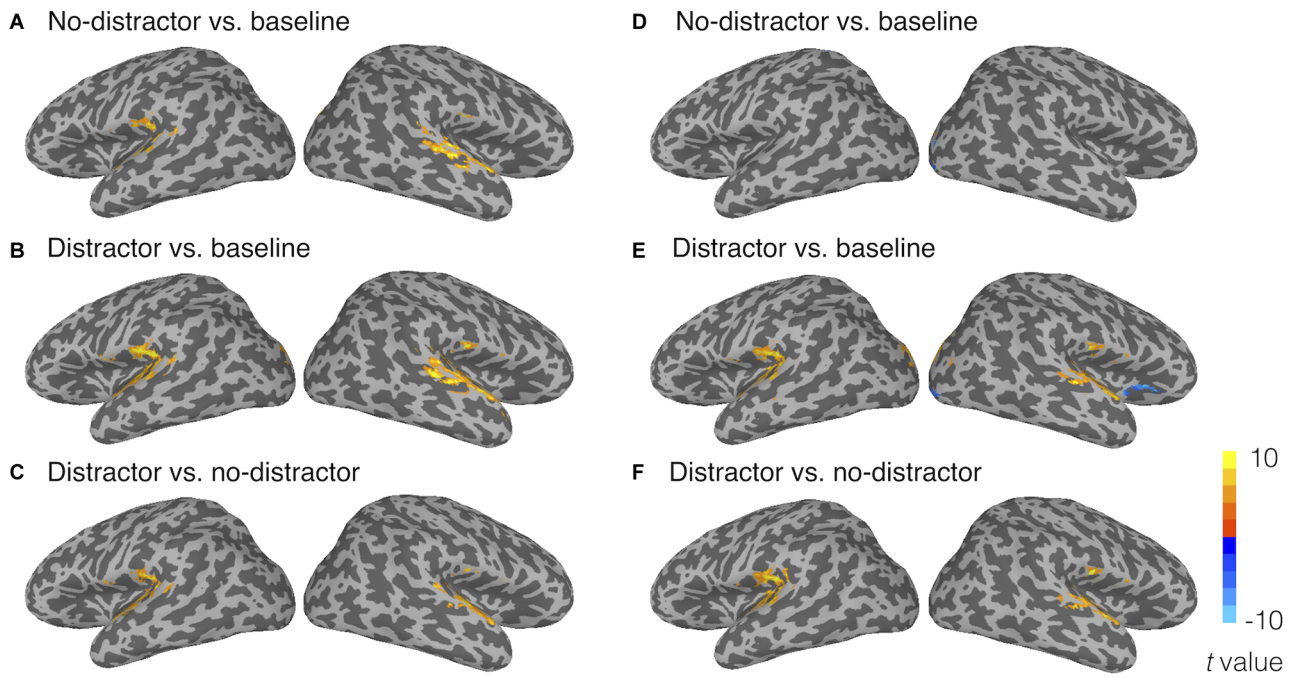

FIGURE 3 | Univariate activation results during **(A–C)** the encoding period and **(D–F)** the delay period. Panels **(A)** and **(D)** show the activated regions for the no-distractor condition relative to the fixation baseline; **(B)** and **(E)** reveal the activated regions for the distractor condition relative to the fixation baseline; **(C)** and **(F)** show the contrasts of distractor vs. no-distractor conditions. The activation threshold was set at voxel-wise $p < 0.001$ and corrected at cluster-wise $\alpha < 0.05$ (cluster size > 29 voxels).

in no-distractor and distractor conditions, see **Supplementary Table S2** in **Supplementary Materials**). A contrast of distractor vs. no-distractor showed that bilateral STG and a cluster near the left SMG were activated more for the distractor condition than the no-distractor condition (**Figure 3F**). Greater activation during the delay period for distractor than no-distractor condition is likely due to two processes: perceiving the distractors and maintaining the memory word. Previous studies using a mismatch negativity paradigm (i.e., used as an index of unattended processing for task-irrelevant materials) have shown that automatic speech processing took place in the left temporal lobe (Auther et al., 2000; Tervaniemi et al., 2000; Pulvermüller et al., 2001; Saint-Amour et al., 2007). Thus, the activation in bilateral STG (basically in the primary auditory cortex) is no doubt due at least in large part to the automatic processing of distractors, whereas the activation in the left SMG might be due to maintenance of the memory word, considering the close location of this region ($x = -45$, $y = -37$, $z = 22$) to a region found in a recent study ($x = -53$, $y = -33$, $z = 24$; Yue et al., 2019). No region showed greater activity for the no-distractor condition than the distractor condition.

Taken together, univariate analyses showed that the memory nonwords activated similar brain regions during the encoding period either with or without distractors presented immediately after the memory nonwords. During the delay period, greater activity was found in bilateral STG for the distractor condition as compared to the no-distractor condition, which can be attributed at least in large part to the automatic activation evoked by the perception of the distracting nonwords. Greater activation in the left SMG is unlikely due to the perception of the distracting nonwords, as this region is not a typical speech processing region. Instead, the memory maintenance explanation for the activation in the left SMG is consistent with the notion that the left SMG plays a critical role in phonological WM in the face of distractors. However, without analyzing the neural representations for memory nonwords in the left SMG, it is hard to tell if this region truly maintained phonological representations in the face of distracting information. Also, the absence of activation in the left STG for memory nonwords during the delay period may just be due to lack of sensitivity with the univariate approach. Next, we performed RSA to address these questions.

RSA Results

Figure 4 shows the RSA evidence for phonological codes during the delay period in the distractor and no distractor conditions in the four ROIs: STG, SMG, IFG, and PreCG. In the left STG, there was significant RSA evidence of phonological coding in the no-distractor condition (similarity $\text{index}_{(\text{mean Spearman rho})} = 0.025$, $t_{(9)} = 2.02$, $p = 0.04$, Cohen's $d = 0.64$), but not in the distractor condition (similarity index < 0). In addition, a paired-sample t-test showed that the neural-model similarity index was significantly smaller for the

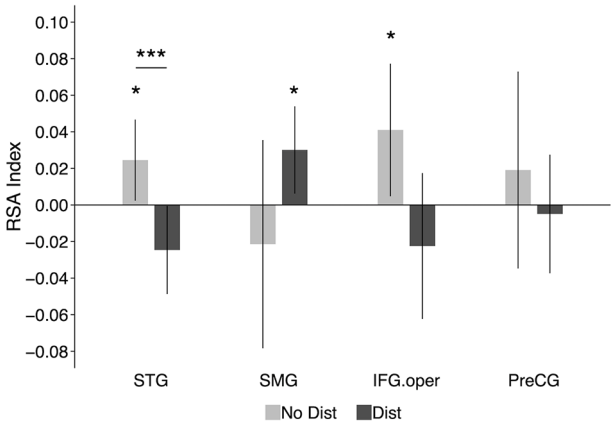

FIGURE 4 | RSA results in functional ROIs defined based on results from Yue et al. (2019): the left STG, the left SMG, the left IFG.oper, and the left PreCG. The graphs show the average neural-model similarity index (i.e., Spearman correlation coefficient) during the delay period. Error bars represent 95% within-subjects confidence intervals around the mean. No Dist, no-distractor condition; Dist, distractor condition. STG, superior temporal gyrus; SMG, supramarginal gyrus; IFG.oper, inferior frontal gyrus (the opercular part); PreCG, precentral gyrus; $^{*}p < 0.05$; $^{***}p < 0.001$.

distractor condition than the no-distractor condition ($t_{(9)} = 4.70$, $p = 0.001$, Cohen's $d = 1.49$). In the left SMG, there was no RSA evidence in the no-distractor condition (similarity index < 0). This was unexpected because this region has been regarded as a phonological buffer and was thus expected to show RSA evidence for phonological WM maintenance when no distractors were presented, as was observed in a recent study (Yue and Martin, 2021). However, when distractors were presented during the delay period, there was significant RSA evidence in the left SMG (similarity index = 0.03, $t_{(9)} = 2.31$, $p = 0.02$, Cohen's $d = 0.73$). The difference between the no-distractor and the distractor conditions was not significant ($t_{(9)} = 1.53$, $p = 0.16$, Cohen's $d = 0.48$). However, a repeated-measure ANOVA with distracting conditions (i.e., no-distractor and distractor) and regions (e.g., STG and SMG) as two within-subject factors showed a significant interaction ($F_{(1, 9)} = 7.7$, $p = 0.02$, partial $\eta^2 = 0.46$), showing that the decoding of phonological representations for the memory items was greater in the distractor than the no distractor condition in the SMG whereas the reverse was the case in the STG. Neither the distractor main effect nor the region main effect was significant (ps > 0.8).

In the left IFG (opercular part), significant RSA evidence was observed in the no-distractor condition (similarity index = 0.041, $t_{(9)} = 2.07$, $p = 0.03$, Cohen's $d = 0.65$), suggesting that this region was involved in maintaining phonological representations during the delay period in the absence of distractors. Given the nonwords used in the experiment, the RSA evidence in the left IFG may imply that subjects relied more on rehearsal to maintain the memory nonwords (i.e., maintaining articulatory codes). When distractors were presented during the delay period, there was no RSA evidence in the IFG (similarity index < 0; see Section "Discussion" below). However, the difference between the distractor condition and no-distractor condition was not significant ($t_{(9)} = 1.75$, $p = 0.11$, Cohen's $d = 0.55$). In the left precentral gyrus, there was no significant RSA evidence with either the presence or absence of distractors during the delay period.

To summarize, although the left STG showed RSA evidence for phonological codes during the delay period in the no-distractor condition, such evidence was absent when there were distractors presented during the delay period. While the findings suggest that the STG may provide support to phonological WM when no distractors are present, stronger causal evidence would be obtained in a paradigm in which neural representations are disrupted during the delay period. In contrast to the STG, the proposed buffer region in the left SMG showed RSA evidence for phonological retention in the distractor condition, suggesting its critical role in maintaining phonological information under distraction. In Experiment 2, we addressed the necessity of these regions in supporting phonological WM using a brain stimulation method.

EXPERIMENT 2: TMS

Previous TMS studies have investigated the roles of specific regions in verbal WM (Romero et al., 2006; Deschamps et al., 2014; Sliwinska et al., 2015). For example, Deschamps et al. (2014), by using repetitive TMS (rTMS), tested whether the supramarginal gyrus is involved in phonological processing or in verbal working memory. To tap phonological processing, they used a same/different judgment task for pairs of two-syllable auditory stimuli (either spoken words or pseudowords) with a short stimulus-onset-asynchrony between items in a pair, which makes minimal demands on verbal WM. To tap verbal WM they used an N-back task with a subset of the same auditory stimuli as in the phonological processing task. The results showed that rTMS delivered to the SMG had no effect on the same/different judgment task but did impair performance in the N-back task (i.e., causing more errors and slower response times). The results from this experiment are consistent with the buffer account claiming that the left SMG, which is not involved in phonological processing, supports phonological WM. However, given the complexity of the N-back task, it is unknown what specific functional component of WM was supported by the SMG. The purpose of the present experiment was to test TMS effects in both the speech processing region and the putative phonological buffer region. Off-line rTMS, presented prior to the behavioral experiment, as in Deschamps et al. (2014), is not preferable because if there is a TMS effect in the speech processing region, it would be unclear whether this effect is attributed to a disruption of perception or memory retention. Instead, we used an online non-repetitive TMS paradigm (triple pulse) in this experiment, which allowed delivery of the stimulation after stimulus presentation during the delay period of a phonological WM task.

Some studies have used single- or triple-pulse online TMS paradigms to examine the causal role of the occipital lobe in visual WM (Cattaneo et al., 2009; van de Ven et al., 2012; van de Ven and Sack, 2013; Rademaker et al., 2017;

van Lamsweerde and Johnson, 2017). For example, in Cattaneo et al.'s (2009) study, subjects were asked to remember the clock hands in a visual WM task, and a single-pulse of TMS was delivered over the occipital lobe either at the start or the end of a 2,000 ms retention period. They found that TMS applied at the start of the retention period caused an interference effect on WM performance (i.e., longer response time for TMS vs. no-TMS conditions), but this interference effect was absent when TMS was applied at the end of the retention period. This timing-sensitive TMS effect has also been observed in other studies (van de Ven et al., 2012; van Lamsweerde and Johnson, 2017) which examined the contribution of the early visual cortex to visual WM. van de Ven et al. (2012) manipulated the onset of a single TMS pulse during the delay period of a visual STM task (i.e., 100 ms, 200 ms, 400 ms after the onset of the 150 ms presentation period for memory items) and included two memory load conditions (i.e., one and three memory items). They observed an interference effect on memory accuracy (i.e., lower accuracy for TMS vs. no-TMS conditions) when a single TMS pulse was delivered at the 200 ms timing condition, but such an interference effect was absent when the TMS pulse was delivered later (i.e., 400 ms). In addition, this time-dependent pattern was only observed in the high memory load condition. These interference effects were claimed to support the embedded processes account for visual WM, in which the visual WM representation was maintained in the visual sensory area and TMS delivered at this region caused interference to WM performance. However, taking the discrepancy between early vs. late timings of TMS pulse into consideration, some researchers suggested another explanation—specifically, the absence of the interference effect at the late delay period reflected a nonessential role of the visual sensory region in WM. That is, once the WM representation has been transformed and consolidated into the visual buffer, TMS to the visual sensory region did not affect WM performance (e.g., Barbosa, 2017; Xu, 2017, 2018).

In this experiment, we employed a triple-pulse TMS paradigm to test the causal roles of the cortical regions showing neural evidence of phonological maintenance in Experiment 1. We used the same set of subjects in Experiment 1, and their RSA-fMRI results were used to locate the target regions for the TMS application. Results from Experiment 1 indicated that the left STG showed RSA evidence for phonological codes during the delay period in the no-distractor condition, and the left SMG showed RSA evidence for phonological storage during the delay period in the distractor condition. These two regions were chosen as the target regions for the TMS experiment. An occipital region was selected as a control region. A phonological WM task was administered to subjects, and triple TMS pulses were delivered to each of the target regions (i.e., the left STG, the left SMG, and the occipital control region) during the delay period of the phonological WM task. To uncover the potential time-course of TMS effects, we also manipulated the timing of the TMS pulses (see "Methods" Section). Recently, using this triple-pulse TMS paradigm, we showed that TMS applied to the left superior temporal lobe disrupted behavioral performance on a speech perception task, confirming the causal role of the left STG in speech processing (Ramos-Nuñez et al., 2020). If the left STG serves as the neural substrate for phonological WM, as predicted by the embedded processes accounts, and the RSA evidence for phonological codes in the left STG from Experiment 1 truly reflects phonological maintenance, then applying TMS to this region during the delay period should cause interference in WM performance. In contrast, the buffer models predict additional regions beyond the speech processing region involved in maintaining information in WM. Thus, buffer accounts would predict that TMS delivered at the left STG region would not affect WM performance, whereas stimulation at the buffer region (SMG) would.

TMS Experiment: Materials and Methods

Participants

The same 10 subjects from the Experiment 1 participated in the TMS experiment. Subjects signed consent forms according to procedures approved by the Rice University Institutional Review Board.

Materials and Procedure

A similar delayed recognition task was employed in the TMS experiment, except that a shorter delay period (3 s) was used, as compared to 9 s used in the fMRI experiment. Each trial began with a fixation cross shown in the center of a PC monitor for 500 ms. At the end of the fixation cross, a nonword was played binaurally *via* earbuds to the subjects for 700 ms, followed by a 3-s delay. Subjects were instructed to remember the nonword over the delay period. Then a probe nonword was played and subjects responded to the probe by pressing buttons indicating whether the probe matched the memory nonword. The task was administered using E-prime 2.0 (Psychology Software Tools[4]). During the delay period, the TMS pulses were delivered to the target or control brain regions (see Section "TMS Procedures" below). Subjects' response times were recorded from the onset of the probe nonword.

One-hundred and twenty nonwords, including the 16 nonwords used in Experiment 1, were used as the memory items in the TMS experiment. The mean duration of the nonwords was 615 ms (range: 481 ms–698 ms). As in Experiment 1, the non-matching probes differed in a single distinctive feature of one phoneme from the target memory nonwords (e.g., sirp vs. sirb). Half of the trials had matching probes and half non-matching.

TMS Procedures

Before the TMS experiment, each subject's anatomical and functional images were acquired in Experiment 1. For the TMS experiment, we used the Brainsight TMS Navigation system (Rogue Research Inc., Canada) to register each subject's head to the anatomical image for that subject by using four anatomical landmarks (i.e., the tip of the nose, the nose bridge, left and right ear notches). The functional data were registered to the anatomical images, thus the brain areas that showed RSA evidence served as the target regions for the TMS experiment. For each subject, three target regions were located based on the center of mass of clusters in RSA results in the fMRI experiment. The anatomical parcellation from Freesurfer (Fischl et al., 2004) was used to help locate the relevant areas—that is,

the search was conducted within the range of the anatomical masks for the corresponding regions. The first target TMS region of interest was in the left SMG, which has been argued to be a buffer area for phonological WM (Martin, 2005; Paulesu et al., 2017; Yue et al., 2019); the second one was in the left STG, which was regarded as the speech processing area (Turkeltaub and Coslett, 2010; Price, 2012; Yi et al., 2019). The last one was a control region, and was located in the posterior occipital lobe, which is a primary visual processing area (Murakami et al., 2015; Ramos-Nuñez et al., 2020). Specifically, considering the results of the fMRI experiment, the selection of the target regions followed these priority criteria: for the left SMG, (1) if RSA evidence of phonological retention during the delay period (with a threshold of voxel-based neural-model similarity index > 0.1) was observed in both distractor and no-distractor conditions, the overlapping cluster was chosen as the SMG target region; (2) or if no overlapping cluster between distractor and no-distractor conditions was found, a cluster showing RSA evidence in the distractor condition was considered first; and (3) or if none of (1) and (2), a cluster showing RSA evidence in the no-distractor condition was chosen. With these criteria, five subjects showed RSA evidence in a left SMG for both distractor and no-distractor conditions, and four subjects showed RSA evidence for the distractor condition only, and one subject showed RSA evidence in the no-distractor condition only. For the left STG, in addition to the criteria described above, RSA evidence during the encoding period in this region was also considered—that is, if a common region in the left STG showed RSA evidence during both the encoding period and the delay period, that region was considered first; otherwise, a region showing RSA evidence during the delay period was chosen. There were four subjects showing delay-period RSA evidence in the distractor condition and six subjects showing delay-period RSA evidence in the no-distractor condition, with one subject showing both and one showing neither. For the control region, a posterior occipital region showing no RSA evidence during either period was chosen. With these criteria, we were able to locate three target regions for all subjects. The Talairach coordinates of three target regions for all subjects are shown in **Table 1**. Notice that all target regions were defined in each individual's native space, and the coordinates in the standard space are only provided for reference.

In TMS trials, during the delay period, triple pulses presented at 100 ms intervals (10 Hz) were delivered to the target region using Magstim Rapid^2 simulator system (Magstim Inc.) with the D70^2 coil being placed perpendicularly to the subject's scalp. For the early timing condition, triple pulses were triggered at 700 ms after the onset of the memory item (i.e., the start of the delay period), and for the late timing condition triple pulses were triggered at 1,300 ms after the onset of the memory item (i.e., 600 ms later after the onset of the delay period). In the no-TMS trials, the coil was placed in the same region, but no pulse was delivered. For each target region and each timing condition, there were 10 trials for the TMS condition and 10 trials for the no-TMS condition, with the order of these 20 trials being pseudo-randomized (i.e., no more than three consecutive TMS trials) and grouped in a block. Orders for three target TMS regions (i.e., SMG, STG, occipital gyrus) and two TMS timing conditions (i.e., early, late) were counterbalanced across subjects. The stimulation intensity was set to the motor threshold for each subject individually at the beginning of the experiment. Before the formal experiment, a short practice session including five TMS trials and five no-TMS trials was administered to subjects with the coil placed at the vertex of the brain, to familiarize subjects with the stimulation procedure.

TMS Results

Accuracy

When the TMS pulses were delivered at the onset of the delay period (**Figure 5A**), there was no significant difference between the TMS condition and the no-TMS condition in either the left SMG (TMS: 98%, no-TMS: 97%; $t_{(9)} = 0.43$, $p = 0.68$, Cohen's $d = 0.14$), the left STG (TMS: 95%, no-TMS: 96%; $t_{(9)} = 0.32$, $p = 0.76$, Cohen's $d = 0.1$), or the occipital gyrus (TMS: 95%, no-TMS: 96%; $t_{(9)} = 0.43$, $p = 0.68$, Cohen's $d = 0.14$). When the TMS pulses were delivered at 600 ms later than the onset of the delay period (**Figure 5B**), no significant TMS effect on accuracy was observed in either the left SMG (TMS: 97%, no-TMS: 96%; $t_{(9)} = 0.56$, $p = 0.59$, Cohen's $d = 0.18$) or the left STG (TMS: 96%, no-TMS: 98%; $t_{(9)} = 0.8$, $p = 0.44$, Cohen's $d = 0.25$). However, in the occipital gyrus, accuracy was slightly higher in

TABLE 1 | Talairach coordinates of the target regions in the TMS experiment.

Subjects	Left STG			Left SMG			Occipital		
	x	y	z	x	y	z	x	y	z
s103	−58	−9.6	−1.5	−45	−55.8	50.4	−4.5	−102.8	8.6
s104	−65.2	−31.9	5.7	−61.5	−39.4	34.4	−13.3	−101.7	12.3
s105	−63.8	−17.5	−2	−60.5	−31.5	41.5	−12.5	−96.5	23.5
s106	−56.7	−31.6	6	−63	−39.7	37.1	−9.6	−94.1	14.4
s107	−65.1	−19.2	9.5	−59	−28.9	40.3	−8.3	−99.1	14.8
s108	−64.6	−23.2	9.7	−58.5	−31.9	41.6	−4.5	−98.5	2.5
s109	−55.3	10	−4.9	−62.2	−37.2	38.6	−7.6	−95.4	19.3
s110	−65.6	−13.5	4.7	−59.1	−37	41.3	−10.5	−100.4	3.4
s111	−64.7	−21.3	5.8	−58.5	−49.1	37.9	−10.6	−97.5	−0.2
s112	−67.3	−23.7	2.7	−66.5	−29.4	25.1	−10.4	−98.8	4.6
Mean	−62.6	−18.2	3.6	−59.4	−38	38.8	−9.2	−98.5	10.3
SD	4.3	12.1	4.9	5.6	8.7	6.4	3	2.7	7.8

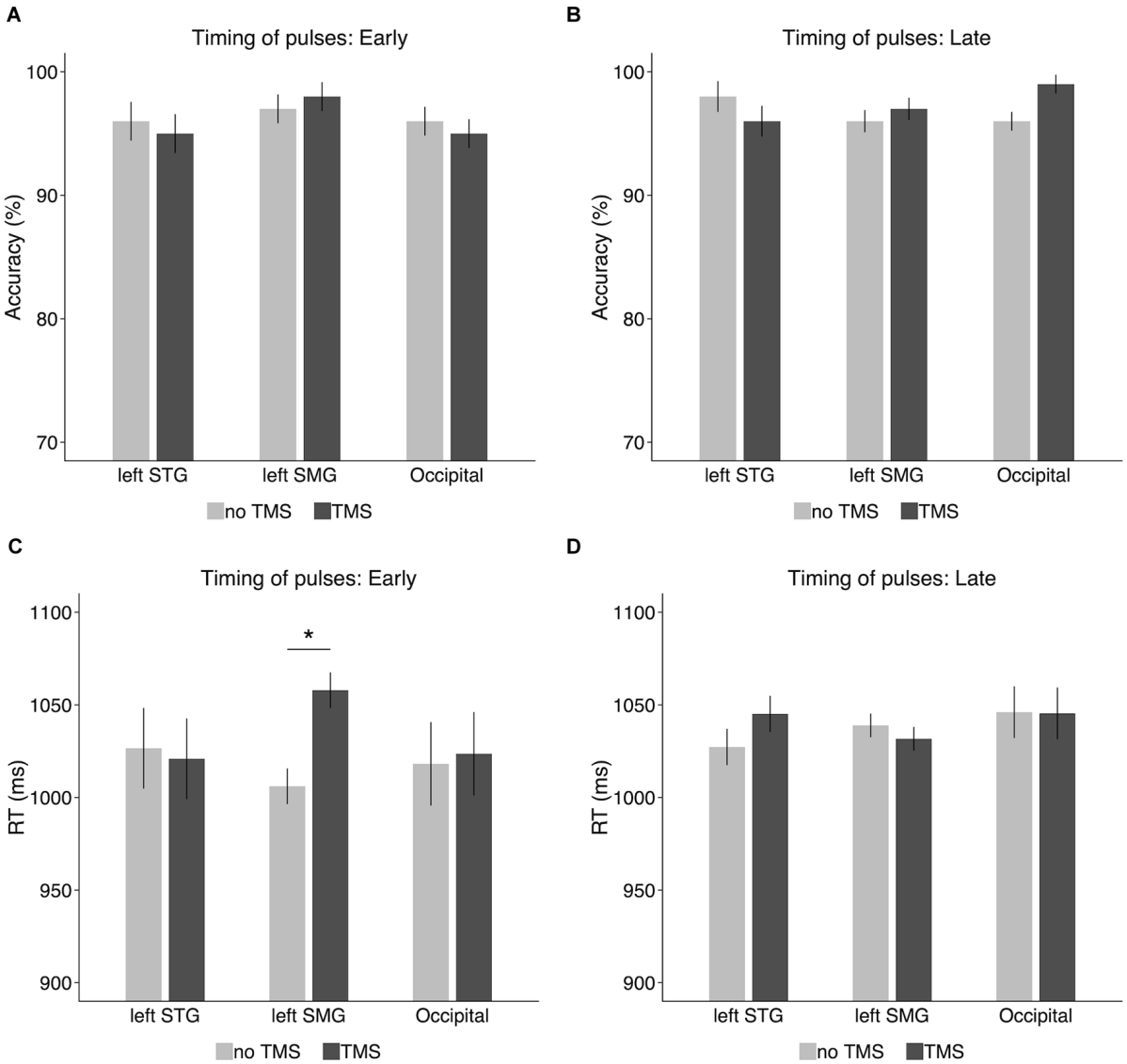

FIGURE 5 | Accuracy and response times in the TMS experiment for **(A,C)** the early timing condition (i.e., the onset of the delay period) and **(B,D)** the late timing condition (i.e., 600 ms after the onset of the delay period). Error bars represent 95% within-subjects confidence intervals around the mean. *$p < 0.05$.

the TMS condition (99%) than on the no-TMS condition (96%), a difference which reached marginal significance ($t_{(9)} = 1.96$, $p = 0.08$, Cohen's $d = 0.62$).

RT

Response times were recorded from the onset of the probe nonword in the TMS experiment and analyzed on the correct trials[7]. As shown in **Figure 5C**, when the TMS pulses were delivered to the left SMG at the onset of the delay period (i.e., offset of the memory nonword), RT was longer for the TMS condition (1,058 ms) than for the no-TMS condition (1,006 ms). A paired-sample *t*test confirmed that the difference was significant ($t_{(9)} = 2.69$, $p = 0.02$, Cohen's $d = 0.85$). However, this TMS effect on RT was not observed in the left STG (TMS: 1,021 ms, no-TMS: 1,027 ms; $t_{(9)} = 0.13$, $p = 0.9$, Cohen's $d = 0.04$) or in the control region (i.e., occipital gyrus; TMS: 1,024 ms, no-TMS: 1,018 ms; $t_{(9)} = 0.12$, $p = 0.91$, Cohen's $d = 0.04$). When the TMS pulses were delivered 600 ms later after the onset of the delay period (**Figure 5D**), there was no significant TMS effect on RT in the left SMG (TMS: 1,032 ms, no-TMS: 1,039 ms; $t_{(9)} = 0.56$, $p = 0.59$, Cohen's $d = 0.18$), the left STG (TMS: 1,045 ms, no-TMS: 1,027 ms; $t_{(9)} = 0.91$, $p = 0.39$, Cohen's $d = 0.29$), or the occipital gyrus (TMS: 1,045 ms, no-TMS: 1,046 ms; $t_{(9)} = 0.02$, $p = 0.98$, Cohen's $d = 0.006$).

[7]In the main text, RT results are algebraic means. We also analyzed the RT data using both the median of response times and the mean of log-transformed response times (see **Supplementary Materials**). These two ways of analyzing response times gave similar results, consistent with what we reported in the main text.

DISCUSSION

Although the buffer vs. embedded processes account of verbal WM have been under debate for decades, the neural locus of short-term retention and how the neural representations are maintained under distraction are poorly understood. In this study, we brought in evidence from two approaches to address these issues. Using fMRI with the RSA approach, we tested distractor interference effects on regions implicated in maintaining phonological representations and, using TMS, we tested the necessity of these regions on phonological WM performance.

If the representation for the memory nonword was maintained in the speech processing region (e.g., left STG), as predicted by the embedded processes account, the neural representation of the target would either persist despite the interference from distractors, or decrease but remain at a level from which the phonological representations were still decodable. However, this was not the case in the current study. Although RSA evidence for phonological retention was observed in the left STG in the no-distractor condition, such evidence was absent in the presence of distractors, and it was significantly different from that without distractors. Taking the lack of an interference effect on behavioral performance into consideration, this does not support a claim that the left STG, the speech processing region, is the neural substrate for phonological WM maintenance.

In contrast, the left SMG showed RSA evidence of phonological retention during the delay period in the distractor condition, supporting the role of buffer in this region in the face of distractors. One issue is that this region did not show RSA evidence of phonological retention when there were no distracting nonwords during the delay period. If this region serves as a buffer, it would be expected to maintain phonological information regardless of whether there were distractors or not. Given the present results, one might argue that the anatomical dissociation evident in the RSA evidence indicates that if there were no distractors, the phonological representations were maintained in the processing region whereas, in the presence of distraction, the phonological WM representations were shifted into a non-perceptual region. In a recent study on visual WM, Lorenc et al. (2018) presented a grating with a given orientation to the subject to remember, and then, for some trials, presented a distracting grating with a different orientation midway during the delay period. Using an inverted encoding model approach (a similar representation modeling method as RSA; Naselaris and Kay, 2015), they found that the orientation information of the memory grating could be successfully reconstructed from both visual sensory areas (e.g., V1-V3) and a parietal area (i.e., IPS) when there were no distractors. However, when a distractor was presented, the orientation representation in the visual sensory area showed a bias towards the distracting orientation whereas in the parietal lobe the representation did not show such a bias, and accurately maintained the memory grating orientation. Based on these results, Lorenc et al. proposed a dynamic trade-off mechanism between the processing region and the parietal region under different task demands (e.g., with or without distractors). However, this explanation does not seem to apply to our case. In the no-distractor condition in the present study, in addition to the left STG, RSA evidence of phonological retention was also observed in a posterior region of the left IFG. This frontal region has often been assumed to be involved in speech rehearsal (Paulesu et al., 1993; Awh et al., 1996; Chein and Fiez, 2001). Under this rehearsal view, one could reasonably assume that this region was involved in rehearsing the memory nonword during the delay period. The co-existence of RSA evidence in the left IFG and the left STG diminishes the possibility that the neural representations in the left STG underlie phonological WM. Instead, the decoding in the STG perhaps just reflects the automatic activation of phonological codes induced by inner speech rehearsal (Shergill et al., 2002).

However, there was a trend for RSA evidence in the left IFG to be modulated by distraction—that is, with RSA evidence with no distraction but not with distraction, although the difference was not significant. One might have expected that subjects would make more use of rehearsal to maintain the memory nonwords when distractors were present, but there was no suggestion of a higher decoding index in the IFG under distraction. However, it is not necessarily the case that RSA evidence in the left IFG should be interpreted as reflecting articulatory rehearsal. Some researchers have argued on the basis of behavioral results that participants do not tend to recirculate items through rehearsal in WM tasks and when instructed to do so, such rehearsal is not an effective means of maintaining information in verbal WM (Oberauer, 2019) and does not benefit performance (Souza and Oberauer, 2018, 2020). Chein and Fiez (2010) put forward a different interpretation of the role of the LIFG in verbal WM, arguing that this region was involved in maintaining novel sequences of phonological representations. If so, one might argue that these representations consist of output phonological representations involved in speech production (Martin et al., 1999; Cogan et al., 2017), rather than input phonological representations involved in speech perception, which might be maintained in the SMG. Chein and Fiez (2010) found that irrelevant auditory information presented during the presentation of the list and during a delay period decreased activity in this LIFG region and suggested that this resulted from a general effect of attention being oriented temporarily towards the irrelevant information. A related interpretation regarding the role of the left IFG is that it may be involved in another mechanism (e.g., refreshing; Barrouillet et al., 2004, 2011) which is used to maintain phonological representations. Thus, the absence of decoding in this region may reflect the diversion of attention by the distractors. It is possible that such a distraction effect occurred here, reducing the ability to decode information in this region, even though the behavioral performance was unaffected by distraction for our one-item memory load.

The findings from the fMRI experiment support predictions from a buffer account of phonological WM that non-perceptual fronto-parietal regions (i.e., the left SMG in the presence of distractors and the left IFG in the absence of distractors) are involved in maintaining phonological representations, although

the left STG also showed decoding evidence in the absence of distractors. There are, however, some remaining issues. For example, it remained unclear whether the neural codes in the left STG in the no-distractor condition support phonological WM. We addressed this question by testing the necessity of the left STG, as well as the proposed buffer region (i.e., left SMG), in phonological WM with a brain stimulation approach. We did not observe any TMS effect on behavioral performance when stimulation was delivered to the left STG. In contrast, a TMS effect on response time was observed when stimulation was delivered at the left SMG at the start of the delay period. Because the left SMG showed RSA decoding evidence in the presence of distractors in Experiment 1 which is assumed to reflect WM storage rather than other processes involved in working memory (e.g., attentional control), and this region also showed neural evidence for phonological maintenance during the delay period without distractors in our recent studies (Yue et al., 2019; Martin et al., 2021b; Purcell et al., 2021; Yue and Martin, 2021), the TMS effect observed in this region serves as evidence supporting the necessity of this region in WM maintenance of phonological codes.

The discrepancy between early vs. late TMS effects in the left SMG makes the interpretation complicated. The early vs. late TMS timing manipulation was originally made to uncover potential time-dependent TMS effects in the processing region, which have been found in the visual WM domain (Cattaneo et al., 2009; van de Ven et al., 2012; Rademaker et al., 2017; van Lamsweerde and Johnson, 2017). However, no TMS effect on behavioral performance was observed in the left STG for either the early or late timing condition. Instead, time-dependent TMS effects were observed in the left SMG. If phonological representations were maintained in the left SMG over the delay period, TMS effects would be expected for both early and late timing conditions. The observed discrepancy may lead one to argue that such a TMS effect in the early timing condition might be due to some disruption of perceptual codes. This explanation seems implausible. If the early TMS effect is attributed to perceptual disruption, such a TMS effect should be observed in the left STG because this region is considered to be actually involved in speech perception, but no TMS effect was found. One explanation for the time-dependent TMS effect in the left SMG is that it may reflect the dynamic nature of WM codes in the buffer. In a recent neurophysiological study, Spaak et al. (2017) evaluated the generalization and dynamics of the single-electrode signal in a WM task recorded from the monkey prefrontal region. Specifically, they trained a decoder based on a given delay period and used this decoder to decode stimulus information during other delay periods. If the decoder shows good generalization in decoding information across different delay periods, the WM representation is assumed to be maintained in a stable state. They found that during the early delay period up to 500 ms after the offset of stimulus presentation, the neural codes for WM information changed dynamically, whereas, during the remaining delay period, the WM codes remained stable. A similar pattern has been observed in another neurophysiological study (Murray et al., 2017). Inspired by these observations, Barbosa (2017) proposed an explanation to reconcile the dynamic and stable nature of WM codes from a dynamic systems perspective—that is, when the sensory input disappears, the WM system evolves towards a stable state, but before that, the WM code remains dynamic and is vulnerable to external disturbance. Once the system achieves a stable state, distractors no longer have an effect on the WM representation. This claim seems to explain the discrepancy of the TMS effects in the present experiment. Immediately after the disappearance of the memory nonword and during the early delay period, the phonological information was being transformed from the speech processing region to the buffer region but the WM representation had not yet been constructed in the buffer, leading the WM code to be susceptible to interference (e.g., by the TMS pulses), but once the WM representation had been consolidated in the buffer, it remained in a stable state and external stimulation had a negligible effect on WM performance. Similar time-dependent interference effects on visual WM from behavioral data have been reported showing that performance on a visual arrays task was impaired by masks which were presented shortly after the memory arrays (e.g., less than 200 ms), but not when masks were presented more than 500 ms later (Vogel et al., 2006). As compared to the behavioral data, the present experiment shows that the neural locus of this interference effect on phonological WM is in the left SMG, implying its role in buffering phonological codes. Then, one question arises as to what kind of stable code is unaffected by TMS during the late delay period. This issue relates to the nature of WM (e.g., a distributed WM representation; Christophel et al., 2017). If the WM representation is maintained in a distributed manner along fronto-parietal regions, disturbance at one region within the fronto-parietal network may not sufficiently affect behavioral performance because a disruption of the neural representation in a local region may be restored or compensated *via* its connection from other regions in this network. This claim seems to be supported by the data from computational modeling work which showed that stronger functional connectivity between the prefrontal and parietal regions was associated with more stable memory representations (Edin et al., 2009; Constantinidis and Klingberg, 2016). If WM has a distributed nature, future studies using a multifocal TMS paradigm which applies TMS over two or more regions simultaneously are needed to test this claim (Hartwigsen et al., 2010). Also, future work using computational modeling approaches (e.g., Kowialiewski et al., 2021; Lemaire et al., 2021) should investigate the nature and functional properties of a phonological WM buffer.

It is possible that multiple non-sensory regions may be found to be involved in maintaining WM information, such as the left IFG implicated in the fMRI experiment. Results suggest that this region plays a different role in phonological maintenance (e.g., in maintaining input vs. output phonological codes; Martin et al., 1999; Cogan et al., 2017). If so, it is possible that the degree of disruptions differs across regions, providing some suggestion that the regions differ in their relative contributions in a given WM task. For example, a recall or a repetition task is assumed to rely more on the output phonological buffer than the input buffer. Then, performance on the recall or repetition task would

be more impaired by TMS stimulations in this frontal region, as compared to TMS stimulations at the input buffer region in the inferior parietal lobe. Future work is needed to pin down the specific contribution of each region by TMS.

The present study with a non-repetitive TMS approach found a TMS effect on response time but not on accuracy. TMS-induced effects on high-level cognitive functions such as language and memory have usually been quantified by either change in RT and/or the accuracy of a given task (Hartwigsen, 2015). Accuracy effects (e.g., decreased accuracy for TMS condition vs. sham condition) on phonological WM have typically been reported in studies with a repetitive TMS approach (Romero et al., 2006; Deschamps et al., 2014), though RT effects have been observed in these studies as well. The triple-pulse TMS procedure used in the present is assumed to induce a short-lived suppression effect, as compared to the repetitive TMS that has a long-lasting suppression effect. Also, it should be noted that those studies which found TMS accuracy effects typically used phonological WM tasks that tapped phonological retention for multiple items (Romero et al., 2006; Deschamps et al., 2014). Thus, the absence of the TMS effect on accuracy might be due to the short-lived suppression effect or a relatively simple phonological WM task (i.e., maintaining the sounds of one item) used in the present study. Future work using a repetitive TMS procedure with pulses filling up the delay interval or using a long-term repetitive TMS prior to the behavioral task would be expected to reveal the accuracy effect.

Limitations

One limitation of the current study is the limited sample size. Some work suggested that a minimum sample size of 12 subjects is required for RSA (Nili et al., 2014; Popal et al., 2019). Thus, the results reported in the current study should be treated with caution. Another limitation is the mixed evidence in the RSA decoding in the left SMG in Experiment 1. We did expect that RSA evidence would be observed in this region regardless of whether there were distractors or not, as we observed RSA decoding evidence for phonological retention for words in a recent study (Yue and Martin, 2021). The discrepancy might be due to the different materials and tasks used in the current study as compared to those in Yue and Martin (2021). Moreover, future work employing a typical list recall task with multiple items is needed to disentangle the different representations for the content of items and their serial order structure in the list (e.g., Fan et al., 2021). Also, with an explicit task on the distractors, future work can test whether an interference effect on the representations in the buffer region is associated with a decrement in WM performance.

CONCLUSION

To summarize, although the speech processing region in the left STG showed RSA evidence of phonological retention for nonwords during the delay period, such evidence was absent when distractors were presented. In contrast, the proposed buffer region in the left SMG showed RSA evidence of phonological retention even in the presence of distractors during the delay period. In addition, a TMS effect on response time for a phonological WM recognition task was observed when the left SMG was stimulated during the delay period, whereas stimulations at the left STG and an occipital control region had no effect on behavior, confirming the causal role of the left SMG in phonological WM. Converging evidence from two approaches provides greater support for a buffer account of phonological WM over an embedded processes account, with the proposed buffer region in the inferior parietal lobe being suggested to play a critical role in maintaining phonological information under distraction. Future work using either functional connectivity or the multi-focal brain stimulation approach is needed to uncover whether the memory representations are maintained in local regions or are distributed across the cerebral cortex in a network, and how such a distributed WM might support a range of behavioral performance.

DATA AVAILABILITY STATEMENT

The raw data supporting the conclusions of this article will be made available by the authors, without undue reservation.

ETHICS STATEMENT

The studies involving human participants were reviewed and approved by Rice University Institutional Review Board. The patients/participants provided their written informed consent to participate in this study.

AUTHOR CONTRIBUTIONS

QY designed the study, conducted the experiments, collected and analyzed the data under the supervision of RM. QY and RM wrote the manuscript and approved the submitted version.

FUNDING

This work was supported by the T.L.L. Temple Foundation Neuroplasticity Laboratory award to Rice University, the Maurin Fund for research in cognitive psychology to the Department of Psychological Sciences at Rice University, a Rice University Social Sciences Research Institute Dissertation Research Improvement Grant (QY), and a Dissertation Fellowship in the Cognitive and Neural Foundations of Language from the William Orr Dingwall Foundation (QY).

ACKNOWLEDGMENTS

We acknowledge the Core for Advanced MRI (CAMRI) at Baylor College of Medicine for assistance with imaging data collection.

SUPPLEMENTARY MATERIAL

The Supplementary Material for this article can be found online at: https://www.frontiersin.org/articles/10.3389/fnhum.2022.890483/full#supplementary-material.

REFERENCES

Allen, B., and Becker, M. (2015). *Learning Alternations From Surface Forms With Sublexical Phonology*. Available online at: http://ling.auf.net/lingbuzz/002503/current.pdf.

Auther, L. L., Wertz, R. T., Miller, T. A., and Kirshner, H. S. (2000). Relationships among the mismatch negativity (MMN) response, auditory comprehension and site of lesion in aphasic adults. *Aphasiology* 14, 461–470. doi: 10.1080/026870300401243

Awh, E., Jonides, J., Smith, E. E., Schumacher, E. H., Koeppe, R. A., Katz, S., et al. (1996). Dissociation of storage and rehearsal in verbal working memory: evidence from positron emission tomography. *Psychol. Sci.* 7, 25–31. doi: 10.1111/j.1467-9280.1996.tb00662.x

Baddeley, A., Hitch, G., and Allen, R. (2021). "A multicomponent model of working memory," in *Working Memory: State of the Science*, eds R. H. Logie, V. Camos and N. Cowan (Oxford, United Kingdom: Oxford University Press), 10–43.

Baldo, J. V., and Dronkers, N. F. (2006). The role of inferior parietal and inferior frontal cortex in working memory. *Neuropsychology* 20, 529–538. doi: 10.1037/0894-4105.20.5.529

Baldo, J. V., Katseff, S., and Dronkers, N. F. (2012). Brain regions underlying repetition and auditory-verbal short-term memory deficits in aphasia: evidence from voxel-based lesion symptom mapping. *Aphasiology* 26, 338–354. doi: 10.1080/02687038.2011.602391

Barbosa, J. (2017). Working memories are maintained in a stable code. *J. Neurosci.* 37, 8309–8311. doi: 10.1523/JNEUROSCI.1547-17.2017

Barrouillet, P., Bernardin, S., and Camos, V. (2004). Time constraints and resource sharing in adults' working memory spans. *J. Exp. Psychol. Gen.* 133, 83–100. doi: 10.1037/0096-3445.133.1.83

Barrouillet, P., Portrat, S., and Camos, V. (2011). On the law relating processing to storage in working memory. *Psychol. Rev.* 118, 175–192. doi: 10.1037/a0022324

Bettencourt, K. C., and Xu, Y. (2016). Decoding the content of visual short-term memory under distraction in occipital and parietal areas. *Nat. Neurosci.* 19, 150–157. doi: 10.1038/nn.4174

Bonte, M., Hausfeld, L., Scharke, W., Valente, G., and Formisano, E. (2014). Task-dependent decoding of speaker and vowel identity from auditory cortical response patterns. *J. Neurosci.* 34, 4548–4557. doi: 10.1523/JNEUROSCI.4339-13.2014

Brown, J. (1958). Some tests of the decay theory of immediate memory. *Q. J. Exp. Psychol.* 10, 12–21.

Buchsbaum, B. R., and D'Esposito, M. (2008). The search for the phonological store: from loop to convolution. *J. Cogn. Neurosci.* 20, 762–778. doi: 10.1162/jocn.2008.20501

Cattaneo, Z., Vecchi, T., Pascual-Leone, A., and Silvanto, J. (2009). Contrasting early visual cortical activation states causally involved in visual imagery and short-term memory. *Eur. J. Neurosci.* 30, 1393–1400. doi: 10.1111/j.1460-9568.2009.06911.x

Chein, J. M., and Fiez, J. A. (2001). Dissociation of verbal working memory system components using a delayed serial recall task. *Cereb. Cortex* 11, 1003–1014. doi: 10.1093/cercor/11.11.1003

Chein, J. M., and Fiez, J. A. (2010). Evaluating models of working memory through the effects of concurrent irrelevant information. *J. Exp. Psychol. Gen.* 139, 117–137. doi: 10.1037/a0018200

Christophel, T. B., Klink, P. C., Spitzer, B., Roelfsema, P. R., and Haynes, J.-D. (2017). The distributed nature of working memory. *Trends Cogn. Sci.* 21, 111–124. doi: 10.1016/j.tics.2016.12.007

Church, J. A., Balota, D. A., Petersen, S. E., and Schlaggar, B. L. (2011). Manipulation of length and lexicality localizes the functional neuroanatomy of phonological processing in adult readers. *J. Cogn. Neurosci.* 23, 1475–1493. doi: 10.1162/jocn.2010.21515

Cogan, G. B., Iyer, A., Melloni, L., Thesen, T., Friedman, D., Doyle, W., et al. (2017). Manipulating stored phonological input during verbal working memory. *Nat. Neurosci.* 20, 279–286. doi: 10.1038/nn.4459

Cohen, L. G., Celnik, P., Pascual-Leone, A., Corwell, B., Falz, L., Dambrosia, J., et al. (1997). Functional relevance of cross-modal plasticity in blind humans. *Nature* 389, 180–183. doi: 10.1038/38278

Constantinidis, C., and Klingberg, T. (2016). The neuroscience of working memory capacity and training. *Nat. Rev. Neurosci.* 17, 438–449. doi: 10.1038/nrn.2016.43

Corman, C. D., and Wickens, D. D. (1968). Retroactive inhibition in short-term memory. *J. Verb. Learn. Verb. Behav.* 7, 16–19.

Cowan, N., Morey, C. C., and Naveh-Benjamin, M. (2021). "An embedded-processes approach to working memory: how is it distinct from other approaches and to what ends?," in *Working Memory: State of the Science*, eds R. H. Logie, V. Camos, and N. Cowan (Oxford, United Kingdom: Oxford University Press), 44–84.

Cox, R. W. (1996). AFNI: software for analysis and visualization of functional magnetic resonance neuroimages. *Comput. Biomed. Res.* 29, 162–173. doi: 10.1006/cbmr.1996.0014

Cox, R. W., Chen, G., Glen, D. R., Reynolds, R. C., and Taylor, P. A. (2017). FMRI clustering in AFNI: false-positive rates redux. *Brain Connect.* 7, 152–171. doi: 10.1089/brain.2016.0475

Crowder, R. G. (1967). Short-term memory for words with a perceptual-motor interpolated activity. *J. Verb. Learn. Verb. Behav.* 6, 753–761. doi: 10.1016/S0022-5371(67)80081-1

Crowder, R. G. (1976). *Principles of Learning and Memory*. Hillsdale, NJ: Lawrence Erlbaum Associates, Inc.

Deschamps, I., Baum, S. R., and Gracco, V. L. (2014). On the role of the supramarginal gyrus in phonological processing and verbal working memory: evidence from rTMS studies. *Neuropsychologia* 53, 39–46. doi: 10.1016/j.neuropsychologia.2013.10.015

Desmond, J. E., Chen, S. H. A., and Shieh, P. B. (2005). Cerebellar transcranial magnetic stimulation impairs verbal working memory. *Ann. Neurol.* 58, 553–560. doi: 10.1002/ana.20604

Diedrichsen, J., and Kriegeskorte, N. (2017). Representational models: a common framework for understanding encoding, pattern-component and representational-similarity analysis. *PLoS Comput. Biol.* 13:e1005508. doi: 10.1371/journal.pcbi.1005508

Dillon, R. F., and Reid, L. S. (1969). Short-term memory as a function of information processing during the retention interval. *J. Exp. Psychol.* 81, 261–269. doi: 10.1037/h0027769

Edin, F., Klingberg, T., Johansson, P., McNab, F., Tegnér, J., and Compte, A. (2009). Mechanism for top-down control of working memory capacity. *Proc. Natl. Acad. Sci. U S A* 106, 6802–6807. doi: 10.1073/pnas.0901894106

Fan, Y., Han, Q., Guo, S., and Luo, H. (2021). Distinct neural representations of content and ordinal structure in auditory sequence memory. *J. Neurosci.* 41, 6290–6303. doi: 10.1523/JNEUROSCI.0320-21.2021

Fischl, B., van der Kouwe, A., Destrieux, C., Halgren, E., Ségonne, F., Salat, D. H., et al. (2004). Automatically parcellating the human cerebral cortex. *Cereb. Cortex* 14, 11–22. doi: 10.1093/cercor/bhg087

Formisano, E., De Martino, F., Bonte, M., and Goebel, R. (2008). "Who" is saying "what?" Brain-based decoding of human voice and speech. *Science* 322, 970–973. doi: 10.1126/science.1164318

Gupta, P. (2003). Examining the relationship between word learning, nonword repetition and immediate serial recall in adults. *Q. J. Exp. Psychol. A.* 56, 1213–1236. doi: 10.1080/02724980343000071

Hallett, M. (2007). Transcranial magnetic stimulation: a primer. *Neuron* 55, 187–199. doi: 10.1016/j.neuron.2007.06.026

Hartwigsen, G. (2015). The neurophysiology of language: insights from non-invasive brain stimulation in the healthy human brain. *Brain Lang.* 148, 81–94. doi: 10.1016/j.bandl.2014.10.007

Hartwigsen, G., Baumgaertner, A., Price, C. J., Koehnke, M., Ulmer, S., Siebner, H. R., et al. (2010). Phonological decisions require both the left and right supramarginal gyri. *Proc. Natl. Acad. Sci. U S A* 107, 16494–16499. doi: 10.1073/pnas.1008121107

Haxby, J. V., Gobbini, M. I., Furey, M. L., Ishai, A., Schouten, J. L., Pietrini, P., et al. (2001). Distributed and overlapping representations of faces and objects in ventral temporal cortex. *Science* 293, 2425–2430. doi: 10.1126/science.1063736

Hayes, B. (2008). *Introductory Phonology*. Hoboken, NJ: Wiley-Blackwell.

Jacquemot, C., Pallier, C., LeBihan, D., Dehaene, S., and Dupoux, E. (2003). Phonological grammar shapes the auditory cortex: a functional magnetic resonance imaging study. *J. Neurosci.* 23, 9541–9546. doi: 10.1523/JNEUROSCI.23-29-09541.2003

Jones, D. M., and Macken, W. J. (1993). Irrelevant tones produce an irrelevant speech effect: implications for phonological coding in working memory. *J. Exp. Psychol. Learn. Mem. Cogn.* 19, 369–381. doi: 10.1037/0278-7393.19.2.369

Jones, D. M., and Macken, W. J. (1995). Phonological similarity in the irrelevant speech effect: within- or between-stream similarity? *J. Exp. Psychol. Learn. Mem. Cogn.* 21, 103–115. doi: 10.1037/0278-7393.21.1.103

Jonides, J., Lacey, S. C., and Nee, D. E. (2005). Processes of working memory in mind and brain. *Curr. Dir. Psychol. Sci.* 14, 2–5. doi: 10.1111/j.0963-7214.2005.00323.x

Kowialiewski, B., Lemaire, B., Majerus, S., and Portrat, S. (2021). Can activated long-term memory maintain serial order information? *Psychon. Bull. Rev.* 28, 1301–1312. doi: 10.3758/s13423-021-01902-3

Kriegeskorte, N., Mur, M., and Bandettini, P. (2008). Representational similarity analysis - connecting the branches of systems neuroscience. *Front. Syst. Neurosci.* 2:4. doi: 10.3389/neuro.06.004.2008

Landauer, T. K. (1974). Consolidation in human memory: retrograde amnestic effects of confusable items in paired-associate learning. *J. Verb. Learn. Verb. Behav.* 13, 45–53. doi: 10.1016/S0022-5371(74)80029-0

Leff, A. P., Schofield, T. M., Crinion, J. T., Seghier, M. L., Grogan, A., Green, D. W., et al. (2009). The left superior temporal gyrus is a shared substrate for auditory short-term memory and speech comprehension: evidence from 210 patients with stroke. *Brain* 132, 3401–3410. doi: 10.1093/brain/awp273

Lemaire, B., Heuer, C., and Portrat, S. (2021). Modeling articulatory rehearsal in an attention-based model of working memory. *Cogn. Comput.* 13, 49–68. doi: 10.1007/s12559-020-09791-9

Lorenc, E. S., Mallett, R., and Lewis-Peacock, J. A. (2021). Distraction in visual working memory: resistance is not futile. *Trends Cogn. Sci.* 25, 228–239. doi: 10.1016/j.tics.2020.12.004

Lorenc, E. S., Sreenivasan, K. K., Nee, D. E., Vandenbroucke, A. R. E., and D'Esposito, M. (2018). Flexible coding of visual working memory representations during distraction. *J. Neurosci.* 38, 5267–5276. doi: 10.1523/JNEUROSCI.3061-17.2018

Majerus, S. (2013). Language repetition and short-term memory: an integrative framework. *Front. Hum. Neurosci.* 7:357. doi: 10.3389/fnhum.2013.00357

Martin, R. C. (2005). Components of short-term memory and their relation to language processing: evidence from neuropsychology and neuroimaging. *Curr. Dir. Psychol. Sci.* 14, 204–208. doi: 10.1111/j.0963-7214.2005.00365.x

Martin, R. C., Ding, J., Hamilton, A. C., and Schnur, T. T. (2021a). Working memory capacities neurally dissociate: evidence from acute stroke. *Cereb. Cortex Commun.* 2:tgab005. doi: 10.1093/texcom/tgab005

Martin, R. C., Rapp, B., and Purcell, J. (2021b). "Domain-specific working memory: perspectives from cognitive neuropsychology," in *Working Memory: State of the Science*, eds R. H. Logie, V. Camos, and N. Cowan (New York, NY: Oxford University Press), 235–281.

Martin, R. C., Lesch, M. F., and Bartha, M. C. (1999). Independence of input and output phonology in word processing and short-term memory. *J. Mem. Lang.* 41, 3–29. doi: 10.1006/jmla.1999.2637

Murakami, T., Kell, C. A., Restle, J., Ugawa, Y., and Ziemann, U. (2015). Left dorsal speech stream components and their contribution to phonological processing. *J. Neurosci.* 35, 1411–1422. doi: 10.1523/JNEUROSCI.0246-14.2015

Murray, J. D., Bernacchia, A., Roy, N. A., Constantinidis, C., Romo, R., and Wang, X.-J. (2017). Stable population coding for working memory coexists with heterogeneous neural dynamics in prefrontal cortex. *Proc. Natl. Acad. Sci. U S A* 114, 394–399. doi: 10.1073/pnas.1619449114

Nairne, J. S. (1990). A feature model of immediate memory. *Mem. Cognit.* 18, 251–269. doi: 10.3758/bf03213879

Naselaris, T., and Kay, K. N. (2015). Resolving ambiguities of MVPA using explicit models of representation. *Trends Cogn. Sci.* 19, 551–554. doi: 10.1016/j.tics.2015.07.005

Neath, I. (2000). Modeling the effects of irrelevant speech on memory. *Psychon. Bull. Rev.* 7, 403–423. doi: 10.3758/bf03214356

Nili, H., Wingfield, C., Walther, A., Su, L., Marslen-Wilson, W., and Kriegeskorte, N. (2014). A toolbox for representational similarity analysis. *PLoS Comput. Biol.* 10:e1003553. doi: 10.1371/journal.pcbi.1003553

Oberauer, K. (2019). Is rehearsal an effective maintenance strategy for working memory? *Trends Cogn. Sci.* 23, 798–809. doi: 10.1016/j.tics.2019.06.002

Oberauer, K., and Lange, E. B. (2008). Interference in verbal working memory: distinguishing similarity-based confusion, feature overwriting and feature migration. *J. Mem. Lang.* 58, 730–745. doi: 10.1016/j.jml.2007.09.006

Oberauer, K., and Lange, E. B. (2009). Activation and binding in verbal working memory: a dual-process model for the recognition of nonwords. *Cogn. Psychol.* 58, 102–136. doi: 10.1016/j.cogpsych.2008.05.003

Oliveri, M., Turriziani, P., Carlesimo, G. A., Koch, G., Tomaiuolo, F., Panella, M., et al. (2001). Parieto-frontal interactions in visual-object and visual-spatial working memory: evidence from transcranial magnetic stimulation. *Cereb. Cortex* 11, 606–618. doi: 10.1093/cercor/11.7.606

Oosterhof, N. N., Connolly, A. C., and Haxby, J. V. (2016). CoSMoMVPA: multi-modal multivariate pattern analysis of neuroimaging data in Matlab/GNU Octave. *Front. Neuroinform.* 10:27. doi: 10.3389/fninf.2016.00027

Pascual-Leone, A., Bartres-Faz, D., and Keenan, J. P. (1999). Transcranial magnetic stimulation: studying the brain-behaviour relationship by induction of 'virtual lesions'. *Philos. Trans. R. Soc. Lond. B. Biol. Sci.* 354, 1229–1238. doi: 10.1098/rstb.1999.0476

Paulesu, E., Frith, C. D., and Frackowiak, R. S. (1993). The neural correlates of the verbal component of working memory. *Nature* 362, 342–345. doi: 10.1038/362342a0

Paulesu, E., Shallice, T., Danelli, L., Sberna, M., Frackowiak, R. S. J., and Frith, C. D. (2017). Anatomical modularity of verbal working memory? Functional anatomical evidence from a famous patient with short-term memory deficits. *Front. Hum. Neurosci.* 11:231. doi: 10.3389/fnhum.2017.00231

Peterson, L. R. (1969). Concurrent verbal activity. *Psychol. Rev.* 76, 376–386.

Peterson, L., and Peterson, M. J. (1959). Short-term retention of individual verbal items. *J. Exp. Psychol.* 58, 193–198. doi: 10.1037/h0049234

Pitcher, D., Parkin, B., and Walsh, V. (2021). Transcranial magnetic stimulation and the understanding of behavior. *Annu. Rev. Psychol.* 72, 97–121. doi: 10.1146/annurev-psych-081120-013144

Popal, H., Wang, Y., and Olson, I. R. (2019). A guide to representational similarity analysis for social neuroscience. *Soc. Cogn. Affect. Neurosci* 14, 1243–1253. doi: 10.1093/scan/nsz099

Posner, M. I., and Rossman, E. (1965). Effect of size and location of informational transforms upon short-term retention. *J. Exp. Psychol.* 70, 496–505. doi: 10.1037/h0022545

Postle, B. R. (2006). Working memory as an emergent property of the mind and brain. *Neuroscience* 139, 23–38. doi: 10.1016/j.neuroscience.2005.06.005

Price, C. J. (2012). A review and synthesis of the first 20 years of PET and fMRI studies of heard speech, spoken language and reading. *Neuroimage* 62, 816–847. doi: 10.1016/j.neuroimage.2012.04.062

Pulvermüller, F., Kujala, T., Shtyrov, Y., Simola, J., Tiitinen, H., Alku, P., et al. (2001). Memory traces for words as revealed by the mismatch negativity. *Neuroimage* 14, 607–616. doi: 10.1006/nimg.2001.0864

Purcell, J., Rapp, B., and Martin, R. C. (2021). Distinct neural substrates support phonological and orthographic working memory: Implications for theories of working memory. *Front. Neurol.* 12:681141. doi: 10.3389/fneur.2021.681141

Rademaker, R. L., van de Ven, V. G., Tong, F., and Sack, A. T. (2017). The impact of early visual cortex transcranial magnetic stimulation on visual working memory precision and guess rate. *PLoS One* 12:e0175230. doi: 10.1371/journal.pone.0175230

Ramos-Nuñez, A. I., Yue, Q., Pasalar, S., and Martin, R. C. (2020). The role of left vs. right superior temporal gyrus in speech perception: an fMRI-guided TMS study. *Brain Lang.* 209:104838. doi: 10.1016/j.bandl.2020.104838

Ravizza, S. M., Hazeltine, E., Ruiz, S., and Zhu, D. C. (2011). Left TPJ activity in verbal working memory: implications for storage- and sensory-specific models of short term memory. *Neuroimage* 55, 1836–1846. doi: 10.1016/j.neuroimage.2010.12.021

Romero, L., Walsh, V., and Papagno, C. (2006). The neural correlates of phonological short-term memory: a repetitive transcranial magnetic stimulation study. *J Cogn. Neurosci.* 18, 1147–1155. doi: 10.1162/jocn.2006.18.7.1147

Roodenrys, S., Miller, L. M., and Josifovski, N. (2022). Phonemic interference in short-term memory contributes to forgetting but is not due to overwriting. *J. Mem. Lang.* 122:104301. doi: 10.1016/j.jml.2021.104301

Saint-Amour, D., De Sanctis, P., Molholm, S., Ritter, W., and Foxe, J. J. (2007). Seeing voices: high-density electrical mapping and source-analysis of the multisensory mismatch negativity evoked during the McGurk illusion. *Neuropsychologia* 45, 587–597. doi: 10.1016/j.neuropsychologia.2006.03.036

Salmon, E., Van der Linden, M., Collette, F., Delfiore, G., Maquet, P., Degueldre, C., et al. (1996). Regional brain activity during working memory tasks. *Brain* 119, 1617–1625. doi: 10.1093/brain/119.5.1617

Shergill, S. S., Brammer, M. J., Fukuda, R., Bullmore, E., Amaro, E., Murray, R. M., et al. (2002). Modulation of activity in temporal cortex during generation of inner speech. *Hum. Brain Mapp.* 16, 219–227. doi: 10.1002/hbm.10046

Shoup, J. E. (1980). "Phonological Aspects of Speech Recognition," in *Trends in Speech Recognition*, eds W. A. Lea (Englewood Cliffs, NJ: Prentice-Hall), 125–138.

Sliwinska, M. W., James, A., and Devlin, J. T. (2015). Inferior parietal lobule contributions to visual word recognition. *J Cogn. Neurosci.* 27, 593–604. doi: 10.1162/jocn_a_00721

Souza, A. S., and Oberauer, K. (2018). Does articulatory rehearsal help immediate serial recall? *Cogn. Psychol.* 107, 1–21. doi: 10.1016/j.cogpsych.2018.09.002

Souza, A. S., and Oberauer, K. (2020). No evidence that articulatory rehearsal improves complex span performance. *J. Cogn.* 3:11. doi: 10.5334/joc.103

Spaak, E., Watanabe, K., Funahashi, S., and Stokes, M. G. (2017). Stable and dynamic coding for working memory in primate prefrontal cortex. *J. Neurosci.* 37, 6503–6516. doi: 10.1523/JNEUROSCI.3364-16.2017

Sreenivasan, K. K., and D'Esposito, M. (2019). The what, where and how of delay activity. *Nat. Rev. Neurosci.* 20, 466–481. doi: 10.1038/s41583-019-0176-7

Sreenivasan, K. K., Curtis, C. E., and D'Esposito, M. (2014). Revisiting the role of persistent neural activity during working memory. *Trends Cogn. Sci.* 18, 82–89. doi: 10.1016/j.tics.2013.12.001

Stoeckel, C., Gough, P. M., Watkins, K. E., and Devlin, J. T. (2009). Supramarginal gyrus involvement in visual word recognition. *Cortex* 45, 1091–1096. doi: 10.1016/j.cortex.2008.12.004

Talairach, J., and Tournoux, P. (1988). *Co-Planar Stereotaxic Atlas of the Human Brain: 3-Dimensional Approach System: an Approach to Cerebral Imaging*. New York, NY: Theime Medical.

Tervaniemi, M., Medvedev, S. V., Alho, K., Pakhomov, S. V., Roudas, M. S., van Zuijen, T. L., et al. (2000). Lateralized automatic auditory processing of phonetic versus musical information: a PET study. *Hum. Brain Mapp.* 10, 74–79. doi: 10.1002/(SICI)1097-0193(200006)10:2<<74::AID-HBM30>>3.0.CO;2-2

Townsend, J. T., and Ashby, F. G. (1983). *Stochastic Modeling of Elementary Psychological Processes*. New York, NY: Cambridge University Press.

Turkeltaub, P. E., and Coslett, H. B. (2010). Localization of sublexical speech perception components. *Brain Lang.* 114, 1–15. doi: 10.1016/j.bandl.2010.03.008

Valero-Cabré, A., Amengual, J. L., Stengel, C., Pascual-Leone, A., and Coubard, O. A. (2017). Transcranial magnetic stimulation in basic and clinical neuroscience: a comprehensive review of fundamental principles and novel insights. *Neurosci. Biobehav. Rev.* 83, 381–404. doi: 10.1016/j.neubiorev.2017.10.006

van de Ven, V., and Sack, A. T. (2013). Transcranial magnetic stimulation of visual cortex in memory: cortical state, interference and reactivation of visual content in memory. *Behav. Brain Res.* 236, 67–77. doi: 10.1016/j.bbr.2012.08.001

van de Ven, V., Jacobs, C., and Sack, A. T. (2012). Topographic contribution of early visual cortex to short-term memory consolidation: a transcranial magnetic stimulation study. *J. Neurosci.* 32, 4–11. doi: 10.1523/JNEUROSCI.3261-11.2012

van Lamsweerde, A. E., and Johnson, J. S. (2017). Assessing the effect of early visual cortex transcranial magnetic stimulation on working memory consolidation. *J. Cogn. Neurosci.* 29, 1226–1238. doi: 10.1162/jocn_a_01113

Vogel, E. K., Woodman, G. F., and Luck, S. J. (2006). The time course of consolidation in visual working memory. *J. Exp. Psychol. Hum. Percept Perform.* 32, 1436–1451. doi: 10.1037/0096-1523.32.6.1436

Wickelgren, W. A. (1965). Acoustic similarity and retroactive interference in short-term memory. *J. Verb. Learn. Verb. Behav.* 4, 53–61. doi: 10.1016/S0022-5371(65)80067-6

Xu, Y. (2017). Reevaluating the sensory account of visual working memory storage. *Trends Cogn. Sci.* 21, 794–815. doi: 10.1016/j.tics.2017.06.013

Xu, Y. (2018). Sensory cortex is nonessential in working memory storage. *Trends Cogn. Sci.* 22, 192–193. doi: 10.1016/j.tics.2017.12.008

Yi, H. G., Leonard, M. K., and Chang, E. F. (2019). The encoding of speech sounds in the superior temporal gyrus. *Neuron* 102, 1096–1110. doi: 10.1016/j.neuron.2019.04.023

Yue, Q., and Martin, R. C. (2021). Maintaining verbal short-term memory representations in non-perceptual parietal regions. *Cortex* 138, 72–89. doi: 10.1016/j.cortex.2021.01.020

Yue, Q., Martin, R. C., Hamilton, A. C., and Rose, N. S. (2019). Non-perceptual regions in the left inferior parietal lobe support phonological short-term memory: evidence for a buffer account? *Cereb. Cortex* 29, 1398–1413. doi: 10.1093/cercor/bhy037

Conflict of Interest: The authors declare that the research was conducted in the absence of any commercial or financial relationships that could be construed as a potential conflict of interest.

Publisher's Note: All claims expressed in this article are solely those of the authors and do not necessarily represent those of their affiliated organizations, or those of the publisher, the editors and the reviewers. Any product that may be evaluated in this article, or claim that may be made by its manufacturer, is not guaranteed or endorsed by the publisher.

frontiers | Frontiers in Human Neuroscience

ORIGINAL RESEARCH
published: 24 June 2022
doi: 10.3389/fnhum.2022.920538

Accounting for Stimulations That Do Not Elicit Motor-Evoked Potentials When Mapping Cortical Representations of Multiple Muscles

Fang Jin[1,2], *Sjoerd M. Bruijn*[1,2] *and Andreas Daffertshofer*[1,2]*

[1] *Department of Human Movement Sciences, Faculty of Behavioural and Movement Sciences, Vrije Universiteit Amsterdam, Amsterdam, Netherlands,* [2] *Faculty of Behavioural and Movement Sciences, Institute Brain and Behavior Amsterdam, Vrije Universiteit Amsterdam, Amsterdam, Netherlands*

The representation of muscles in the cortex can be mapped using navigated transcranial magnetic stimulation. The commonly employed measure to quantify the mapping are the center of gravity or the centroid of the region of excitability as well as its size. Determining these measures typically relies only on stimulation points that yield motor-evoked potentials (MEPs); stimulations that do not elicit an MEP, i.e., non-MEP points, are ignored entirely. In this study, we show how incorporating non-MEP points may affect the estimates of the size and centroid of the excitable area in eight hand and forearm muscles after mono-phasic single-pulse TMS. We performed test-retest assessments in twenty participants and estimated the reliability of centroids and sizes of the corresponding areas using inter-class correlation coefficients. For most muscles, the reliability turned out good. As expected, removing the non-MEP points significantly decreased area sizes and area weights, suggesting that conventional approaches that do not account for non-MEP points are likely to overestimate the regions of excitability.

Keywords: TMS, motor evoked potential (MEP), muscle mapping, cortical representation, primary motor cortex (M1)

OPEN ACCESS

Edited by:
Thomas R. Knösche, Max Planck Institute for Human Cognitive and Brain Sciences, Germany

Reviewed by:
Mitsuaki Takemi, The University of Tokyo, Japan
Anders Korshoej, Aarhus University Hospital, Denmark

***Correspondence:**
Andreas Daffertshofer
a.daffertshofer@vu.nl

Specialty section:
This article was submitted to Brain Imaging and Stimulation, a section of the journal Frontiers in Human Neuroscience

Received: *14 April 2022*
Accepted: *31 May 2022*
Published: *24 June 2022*

Citation:
Jin F, Bruijn SM and Daffertshofer A (2022) Accounting for Stimulations That Do Not Elicit Motor-Evoked Potentials When Mapping Cortical Representations of Multiple Muscles. Front. Hum. Neurosci. 16:920538. doi: 10.3389/fnhum.2022.920538

INTRODUCTION

Single-pulse transcranial magnetic stimulation (TMS) is a non-invasive and painless technique that monitors neurophysiological alterations of the human motor cortex (Barker et al., 1985; Schambra et al., 2003). A TMS coil discharge at suitable intensity will induce transient currents and cause depolarization of axons of nerve cells (Rossini et al., 2015). When applied over the motor cortex, this can elicit a motor-evoked potential (MEP) that can be recorded in contralateral target muscles using conventional electromyography (EMG). Amplitudes and latencies of the MEPs reveal the excitability and conduction times of the cortical-spinal tract. Both have been conceived as valid outcomes of TMS motor mapping (Rossini et al., 1994). Neuroscientists and physicians alike utilized TMS motor mapping to evaluate muscle synergies and motor cortical plasticity (Siebner and Rothwell, 2003), to plan brain tumor surgery (Krieg et al., 2012), or to follow recovery after stroke (Mark et al., 2006; Sondergaard et al., 2021). There is ample evidence that the location at

which TMS elicits the maximum MEP is particularly close to the location found using direct cortical stimulation, which is considered the gold standard in motor mapping. The localization clearly outperforms other modalities like magnetoencephalography (Tarapore et al., 2012) or functional magnetic resonance imaging (Forster et al., 2011).

TMS combined with neuro-navigation increases mapping accuracy (Krieg et al., 2017). A popular approach for coil positioning is a pseudo-random walk. Delivering stimulations at random locations roughly evenly spaced over the motor cortex is more efficient and potentially more accurate than time-consuming, course-grained grid-based positioning. Likely, this random placement will also elicit MEPs in muscles other than the target muscle. Often considered a confounder, this is—in fact—particularly useful when multiple muscles are being evaluated, presuming that the muscles have similar resting motor thresholds (Krieg et al., 2017) and close-by cortical representations (Schieber, 2001). Very recently, Tardelli et al. (2021) used the pseudo-random walk method to assess the cortical representation of abductor digiti minimi, flexor carpi radialis, and flexor pollicis brevis. As a rule of thumb: the more muscles are measured simultaneously, the more efficient assessments *via* pseudo-random coil positioning can be.

Irrespective of the experimental protocol, navigated TMS derived cortical map outcomes should have good reliability (Novikov et al., 2018). Nonetheless, "even most commonly used outcomes such as areas, volumes, the location of centers of gravity (CoGs), and hotspots have (hardly) been validated for being reliable measures in test-retest studies (Kraus and Gharabaghi, 2016)." We slightly modified this quote from Novikov et al. (2018), because they and other likewise recent reports did indeed test for the reliability of navigated TMS outcomes considered in the respective studies. For instance, Nazarova et al. (2021) evaluated the reliability of the CoG and the size of the area (volume) of excitability, next to the position of the MEP hotspot. In a grid-based approach, all measures displayed high relative but low absolute reliability, with the latter arguably reflecting between-subject variability.

The area of excitability can be defined as the cortical region within which TMS elicits an MEP. It is usually determined by projecting the focal point of the coil's magnetic field on a (re-)constructed spherical surface or volume and determining the resulting convex hull. State-of-the-art fine-tuning of this approach is to a priori concentrate on the cortical patch of interest. However, a mapping that agrees with the "real" anatomical structure generally provides better area estimates. This is particularly true when realizing that the gray matter border may have large curvatures along gyral ridges (Van Essen, 2004), where spherical approximations will be poor. We followed these lines and extracted subject-specific cortical surfaces at high resolution, projected the stimulation points to that surface and estimated the area spanned by the pair-wise shortest paths connecting the stimulation points. More importantly, we also projected the stimulation points where TMS did *not* elicit an MEP and removed these points from the estimated area. As will be shown, together these steps circumvent potential over-estimation of the area of excitability.

MATERIALS AND METHODS

Participants

Twenty healthy, right-handed volunteers (average age: 29.6 ± 7.5, eight females) participated in the study. Prior to the experiment, all participants were screened for contraindications of MRI and TMS through questionnaires (Rossi et al., 2011). All of them provided signed informed consent prior to joining the experimental sessions. The Edinburgh Handedness Inventory served to determine hand dominance (Oldfield, 1971). The study had been approved by the medical ethics committee of Amsterdam University Medical Center (VUmc, 018.213–NL65023.029.18).

Materials

Our set-up consisted of three devices: a TMS system, an EMG amplifier, and a neural navigation system. Single-pulse TMS was delivered by a Magstim 200[2] stimulator (Magstim Company Ltd., Whitland, Dyfed, United Kingdom) using a figure-of-eight coil with 70 mm windings. Eight bipolar EMG signals were recorded using a 16-channel EMG amplifier (Porti, TMSi, Oldenzaal, Netherlands) and continuously sampled at a rate of 2 kHz. The EMG recordings were triggered by the TMS to allow for online EMG assessments using a custom-made Labview-program with embedded Matlab functions (designed at our department using Labview 2016, National Instruments, Austin, TX, and Matlab 2018b, The MathWorks, Natick, MA). In brief, upon receiving a trigger, peak-to-peak amplitudes and latencies of MEPs were estimated from all EMG signals during the following 500 ms. These outcomes, as well as the original EMG signals (duration = 500 ms), were sent to the neural navigation system (Neural Navigator, Brain Science Tools, De Bilt, Netherlands)[1] for online monitoring and storage. The neural navigation software also stored the position and orientation of the coil with respect to the head.

Prior to running the TMS protocol, we acquired the participants' anatomical T1-weighted MRI (3 Tesla Philips Achieva System, Philips, Best, Netherlands; matrix size $256 \times 256 \times 211$, voxel size $1.0 \times 1.0 \times 1.0$ mm^3, TR/TE 6.40/2.94 ms). For online neuro-navigation, gray matter was segmented using SPM[2]; note that for offline analysis, we employed a more detailed segmentation *via* Freesurfer.[3]

We considered the first dorsal interosseous (FDI), abductor digiti minimi (ADM), abductor pollicis brevis (APB), flexor pollicis brevis (FPB), extensor digitorum communis (EDC), flexor digitorum superficialis (FDS), extensor carpi radialis (ECR), and flexor carpi radialis (FCR) muscles, which were measured using bipolar electrodes (Blue Sensor N-00-S, Ambu, Ballerup, Denmark), placed after cleaning the skin with alcohol (cf. **Figure 1**). The ground electrode was attached to the ulnar styloid process. We monitored and kept the electrode impedance below 5 k**Ω**. During the experiment, the orientation of the TMS coil was held 45 degrees to the sagittal plane, and tangential to the

[1] www.brainsciencetools.com

[2] https://www.fil.ion.ucl.ac.uk/spm/software/spm12/

[3] https://surfer.nmr.mgh.harvard.edu/fswiki

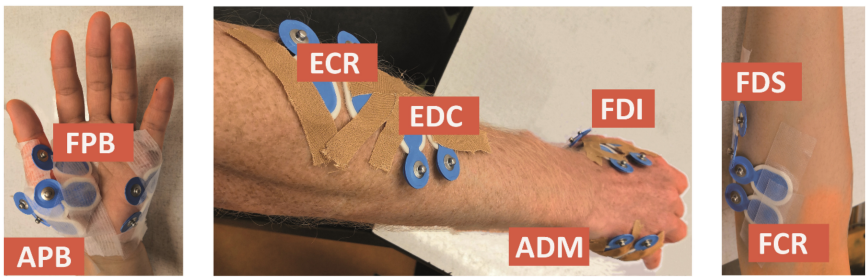

FIGURE 1 | Electrode placement for the first dorsal interosseous (FDI), abductor digiti minimi (ADM), abductor pollicis brevis (APB), flexor pollicis brevis (FPB), extensor digitorum communis (EDC), flexor digitorum superficialis (FDS), extensor carpi radialis (ECR), and flexor carpi radialis (FCR) muscles.

scalp. By this, we meant to induce currents in the cortex along the posterior-to-anterior direction. To control the TMS output, we used the Matlab-toolbox Rapid2.[4]

Experimental Procedures

Participants were seated comfortably in an armchair, relaxing muscles of hands and arms. The experiment consisted of two identical sessions, *Session 1* and *Session 2*. These sessions were separated by 1h and served to test for test-retest reliability of our outcomes. EMG electrodes were kept fixed to minimize placement errors. The interval of 1h was set to prevent drying of the conductive electrolyte gel.

In each session, we searched for the hotspot positions for FDI, EDC and FCR before testing the RMTs. First, the stimulation intensity was identified that yielded MEPs for all three muscles when stimulating in the omega-shaped area ("hand knob") of the precentral gyrus. We started at 45% of the maximum stimulator output and increased or decreased the intensity until a consistent MEP was present. Then, we performed thirty stimulations around the hand knob region along the precentral gyrus. From these stimulations, we determined the position with the largest peak-to-peak amplitude for every muscle and labeled that position as the hotspot. Next, the RMT for every muscle was determined at the muscle-specific hotspot as the minimum stimulator output at which peak-to-peak amplitudes exceeded 50 μV in five out of ten stimuli. This was followed by the actual mapping procedure.

The TMS coil was pseudo-randomly positioned such that stimulations covered the entire left precentral gyrus. We applied 120 stimulations (Cavaleri et al., 2017) and repeated this at three intensities: 105% RMT of FDI, EDC, and FCR, respectively. In total, we performed 360 stimulations in every session. We chose 105% RMT because previous studies suggested it to be the lowest possible intensity for upper limb muscles mapping (Krieg et al., 2017), thus leading to the least stimulation cross-talk. Finally, we estimated the hotspots of the other five muscles (ADM, APB, FPB, FDS, and ECR) and determined the respective RMTs.

Motor-Evoked Potentials Definition

We discriminated between TMS with and without eliciting MEPs, i.e., MEP and non-MEP points. MEPs were considered proper if their amplitude exceeded 20 times the EMG-baseline's standard deviation (defined over 100 ms prior to each stimulation). While on average these thresholds were [51, 51, 76, 63, 59, 55, 70, and 64] μV for FDI, ADM, APB, FPB, EDC, FDS, ECR, and FCR, respectively, the baseline's standard deviations differed substantially over the group rendering a subject-specific threshold definition appropriate—see **Supplementary Figure 2** for the corresponding boxplots and median values. Amplitudes were also required to stay below 10 mV (to exclude movement and cable artifacts) and the peak's latency had to fall within the range of 5–50 ms after stimulation. All other stimulations were marked as non-MEP points; see below under *Outcome measures* for further details.

Area Estimate

The area estimates were based on triangulated cortical surface meshes that we extracted using Freesurfer (see text footnote 3; version 7). We imported the meshes into Brainstorm (version 3)[5] to ease converting between world and subject-specific MRI coordinates. Next to the original meshes with about 230,000–340,000 vertices dependent on the participant, we also generated low-resolution version by downsampling the mesh to either 15,000 or 100,000 vertices. This enabled us to test for effects of surface resolution. In all cases, we assigned the Mindboggle anatomical atlas (version 6; see also Klein et al., 2017)[6] to select left primary motor cortex. The area construction consisted of four steps:

(i) Stimulation points were projected to the triangulated cortical surface mesh yielding a set of vertices as illustrated in **Figure 2** and further detailed under *Outcome measures*.
(ii) Vertices that did not fall in left primary motor cortex were excluded (label "precentral L" in the Mindboggle6 atlas).
(iii) We connected the vertices along their shortest connecting paths. In brief, we converted the mesh into a sparse, weighted graph. The edges of triangularization served as adjacencies that we weighted by the Euclidean distance between the corresponding vertices. Then, we searched for the shortest paths between all MEP points (Dijkstra, 1959). We repeated this iteratively for all points of the

[4]https://github.com/armanabraham/Rapid2

[5]https://neuroimage.usc.edu/brainstorm/

[6]https://mindboggle.info

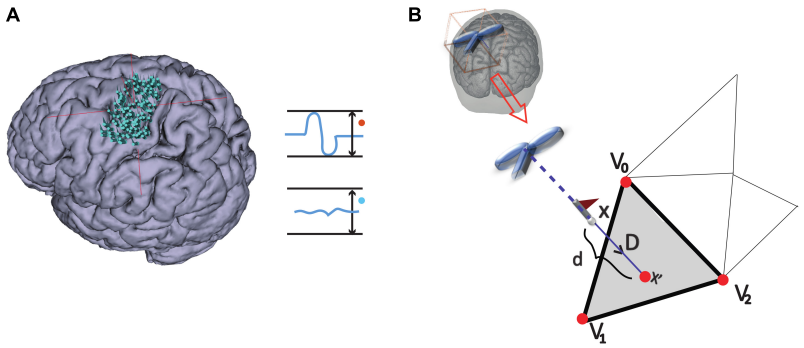

FIGURE 2 | MEP definition and point projection along the direction of coil orientation. **(A)** Stimulation points over the cortex that either elicited an MEP or not: MEP and non-MEP points, respectively. **(B)** The cortical surface nearest to a given stimulation location along the TMS coil orientation is represented by the gray triangle (step ii). The three vertices in the triangle are shown by the red points, while the flagged spots indicate the stimulation points.

connecting paths until no points were added. **Figure 3A** briefly summarizes this iteration. Further details can be found at github.[7]

(iv) Finally, we excluded the vertices (and triangles) corresponding to non-MEP points from the resulting area as sketched in **Figure 3B**. Note that if a triangle contained both, one or more stimulations that elicited a MEP and one or more stimulations that did not, we kept the triangle. By this we limited the risk of underestimation that may stem only from falsely considering stimulation points as non-MEP points.

By construction, removing non-MEP points will reduce the size of the active areas. To appreciate the benefits of non-MEP point removal, consider the case in which the true area of excitability has a non-convex boundary, e.g., if the area is U-shaped. Conventional estimates, in particular ones based on estimating the convex hull of the cloud of stimulation points, will clearly provide an overestimate of the excitable area. Rather than opting for non-convex hull estimates, we used a more general approach that also allows for removing points that are scattered across the area spanned by MEP points. We briefly illustrate this in **Figure 4** showing data of a single subject where isolated triangles that are being removed.

From here on, we refer to the reconstruction without accounting for non-MEP points as method M1, whilst the removal of non-MEP points will be method M2 (with examples in **Figures 4A,B**, respectively).

Outcome Measures

Most of the outcome measures were based on the MEP amplitudes and latencies. We quantified them for every TMS pulse and for every muscle using the original EMG signals, from which we removed the stimulation artifact *via* linear interpolation (−1 to +2 ms around stimulation) followed by high pass filtering at 10 Hz (2nd order, bi-directional Butterworth design). We defined the epoch −100 to −1 ms before the stimulus as a baseline and determined its mean value μ and the standard deviation σ. A peak in the interval 5–100 ms after the stimulus was considered an MEP if its value exceeded $\mu \pm 20\sigma$. Its latency was set as the first sample after the stimulus at which the signal exceeded $\mu + 2\sigma$ ($\mu - 2\sigma$) if the first peak is a maximum (minimum). Finally, we removed MEPs with peak-to-peak amplitude larger than 10 mV as we considered them artifacts. Except for the latter artifact definition, we opted for relative-to-baseline changes when identifying MEPs to circumvent between-subject variability in skin conductance; the choices for $\pm 20\sigma$ and $\pm 2\sigma$ were based on visually inspecting the EMG traces.

The stimulation points were mapped onto cortical surfaces given as triangulated meshes. The triangle of the surface mesh closest to a stimulation point along the direction of coil orientation was determined following the approach by Möller and Trumbore (1997) (see **Figure 2**). We assigned the vertices $\vec{v}_0$, $\vec{v}_1$, and $\vec{v}_2$ of the closest triangle the corresponding amplitude value, a. If two or more stimulations with an MEP shared a vertex, we averaged their amplitudes at the shared point. Since the total area of excitability possibly covered points that were not projected directly, we set all amplitude values *via* natural interpolation with C^1 continuity to $\hat{a}$; note that if interpolation was not needed, i.e., at the original vertices $\vec{v}_0$, $\vec{v}_1$, and $\vec{v}_2$, then $\hat{a} = a$. For every triangle we defined the length between their vertices as $\lambda_0 = \|\vec{v}_0 - \vec{v}_1\|$, $\lambda_1 = \|\vec{v}_1 - \vec{v}_2\|$ and $\lambda_2 = \|\vec{v}_2 - \vec{v}_0\|$, with $\|\cdots\|$ denoting the Euclidean distance between vertices. That is, given Cartesian coordinates $\vec{v}_i = (x_i, y_i, z_i)$, we used, e.g., $\lambda_0^2 = (x_0 - x_1)^2 + (y_0 - y_1)^2 + (z_0 - z_1)^2$.

The total area A of $k = 1, \ldots, M$ triangles weighted by the MEP amplitudes was computed *via* a slight modification of Heron's formula, namely the triangular prism, that reads:

$$A = \sum_{k=1}^{M} \bar{a}_k \sqrt{\Lambda_k \left(\Lambda_k - \lambda_{1,k}\right)\left(\Lambda_k - \lambda_{2,k}\right)\left(\Lambda_k - \lambda_{3,k}\right)}$$

$$\text{with } \Lambda_k = \frac{1}{2}\sum_{i=0}^{2} \lambda_{i,k} \tag{1}$$

[7]https://github.com/marlow17/surfaceanalysis

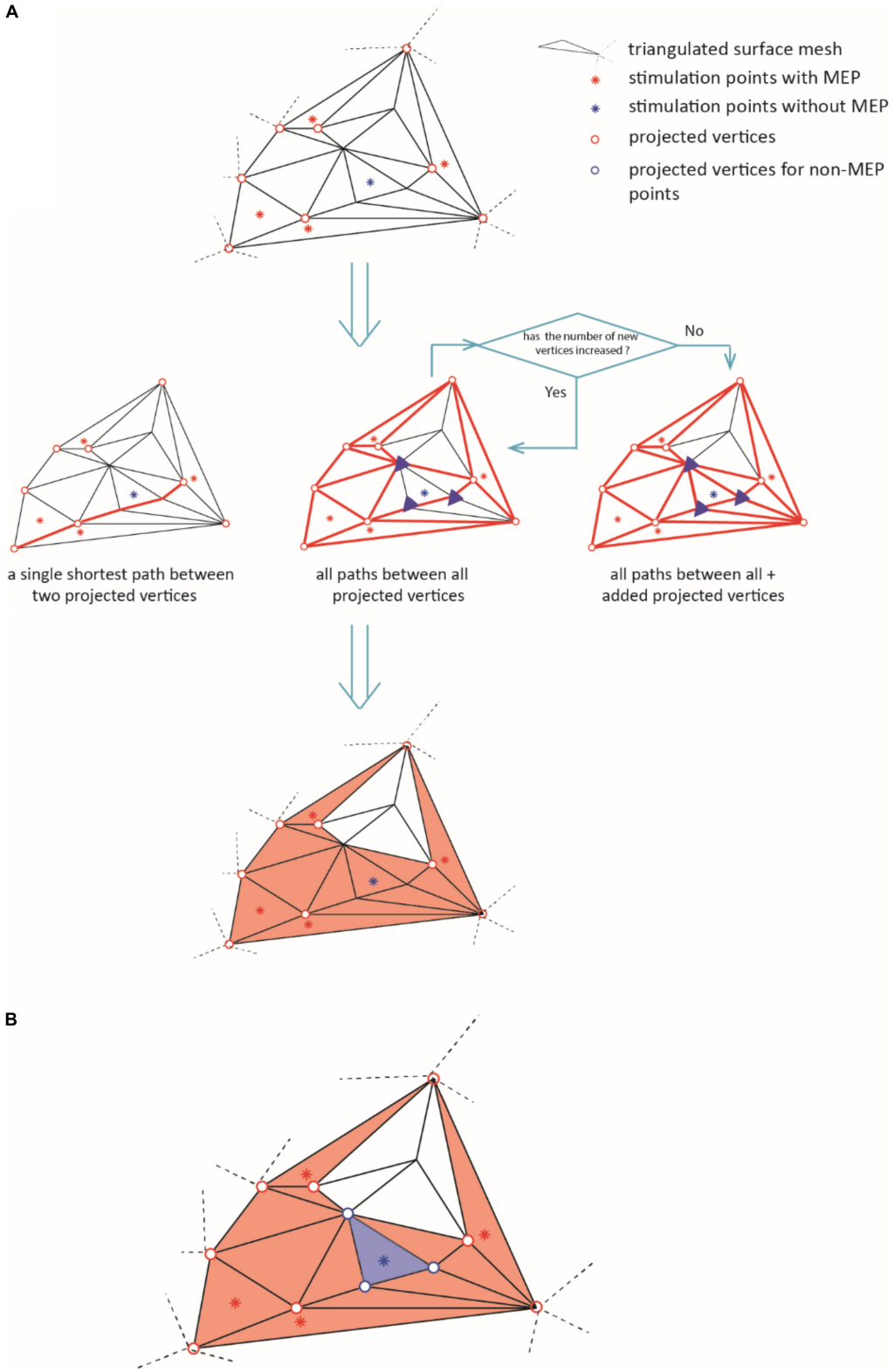

FIGURE 3 | The diagram illustrates the iteration for defining the area of excitability (step iii). In **(A)**, the red dots represent the active points and the blue dots the non-MEP one. Bold red lines indicate the shortest paths between the active points resulting in the orange shaded active area. **(B)** Removal of non-MEP points (step iv). The red dots represent the active points and the blue dots the non-MEP one. Bold lines indicate the shortest paths between the active points resulting in the orange shaded active area, and the blue background shows the (to-be-removed) non-active area.

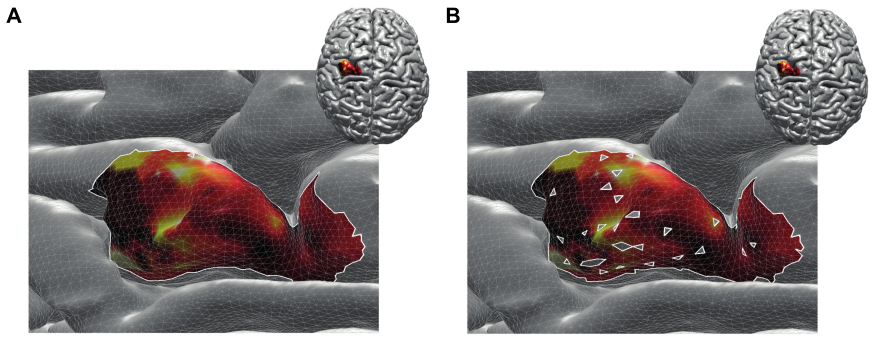

FIGURE 4 | Reconstructed active area in primary motor cortex given a set of stimulation points (orange dots). The color coding indicates the size of the MEP amplitude, with yellow being high and dark red being low. **(A)** Area without removing the non-MEP points (these points are marked in cyan); **(B)** area after removing the non-MEP points. By construction, the area shown in **(B)** is smaller than that in **(A)**. In both cases, the white lines represent an area's boundary; note that this boundary does not necessarily equal the area's convex hull, even when ignoring the non-MEP points **(A)**.

and $\overline{a}_k = \frac{1}{3}\sum_{i=0}^{2} \hat{a}_{i,k}$ being the mean value of (interpolated) MEP amplitudes at the three vertices of triangle k.

Given all $i = 1, \ldots, N$ area vertices, we further defined the centroid of the total area in line with the conventional form of the center of gravity (Opitz et al., 2014) as:

$$C = \begin{pmatrix} C_x \\ C_y \\ C_z \end{pmatrix} = \frac{1}{\sum_{i=1}^{N} \hat{a}_i} \sum_{i=1}^{N} \hat{a}_i \begin{pmatrix} x_i \\ y_i \\ z_i \end{pmatrix} \quad (2)$$

Statistics

We first estimated the reliability between Session 1 and Session 2 *via* the intraclass correlation coefficients (ICC) of the centroid (C), the weighted area size (A) for every muscle and intensity level. In more detail, we use a two-way mixed-effects model for single measurement type and estimated the absolute agreement, i.e., ICC (2,1) conform the Shrout and Fleiss convention (Koo and Li, 2016). We ran this analysis separately for the three representations of the cortex (i.e., three mesh resolutions) and for the three intensities. While the highest resolution for the intensity of 105% RMT of FCR will be reported below, all the other results can be found as **Supplementary Material**. There we also report the ICCs for centers of gravity (*CoG*) and for both the MEP amplitudes and the latencies.

To further confirm the absence of significant differences between Sessions 1 and 2, we performed a two-way ANOVA with repeated measures including factors of *intensity* and *session*. This also allowed for assessing effects of stimulation intensity. We applied a Bonferroni correction for multiple comparisons. Again, we restrict ourselves to reporting "only" the findings of the estimates at maximum resolution in the body text and refer to **Supplementary Material** for all other cases.

Finally, to assess effects of cortex mesh resolution and of ignoring/removing non-MEP stimulation points, we used a two-way repeated ANOVA with factors *method* and *resolution* (again with Bonferroni correction for multiple comparisons).

Prior to conducting the ANOVAs, sphericity was verified *via* Mauchly's test. A Greenhouse-Geisser correction was performed if necessary. Throughout hypothesis testing, we used a significance threshold of $\alpha = 0.05$. All statistical analyses were conducted using Matlab (The Mathworks Inc., Natwick MA, version 2020b).

RESULTS

All $N = 20$ participants completed the experimental procedure without adverse reactions. Of all mappings (subjects × muscle × intensity × session = 960, each containing 120 stimulations) 2% did not contain any valid MEP, and thus did not enter further analyses. In 11/320 (subjects × muscles × session) cases this was for 105% RMT of FDI, 5/320 for 105% RMT of EDC, and 1/320 for 105% RMT of FCR; see **Supplementary Table 1**). For five subjects, we could not detect any MEPs for ADM when using the second intensity in both sessions.

When averaged over participants and sessions, the RMTs were FDI: 44.90 ± 1.46%, ADM: 47.90 ± 1.64%, APB: 46.15 ± 1.45%, FPB: 46.78 ± 1.73%, EDC: 45.28 ± 1.50%, FDS: 47.75 ± 1.51%, ECR: 46.55 ± 1.50%, and FCR: 48.00 ± 1.52%, when expressed in stimulator intensity.

Table 1 provides an overview of ICC with the values obtained for maximum cortical resolution (results of the other resolutions and intensities can be found as **Supplementary Tables 2A–C**). For the sake of legibility, we defined distinct classes as follows: excellent: $0.8 \leq$ ICC, good: $0.65 \leq$ ICC < 0.8, moderate: $0.5 \leq$ ICC < 0.65 and poor: ICC < 0.5 (Cavaleri et al., 2018), and color-coded the table entries accordingly.

The ICCs appeared consistent between methods M1 (ignoring non-MEP points) and M2 (removing non-MEP points). Most of them were moderate to good. Good-excellent reliability was found for estimated centroids in the anterior/posterior and superior/inferior directions (x and z coordinates, respectively). While the area sizes' ICCs of FDI, FDS, and FCR were poor, the ANOVA did not reveal any significant differences between the area estimates between sessions. We illustrate this in **Table 2** for the highest cortex resolution and refer to **Supplementary Tables 3A,B** for the ANOVA results for the other cortex

TABLE 1 | ICC values of area sizes A and centroids $C = (C_x, C_y, C_z)^T$ estimated for intensity of 105% RMT of FCR using the cortical meshes with maximum resolution when ignoring non-MEP points (M1) or removing them (M2)*.

	FDI		ADM		APB		FPB		EDC		FDS		ECR		FCR	
	M1	**M2**	**M1**	**M2**	**M1**	**M2**	**M1**	**M2**	**M1**	**M2**	**M1**	**M2**	**M1**	**M2**	**M1**	**M2**
A	0.41	0.42	0.67	0.67	0.55	0.55	0.69	0.69	0.73	0.72	0.32	0.31	0.58	0.57	0.15	0.14
C_x	0.90	0.90	0.88	0.88	0.89	0.89	0.89	0.89	0.92	0.92	0.89	0.89	0.92	0.92	0.91	0.91
C_y	0.58	0.59	0.55	0.55	0.69	0.70	0.61	0.61	0.56	0.57	0.51	0.51	0.51	0.51	0.53	0.53
C_z	0.80	0.80	0.68	0.68	0.76	0.76	0.81	0.82	0.76	0.76	0.66	0.66	0.72	0.72	0.83	0.83

Excellent: 0.8 ≤ ICC (dark green, bold); good: 0.65 ≤ ICC < 0.8 (light green); moderate: 0.5 ≤ ICC < 0.65 (yellow); poor: ICC < 0.5 (light red).

TABLE 2 | Outcomes of the two-way ANOVA for the area sizes A (in $mm^2 \cdot \mu V \cdot 10^5$) with factors of *intensity* and *session* when considering the highest cortex mesh resolution and when removing the non-MEP points (M2)*.

	⟨A⟩ at 105% RMT			Intensity		Session		Intensity × session		*p*-value pairwise comparison		
	FDI	**EDC**	**FCR**	***F***	***p***	***F***	***p***	***F***	***p***	**FDI/EDC**	**FDI/FCR**	**EDC/FCR**
FDI	1.61 ± 0.24	2.48 ± 0.60	4.86 ± 1.41	**$F(2, 36) = 4.855$**	**0.032**	$F(1, 18) = 1.390$	0.254	$F(2, 36) = 0.634$	0.454	0.307	0.087	0.195
ADM	0.92 ± 0.21	0.99 ± 0.17	2.16 ± 0.60	**$F(2, 24) = 5.385$**	**0.032**	$F(1, 12) = 1.216$	0.292	$F(2, 24) = 0.238$	0.790	1.00	0.076	0.137
APB	1.63 ± 0.41	1.89 ± 0.45	3.74 ± 1.28	$F(2, 34) = 3.050$	0.093	$F(1, 17) = 0.939$	0.346	$F(2, 34) = 1.337$	0.267	1.00	0.213	0.364
FPB	1.18 ± 0.28	1.53 ± 0.37	2.41 ± 0.69	$F(2, 34) = 3.439$	0.073	$F(1, 17) = 4.425$	0.051	$F(2, 34) = 1.398$	0.260	0.273	0.158	0.406
EDC	1.01 ± 0.21	0.94 ± 0.12	1.75 ± 0.36	**$F(2, 34) = 5.960$**	**0.016**	$F(1, 17) = 0.082$	0.778	$F(2, 34) = 0.146$	0.865	1.00	**0.031**	0.078
FDS	0.83 ± 0.12	0.97 ± 0.18	1.60 ± 0.25	**$F(2, 30) = 6.345$**	**0.005**	$F(1,15) = 1.090$	0.313	$F(2, 30) = 1.174$	0.323	1.00	**0.020**	0.077
ECR	1.24 ± 0.20	1.62 ± 0.43	2.45 ± 0.53	**$F(2, 30) = 4.730$**	**0.016**	$F(1, 15) = 0.319$	0.580	$F(2, 30) = 0.867$	0.388	0.947	**0.030**	0.217
FCR	0.69 ± 0.11	0.99 ± 0.20	1.39 ± 0.20	**$F(2, 30) = 5.173$**	**0.012**	$F(1, 15) = 2.079$	0.170	$F(2, 30) = 1.388$	0.265	0.473	**0.011**	0.376

Bold face implies $p < 0.05$.

TABLE 3 | The outcome of the two-way ANOVA for the area sizes A (in $mm^2 \cdot \mu V \cdot 10^5$) with factors of *method* and *resolution* for the intensity of 105% RMT of FCR; M1, ignoring non-MEP points, M2, removing them*.

	⟨A⟩ at 105% RMT of FCR		Method		Resolution		Method × resolution	
	M1	**M2**	***F***	***p***	***F***	***p***	***F***	***p***
FDI	4.81 ± 1.48	4.27 ± 1.25	**$F(1, 19) = 5.335$**	**0.032**	$F(2, 38) = 1.655$	0.212	**$F(2, 38) = 3.128$**	0.093
ADM	1.68 ± 0.50	1.50 ± 0.43	**$F(1, 17) = 5.158$**	**0.036**	$F(2, 34) = 1.927$	0.173	**$F(2, 34) = 2.638$**	0.122
APB	3.54 ± 1.12	3.25 ± 1.03	**$F(1, 19) = 7.967$**	**0.011**	$F(2, 38) = 1.002$	0.342	**$F(2, 38) = 3.404$**	0.079
FPB	2.21 ± 0.59	2.00 ± 0.53	**$F(1, 19) = 9.775$**	**0.006**	$F(2, 38) = 1.286$	0.273	**$F(1, 19) = 9.775$**	**0.006**
EDC	1.63 ± 0.33	1.49 ± 0.29	**$F(1, 19) = 19.435$**	**0.000**	$F(2, 38) = 2.625$	0.086	**$F(1, 19) = 19.435$**	**0.000**
FDS	1.40 ± 0.22	1.29 ± 0.20	**$F(1, 19) = 24.526$**	**0.000**	$F(2, 38) = 0.582$	0.517	**$F(2, 38) = 11.278$**	**0.002**
ECR	2.09 ± 0.43	1.93 ± 0.39	**$F(1, 19) = 13.025$**	**0.002**	$F(2, 38) = 2.576$	0.089	**$F(2, 38) = 5.639$**	**0.023**
FCR	1.43 ± 0.19	1.33 ± 0.17	**$F(1, 17) = 20.599$**	**0.000**	$F(2, 34) = 0.096$	0.830	**$F(2, 34) = 9.791$**	**0.004**

Bold face implies $p < 0.05$.

resolutions. In **Supplementary Tables 4–6A–C**, we also provide the results for the corresponding centroid positions. In a nutshell there were hardly any significant effects of session or intensity (let alone their interaction) on the centroids; when correcting for multiple comparisons all effects will turn out not significant.

Here we would like to note that this dependency on stimulation intensity can be understood when looking at the effects of intensity on the mere MEP amplitudes, i.e., without projecting them onto the cortex. The corresponding results can be found as **Supplementary Table 7**. In a nutshell, the amplitudes of FDI, EDC, FCR, FDS, and FCR significantly increased with increasing stimulation intensity.

As expected, ignoring non-MEP points (M1) consistently resulted in larger area sizes when compared to the case when non-MEP points were removed (M2). Our second ANOVA confirmed this. We summarized this in **Table 3** where we highlighted the main effects of *method*. Yet, we also would like to note the interaction effect with *resolution*, suggesting that the correction for non-MEP points is especially relevant when incorporating low-resolution cortical meshes (see also **Figure 5**, upper row).

The main effect of *method* (ignoring non-MEPs vs. removing them) is also illustrated in **Figure 6** where we show the relative change in the estimated area sizes. Irrespective of resolution, not removing the non-MEP points yields an overestimation of the

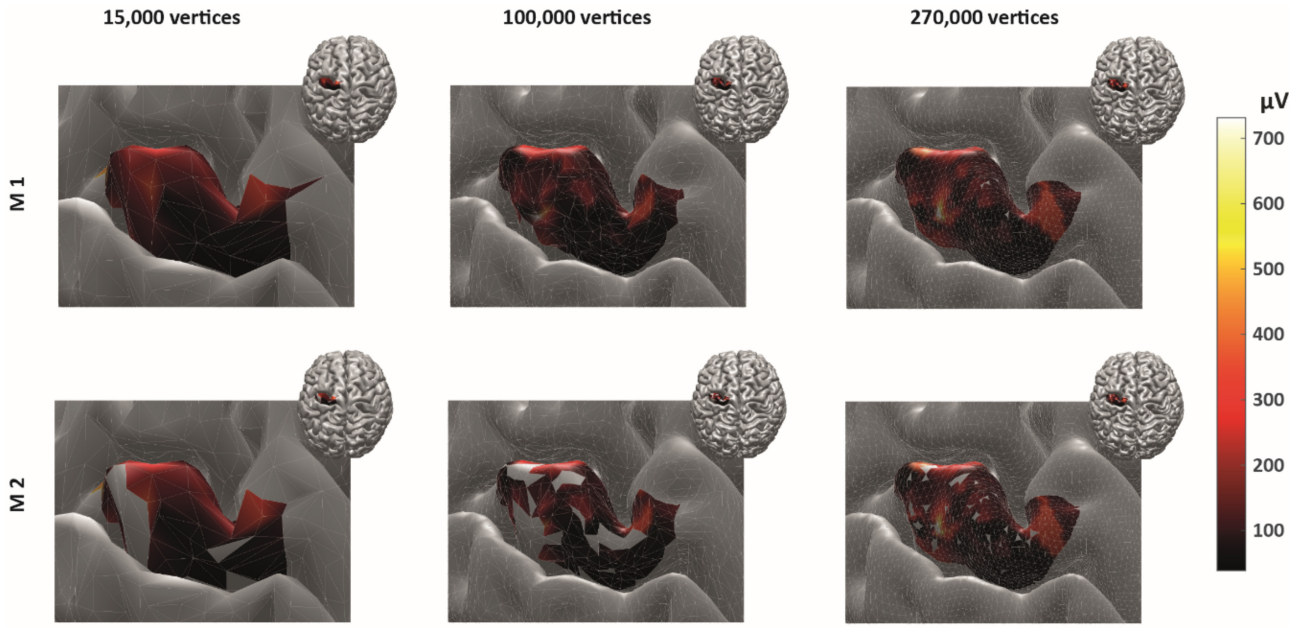

FIGURE 5 | The cortical representation for Session 1 intensity of 105% RMT of FCR in a representative participant. In M1 (upper row), we ignored non-MEP points, and in M2 (lower row), we removed them. Left: surface mesh resolution of 15,000 vertices; center: 100,000 vertices; right: maximum number of vertex number (in this participant, about 270,000 vertices). Color coding represents the value of the (interpolated) MEP-amplitude (in μV). The effects of non-MEP point removal are especially visible at a lower resolution, but in all cases, removing these stimulation points cause the estimated area to shrink.

active areas, though this effect appears particularly pronounced at low resolution (top panel in **Figure 6**).

We finally illustrate the effect of removing non-MEP points in **Figure 5**, where it can be clearly seen that higher resolutions lead to less area being removed.

DISCUSSION

We assessed the reliability of the cortical representation of eight muscles mapped simultaneously using navigated TMS. We distinguished two methods to estimate the active area of a muscle. In the first, more conventional one (M1), we included all stimulation points that elicited an MEP. In the second method (M2), we included the same points but also excluded all stimulation points that did not elicit an MEP. We tested for the effects of the type of measure with the obvious expectation that the latter will yield smaller active areas. We also tested for effects of stimulation intensity and cortical mesh resolution in two consecutive sessions. By and large, we found that the reliabilities of the size and the centroids of the active areas for all the muscles were excellent, good, or moderate. Exceptions were the area size estimates in three muscles (**Table 1**) that came with small areas sizes but strong outliers when looking at their representation at high-resolution cortical surface meshes (**Figure 6**, lower panel). The ICCs of amplitude and latency were excellent or good for all the muscles, again supporting the reliability of our experimental approach (cf. **Supplementary Table 8**).

One must realize that designing multiple muscle mapping experiments can—in general—be problematic as the RMT of a single muscle must be considered a reference when setting the stimulation intensity. In our case, the difference of RMTs values between different stimulation intensities was small (on average 3.1% of stimulator output; when looking at the individual subjects we found maximum differences of $|\,RMT_{FDI}\text{-}RMT_{EDC}|$ = $|\,RMT_{FCR}\text{-}RMT_{EDC}|$ = 9%, and $|\,RMT_{FDI}\text{-}RMT_{FCR}|$ = 8%). Intensities of 105%, 110–120% (Akiyama et al., 2006) RMT have been widely used in motor mapping (Bohning et al., 2001; Akiyama et al., 2006; Tarapore et al., 2012), suggesting that the here-observed difference is acceptable if not negligible. Hence, forearm and hand muscles might be pooled in a group of muscles with "similar RMTs" and may be evaluated at the same intensity.

For all the muscles, the ICCs of the centroids' positions were moderate to excellent. In the **Supplementary Tables 2A–C** we show the likewise good results for the more conventional CoGs. Both the estimated centroid as well as the centers-of-gravity hence appeared very consistent and should be considered reliable outcomes in motor mapping, in particular also the anterior/posterior and superior/inferior directions, in line with previous studies (Weiss et al., 2013; Cavaleri et al., 2018). The CoG is commonly employed to quantify the cortical representation of muscles (Massé-Alarie et al., 2017; Nazarova et al., 2021). However, there are several issues with the notion of "CoG" itself. For instance, for many shapes (of cortical representations), the CoG will lie outside the actual stimulation area itself (consider a banana, whose CoG will not be inside the banana itself). The CoG may hence be a tricky measure to give an estimate of the cortical representation of a muscle, especially when the true cortical representation is non-trivially shaped and on a curved surface. Supplementing the CoG, or in our case the

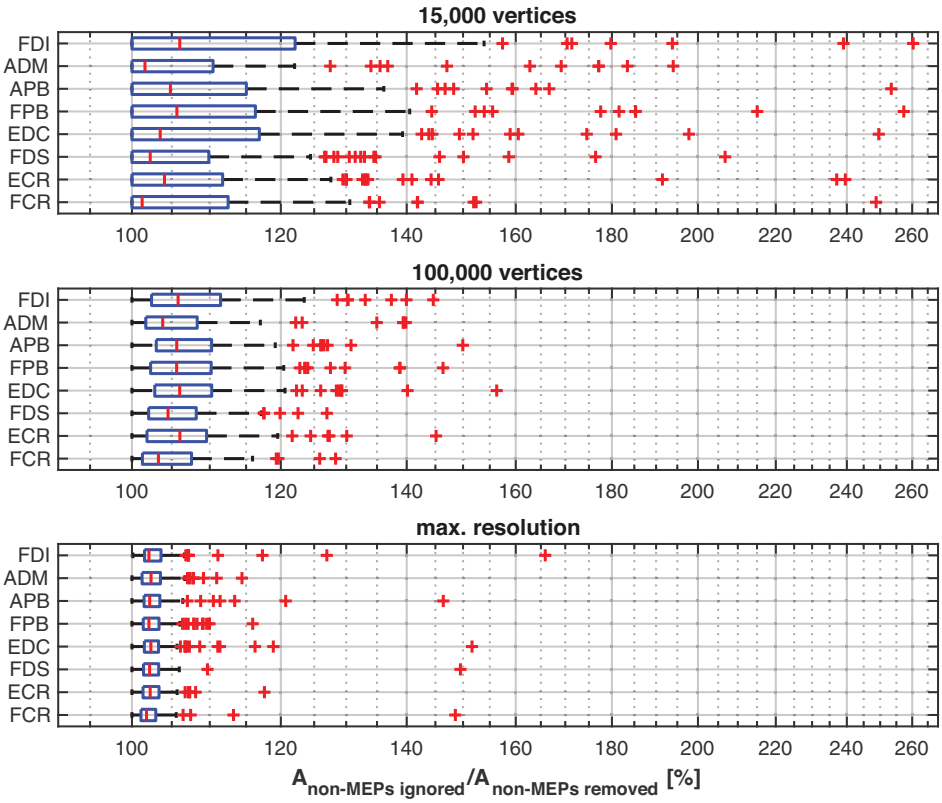

FIGURE 6 | The relative change of the size of the estimated active area per muscle using different resolutions of the cortex mesh. The maximum number of vertices was subject specific and ranged from about 230,000 to 340,000 vertices. The figure shows boxplots with red crosses marking outliers (all subjects/sessions entered the median and quantile estimates). Throughout mesh resolution the removal of non-MEP points yielded larger area sizes suggesting an overestimation of the active area.

centroid, by the area of excitability is clearly needed, especially when the area estimate is weighted by the MEP amplitude. Again, we advocate incorporating the non-MEP stimulation points in these estimates.

When removing non-MEP points, the areas of excitability became significantly smaller than when non-MEP points were simply ignored. We argue that by ignoring the stimulation points that do not elicit MEPs one runs the risk of overestimating the area of excitability and thus to mis-represent muscles in the cortex. Our results show that accounting for non-MEP points does not jeopardize the reliability of assessments. As such we advocate for correcting any potential structural error and provide the tools to do so. Of course, one may counter the fear for structural errors by subsuming that the neuronal population that ought to be covered by our cortical map are likely to be homogeneously distributed. However, several invasive studies already speak against this (e.g., Schieber, 2001). By using intracortical micro-stimulation, Nudo et al. (1996) revealed that the cortical representation of distal forelimb muscles is quite complicated and clearly not uniform. Moreover, to date most area measures rely on estimating convex hulls that clear yield weak approximations if the excitable area has a non-convex boundary—when looking at precentral gyrus that might be the rule rather than the exception.

CONCLUSION

Estimating the active area can be improved when incorporation points at which TMS does not elicit an MEP. Navigated TMS and a pseudo-random coil placement allow for correcting area estimates post-hoc and hence reduce the risk of overestimating the cortical representation of active areas. As such, the very fact that at certain points, a stimulation does not yield a measurable response appears informative. And, even when assessing multiple muscles in unison, this approach comes with high reliability, albeit under the provison that stimulation intensity has been chosen properly.

DATA AVAILABILITY STATEMENT

The raw data supporting the conclusions of this article will be made available by the authors, without undue reservation.

ETHICS STATEMENT

The studies involving human participants were reviewed and approved by the Medisch Ethische Toetsingscommissie VUmc.

The patients/participants provided their written informed consent to participate in this study. Written informed consent was obtained from the individual(s) for the publication of any potentially identifiable images or data included in this article.

AUTHOR CONTRIBUTIONS

FJ designed and conducted the experiment, analyzed the data, and wrote the draft. SB designed and conducted the experiment, analyzed the data, and modified the draft. AD designed the experiment, analyzed the data, and modified the draft. All authors contributed to the article and approved the submitted version.

SUPPLEMENTARY MATERIAL

The Supplementary Material for this article can be found online at: https://www.frontiersin.org/articles/10.3389/fnhum.2022.920538/full#supplementary-material

REFERENCES

Akiyama, T., Ohira, T., Kawase, T., and Kato, T. (2006). TMS orientation for NIRS-functional motor mapping. *Brain Topogr.* 19, 1–9. doi: 10.1007/s10548-006-0007-9

Barker, A. T., Jalinous, R., and Freeston, I. L. (1985). Non-invasive magnetic stimulation of human motor cortex. *Lancet* 325, 1106–1107. doi: 10.1016/s0140-6736(85)92413-4

Bohning, D., He, L., George, M., and Epstein, C. (2001). Deconvolution of transcranial magnetic stimulation (TMS) maps. *J. Neural Transm.* 108, 35–52. doi: 10.1007/s007020170095

Cavaleri, R., Schabrun, S. M., and Chipchase, L. S. (2017). The number of stimuli required to reliably assess corticomotor excitability and primary motor cortical representations using transcranial magnetic stimulation (TMS): a systematic review and meta-analysis. *Syst. Rev.* 6, 1–11.

Cavaleri, R., Schabrun, S. M., and Chipchase, L. S. (2018). The reliability and validity of rapid transcranial magnetic stimulation mapping. *Brain Stimul.* 11, 1291–1295. doi: 10.1016/j.brs.2018.07.043

Dijkstra, E. W. (1959). A note on two problems in connexion with graphs. *Numer. Math.* 1, 269–271.

Forster, M.-T., Hattingen, E., Senft, C., Gasser, T., Seifert, V., and Szelényi, A. (2011). Navigated transcranial magnetic stimulation and functional magnetic resonance imaging: advanced adjuncts in preoperative planning for central region tumors. *Neurosurgery* 68, 1317–1325.

Klein, A., Ghosh, S. S., Bao, F. S., Giard, J., Häme, Y., Stavsky, E., et al. (2017). Mindboggling morphometry of human brains. *PLoS Comput. Biol.* 13:e1005350. doi: 10.1371/journal.pcbi.1005350

Koo, T. K., and Li, M. Y. (2016). A guideline of selecting and reporting intraclass correlation coefficients for reliability research. *J. Chiropr. Med.* 15, 155–163.

Kraus, D., and Gharabaghi, A. (2016). Neuromuscular plasticity: disentangling stable and variable motor maps in the human sensorimotor cortex. *Neural Plast.* 2016:7365609. doi: 10.1155/2016/7365609

Krieg, S. M., Lioumis, P., Mäkelä, J. P., Wilenius, J., Karhu, J., Hannula, H., et al. (2017). Protocol for motor and language mapping by navigated TMS in patients and healthy volunteers. workshop report. *Acta Neurochirurgica* 159, 1187–1195. doi: 10.1007/s00701-017-3187-z

Krieg, S. M., Shiban, E., Buchmann, N., Gempt, J., Foerschler, A., Meyer, B., et al. (2012). Utility of presurgical navigated transcranial magnetic brain stimulation for the resection of tumors in eloquent motor areas. *J. Neurosurg.* 116, 994–1001. doi: 10.3171/2011.12.JNS111524

Mark, V., Taub, E., and Morris, D. (2006). Neuroplasticity and constraint-induced movement therapy. *Eura. Medicophys.* 42:269.

Massé-Alarie, H., Bergin, M. J., Schneider, C., Schabrun, S., and Hodges, P. W. (2017). "Discrete peaks" of excitability and map overlap reveal task-specific organization of primary motor cortex for control of human forearm muscles. *Hum. Brain Mapp.* 38, 6118–6132. doi: 10.1002/hbm.23816

Möller, T., and Trumbore, B. (1997). Fast, minimum storage ray-triangle intersection. *J. Graphics Tools* 2, 21–28.

Nazarova, M., Novikov, P., Ivanina, E., Kozlova, K., Dobrynina, L., and Nikulin, V. V. (2021). Mapping of multiple muscles with transcranial magnetic stimulation: absolute and relative test–retest reliability. *Hum. Brain Mapp.* 42, 2508–2528. doi: 10.1002/hbm.25383

Novikov, P. A., Nazarova, M. A., and Nikulin, V. V. (2018). TMSmap-software for quantitative analysis of TMS mapping results. *Front. Hum. Neurosci.* 12:239. doi: 10.3389/fnhum.2018.00239

Nudo, R. J., Milliken, G. W., Jenkins, W. M., and Merzenich, M. M. (1996). Use-dependent alterations of movement representations in primary motor cortex of adult squirrel monkeys. *J. Neurosci.* 16, 785–807. doi: 10.1523/JNEUROSCI.16-02-00785.1996

Oldfield, R. C. (1971). The assessment and analysis of handedness: the Edinburgh inventory. *Neuropsychologia* 9, 97–113. doi: 10.1016/0028-3932(71)90067-4

Opitz, A., Zafar, N., Bockermann, V., Rohde, V., and Paulus, W. (2014). Validating computationally predicted TMS stimulation areas using direct electrical stimulation in patients with brain tumors near precentral regions. *NeuroImage Clin.* 4, 500–507. doi: 10.1016/j.nicl.2014.03.004

Rossi, S., Hallett, M., Rossini, P. M., and Pascual-Leone, A. (2011). Screening questionnaire before TMS: an update. *Clin. Neurophysiol.* 122:1686. doi: 10.1016/j.clinph.2010.12.037

Rossini, P. M., Barker, A., Berardelli, A., Caramia, M., Caruso, G., Cracco, R., et al. (1994). Non-invasive electrical and magnetic stimulation of the brain, spinal cord and roots: basic principles and procedures for routine clinical application. Report of an IFCN committee. *Electroencephalogr. Clin. Neurophysiol.* 91, 79–92. doi: 10.1016/0013-4694(94)90029-9

Rossini, P. M., Burke, D., Chen, R., Cohen, L., Daskalakis, Z., Di Iorio, R., et al. (2015). Non-invasive electrical and magnetic stimulation of the brain, spinal cord, roots and peripheral nerves: basic principles and procedures for routine clinical and research application. An updated report from an IFCN Committee. *Clin. Neurophysiol.* 126, 1071–1107. doi: 10.1016/j.clinph.2015.02.001

Schambra, H., Sawaki, L., and Cohen, L. (2003). Modulation of excitability of human motor cortex (M1) by 1 Hz transcranial magnetic stimulation of the contralateral M1. *Clin. Neurophysiol.* 114, 130–133. doi: 10.1016/s1388-2457(02)00342-5

Schieber, M. H. (2001). Constraints on somatotopic organization in the primary motor cortex. *J. Neurophysiol.* 86, 2125–2143. doi: 10.1152/jn.2001.86.5.2125

Siebner, H., and Rothwell, J. (2003). Transcranial magnetic stimulation: new insights into representational cortical plasticity. *Exp. Brain Res.* 148, 1–16. doi: 10.1007/s00221-002-1234-2

Sondergaard, R. E., Martino, D., Kiss, Z. H., and Condliffe, E. G. (2021). TMS motor mapping methodology and reliability: a structured review. *Front. Neurosci.* 15:709368. doi: 10.3389/fnins.2021.709368

Tarapore, P. E., Tate, M. C., Findlay, A. M., Honma, S. M., Mizuiri, D., Berger, M. S., et al. (2012). Preoperative multimodal motor mapping: a comparison of magnetoencephalography imaging, navigated transcranial magnetic stimulation, and direct cortical stimulation. *J. Neurosurg.* 117, 354–362. doi: 10.3171/2012.5.JNS112124

Tardelli, G. P., Souza, V. H., Matsuda, R. H., Garcia, M. A. C., Novikov, P., Nazarova, M., et al. (2021). Forearm and hand muscles exhibit high coactivation and overlapping of cortical motor representations. *Biorxiv[preprint]* doi: 10.1007/s10548-022-00893-1

Van Essen, D. C. (2004). Surface-based approaches to spatial localization and registration in primate cerebral cortex. *NeuroImage* 23, S97–S107. doi: 10.1016/j.neuroimage.2004.07.024

Weiss, C., Nettekoven, C., Rehme, A. K., Neuschmelting, V., Eisenbeis, A., Goldbrunner, R., et al. (2013). Mapping the hand, foot and face representations in the primary motor cortex – retest reliability of neuronavigated TMS versus functional MRI. *NeuroImage* 66, 531–542. doi: 10.1016/j.neuroimage.2012.10.046

Conflict of Interest: The authors declare that the research was conducted in the absence of any commercial or financial relationships that could be construed as a potential conflict of interest.

Publisher's Note: All claims expressed in this article are solely those of the authors and do not necessarily represent those of their affiliated organizations, or those of the publisher, the editors and the reviewers. Any product that may be evaluated in this article, or claim that may be made by its manufacturer, is not guaranteed or endorsed by the publisher.

frontiers | Frontiers in Human Neuroscience

BRIEF RESEARCH REPORT
published: 05 July 2022
doi: 10.3389/fnhum.2022.920383

Transcranial Magnetic Stimulation for Long-Term Smoking Cessation: Preliminary Examination of Delay Discounting as a Therapeutic Target and the Effects of Intensity and Duration

Alina Shevorykin[1†], Ellen Carl[1], Martin C. Mahoney[1], Colleen A. Hanlon[2], Amylynn Liskiewicz[1], Cheryl Rivard[1], Ronald Alberico[1], Ahmed Belal[1], Lindsey Bensch[1], Darian Vantucci[1], Hannah Thorner[1], Matthew Marion[1], Warren K. Bickel[3] and Christine E. Sheffer[1†]*

[1] Roswell Park Comprehensive Cancer Center, Buffalo, NY, United States, [2] Wake Forest School of Medicine, Winston-Salem, NC, United States, [3] Fralin Biomedical Research Institute at Virginia Tech Carilion, Roanoke, VA, United States

OPEN ACCESS

Edited by:
Joao Miguel Castelhano, University of Coimbra, Portugal

Reviewed by:
David Conversi, Sapienza University of Rome, Italy
Mauro Pettorruso, University of Studies G. d'Annunzio Chieti and Pescara, Italy

***Correspondence:**
Alina Shevorykin
alina.shevorykin@roswellpark.org

[†] These authors have contributed equally to this work

Specialty section:
This article was submitted to Brain Imaging and Stimulation, a section of the journal Frontiers in Human Neuroscience

Received: 14 April 2022
Accepted: 20 June 2022
Published: 05 July 2022

Citation:
Shevorykin A, Carl E, Mahoney MC, Hanlon CA, Liskiewicz A, Rivard C, Alberico R, Belal A, Bensch L, Vantucci D, Thorner H, Marion M, Bickel WK and Sheffer CE (2022) Transcranial Magnetic Stimulation for Long-Term Smoking Cessation: Preliminary Examination of Delay Discounting as a Therapeutic Target and the Effects of Intensity and Duration. Front. Hum. Neurosci. 16:920383. doi: 10.3389/fnhum.2022.920383

Background: Repetitive transcranial magnetic stimulation (rTMS) is a novel treatment for smoking cessation and delay discounting rate is novel therapeutic target. Research to determine optimal therapeutic targets and dosing parameters for long-term smoking cessation is needed. Due to potential biases and confounds introduced by the COVID-19 pandemic, we report preliminary results from an ongoing study among participants who reached study end prior to the pandemic.

Methods: In a 3 × 2 randomized factorial design, participants (n = 23) received 900 pulses of 20 Hz rTMS to the left dorsolateral prefrontal cortex (PFC) in one of three Durations (8, 12, or 16 days of stimulation) and two Intensities (1 or 2 sessions per day). We examined direction and magnitude of the effect sizes on latency to relapse, 6-month point-prevalence abstinence rates, research burden, and delay discounting rates.

Results: A large effect size was found for Duration and a medium for Intensity for latency to relapse. Increasing Duration increased the odds of abstinence 7–8-fold while increasing Intensity doubled the odds of abstinence. A large effect size was found for Duration, a small for Intensity for delay discounting rate. Increasing Duration and Intensity had a small effect on participant burden.

Conclusion: Findings provide preliminary support for delay discounting as a therapeutic target and for increasing Duration and Intensity to achieve larger effect sizes for long-term smoking cessation and will provide a pre-pandemic comparison for data collected during the pandemic.

Clinical Trial Registration: [www.ClinicalTrials.gov], identifier [NCT03865472].

Keywords: transcranial magnetic stimulation, smoking cessation, tobacco dependence treatment, delay discounting, self-regulation, brain stimulation

INTRODUCTION

"Making progress on longstanding challenges requires a different lens and a new approach."

Ayanna Pressley.

Over one-half of individuals who smoke cigarettes in the US attempt to quit every year, but over 90% rapidly reverse this decision, choosing the immediate reward of smoking over the long-term benefits of quitting (Babb et al., 2017). Despite the increased availability of evidence-based behavioral and pharmacological treatments for cigarette smoking, less than one-third of cigarette smokers use them (Babb et al., 2017; Office on Smoking and United States Public Health Service Office of the Surgeon General, and National Center for Chronic Disease Prevention and Health Promotion (US) Office on Smoking and Health, 2020). Negative attitudes about taking medications for smoking cessation are a commonly endorsed barrier to using pharmacological treatments (Mooney et al., 2006; Gross et al., 2008; Morphett et al., 2015; Smith et al., 2015). Novel, non-pharmacological treatment approaches have the potential to provide cigarette smokers with more smoking cessation treatment options.

Tremendous progress has been made in the development of brain stimulation techniques to support smoking cessation (Ekhtiari et al., 2019). High frequency (HF) (rTMS) is a non-invasive brain stimulation technique that can selectively modulate neuronal plasticity (Ekhtiari et al., 2019). Using a variety of different coil configurations, rTMS generates brief focal electromagnetic pulses that penetrate the skull to stimulate brain regions via localized axonal depolarization (Fitzgerald et al., 2006; Thut and Pascual-Leone, 2010). rTMS coil selection is based on the need for stimulation depth and focality (Lu and Ueno, 2017). HF rTMS using an H4-coil was recently cleared by the Federal Drug Administration (K200957) for short-term smoking cessation (Zangen et al., 2021). The H4-coil stimulates broad swaths of the (PFC) and insula (Fiocchi et al., 2018). The conventional figure of 8 coil delivers stimulation with more focality than the H4 coil (i.e., targets with more specificity) (Lu and Ueno, 2017). HF rTMS of the left dorsolateral PFC (dlPFC) using a figure of 8 coil is emerging as a novel non-pharmacological treatment approach for long-term smoking cessation (Ekhtiari et al., 2019).

The Competing Neurobehavioral Decisions Systems (CNDS) Model is a broad, fundamental framework grounded in neuroeconomics and dual processing theory (Mukherjee, 2010). The CNDS Model describes the general neurobiological underpinnings involved with making far-sighted decisions about one's health (e.g., maintaining abstinence from smoking) in the context of immediately rewarding, though less healthy choices (e.g., continued smoking) (Bickel et al., 2007; McClure and Bickel, 2014). The Model posits that these decisions are broadly driven by the interaction between two functional neurobiological networks: the executive function network, embodied in the PFC; and the impulsive network, embodied in the limbic and paralimbic regions of the brain (Bickel et al., 2014, 2016; Hanlon et al., 2015). The balance of activity in these two networks shapes reward-related decision-making (Hanlon et al., 2015). Greater activity in the PFC is linked with a higher likelihood of more prudent decision-making, even in the context of temptation (McClure et al., 2007; MacKillop et al., 2012). However, chronic nicotine administration can significantly impact reward-related decision-making (Koob, 2008a,b) and over time, the balance and functioning of these networks can become dysregulated, resulting in significant deficits in executive function neural processing (Ernst et al., 2001; Xu et al., 2005; McClure and Bickel, 2014; Koob et al., 2014). Dysfunction or hypo-activation of the executive function network contributes to undervaluation of the long-term rewards from cessation (Hanlon et al., 2015), adding to the behavioral and psychosocial challenges of achieving long-term abstinence from cigarettes.

Most individuals prefer immediate rewards because reinforcement loses value the longer one waits to receive it, but individuals demonstrate considerable variability in these preferences. Delay discounting rate represents the degree to which individuals discount the value of a reward as a function of time to receipt (Kirby, 1997; Odum, 2011; Commons et al., 2013). Delay discounting rate is considered a transdiagnostic biological marker for the relative balance between the executive and impulsive networks consistent with the CNDS model (Bickel et al., 2012, 2019), and is a well-established prognostic factor for smoking cessation treatment outcomes (Sheffer et al., 2012, 2014; Coughlin et al., 2020). Importantly, delay discounting rates are malleable, with decreases associated with improved health behaviors (Koffarnus et al., 2013; Bickel et al., 2014; Rung and Madden, 2018).

The frontolimbic balance outlined by the CNDS Model and its application to cigarette smoking, however, must be viewed as a general framework within the context of the multiple complex neurobiological, psychological, affective, environmental, socio-cultural, and evolutionary factors that contribute to the development and maintenance of dysfunctional human decision-making, a review of which is outside the scope of this manuscript (Alcaro et al., 2021). For instance, the well-established role of classical and operant conditioning in decision-making is optimized by the mesolimbic dopaminergic (MS DA) system (Robinson and Berridge, 2001, 2003, 2008; Salamone and Correa, 2002; Everitt and Robbins, 2005; Alcaro et al., 2007) and contributes significantly to the development and maintenance of the imbalance described by the CNDS Model. A significant body of research also shows that the SEEKING or exploring drive is neurologically foundational to all appetitively motivated behaviors (Alcaro et al., 2021). Addiction likely reflects dysfunction of the SEEKING drive, linked with the MS DA system and consistent with results predicted by the CNDS Model (Alcaro et al., 2021). In addition, delay discounting is one of many potential transdiagnostic dimensions that are relevant to reward dysfunction. Anhedonia, defined as the inability to feel pleasure, is a transdiagnostic dimension present in a wide variety of mental health and substance use disorders (Spano et al., 2019). As a symptom of abstinence from many substances, anhedonia can prevent adequate reinforcement from non-substance related reinforcers (Garfield et al., 2014).

The dlPFC, a functional node in the PFC, has a significant role in executive function and the controlled response inhibition associated with drug-related craving and self-regulation (Ernst et al., 2001; Brody et al., 2002; McBride et al., 2006). The proposed mechanism by which HF rTMS of the left dlPFC supports smoking cessation is by increasing neuronal activity and plasticity in the left dlPFC, thereby improving executive functions mediated by the dlPFC. Preliminary evidence indicates that the approach is feasible and can reduce delay discounting rates and increase short-term latency to relapse, abstinence rates, and uptake of psychoeducational material (Sheffer et al., 2013, 2018; Ekhtiari et al., 2019). Prior to conducting a large-scale study of efficacy, however, research is needed to determine the optimal dosing strategies to achieve long-term abstinence (i.e., 6 months or more).

The parent project from which this study is derived is an ongoing 5-year study aimed to determine the optimal dosing strategies of rTMS of the left dlPFC for long-term smoking cessation (Carl et al., 2020). This study employs a fully crossed, $3 \times 2 \times 2$ randomized double-blinded factorial design, where Duration is defined as 8, 12, and 16 days of stimulation, Intensity is a number of pulses per day (900 in one session vs. 1,800 in two sessions), and participants are randomized to active/sham conditions.

The onset of the COVID-19 pandemic paused all in-person study-related activities in the parent study in late March of 2020. Once the study resumed, multiple factors associated with COVID-19 introduced possible biases and confounds on recruitment, retention, and outcomes. These factors include the need to use different recruitment strategies (social media vs. flyers in the community), increased participant burden due to safety precautions, concerns about physical distancing, and COVID-19 stress-related effects on engagement and outcomes. Thus, we report preliminary results from participants who reached study end prior to the COVID-19 outbreak in Western New York.

Our primary goal was to examine the effects of increasing rTMS Duration and Intensity of active stimulation on latency to relapse, 6-month point prevalence abstinence rates, participant burden, and delay discounting rates among participants who reached study end. The hypotheses were consistent with the parent study (see above). Given the preliminary nature of this study, the focus on pre-COVID participation, the 3–1 active/sham randomization in the parent study, and the limited sample size, we included only active participants, limited comparisons, and focused on effect sizes. Statistical significance, while reported, must be viewed with caution in this context, however, multiple statistical approaches were employed to establish consistency among the findings.

MATERIALS AND METHODS

Participants

We recruited right-handed adults (age 18–65) who smoked 6–25 cigarettes daily and who were motivated to quit smoking. Participants were required to pass a 12-panel urine drug test, a pregnancy test, the TMS Adult Safety and Screening Questionnaire (TASS) (Rossi et al., 2011), claustrophobia screen to assess the ability to undergo a closed MRI of the head (Carl et al., 2020). Participants were recruited using flyers in the community, print advertisement, and social media.

Design

This study is a fully crossed 3×2 randomized factorial design. The two factors were Duration (8, 12, or 16 days of stimulation) and Intensity (900 or 1,800 pulses per day). Although only those participants who received active stimulation were included in the analyses, all participants and technicians were blinded to active/sham condition. Participants were followed for 6 months after the quit date. Daily number of cigarettes smoked per day was collected every 2 weeks. Exhaled carbon monoxide (CO) level was assessed at each in-person outcome assessment (4-, 8-, 12-, 18-, and 24-weeks after the quit date). Given the preliminary nature of this study, the focus on pre-COVID participation, the 3–1 active/sham randomization in the parent study, and the limited sample size, only those participants who received active stimulation and reached study end prior to April 4, 2020 were included in this study.

Procedure

Participants were screened over the telephone and invited to an in-person interview during which urine drug and pregnancy tests were administered. After informed consent, participants completed baseline assessments and were scheduled for an MRI. Prior to the MRI, the International 10-10 Electrode System was used to place a vitamin E capsule at the AF3 electrode position as a fiducial marker on the image. AF3 was chosen because the cognitive functions of interest are located in the anterior region of the dlPFC (Cieslik et al., 2012). The MRI was uploaded into the neuronavigation system with the fiducial marker readily apparent on the image. The MRI was also used to identify brain abnormalities that might impact participant safety. Eligible participants were randomized and scheduled for quit counseling, a quit date, and rTMS sessions.

The quit day was the day immediately prior to the first rTMS session. Participants were provided 30 min of brief structured cognitive behavioral counseling over the telephone 2 days prior to the quit date. Participants were required to abstain from smoking for at least 24 h prior to the first stimulation session, as evidenced by an expired breath CO level of < 10 ppm (SRNT Subcommittee on Biochemical Verification, 2002). Immediately prior to initiating rTMS, participants were randomized using permuted block randomization stratified by high or low nicotine dependence level [FTND; high ($\geq$5) or low ($<$5)] (Heatherton et al., 1991).

TMS power was tailored to the Motor Threshold (MT), which was defined as the minimum stimulation power required to elicit a motor evoked potential of 50 μV from the abductor pollicis brevis (APB) in 3 of 6 trials. Each rTMS session provided 900 pulses of 20 Hz rTMS to the left dlPFC at 110% of the MT. Magstim Super RAPID^2 PLUS1 System with Magstim 70 mm Double Air Film Active Figure of 8 Coil was used. The Brainsight Neuronavigational system (Rouge Research, Inc.) was used to track the placement of the coil in real time with respect to an MRI-derived image. Pulses were delivered in 45 20-pulse trains of 1 s duration with

an inter-train interval of 20 s. Stimulation time was 16 min. Participants read psychoeducational materials (Forever Free® self-help booklets) during the first 8 stimulation sessions. Participants were compensated $20 after each in-person visit, a weekly $50 bonus for completing all scheduled rTMS sessions, and $100 bonus for completing all five outcome assessments.

Bioethics

The study was approved by the Institutional Review Board of Roswell Park Comprehensive Cancer Center (#I-65718). Informed consent was obtained from all participants.

Measures

Demographic information collected at baseline included age, sex, race, ethnicity, partnered status, education, and household income. Other measures included the Fagerström Test for Nicotine Dependence (FTND) (Heatherton et al., 1991; Fagerstrom, 2012) and other clinical factors such as impulsivity measured by Barratt Impulsiveness Scale (Patton et al., 1995). Delay discounting and participant research burden were assessed at baseline and at each outcome assessment point. Primary outcomes included latency to relapse (number of days to relapse), 6-month point prevalence abstinence rates, participant research burden, and delay discounting rates.

Delay discounting rates were assessed using the 5-trial adjusting delay task for $100 and $1,000 magnitudes (Koffarnus and Bickel, 2014). During this task, participants were presented with a choice between two hypothetical monetary amounts ($100 vs. $50 in the $100 condition and $1,000 vs. $500 in the $1,000 condition). In each of the seven choice presentations, the smaller amount was available immediately, and the higher amount available at a discrete delay, beginning with 3 weeks. Based on the participant's choice, delay either increased (when participants select the delayed option) or decreased (when participants select the immediate option). Participants made this choice for five trials, resulting in potential *k*-values which were subsequently log transformed into ln*k*.

Latency to relapse and point prevalence abstinence were assessed using the Timeline Follow Back procedure (TLFB) every 2 weeks (Sobell and Sobell, 1992; Brown et al., 1998) by telephone and during the in-person outcome assessments. Relapse was defined as 7 consecutive days of any cigarette smoking (Hughes et al., 2003). CO in exhaled breath of $\leq$ 5 ppm as measured by the Micro + Smokerlyzer (Covita, Inc.) was considered abstinent from cigarette smoking (SRNT Subcommittee on Biochemical Verification, 2002).

Participant research burden was assessed with the 21-item Perceived Research Burden Assessment (PeRBA) (Lingler et al., 2014). Total scores range from 21 to 105, with lower scores reflecting lower participant burden.

Statistical Analyses

Descriptive analyses were used to characterize the sample. Because the aim was to examine the direction and strength of effect sizes, the primary tests were Cohen's d, partial eta squared (η^2), Cramer's Phi squared (Φ^2), and odds ratios (OR), as appropriate (Rhea, 2004; Le and Marcus, 2012; Tomczak and Tomczak, 2014; Enzmann, 2015; Kim, 2015). Cohen's d provides a standardized difference between two means by expressing the difference in units of standard deviation. With Cohen's d, a small effect size is ∼0.2, medium is ∼0.5, and large is ∼0.8 or greater. Partial η^2 measures the proportion of variance explained by the dependent variable attributable to the independent variable. With η^2, a small effect size is ∼ 0.01, medium is ∼0.06, and large is ∼0.14 or greater. Cramer's Phi (Φ) reflects the strength of the association between two variables, and when squared, reflects how much variance is accounted for by the association. With Φ^2, a small effect size is ∼0.01, medium is ∼0.09, and large is ∼0.25 or greater (Maher et al., 2013; Ialongo, 2016). OR reflect the direction and strength of the effect relative to the comparison group. Hazard ratios, chi square, confidence intervals, F-statistics, and *p*-values are reported as appropriate, but given small sample size, must be viewed with caution.

Cox proportional hazard (CPH) models were used to examine the effects of Duration and Intensity on latency to relapse. Days to relapse were right-censored. Right censoring was defined as participants who did not relapse while under observation, either because they maintained abstinence to the end of the study period or were lost to follow-up. Participants were considered abstinent at least as long as they were observed to have been abstinent. Cohen's d was calculated for CPH results using the formula: $d = ln(HR)x\checkmark(6/\pi)$ (Azuero, 2016).

Binary logistic regression models were used to examine the effects of Duration and Intensity on 6-month/7-day point prevalence abstinence rates. Missing data was imputed as smoking for the Intention to treat analysis (ITT). Missing data was excluded for complete case analysis (CCA). For Duration, 8 days was used as the comparison group. For intensity, 1 session per day (900 pulses) was used as the comparison group. OR and confidence intervals are reported.

The analysis of delayed discounting rate and PeRBA was conducted in two ways: (1) Repeated measures multivariate analysis of variance (MANOVA) was used to examine main effects, and (2) Generalized estimating equations (GEE) was used to examine rate of change across time. Dependent variables were discounting (ln*k*) of $100 and $1,000 magnitudes, and the total score of the PeRBA. Time was entered as a within-subject factor, with six timepoints: baseline and 5 outcome assessments (4-, 8-, 12-, 16-, and 24-weeks after the first rTMS session). The Bonferroni adjustment was used to control for multiple comparisons. When Mauchly's test statistic was significant, Greenhouse–Geisser correction was applied. Partial η^2 was calculated for MANOVA results using the formula: $\eta^2 = SS_{effect}/SS_{total}$ (Lakens, 2013). Cramer's Phi (Φ) was calculated for GEE results using the formula: $\Phi = \checkmark(\chi^2/N)$; Φ^2 was calculated to show shared variance (Phi/Cramer's Phi; Sharpe, 2015).

RESULTS

Participant Characteristics

Prior to pausing the parent project, n = 23 participants in the active condition reached study end. Participants were primarily

middle-aged (M = 50.78, SD = 10.96). About 30% identified as non-white and 70% as women. Participants included a high proportion of individuals of lower income and were diverse in terms of employment status. Nearly 80% were Medicaid and/or Medicare beneficiaries, over half had household incomes less than $25,000 per year, and 40% did not attend college. Participants were highly dependent on smoking. Most began smoking as adolescents, and over half had not made a quit attempt in the past year. Participants were moderately confident in their ability to quit smoking and maintained relatively high levels of motivation to quit throughout the study. Baseline levels of overall impulsivity were moderate and remained steady throughout the study (see **Table 1** and **Supplementary Table 1**).

Engagement and retention were high; 98.35% of rTMS sessions were completed and 78.30% (n = 18) completed the final outcome assessment (see **Supplementary Table 2**).

TABLE 1 | Participant (n = 23) characteristics at baseline.

Variable	Range or categories	M (SD) or% (n)
Age	20–64 years	50.78 (10.96)
Sex	Female	69.6% (16)
Race	White or Caucasian	69.6% (16)
	Black or African American	13% (3)
	Other	17.3% (4)
Ethnicity	Non-Hispanic	87% (20)
Partnered status	Un-partnered	52.2% (12)
Annual household income	<$10,000	17.4% (4)
	$10,000–$24,999	39.1% (9)
	$25,000–$74,999	39.1% (9)
	>$75,000	4.3% (1)
Highest education level	High school	39.1% (9)
	College	47.8% (11)
	Graduate school	13% (3)
Employment status	Full time	30.4% (7)
	Part-time	13% (3)
	Retired	13% (3)
	Disabled	8.7% (2)
	Unemployed	17.4% (4)
	Homemaker	17.4% (4)
Health insurance status	Medicare and/or Medicaid	78.2% (18)
	Private	17.4% (4)
	None	4.3% (1)
Cigarettes per day	6–25	14 (5.510)
Categories	6–10	39.1% (9)
	>10	60.9% (14)
FTND	0–8	5.0 (2.00)
Age started smoking, years	8–44 years	17.96 (6.609)
Last quit attempt	Never	13% (3)
	Past year	34.7% (8)
	Greater than 1 year ago	52.2% (12)
Self-efficacy for quitting	0–10	6.35 (2.740)
Motivation for quitting	1–10	7.91 (2.521)
Delay discounting rates of	$100	−3.449 (2.781)
	$1,000	−3.948 (2.707)

Unpartnered, single, divorced, separated, widowed; Partnered, married, partnered, or living with significant other. FTND, Fagerström Test for Nicotine Dependence.

Latency to Relapse

Although the standard deviations and interquartile ranges were large, the mean and median latency to relapse increased as Duration and Intensity increased, as hypothesized. Compared to 8 days of stimulation, 12 days showed a medium effect size (Cohen's d = 0.310) and 16 days showed a large effect size (Cohen's d = 0.741). Increasing Duration from 8 to 16 days significantly reduced the relative risk of relapse [HR 0.29 (0.09, 1.00); p = 0.049], such that with 16 days of stimulation the mean days to relapse increased from 17 days to 76 and the median from 2 to 31 days. Increasing Intensity from 900 to 1,800 pulses per day approached a medium effect size (Cohen's d = 0.381). Increasing Intensity from 900 pulses per day to 1800 pulses reduced the relative risk of relapse [HR 0.53 (0.17, 1.66); p = 0.28], such that with 1,800 pulses the mean days to relapse increased from 26 to 64 and the median from 2 to 28 days (see **Supplementary Table 3** and **Figure 1**).

Point Prevalence Abstinence

Using both ITT and CCA analysis, the proportion of participants abstinent from smoking consistently increased as Duration and Intensity increased. Logistic regressions revealed that increasing Duration from 8 to 12 days and from 8 to 16 days increased the odds of abstinence 4 and 7–8 fold, respectively. Increasing Intensity doubled the odds of long-term abstinence. Nevertheless, the confidence intervals were quite large. Differences were not statistically significant (Duration ITT: χ^2 = 3.260, p = 0.196, R^2 = 0.187; CCA: χ^2 = 2.885, p = 0.236, R^2 = 0.178) (Intensity ITT: χ^2 = 0.712, p = 0.399, R^2 = 0.043; CCA: χ^2 = 0.421, p = 0.516, R^2 = 0.028) (see **Supplementary Table 4**).

Participant Burden

MANOVAs revealed small effect sizes for both Duration and Intensity on the total PeRBA score (Duration: F = 0.376, p = 695, η^2 = 0.059 and Intensity: F = 0.008, p = 0.930, η^2 = 0.001). Similarly, GEE revealed small effect sizes for Duration and Intensity on total PeRBA scores (Duration: χ^2 = 1.921, p = 0.383, Φ = 0.289, Φ^2 = 0.084 and Intensity: χ^2 = 0.901, p = 0.343, Φ = 0.198, Φ^2 = 0.039). Increasing Duration or Intensity did not increase research burden and the scores were in the lower range (possible range is 21–105) (see **Supplementary Table 5**).

Delay Discounting

MANOVAs revealed large effect sizes for Duration (between 8, 12, and 16 days) for the $100 and $1000 magnitudes and these differences were statistically significant ($100: F = 4.500, p = 0.035, η^2 = 0.429; and $1,000 F = 5.657, p = 0.019, η^2 = 0.485). See **Figure 2A** the difference for Intensity (between 900 and 1,800 pulses per day) was in the expected direction, with small effect size, and not statistically significant ($100 F = 0.083, p = 0.779, η^2 = 0.007; and $1000 F = 0.023, p = 0.883, η^2 = 0.002) (see **Figure 2B**).

GEE revealed an overall decrease in delay discounting rate over time (see **Figure 3**) for Duration but not Intensity. Overall, large effect sizes were found for Duration ($100: χ^2 = 16.008, p < 0.001, Φ = 0.834, Φ^2 = 0.696; and $1,000: χ^2 = 19.042,

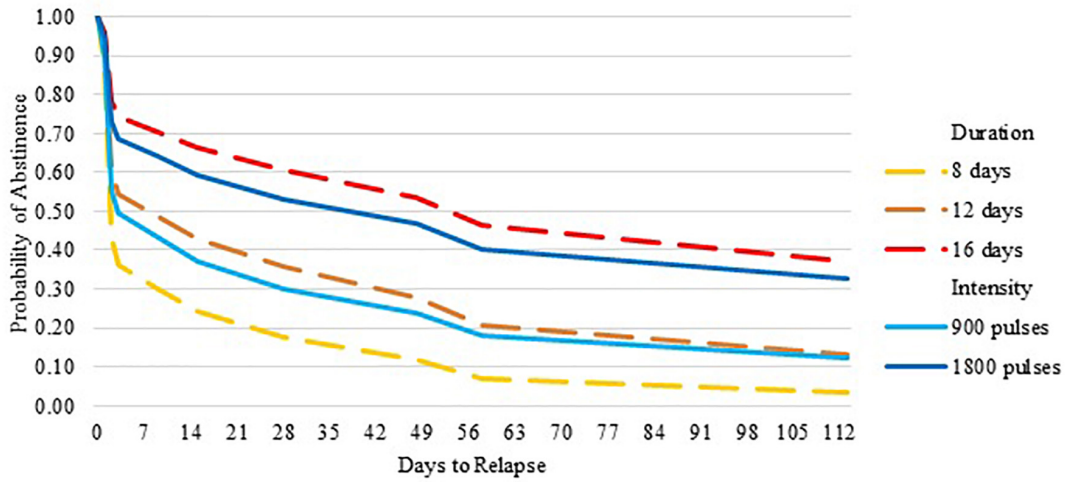

FIGURE 1 | Probability of abstinence over 6 months by duration and intensity of repetitive transcranial magnetic stimulation.

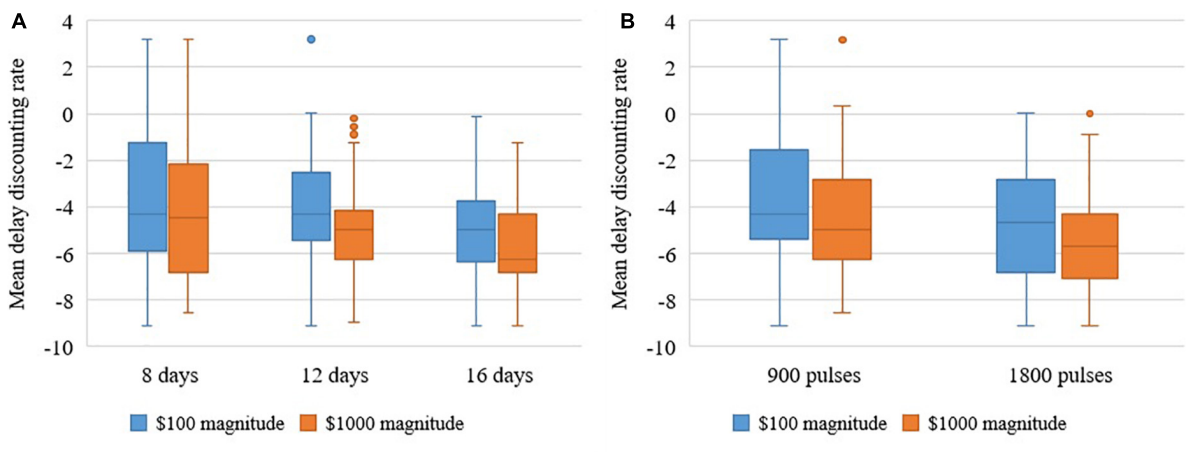

FIGURE 2 | (A) Repeated measures analysis of variance shows that increasing duration decreases delay discounting rates of $100 and $1000 overall over 6 months. **(B)** Repeated measures analysis of variance shows that increasing intensity decreases delay discounting rates of $100 and $1000 overall over 6 months.

$p < 0.001$, $\Phi = 0.909$, $\Phi^2 = 0.827$). Participants who received 16 days of rTMS had a more robust change in $100 and $1,000 magnitudes across time compared to those receiving 8 days of rTMS. The difference between 900 and 1,800 pulses per day was in the expected direction, with small effects size, and not statistically significant ($100: $\chi^2 = 1.187$, $p = 0.28$, $\Phi = 0.227$, $\Phi^2 = 0.051$; and $1,000: $\chi^2 = 2.161$, $p = 0.14$, $\Phi = 0.307$, $\Phi^2 = 0.094$) (see **Supplementary Table 5**).

DISCUSSION

Using multiple outcomes and statistical approaches, these findings provide consistent preliminary support for the primary smoking cessation hypotheses. Greater Duration and Intensity had greater effects on increasing latency to relapse, improving abstinence rates, and decreasing delay discounting rates. Findings also provided support, though weak, for the hypothesis that increased Duration and Intensity also increase participant research burden. Finally, these findings suggest that the therapeutic target, delay discounting, was robustly engaged and demonstrated the predicted concurrent effects on delay discounting and efficacy outcomes.

These findings suggest that prior to the onset of the COVID-19 pandemic, engagement was sufficiently high among participants who received higher doses of rTMS in terms of Duration and Intensity to support larger efficacy trials. In this sample, 98% of the rTMS sessions were completed, 78% completed the final outcome assessment, and at least some daily cigarette use was collected for all participants. Most participants were of lower income, were diverse in terms of employment, and over 30% identified as racial and/or ethnic minorities suggesting that rTMS studies are able to attract racially and socioeconomically diverse cigarette smokers.

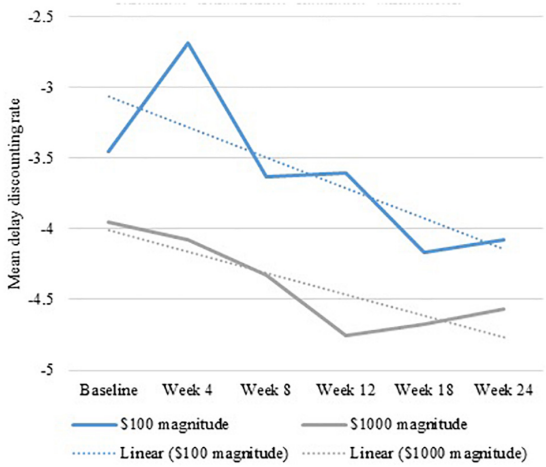

FIGURE 3 | Generalized estimating equation show an overall decrease in delay discounting rate over 6 months of repetitive transcranial magnetic stimulation.

Although increasing both Duration and Intensity increased effect sizes across multiple outcomes, it appears that the number of days of stimulation might have a larger impact on outcomes than the number of pulses per day. This suggests that effects of rTMS on smoking cessation are cumulative and might require time to produce changes in behavior. Future studies with larger sample sizes, should examine whether Duration and Intensity interact to produce higher effect sizes.

Although clearly not conclusive, the impact of increasing Duration and Intensity on perceived research burden was less than expected. We speculate these findings might be an artifact of including only participants who received active stimulation because they were more likely to receive benefits of cessation, which might have outweighed the greater requirements. Future research will need to examine differences in perceived research burden between participants who received active and sham stimulation. Nonetheless, these findings suggest that the burden of participating in this study was not strongly linked with the actual number of rTMS sessions required. Future research will examine whether participants who reached study end after the onset of the pandemic experienced greater participant burden.

The parent study is ongoing and expected to meet modified accrual objectives in 2022. Findings from this study will provide a pre-pandemic comparison for the data collected during the pandemic. Reporting on pre-pandemic findings is important because the pandemic created an environment in which possible biases and confounds potentially impact outcomes. Pre- and post-pandemic comparisons can inform interpretations about biases and confounds should pre- and post-pandemic findings differ.

Finally, future research needs to examine the potential long-term neural adaptations from multiple sessions of rTMS. Although an isolated finding, one study reported a reflection effect, whereby one session of rTMS decreased DD of monetary gains, but also increased DD of monetary losses, a potentially negative finding (Sheffer et al., 2013). Therefore, future research should incorporate the examination of long-term paradoxical or counter therapeutic effects.

The strengths of this study include factorial design in which each participant is exposed to a level of each factor, allowing for the efficient examination of the main effects for Duration and Intensity in one study, eliminating confounds associated with systematic differences among pilot studies using different doses. This design also provides an estimate of the main effects of each factor in the presence of the other factor. Nonetheless, these findings are limited by a small sample size and lack of sham control comparisons. We did not include participants who received sham in this preliminary analysis for multiple reasons. Including sham participants would have doubled the number of cells and comparisons. In addition to the small number of participants who reached study end prior to the onset of the pandemic, the parent study randomized participants to active or sham in a 3–1 ratio. Many of the cells were simply too small to feasibly compare Duration and Intensity when the sham was included. Although including participants who smoke from 6 to 25 cigarettes per day might introduce uncontrolled variability, this limitation is tempered by permuted block randomization stratified by nicotine dependence level. Finally, all participants were motivated to quit based on the inclusion criteria, which limits generalizability of the results to treatment seeking individuals.

CONCLUSION

These findings provide preliminary support for targeting delay discounting as a therapeutic target for smoking cessation with rTMS. Greater Duration and Intensity of rTMS appear to have greater effects on delay discounting rates and multiple indicators of abstinence, with a small effect on participant burden. Findings provide a pre-pandemic comparison for the data collected during the pandemic and a basis to examine possible biases and confounds created by the COVID-19 pandemic in the parent study.

DATA AVAILABILITY STATEMENT

The data analyzed in this study is subject to the following licenses/restrictions: All data, and research materials will be available upon completion of the associated clinical trial with the appropriate permissions (clinical trial identifier: NCT03865472). Requests to access these datasets should be directed to the corresponding author or Clinicaltrials.gov.

ETHICS STATEMENT

The studies involving human participants were reviewed and approved by the Institutional Review Board of Roswell Park Comprehensive Cancer Center (#I-65718). The patients/participants provided their written informed consent to participate in this study.

AUTHOR CONTRIBUTIONS

AS, EC, MM, CH, WB, and CS: conceptualization. AS, AL, CR, RA, AB, LB, DV, HT, MM, and CS: methodology. AS, EC, and CS: formal analysis. MM, AL, CR, RA, AB, LB, DV, HT, MM, and CS: investigation. CS: resources, supervision, and funding acquisition. AS, EC, and AL: data curation. AS and CS: writing—original draft preparation. AS, EC, MM, CH, AL, CR, RA, AB, LB, DV, HT, MM, WB, and CE: writing—review and editing. AS: visualization. AL and CS: project administration. All authors have read and agreed to the published version of the manuscript.

FUNDING

This research was funded by the National Cancer Institute (R01 CA229415 PI: Sheffer). The content was solely the responsibility of the authors and does not necessarily represent the official views of the National Cancer Institute or the National Institutes of Health.

ACKNOWLEDGMENTS

We want to acknowledge all our participants who devoted their time and effort to our scientific community over many years and made advances in science possible. We also would like to acknowledge all the lab members, students, and trainees who helped with this project.

SUPPLEMENTARY MATERIAL

The Supplementary Material for this article can be found online at: https://www.frontiersin.org/articles/10.3389/fnhum.2022.920383/full#supplementary-material

REFERENCES

Alcaro, A., Brennan, A., and Conversi, D. (2021). The SEEKING drive and its fixation: a neuro-psycho-evolutionary approach to the pathology of addiction. *Front. Hum. Neurosci.* 15:635932. doi: 10.3389/fnhum.2021.635932

Alcaro, A., Huber, R., and Panksepp, J. (2007). Behavioral functions of the mesolimbic dopaminergic system: an affective neuroethological perspective. *Brain Res. Rev.* 56, 283–321. doi: 10.1016/j.brainresrev.2007.07.014

Azuero, A. (2016). A note on the magnitude of hazard ratios. *Cancer* 122, 1298–1299. doi: 10.1002/cncr.29924

Babb, S., Malarcher, A., Schauer, G., Asman, K., and Jamal, A. (2017). Quitting smoking among adults — united states, 2000–2015. *MMWR. Morb. Mortal. Wkly. Rep.* 65, 1457–1464. doi: 10.15585/mmwr.mm6552a1

Bickel, W. K., Athamneh, L. N., Basso, J. C., Mellis, A. M., DeHart, W. B., Craft, W. H., et al. (2019). Excessive discounting of delayed reinforcers as a trans-disease process: update on the state of the science. *Curr. Opin. Psychol.* 30, 59–64. doi: 10.1016/j.copsyc.2019.01.005

Bickel, W. K., Jarmolowicz, D. P., Terry Mueller, E., Koffarnus, M. N., and Gatchalian, K. M. (2012). Excessive discounting of delayed reinforcers as a trans-disease process contributing to addiction and other disease-related vulnerabilities: emerging evidence. *Pharmacol. Ther.*134, 287–297. doi: 10.1016/j.pharmthera.2012.02.004

Bickel, W. K., Koffarnus, M. N., Moody, L., and Wilson, A. G. (2014). The behavioral- and neuro-economic process of temporal discounting: a candidate behavioral marker of addiction. *Neuropharmacology* 76, 518–527. doi: 10.1016/j.neuropharm.2013.06.013

Bickel, W. K., Miller, M. L., Yi, R., Kowal, B. P., Lindquist, D. M., and Pitcock, J. A. (2007). Behavioral and neuroeconomics of drug addiction: competing neural systems and temporal discounting processes. *Drug Alcohol Depend.* 90, S85–S91. doi: 10.1016/j.drugalcdep.2006.09.016

Bickel, W. K., Snider, S. E., Quisenberry, A. J., Stein, J. S., and Hanlon, C. A. (2016). Competing neurobehavioral decision systems theory of cocaine addiction: from mechanisms to therapeutic opportunities. *Prog. Brain Res.* 223, 269–293. doi: 10.1016/bs.pbr.2015.07.009

Brody, A. L., Mandelkern, M. A., London, E. D., Childress, A. R., Lee, G. S., Bota, R. G., et al. (2002). Brain metabolic changes during cigarette craving. *Arch. Gen. Psychiatry* 59, 1162–1172. doi: 10.1001/archpsyc.59.12.1162

Brown, R. A., Burgess, E. S., Sales, S. D., Whiteley, J. A., Evans, D. M., and Miller, I. W. (1998). Reliability and validity of a smoking timeline follow-back interview. *Psychol. Addict. Behav.* 12, 101–112. doi: 10.1037/0893-164X.12.2.101

Carl, E., Liskiewicz, A., Rivard, C., Alberico, R., Belal, A., Mahoney, M. C., et al. (2020). Dosing parameters for the effects of high-frequency transcranial magnetic stimulation on smoking cessation: study protocol for a randomized factorial sham-controlled clinical trial. *BMC Psychol.* 8:42. doi: 10.1186/s40359-020-00403-7

Cieslik, E. C., Zilles, K., Caspers, S., Roski, C., Kellermann, T. S., Jakobs, O., et al. (2012). Is There "One" DLPFC in cognitive action control? Evidence for heterogeneity from co-activation-based parcellation. *Cereb. Cortex* 23, 2677–2689. doi: 10.1093/cercor/bhs256

Commons, M. L., Mazur, J. E., Nevin, J. A., and Rachlin, H. (2013). *The Effect of Delay and of Intervening Events on Reinforcement Value: Quantitative Analyses of Behavior*, Vol. V. London: Psychology Press. doi: 10.4324/9781315825502

Coughlin, L. N., Tegge, A. N., Sheffer, C. E., and Bickel, W. K. (2020). A machine-learning approach to predicting smoking cessation treatment outcomes. *Nicotine Tob. Res.* 22, 415–422. doi: 10.1093/ntr/nty259

Ekhtiari, H., Tavakoli, H., Addolorato, G., Baeken, C., Bonci, A., Campanella, S., et al. (2019). Transcranial electrical and magnetic stimulation (tES and TMS) for addiction medicine: a consensus paper on the present state of the science and the road ahead. *Neurosci. Biobehav. Rev.* 104, 118–140. doi: 10.1016/j.neubiorev.2019.06.007

Enzmann, D. (2015). Notes on effect size measures for the difference of means from two independent groups: the case of Cohen'sd and Hedges'g. *January* 12:2015.

Ernst, M., Heishman, S. J., Spurgeon, L., and London, E. D. (2001). Smoking history and nicotine effects on cognitive performance. *Neuropsychopharmacology* 25, 313–319. doi: 10.1016/S0893-133X(01)00257-3

Everitt, B. J., and Robbins, T. W. (2005). Neural systems of reinforcement for drug addiction: from actions to habits to compulsion. *Nat. Neurosci.* 8, 1481–1489. doi: 10.1038/nn1579

Fagerstrom, K. (2012). Determinants of tobacco use and renaming the FTND to the fagerstrom test for cigarette dependence. *Nicotine Tob. Res.* 14, 75–78. doi: 10.1093/ntr/ntr137

Fiocchi, S., Chiaramello, E., Luzi, L., Ferrulli, A., Bonato, M., Roth, Y., et al. (2018). Deep transcranial magnetic stimulation for the addiction treatment: electric field distribution modeling. *IEEE J. Electromagn. RF Microw. Med. Biol.* 2, 242–248. doi: 10.1109/JERM.2018.2874528

Fitzgerald, P. B., Fountain, S., and Daskalakis, Z. J. (2006). A comprehensive review of the effects of rTMS on motor cortical excitability and inhibition. *Clin. Neurophysiol.* 117, 2584–2596. doi: 10.1016/j.clinph.2006.06.712

Garfield, J. B. B., Lubman, D. I., and Yücel, M. (2014). Anhedonia in substance use disorders: a systematic review of its nature, course and clinical correlates. *Aust. N. Z. J. Psychiatry* 48, 36–51. doi: 10.1177/0004867413508455

Gross, B., Brose, L., Schumann, A., Ulbricht, S., Meyer, C., Völzke, H., et al. (2008). Reasons for not using smoking cessation aids. *BMC Public Health* 8:129. doi: 10.1186/1471-2458-8-129

Hanlon, C. A., Dowdle, L. T., Austelle, C. W., DeVries, W., Mithoefer, O., Badran, B. W., et al. (2015). What goes up, can come down: novel brain stimulation paradigms may attenuate craving and craving-related neural circuitry in

substance dependent individuals. *Brain Res.* 1628, 199–209. doi: 10.1016/j.brainres.2015.02.053

Heatherton, T. F., Kozlowski, L. T., Frecker, R. C., and Fagerström, K. O. (1991). The fagerström test for nicotine dependence: a revision of the fagerström tolerance questionnaire. *Br. J. Addict.* 86, 1119–1127. doi: 10.1111/j.1360-0443.1991.tb01879.x

Hughes, J. R., Keely, J. P., Niaura, R. S., Ossip-Klein, D. J., Richmond, R. L., and Swan, G. E. (2003). Measures of abstinence in clinical trials: issues and recommendations. *Nicotine Tob. Res.* 5, 13–25. doi: 10.1080/1462220031000070552

Ialongo, C. (2016). Understanding the effect size and its measures. *Biochem. Med.* 26, 150–163. doi: 10.11613/BM.2016.015

Kim, H.-Y. (2015). Statistical notes for clinical researchers: effect size. *Restor. Dent. Endod.* 40, 328–331. doi: 10.5395/rde.2015.40.4.328

Kirby, K. N. (1997). Bidding on the future: evidence against normative discounting of delayed rewards. *J. Exp. Psychol. Gen.* 126, 54–70. doi: 10.1037/0096-3445.126.1.54

Koffarnus, M. N., and Bickel, W. K. (2014). A 5-trial adjusting delay discounting task: accurate discount rates in less than one minute. *Exp. Clin. Psychopharmacol.* 22, 222–228. doi: 10.1037/a0035973

Koffarnus, M. N., Jarmolowicz, D. P., Mueller, E. T., and Bickel, W. K. (2013). Changing delay discounting in the light of the competing neurobehavioral decision systems theory: a review. *J. Exp. Anal. Behav.* 99, 32–57. doi: 10.1002/jeab.2

Koob, G. F. (2008a). A role for brain stress systems in addiction. *Neuron* 59, 11–34. doi: 10.1016/j.neuron.2008.06.012

Koob, G. F. (2008b). Hedonic homeostatic dysregulation as a driver of drug-seeking behavior. *Drug Discov. Today Dis. Models* 5, 207–215. doi: 10.1016/j.ddmod.2009.04.002

Koob, G. F., Arends, M. A., and Le Moal, M. (2014). *Drugs, Addiction, and the Brain*. Cambridge, MA: Academic Press.

Lakens, D. (2013). Calculating and reporting effect sizes to facilitate cumulative science: a practical primer for t-tests and ANOVAs. *Front. Psychol.* 4:863. doi: 10.3389/fpsyg.2013.00863

Le, H., and Marcus, J. (2012). The overall odds ratio as an intuitive effect size index for multiple logistic regression. *Educ. Psychol. Meas.* 72, 1001–1014. doi: 10.1177/0013164412445298

Lingler, J. H., Schmidt, K. L., Gentry, A. L., Hu, L., and Terhorst, L. A. (2014). A new measure of research participant burden: brief report. *J. Empir. Res. Hum. Res. Ethics* 9, 46–49. doi: 10.1177/1556264614545037

Lu, M., and Ueno, S. (2017). Comparison of the induced fields using different coil configurations during deep transcranial magnetic stimulation. *PLoS One* 12:e0178422. doi: 10.1371/journal.pone.0178422

MacKillop, J., Amlung, M. T., Wier, L. M., David, S. P., Ray, L. A., Bickel, W. K., et al. (2012). The neuroeconomics of nicotine dependence: a preliminary functional magnetic resonance imaging study of delay discounting of monetary and cigarette rewards in smokers. *Psychiatry Res. Neuroimaging* 202, 20–29. doi: 10.1016/j.pscychresns.2011.10.003

Maher, J. M., Markey, J. C., and Ebert-May, D. (2013). The other half of the story: effect size analysis in quantitative research. *CBE Life Sci. Educ.* 12, 345–351. doi: 10.1187/cbe.13-04-0082

McBride, D., Barrett, S. P., Kelly, J. T., Aw, A., and Dagher, A. (2006). Effects of expectancy and abstinence on the neural response to smoking cues in cigarette smokers: an fMRI study. *Neuropsychopharmacology* 31, 2728–2738. doi: 10.1038/sj.npp.1301075

McClure, S. M., and Bickel, W. K. (2014). A dual-systems perspective on addiction: contributions from neuroimaging and cognitive training. *Ann. N. Y. Acad. Sci.* 1327, 62–78. doi: 10.1111/nyas.12561

McClure, S. M., Ericson, K. M., Laibson, D. I., Loewenstein, G., and Cohen, J. D. (2007). Time discounting for primary rewards. *J. Neurosci.* 27, 5796–5804. doi: 10.1523/JNEUROSCI.4246-06.2007

Mooney, M., Leventhal, A., and Hatsukami, D. (2006). Attitudes and knowledge about nicotine and nicotine replacement therapy. *Nicotine Tob. Res.* 8, 435–446. doi: 10.1080/14622200600670397

Morphett, K., Partridge, B., Gartner, C., Carter, A., and Hall, W. (2015). Why don't smokers want help to quit? A qualitative study of smokers' attitudes towards assisted vs. unassisted quitting. *Int. J. Environ. Res. Public Health* 12, 6591–6607. doi: 10.3390/ijerph120606591

Mukherjee, K. (2010). A dual system model of preferences under risk. *Psychol. Rev.* 117, 243–255. doi: 10.1037/a0017884

Odum, A. L. (2011). Delay discounting: i'm a k. you're a k. *J. Exp. Anal. Behav.* 96, 427–439. doi: 10.1901/jeab.2011.96-423

Patton, J. H., Stanford, M. S., and Barratt, E. S. (1995). Factor structure of the barratt impulsiveness scale. *J. Clin. Psychol.* 51, 768–774. doi: 10.1002/1097-4679(199511)51:6<768::AID-JCLP2270510607>3.0.CO;2-1

Rhea, M. R. (2004). Determining the magnitude of treatment effects in strength training research through the use of the effect size. *J. Strength Cond. Res.* 18, 918–920. doi: 10.1519/00124278-200411000-00040

Robinson, T. E., and Berridge, K. C. (2001). Incentive-sensitization and addiction. *Addiction* 96, 103–114. doi: 10.1046/j.1360-0443.2001.9611038.x

Robinson, T. E., and Berridge, K. C. (2003). Addiction. *Annu. Rev. Psychol.* 54, 25–53. doi: 10.1146/annurev.psych.54.101601.145237

Robinson, T. E., and Berridge, K. C. (2008). Review. the incentive sensitization theory of addiction: some current issues. *Philos. Trans. R. Soc. Lond. B Biol. Sci.* 363, 3137–3146. doi: 10.1098/rstb.2008.0093

Rossi, S., Hallett, M., Rossini, P. M., and Pascual-Leone, A. (2011). Screening questionnaire before TMS: an update. *Clin. Neurophysiol.* 122:1686. doi: 10.1016/j.clinph.2010.12.037

Rung, J. M., and Madden, G. J. (2018). Experimental reductions of delay discounting and impulsive choice: a systematic review and meta-analysis. *J. Exp. Psychol. Gen.* 147, 1349–1381. doi: 10.1037/xge0000462

Salamone, J. D., and Correa, M. (2002). Motivational views of reinforcement: implications for understanding the behavioral functions of nucleus accumbens dopamine. *Behav. Brain Res.* 137, 3–25. doi: 10.1016/S0166-4328(02)00282-6

Sharpe, D. (2015). Chi-Square test is statistically significant: now what? *Pract. Assess. Res. Eval.* 20:8.

Sheffer, C. E., Bickel, W. K., Brandon, T. H., Franck, C. T., Deen, D., Panissidi, L., et al. (2018). Preventing relapse to smoking with transcranial magnetic stimulation: feasibility and potential efficacy. *Drug Alcohol Depend.* 182, 8–18. doi: 10.1016/j.drugalcdep.2017.09.037

Sheffer, C. E., Christensen, D. R., Landes, R., Carter, L. P., Jackson, L., and Bickel, W. K. (2014). Delay discounting rates: a strong prognostic indicator of smoking relapse. *Addict. Behav.* 39, 1682–1689. doi: 10.1016/j.addbeh.2014.04.019

Sheffer, C. E., Mennemeier, M., Landes, R. D., Bickel, W. K., Brackman, S., Dornhoffer, J., et al. (2013). Neuromodulation of delay discounting, the reflection effect, and cigarette consumption. *J. Subst. Abuse Treat.* 45, 206–214. doi: 10.1016/j.jsat.2013.01.012

Sheffer, C., Mackillop, J., McGeary, J., Landes, R., Carter, L., Yi, R., et al. (2012). Delay discounting, locus of control, and cognitive impulsiveness independently predict tobacco dependence treatment outcomes in a highly dependent, lower socioeconomic group of smokers. *Am. J. Addict.* 21, 221–232. doi: 10.1111/j.1521-0391.2012.00224.x

Smith, A. L., Carter, S. M., Chapman, S., Dunlop, S. M., and Freeman, B. (2015). Why do smokers try to quit without medication or counselling? A qualitative study with ex-smokers. *BMJ Open* 5:e007301. doi: 10.1136/bmjopen-2014-007301

Sobell, L. C., and Sobell, M. B. (1992). "Timeline Follow-Back," in *Measuring Alcohol Consumption: Psychosocial and Biochemical Methods*, eds R. Z. Litten and J. P. Allen (Totowa, NJ: Humana Press), 41–72. doi: 10.1007/978-1-4612-0357-5_3

Spano, M. C., Lorusso, M., Pettorruso, M., Zoratto, F., Di Giuda, D., Martinotti, G., et al. (2019). Anhedonia across borders: transdiagnostic relevance of reward dysfunction for noninvasive brain stimulation endophenotypes. *CNS Neurosci. Ther.* 25, 1229–1236. doi: 10.1111/cns.13230

SRNT Subcommittee on Biochemical Verification (2002). Biochemical verification of tobacco use and cessation. *Nicotine Tob. Res.* 4, 149–159. doi: 10.1080/14622200210123581

Thut, G., and Pascual-Leone, A. (2010). A review of combined TMS-EEG studies to characterize lasting effects of repetitive TMS and assess their usefulness in cognitive and clinical neuroscience. *Brain Topogr.* 22, 219–232. doi: 10.1007/s10548-009-0115-4

Tomczak, M., and Tomczak, E. (2014). The need to report effect size estimates revisited. An overview of some recommended measures of effect size. *Trends Sport Sci.* 1, 19–25.

United States Public Health Service Office of the Surgeon General, and National Center for Chronic Disease Prevention and Health Promotion

(US) Office on Smoking and Health (2020). *Smoking Cessation: A Report of the Surgeon General*. Washington, DC: US Department of Health and Human Services.

Xu, J., Mendrek, A., Cohen, M. S., Monterosso, J., Rodriguez, P., Simon, S. L., et al. (2005). Brain activity in cigarette smokers performing a working memory task: effect of smoking abstinence. *Biol. Psychiatry* 58, 143–150. doi: 10.1016/j.biopsych.2005.03.028

Zangen, A., Moshe, H., Martinez, D., Barnea-Ygael, N., Vapnik, T., Bystritsky, A., et al. (2021). Repetitive transcranial magnetic stimulation for smoking cessation: a pivotal multicenter double-blind randomized controlled trial. *World Psychiatry* 20, 397–404. doi: 10.1002/wps.20905

Conflict of Interest: MM had provided expert testimony on the health effects of smoking in lawsuits filed against the tobacco industry. He has also received research support from Pizer, Inc., for an on-going clinical trial of smoking cessation, and has previously served on external advisory panels sponsored by Pfizer to promote smoking cessation in clinical settings.

The remaining authors declare that the research was conducted in the absence of any commercial or financial relationships that could be construed as a potential conflict of interest.

Publisher's Note: All claims expressed in this article are solely those of the authors and do not necessarily represent those of their affiliated organizations, or those of the publisher, the editors and the reviewers. Any product that may be evaluated in this article, or claim that may be made by its manufacturer, is not guaranteed or endorsed by the publisher.

frontiers | Frontiers in Human Neuroscience

TYPE Systematic Review
PUBLISHED 04 August 2022
DOI 10.3389/fnhum.2022.940759

OPEN ACCESS

EDITED BY
Joao Miguel Castelhano,
University of Coimbra, Portugal

REVIEWED BY
Alena Damborská,
Masaryk University, Czechia
Shalini S. Naik,
Post Graduate Institute of Medical Education and Research (PGIMER), India

*CORRESPONDENCE
Daphne Voineskos
daphne.voineskos@camh.ca

SPECIALTY SECTION
This article was submitted to Brain Imaging and Stimulation, a section of the journal Frontiers in Human Neuroscience

RECEIVED 11 May 2022
ACCEPTED 28 June 2022
PUBLISHED 04 August 2022

CITATION
Strafella R, Chen R, Rajji TK, Blumberger DM and Voineskos D (2022) Resting and TMS-EEG markers of treatment response in major depressive disorder: A systematic review. *Front. Hum. Neurosci.* 16:940759. doi: 10.3389/fnhum.2022.940759

Resting and TMS-EEG markers of treatment response in major depressive disorder: A systematic review

Rebecca Strafella[1,2], Robert Chen[1,3,4], Tarek K. Rajji[1,2,5,6], Daniel M. Blumberger[1,2,5] and Daphne Voineskos[1,2,3,5]*

[1]Institute of Medical Science, University of Toronto, Toronto, ON, Canada, [2]Temerty Centre for Therapeutic Brain Intervention, Campbell Family Mental Health Research Institute, Centre for Addiction and Mental Health, Toronto, ON, Canada, [3]Krembil Research Institute, Toronto Western Hospital, University Health Network, Toronto, ON, Canada, [4]Division of Neurology, Department of Medicine, University of Toronto, Toronto, ON, Canada, [5]Department of Psychiatry, Temerty Faculty of Medicine, University of Toronto, Toronto, ON, Canada, [6]Toronto Dementia Research Alliance, University of Toronto, Toronto, ON, Canada

Electroencephalography (EEG) is a non-invasive method to identify markers of treatment response in major depressive disorder (MDD). In this review, existing literature was assessed to determine how EEG markers change with different modalities of MDD treatments, and to synthesize the breadth of EEG markers used in conjunction with MDD treatments. PubMed and EMBASE were searched from 2000 to 2021 for studies reporting resting EEG (rEEG) and transcranial magnetic stimulation combined with EEG (TMS-EEG) measures in patients undergoing MDD treatments. The search yielded 966 articles, 204 underwent full-text screening, and 51 studies were included for a narrative synthesis of findings along with confidence in the evidence. In rEEG studies, non-linear quantitative algorithms such as theta cordance and theta current density show higher predictive value than traditional linear metrics. Although less abundant, TMS-EEG measures show promise for predictive markers of brain stimulation treatment response. Future focus on TMS-EEG measures may prove fruitful, given its ability to target cortical regions of interest related to MDD.

KEYWORDS

major depressive disorder (MDD), electroencephalography (EEG), transcranial magnetic stimulation (TMS), TMS-EEG, biomarkers, repetitive transcranial magnetic stimulation (rTMS), antidepressant, treatment

Introduction

Major depressive disorder (MDD) is a leading cause of disability worldwide and is increasing in prevalence (Friedrich, 2017). Unfortunately, little progress has been made in identifying biological indicators of treatment response, and much intervention is *via* trial-and-error. While some possible neurobiological indicators of response have been identified using genetic and imaging studies (reviewed Belmaker, 2008; Kupfer et al., 2012), a less-costly, non-invasive option is electroencephalography (EEG), which indexes neural activity with high temporal resolution (Berger, 1929).

EEG has several investigational uses, characterizing cortical activity after perturbation, or reflecting frequency bands associated with specific cognitive patterns (Freeman and Quiroga, 2013). The combination of transcranial magnetic stimulation with EEG (TMS-EEG) has sparked interest as a way to record direct and downstream cortical responses to a targeted magnetic stimulus (Farzan et al., 2016).

EEG provides multiple avenues to identify putative markers differentiating treatment responders and non-responders in MDD. Common interventions for MDD include pharmacotherapy, psychotherapy, and brain stimulation (Voineskos et al., 2020). However, there is a lack of synthesis of evidence in the MDD literature regarding the utility of EEG indices as markers of treatment response. To date, one meta-analysis has focused solely on quantitative EEG to examine markers of treatment response (Widge et al., 2019), but did not find reliable indices or include other types of EEG investigations, such as TMS-EEG. Due to the breadth of EEG markers in the existing literature, there is a need to combine evidence to understand which markers consistently demonstrate the potential for clinical utility across therapeutic interventions for MDD. Identifying potential biological predictors of response will hopefully lead to a departure from the trial-and-error approach of MDD treatment, although several steps remain before declaring this achievement. Below, we will briefly define both resting EEG (rEEG) and TMS-EEG prior to presenting our systematic review of relevant findings.

Resting EEG

Resting EEG (rEEG) indexes brain activity without stimulus presentation, typically *via* 64 electrodes distributed with the 10–20 system (Jasper, 1958). REEG frequency bands characterize the signal in delta to gamma domains (Niedermeyer, 1999). The low frequency delta band (<4 Hz) appears in stage 3 non-rapid eye movement sleep and is not typically seen in rEEG (Amzica and Steriade, 1998). Theta (4–8 Hz) is related to emotional processing and internal focus (Aftanas and Golocheikine, 2001; Aftanas et al., 2002). Frontal theta activity may reflect neurotransmission to and from the anterior cingulate cortex (ACC) (Asada et al., 1999), regions implicated in MDD (Spellman and Liston, 2020). The alpha (8–12 Hz) band appears during relaxation and is the most dominant band present in occipital or posterior regions (Niedermeyer, 1999). In MDD, the presence of alpha indicates brain regions with lower activity (Bruder et al., 1997). Beta (12–30 Hz) and gamma bands (>30 Hz) are considered "high-frequency", reflecting alertness and concentration (Abhang et al., 2016) and attention and executive functioning (Freeman and Quiroga, 2013), respectively. Deciphering the relevance of frequency band activity may have potential for MDD response markers.

TMS-EEG

Transcranial magnetic stimulation (TMS) non-invasively stimulates the brain, inducing electric currents in neurons *via* electromagnetic induction (i.e., Faraday's law) (Barker et al., 1985). The TMS stimulus is thought to act on inhibitory interneurons and results in the depolarization of pyramidal cells (Kobayashi and Pascual-Leone, 2003), which can be captured *via* EEG. The combination of TMS-EEG then provides an accurate window into the direct localized and downstream cortical effects of the TMS pulse, and can provide measurable output for cortical regions outside of the motor and somatosensory cortices. Single-pulse TMS-EEG produces TMS evoked potentials (TEPs) reflecting excitatory and inhibitory neurotransmission (Farzan et al., 2016) and can index both inter and intra-regional connectivity between cortico-cortical and cortico-subcortical areas (Daskalakis et al., 2012). Unlike rEEG, TMS-EEG allows for both direct stimulation and recording of output from the cortical region of interest. Both cortical responses at the stimulated region, as well as downstream effects can then be interpreted. These measures have identified cortical abnormalities in MDD, that may be used as markers of treatment response.

Objectives of review

We conducted a formal narrative synthesis of the included studies, which focused on rEEG and TMS-EEG indexing the effects of antidepressant interventions (pharmacotherapy, brain stimulation, other therapies) on resulting outcomes (response or remission from a major depressive episode). The objectives were to: report changes in EEG measures of treatment; compare changes in EEG measures following treatment in responders and non-responders; report whether EEG measures at baseline predicted response.

Methods

Search strategy

PubMed and EMBASE were searched between January 1st, 2000 and December 31st, 2021 for publications studying treatment effects (i.e., pharmacotherapies and non-pharmacotherapies) on EEG (rEEG and TMS-EEG) in patients with MDD. Search terms are detailed in the Appendix. Results were filtered to only include human studies reported in English.

Inclusion criteria

Studies included examined subjects with unipolar MDD (DSM-IV and DSM-5 criteria) who underwent antidepressant treatment in conjunction with EEG measures. Studies must have reported rEEG or TMS-EEG measures before, during, or post-treatment.

Exclusion criteria

Case studies, review articles, protocols, posters, and conference abstracts were excluded (i.e., incorrect design). Studies reporting on animal populations, healthy subjects, bipolar depression, or conditions other than unipolar MDD were excluded (i.e., incorrect patient population). Non-therapeutic interventions were also excluded (i.e., incorrect intervention). Studies reporting antidepressant effects using techniques other than EEG (i.e. magnetoencephalography and electromyography), were excluded (i.e., incorrect EEG type). Sleep EEG, ictal EEG, neurofeedback studies, resting connectivity EEG, event-related EEG, and machine learning studies were excluded for focus and brevity (i.e., incorrect outcome). For the purpose of this review, *incorrect* was used to denote criteria that deemed to be out of scope.

Data extraction

Two study authors (RS, DV) conducted an independent literature search using pre-defined inclusion and exclusion criteria following duplicate removal. Covidence (www.covidence.org), an internet-based software, facilitated screening and extraction. Following initial screening, eligible studies underwent full-text review. Conflicts between authors were resolved by discussion. Approved studies were then moved to data extraction.

Quality of evidence assessment

Quality of evidence assessment was performed using the Grading of Recommendations Assessment, Development, and Evaluation (GRADE) working group methodology (Schünemann et al., 2008). Quality was marked with four levels: high, moderate, low, very low. High studies were randomized, double-blinded, and placebo-controlled; moderate were randomized without blinding; low were non-randomized with a placebo or control group; very low were non-randomized without a placebo or control group. Studies marked *Very low* were excluded to focus on higher quality, and reliable designs.

Results

Study selection

Figure 1 provides full information on the study selection process, using the Preferred Reporting Items for Systematic Reviews and Meta-Analysis (PRISMA).

Included study characteristics

Search terms yielded 966 studies after applying filters, 916 after removing duplicates. Primary screening excluded 712 for irrelevance based on the abstract. Two hundred and four underwent full-text review. One hundred and eighteen were excluded for incorrect design, outcomes, EEG type, patient population, or intervention. For more details on reasons for exclusion, see Section Exclusion criteria. Thirty-five studies had a *Very low* quality assessment and were removed for brevity. Overall, 51 studies underwent qualitative synthesis.

Quality ratings are included in Tables 1, 2. After exclusion of *Very low* quality studies, the vast majority of studies were marked as *High*, followed by *Moderate* and *Low* ratings. The following sections are presented in order of decreasing quality rating.

Resting EEG studies

Forty-seven studies examined rEEG markers of treatment response to pharmacotherapies, brain stimulation therapies, and other therapies (Table 1). These studies reported quantitative rEEG measures such as power analysis (Cook, 2002; Knott et al., 2002; Deslandes et al., 2010; Widge et al., 2013; Gollan et al., 2014; Jaworska et al., 2014, p. 201; Leuchter et al., 2002, 2017; Arns et al., 2014, 2016; Alexander et al., 2019; Bailey et al., 2019; Cao et al., 2019; Cook et al., 2019; McMillan et al., 2020; Szumska et al., 2021), cordance (Cook, 2002; Leuchter et al., 2002; Hunter et al., 2006, 2009, 2010a,b; Cook et al., 2009; Bares et al., 2015a; Bailey et al., 2019; Cao et al., 2019; de la Salle et al., 2020), current density (Pizzagalli et al., 2001, 2018; Mulert et al., 2007a,b; Korb et al., 2009, 2011; Narushima et al., 2010; Tenke et al., 2011; Hunter et al., 2013, p. 201; Jaworska et al., 2014; Almeida Montes et al., 2015; Arns et al., 2015), a weighted combination of alpha and theta power compared over time (termed: antidepressant treatment response (ATR) index) (Leuchter et al., 2009a,b; Hunter et al., 2011; Cook et al., 2013; Widge et al., 2013), vigilance (Olbrich et al., 2016; Schmidt et al., 2017; Sander et al., 2018; Ip et al., 2021), normalizations and abnormalities (Arns et al., 2017; van der Vinne et al., 2019a,b), individualized alpha-peak frequency (iAPF) (Bailey et al., 2019; Philip et al., 2019), entropy (Jaworska et al., 2017), and other algorithms (Arns et al., 2014).

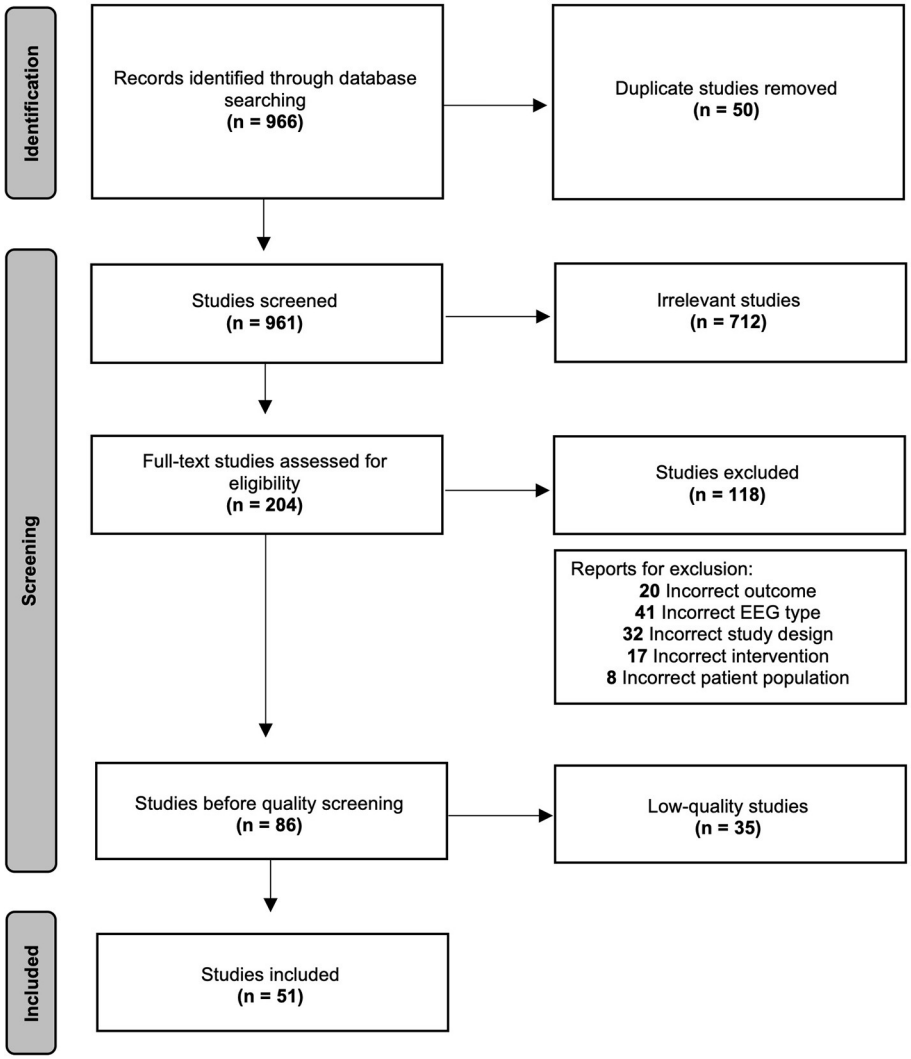

FIGURE 1
Preferred reporting items for systematic reviews and meta-analysis (PRISMA) flow diagram.

rEEG studies included a variety of pharmacotherapies, brain stimulation therapies, and other therapies. Pharmacotherapy studies used various dosages, schedules, and antidepressant classes of medication [serotonin-reuptake inhibitors (SSRI), serotonin-norepinephrine reuptake inhibitors (SNRI), tricyclic antidepressants (TCA), dopamine reuptake inhibitors (DRI), mirtazapine, or combinations]. Some used fixed dosages and treatment lengths, others followed naturalistic designs. Brain stimulation interventions included repetitive transcranial magnetic stimulation (rTMS), synchronized transcranial magnetic stimulation (sTMS), and transcranial alternating current stimulation (tACS). Treatment parameters varied by stimulation target, intensity, and number of treatments. Other therapies included IV ketamine, psychotherapies (i.e., mindfulness-based cognitive therapy, behavioral activation treatment), aerobic training, and partial sleep deprivation. Across treatment types, rEEG protocols varied in recording length, electrode placement, number of electrodes of interest, eyes closed vs. open and outcome measures. The following section will focus on reported rEEG measures by treatment type.

Power analysis

Frequency bands are computed by absolute or relative band power. Absolute band power measures all activity within a specific range, whereas relative band power expresses band power as a percentage of total signal power.

Antidepressant pharmacotherapies

Three high quality rated studies reported power analysis findings. One week of SSRI resulted in decreased relative alpha power and increased relative delta-theta (Leuchter et al.,

10.3389/fnhum.2022.940759

TABLE 1 Resting EEG outcomes for antidepressant, brain stimulation, and other studies.

rEEG measure	References	*n* (F)	EEG protocol (# of electrode; reference; electrode placement)	rEEG protocol (recording time; EO vs. EC; rEEG measure)	Recording period	Treatment type	Treatment name	Treatment protocol	Treatment length	Quality assessment	Outcome measure	Brain region	Change in measure following treatment	Association with response
Power analysis														
	Szumska et al., 2021	20 (11)	64 electrodes; Cz reference; 10–20 system	3 min; EO and EC; α (8–13 Hz) band.	Baseline, post-treatment	Other therapies	Mindfulness-based cognitive therapy	2.5 h group sessions	8 sessions	Moderate	α asymmetry	FR	NS	NA
	McMillan et al., 2020	26 (13)	64 electrodes; FCz reference; NA	NA; NA; δ (1–4 Hz), θ (4–8 Hz), α (8–13 Hz), High β (28–40 Hz), Low γ (42–53 Hz), High γ (55–67 Hz) bands.	From time of infusion (few mins)	Other therapies	Ketamine or placebo	Ketamine 0.25 mg/kg.	1 infusion	High	θ power; High β power; Low γ power; High γ power; δ power; α power; Low β power	NA	↑; ↑; ↑; ↑; ↓; ↓; ↓	No; No; No; No; No; No; No
	Alexander et al., 2019	32 (27)	128 electrodes; Cz reference; 10–20 system	2 min; EC and EO; α (8–12 Hz) band.	Baseline, After 5 days of treatment, 4 week follow-up	Brain stimulation therapies	tACS or sham	10 Hz-tACS ($n = 10$) or 40 Hz-tACS ($n = 11$) or Active sham at 10 Hz ($n = 11$).	5 sessions	High	α power	FR	↓ Over LH (10 Hz- tACS only)	No
	Bailey et al., 2019	42 (23)	30 electrodes; CPz reference; NA	3 min; EO and EC; θ (4–8 Hz), α (8–13 Hz) bands.	Baseline, After 1-week of treatment, post-treatment	Brain stimulation therapies	rTMS	110% RMT, HF L-DLPFC or LF R-DLPFC or BL rTMS (CJ).	15 sessions	Low	θ power; α power	NA	NS; NS	No; No
	Cao et al., 2019	37 (32)	4 electrodes; A2 reference; NA	10 min; EC; δ (1–3.5 Hz), θ (4–7.5 Hz), lower α (8–10 Hz), upper α (10.5–12 Hz) bands.	Baseline, post-treatment	Other therapies	Ketamine or placebo	Ketamine 0.5 or 0.2 mg/kg.	1 infusion	High	Relative θ power; Relative α power	NA	↓; ↓	Yes; Yes
	Cook et al., 2019	16 (NA)	35 electrodes; Pz reference; 10–20 system	NA; EC; δ (0.5–4 Hz), θ (4–8 Hz), α (8–12 Hz), β (12–20 Hz) bands.	Baseline, Post-treatment	Brain stimulation therapies	sTMS or sham	sTMS ($n = 10$) or sham ($n = 6$).	6 weeks	High	Absolute power; Relative power	NA	NS; NS	NA; NA

(Continued)

TABLE 1 Continued

rEEG measure	References	*n* (F)	EEG protocol (# of electrode; reference; electrode placement)	rEEG protocol (recording time; EO vs. EC; rEEG measure)	Recording period	Treatment type	Treatment name	Treatment protocol	Treatment length	Quality assessment	Outcome measure	Brain region	Change in measure following treatment	Association with response
	Leuchter et al., 2017	194 (124)	35 electrodes; Pz reference; NA	10 min; EC; δ + θ (2.5–8 Hz) or α (8–12 Hz) bands.	Baseline, After 1-week of treatment	Antidepressant pharmacotherapies	Escitalopram (SSRI) or placebo	Escitalopram ($n = 143$) 10 mg.	7 weeks	High	δ-θ power; α power	NA	↑ in SSRI group; ↓ in SSRI group	Yes; Yes
	Arns et al., 2016	655 (378)	26 electrodes; Average mastoid reference; 10–20 system	2 min; EO and EC; α (NA) band.	Baseline	Antidepressant pharmacotherapies	Escitalopram (SSRI) or Sertraline (SSRI) or Venlafaxine-XR (SNRI)	Escitalopram ($n = 217$) 10–20 mg. Sertraline ($n = 234$) 50–200 mg. Venlafaxine-XR ($n = 204$) 75–255 mg.	8 weeks	Moderate	α power	FR	↑ Right FR in SSRI group only.	Yes, for F only
	Arns et al., 2014	90 (49)	26 electrodes; Average mastoid reference; 10–20 system	2 min; EC and EO; α (7–13 Hz) band.	Baseline	Brain stimulation therapies	rTMS and psychotherapy	110% MT, HF L-DLPFC or LF R-DLPFC rTMS/	21 sessions	Low	α power	NA	NS	NA
	Gollan et al., 2014	37 (26)	20 electrodes; Average mastoid reference; 10–20 system	8 min; EC and EO; α (8–13 Hz) bands.	Baseline, Post-treatment	Other therapies	Behavioral Activation Treatment	CJ	16 sessions	Low	α asymmetry	FR	NS	No
	Jaworska et al., 2014	51 (28)	32 electrodes; Average mastoid reference; 10-10 system	3 min; EC; α (10.5–13 Hz) band.	Baseline, After 1-week of treatment	Antidepressant pharmacotherapies	Escitalopram (SSRI) or Bupropion (DRI) or SSRI + DRI	Escilatopram ($n = 17$) 10–40 mg. Bupropion ($n = 16$) 150–450 mg.	12 weeks	Moderate (without placebo-controlled)	α power	FR	↓ in SSRI group	Yes
	Widge et al., 2013	180 (NA)	4 electrodes; NA; NA	30 s; EO; α (8.5–12 Hz), β (12–20 Hz), θ (2–8.5 Hz) bands.	Baseline	Brain stimulation therapies	rTMS or sham	120% MT, HF L-DLPFC rTMS or sham.	6 weeks	Moderate (single-blinded)	α power; β power; θ power	NA	NA; NA; NA	NS; NS; NS
	Deslandes et al., 2010	20 (14)	20 electrodes; Linked ears reference; 10–20 system	8 min; NA; α (8–13 Hz) band.	Baseline, Post-treatment	Other therapies	Exercise + pharmacotherapy (Decided by physician)	Exercise group + pharmacotherapy (CJ) ($n = 10$) or pharmacotherapy only (CJ) (n=10)	1 year (2 exercise	Low	Absolute α power	NA	↓ pharmacotherapy group only	No

(Continued)

10.3389/fnhum.2022.940759

TABLE 1 Continued

rEEG measure	References	*n* (F)	EEG protocol (# of electrode; reference; electrode placement)	rEEG protocol (recording time; EO vs. EC; rEEG measure)	Recording period	Treatment type	Treatment name	Treatment protocol	Treatment length	Quality assessment	Outcome measure	Brain region	Change in measure following treatment	Association with response
	Cook, 2002	51 (32)	35 electrodes; Pz reference; 10–20 system	NA; EC; θ (4–8 Hz) band.	Baseline, After 48 h, 1 week of treatment	Antidepressant pharmacotherapies	Fluoxetine (SSRI) or Venlafaxine (SNRI) or placebo	Fluoxetine 20 mg. Venlafaxine 37.5–150 mg.	8 weeks	High	Absolute or relative power	NA	NS	NA
	Knott et al., 2002	25 (NA)	21 electrodes; Linked-ears reference; 10–20 system	20 min; EC; δ (1.5–3.5 Hz), θ (3.5–7.5 Hz), α (7.5–12.5 Hz), β (12.5–25 Hz) bands.	Baseline, post-treatment	Antidepressant pharmacotherapies	Paroxetine (SSRI) or placebo	Paroxetine 20 mg.	6 weeks	Low	Absolute α power; Absolute β power; Relative δ power; Relative β power; Relative θ power; Relative α power	NA	↓; ↑; ↑; ↑; ↑; ↓	No; No; No; No; No; No
	Leuchter et al., 2002	51 (31)	35 electrodes; Pz reference; 10–20 system	NA; EC; δ (0.5–4 Hz), θ (4–8 Hz), α (8–12 Hz), β (12–10 Hz) bands.	Baseline, 1-week post placebo, After 2, 3, 8 weeks of treatment	Antidepressant pharmacotherapies	Fluoxetine (SSRI) or Venlafaxine (SNRI) or placebo	Fluoxetine (n = 24) 20 mg. Venlafaxine (n = 27) 37.5–150 mg.	7–8 weeks	High	Absolute δ power; Absolute θ power; Absolute α power; Absolute β power	NA	NS; NS; NS; NS	No; No; No; No
Cordance														
	de la Salle et al., 2020	46 (26)	32 electrodes; Common average reference; 10–10 system	3 min; EC; PF (Fpz, Fp2) and MRF (FZ, Fp1, F4, F8) θ (4–8 Hz) Cordance calculated.	Baseline, After 1-week of treatment	Antidepressant pharmacotherapies	Escitalopram (SSRI) or Bupropion (DRI) or SSRI + DRI	CJ	12 weeks	Moderate (without placebo-controlled)	θ cordance	PF, MRF	↓	Yes (+ Remission)
	Bailey et al., 2019	42 (23)	30 electrodes; CPz reference; NA	3 min; EO and EC; θ (4–8 Hz) Cordance calculated.	Baseline, After 1-week of treatment, post-treatment	Brain stimulation therapies	rTMS	110% RMT, HF L-DLPFC or LF R-DLPFC or BL rTMS (CJ)	15 sessions	Low	θ cordance	NA	NS	No
	Cao et al., 2019	37 (32)	4 electrodes; A2 reference; NA	10 min; EC; θ (4–7.5 Hz) Cordance calculated.	Baseline, post-treatment	Other therapies	Ketamine or placebo	Ketamine 0.5 or 0.2 mg/kg.	1 infusion	High	θ cordance	NA	↓	Yes

(Continued)

10.3389/fnhum.2022.940759

TABLE 1 Continued

rEEG measure	References	*n* (F)	EEG protocol (# of electrode; reference; electrode placement)	rEEG protocol (recording time; EO vs. EC; rEEG measure)	Recording period	Treatment type	Treatment name	Treatment protocol	Treatment length	Quality assessment	Outcome measure	Brain region	Change in measure following treatment	Association with response
	Bares et al., 2015a	25 (20)	21 electrodes; FCz reference; 10–20 system	10 min; EC; PF (FP1, FP2, Fz) θ (4–8 Hz) Cordance calculated.	Baseline, After 1-week of treatment	Brain stimulation therapies	rTMS + placebo	100% MT, LF R-DLPFC rTMS	4 weeks	Moderate (without placebo-)	θ cordance	NA	↓	Yes
	Bares et al., 2015b	25 (20)	21 electrodes; FCz reference; 10–20 system	10 min; EC; PF (FP1, FP2, Fz) θ (4–8 Hz) Cordance calculated.	Baseline, After 1-week of treatment	Antidepressant pharmacotherapies	Venlafaxine (SNRI) + sham	∼267 mg/day	4 weeks	Moderate (without placebo-controlled)	θ cordance	PF	↓	Yes
	Hunter et al., 2010a	72 (43)	35 electrodes; Pz reference; 10–20 system	NA; EC; MRF (FPz, Fz, FP2, AF2, F4) θ (4–8 Hz) Cordance calculated.	Baseline, 1-week post-placebo, After 48, 1, 2, and 4 h of treatment, post-treatment	Antidepressant pharmacotherapies	Fluoxetine (SSRI) or Venlafaxine (SNRI) or placebo	Fluoxetine (n = 13) 20 mg. Venlafaxine (n = 24) 150 mg.	8 weeks	High	θ cordance	MRF	↓	Associated with treatment-emergent suicidal ideation
	Hunter et al., 2010b	94 (58)	35 electrodes; Pz reference; 10–20 system	NA; EC; MRF (AF2, F4, F8, FP2, FPz, Fz) θ (4–8 Hz) Cordance calculated.	Baseline, After 48 h, 1-week of treatment	Antidepressant pharmacotherapies	Fluoxetine (SSRI) or Venlafaxine (SNRI) or placebo	Fluoxetine (n = 14) 20 mg. Venlafaxine (n = 35) 150 mg.	8 weeks	High	θ cordance	MRF	↓	Yes
	Cook et al., 2009	37 (23)	35 electrodes; Pz reference; 10–20 system	NA; EC; MRF (FPz, Fz, FP2, AF2, F4, F8) θ (4–8 Hz) Cordance calculated.	After 48 h, 1-week, 2 weeks of treatment	Antidepressant pharmacotherapies	Fluoxetine (SSRI) or Venlafaxine (SNRI) or placebo	Fluoxetine (n = 13) 20 mg. Venlafaxine (n = 24) 150 mg.	8 weeks	High	θ cordance	MRF	↓	Yes (+ Remission)
	Hunter et al., 2009	58 (NA)	35 electrodes; Pz reference; 10–20 system	NA; EC; PF (FP1, FPz, FP2) θ (4–8 Hz) Cordance calculated.	Baseline, 1-week post-placebo	Antidepressant pharmacotherapies	Fluoxetine (SSRI) or Venlafaxine (SNRI) or placebo	Fluoxetine (n = 13) 20 mg. Venlafaxine (n = 24) 150 mg.	8 weeks	High	θ cordance	PF	↓	Yes, during placebo lead-in in F only
	Hunter et al., 2006	51 (35)	35 electrodes; Pz reference; 10–20 system	NA; EC; θ (4–8 Hz) Cordance calculated.	Baseline, 1-week post-placebo, After 48, 1, 2, and 4 h of treatment, post-treatment	Antidepressant pharmacotherapies	Fluoxetine (SSRI) or Venlafaxine (SNRI) or placebo	Fluoxetine (n = 24) 20 mg. Venlafaxine (n = 27) 150 mg.	8 weeks	High	θ cordance	PF	↓	Yes, during placebo lead-in

(Continued)

10.3389/fnhum.2022.940759

TABLE 1 Continued

rEEG measure	References	*n* (F)	EEG protocol (# of electrode; reference; electrode placement)	rEEG protocol (recording time; EO vs. EC; rEEG measure)	Recording period	Treatment type	Treatment name	Treatment protocol	Treatment length	Quality assessment	Outcome measure	Brain region	Change in measure following treatment	Association with response
	Cook, 2002	51 (32)	35 electrodes; Pz reference; 10–20 system	NA; EC; θ (4–8 Hz) Cordance calculated.	Baseline, After 48 h, 1 week of treatment	Antidepressant pharmacotherapies	Fluoxetine (SSRI) or Venlafaxine (SNRI) or placebo	Fluoxetine 20 mg. Venlafaxine 37.5–150 mg.	8 weeks	High	θ cordance	PF	↓	Yes
	Leuchter et al., 2002	51 (31)	35 electrodes; Pz reference; 10–20 system	NA; EC; θ (4–8 Hz) Cordance calculated.	Baseline, 1-week post-placebo, After 2, 3, 8 weeks of treatment	Antidepressant pharmacotherapies	Fluoxetine (SSRI) or Venlafaxine (SNRI) or placebo	Fluoxetine (n = 24) 20 mg. Venlafaxine (n = 27) 37.5–150 mg.	7–8 weeks	High	θ cordance	PF	↑ Placebo responders and ↓ medication responders	Yes; Yes
Current density														
	Pizzagalli et al., 2018	248 (160)	72 electrodes; Common average reference; NA	2 min; EC; θ current density calculated.	Baseline, After 1-week of treatment	Antidepressant pharmacotherapies	Sertraline (SSRI) or placebo	Sertraline (n = 121) ∼200 mg.	8 weeks	High	θ current density	rACC	↑ (Non-specific for treatment group)	Yes
	Arns et al., 2015	655 (378)	26 electrodes; Average mastoid reference; 10–20 system	2 min; EC; θ current density calculated.	Baseline, post-treatment	Antidepressant pharmacotherapies	Escitalopram (SSRI) or Sertraline (SSRI) or Venlafaxine-XR (SNRI)	Escitalopram (n = 217) 10–20 mg. Sertraline (n = 234) 50–200 mg.Venlafaxine-XR (n = 204) 75–255 mg.	8 weeks	Moderate	θ current density	rACC, PF	↓ (More pronounced in TRD)	Yes
	Almeida Montes et al., 2015	74 (64)	32 electrodes; Average mastoid reference; 10–20 system	20 min; EC; α current density calculated.	Baseline, After 1- and 2-weeks of treatment, After 1,2, 6, 9, and 12 months of treatment	Antidepressant pharmacotherapies	Fluoxetine (SSRI)	Fluoxetine (SSRI) 20 mg during week 1, 40 mg from week 2- 1 year	1 year	Low	α current density	Occipital, Parietal, ACC, mOFC, thalamus, caudate nucleus	↓	No
	Jaworska et al., 2014	51 (28)	32 electrodes; Average mastoid reference; 10–10 system	3 min; EC; current density calculated.	Baseline, After 1-week of treatment	Antidepressant pharmacotherapies	Escitalopram (SSRI) or Bupropion (DRI) or SSRI + DRI	Escilatopram (n = 17) 10–40 mg. Bupropion (n =16) 150–450 mg.	12 weeks	Moderate (without placebo-controlled)	θ current density	rACC	↑ In SSRI + DRI group	Yes

(Continued)

10.3389/fnhum.2022.940759

TABLE 1 Continued

rEEG measure	References	*n* (F)	EEG protocol (# of electrode; reference; electrode placement)	rEEG protocol (recording time; EO vs. EC; rEEG measure)	Recording period	Treatment type	Treatment name	Treatment protocol	Treatment length	Quality assessment	Outcome measure	Brain region	Change in measure following treatment	Association with response
	Hunter et al., 2013	22 (12)	36 electrodes; Pz reference; 10–20 system	20 min; EC; θ current density calculated.	5-weeks pre-treatment, immediately post-treatment (baseline)	Antidepressant pharmacotherapies	Sertraline (SSRI) or placebo	Sertraline 50–150 mg.	8 weeks	High	θ current density	rACC	↑	Yes
	Korb et al., 2011	72 (43)	36 electrodes; Pz reference; 10–20 system	20 min; EC; θ current density calculated.	Baseline	Antidepressant pharmacotherapies	Fluoxetine (SSRI) or Venlafaxine (SNRI) or placebo	Fluoxetine (n = 37) 150 mg. Venlafaxine (n = 35) 20 mg.	8 weeks	High	θ current density	rACC; mOFC	↑; NS	Yes; NA
	Tenke et al., 2011	41 (24)	67 electrodes; Average PO1 and PO2 references; NA	2 min; EC and EO; α current density calculated.	Baseline	Antidepressant pharmacotherapies	SSRI or SNRI or SSRI + NDRI	CJ	8–12 weeks	Low	α current density	NA	↑	Yes
	Narushima et al., 2010	43 (25)	19 electrodes; Linked ears reference; 10–20 system	20 min; EC; θ current density calculated.	Baseline, post-treatment	Brain stimulation therapies	rTMS or sham	110% MT, HF L-DLPFC rTMS (n = 32) or sham (n = 11).	2 weeks	Moderate	θ current density	sACC; rACC	↑; ↓	Yes; Yes
	Korb et al., 2009	72 (43)	36 electrodes; Pz reference; 10–20 system	20 min; EC; θ current density calculated.	Baseline	Antidepressant pharmacotherapies	Fluoxetine (SSRI) or Venlafaxine (SNRI) or placebo	Fluoxetine (n = 13) 150 mg. Venlafaxine (n = 24) 20 mg.	8 weeks	High	θ current density	rACC; mOFC	↑; ↑	Yes; Yes
	Mulert et al., 2007a	20 (13)	33 electrodes; Cz reference; 10–20 system	5 min; EC; θ current density calculated.	Baseline	Antidepressant pharmacotherapies	Citalopram (SSRI) or Reboxetine (NRI)	Citalopram (n = 11) 20–60 mg. Reboxetine (n = 7) 4–12 mg.	4 weeks	Moderate	θ current density	rACC; mOFC	↑; ↑	Yes; Yes
	Mulert et al., 2007b	20 (13)	33 electrodes; Cz reference; 10–20 system	5 min; EC; θ current density calculated.	Baseline	Antidepressant pharmacotherapies	Citalopram (SSRI) or Reboxetine (NRI)	Citalopram (n = 11) 20–60 mg. Reboxetine (n = 7) 4–12 mg.	4 weeks	Moderate	θ current density	rACC	↑	Yes

(Continued)

10.3389/fnhum.2022.940759

TABLE 1 Continued

rEEG measure	References	*n* (F)	EEG protocol (# of electrode; reference; electrode placement)	rEEG protocol (recording time; EO vs. EC; rEEG measure)	Recording period	Treatment type	Treatment name	Treatment protocol	Treatment length	Quality assessment	Outcome measure	Brain region	Change in measure following treatment	Association with response
	Pizzagalli et al., 2001	18 (10)	28 electrodes; Average reference; 10–10 system	30 min; EC; θ current density calculated.	Baseline	Antidepressant pharmacotherapies	Nortriptyline (TCA)	Nortriptyline 50–150 ng/ml.	4–6 months	Low	θ current density	rACC	↑	Yes
ATR														
	Widge et al., 2013	180 (NA)	4 electrodes; NA; NA	30 s; EO; ATR calculated.	Baseline	Brain stimulation therapies	rTMS or sham	120% MT, HF L-DLPFC rTMS or sham.	6 weeks	Moderate (single-blinded)	ATR	NA	NS	NA
	Cook et al., 2013	67 (45)	4 electrodes; NA; NA	6 min and 2 min EO; EC; ATR calculated.	Baseline, After 1-week of treatment	Antidepressant pharmacotherapies	Escitalopram (SSRI) or Bupropion (DRI) or SSRI + DRI	Escitalopram 10 mg. Bupropion 300 mg.	13 weeks	Moderate	ATR	NA	↑	Yes (+Remission)
	Hunter et al., 2011	23 (15)	35 electrodes; Pz reference; 10–20 system	NA; EC; ATR calculated.	Baseline, post-treatment	Antidepressant pharmacotherapies	Fluoxetine (SSRI) or placebo	Fluoxetine (n = 13) 20 mg.	8 weeks	High	ATR	NA	↑ In SSRI group	Yes
	Leuchter et al., 2009b	220 (137)	2 electrodes; Fpz reference; NA	6 min EC and 2 min EO; ATR calculated.	Baseline, After 1-week of treatment	Antidepressant pharmacotherapies	Escitalopram (SSRI) or Bupropion (DRI) or SSRI + DRI	Escitalopram (n = 73) 10 mg. Bupropion (n = 73) 300 mg. Escitalopram + Bupropion (n = 74).	7 weeks	Moderate	ATR	NA	↑ In SSRI group	Yes (+Remission)
	Leuchter et al., 2009a	220 (137)	2 electrodes; Fpz reference; NA	6 min EC and 2 min EO; ATR calculated.	Baseline, After 1-week of treatment	Antidepressant pharmacotherapies	Escitalopram (SSRI) or Bupropion (DRI) or SSRI + DRI	Escitalopram (n = 73) 10 mg. Bupropion (n = 73) 300 mg. Escitalopram + Bupropion (n = 74).	7 weeks	Moderate	ATR	NA	↑ In SSRI group, ↓ in DRI group	Yes (+Remission); Yes
Vigilance														
	Ip et al., 2021	91 (66)	256 electrodes; Vertex reference; NA	3 min; EC and EO; EEG vigilance calculated using algorithm.	Baseline, post-treatment	Antidepressant pharmacotherapies	Escitalopram (SSRI) or Duloxetine (SNRI)	Escitalopram (n = 76) ∼5–20 mg. Duloxetine (n =15) ∼30–120 mg.	8 weeks	Low	Stage 0; Sub-Stage A2; Stage B; Sub-stage B1	NA	NS; NS; NS; ↑	No; No; No; Yes
	Sander et al., 2018	27 (17)	31 electrodes; NA; 10–20 system	15 min; EC; EEG vigilance calculated using algorithm.	Baseline, post-treatment	Other therapies	Partial Sleep Deprivation	Awake from 1 a.m. to 8 p.m.	1 session	Low	Mean Vigilance Value	NA	↓	Yes

(Continued)

10.3389/fnhum.2022.940759

TABLE 1 Continued

rEEG measure	References	*n* (F)	EEG protocol (# of electrode; reference; electrode placement)	rEEG protocol (recording time; EO vs. EC; rEEG measure)	Recording period	Treatment type	Treatment name	Treatment protocol	Treatment length	Quality assessment	Outcome measure	Brain region	Change in measure following treatment	Association with response
	Schmidt et al., 2017	65 (33)	31 electrodes; Common average reference; 10–20 system	NA; NA; EEG vigilance calculated using algorithm.	Baseline, post-treatment	Antidepressant pharmacotherapies	Escitalopram (SSRI) or Mirtazapine (atypical) or other	CJ	4 weeks	Low	Stage 0; Sub-Stage A2; Stage B; Sub-stage B1	NA	↓; ↓; ↑; ↑	Yes; Yes; Yes; Yes
	Olbrich et al., 2016	1,008 (NA)	26 electrodes; Average mastoid reference; 10–20 system	3 min; EC; EEG vigilance calculated using algorithm.	Baseline, post-treatment	Antidepressant pharmacotherapies	Escitalopram (SSRI) or Sertraline (SSRI) or Venlafaxine-XR (SNRI)	Escitalopram ($n = 198$) 10–20 mg. Sertraline ($n = 216$) 50–200 mg.Venlafaxine-XR ($n = 184$) 75–225 mg.	8 weeks	Moderate	CNS arousal	NA	↓ SSRI only	Yes (+Remission)
Normalizations and abnormalities														
	van der Vinne et al., 2019b	453 (247)	26 electrodes; Average mastoid reference; 10–20 system	2 min; EO and EC; α asymmetry calculated.	Baseline, post-treatment	Antidepressant pharmacotherapies	Escitalopram (SSRI) or Sertraline (SSRI) or Venlafaxine-XR (SNRI)	Escitalopram ($n = 136$) 10–20 mg. Sertraline ($n = 169$) 50–200 mg. Venlafaxine-XR ($n = 148$) 75–225 mg.	8 weeks	Moderate	α asymmetry	FR	↑ Over RH in SSRI group	Yes, in F only
	van der Vinne et al., 2019a	57 (NA)	26 electrodes; Average mastoid reference; 10–20 system	2 min; EO and EC; Presence of abnormal EEG activity	Baseline, post-treatment	Antidepressant pharmacotherapies	Escitalopram (SSRI) or Sertraline (SSRI) or Venlafaxine-XR (SNRI) or other	Escitalopram ($n = 19$) 10–20 mg. Sertraline ($n = 10$) 50–200 mg. Venlafaxine-XR ($n = 10$) 75–225 mg.	8 weeks	Moderate	Normalization	NA	NA	Yes, associated with 5.2x likelihood of response to Sertraline
	Arns et al., 2017	622 (356)	26 electrodes; Average mastoid reference; 10–20 system	2 min; EC; Presence of abnormal EEG activity	Baseline	Antidepressant pharmacotherapies	Escitalopram (SSRI) or Sertraline (SSRI) or Venlafaxine-XR (SNRI)	Escitalopram 10–20 mg. Sertraline 50–200 mg. Venlafaxine-XR 75–255 mg.	8 weeks	Moderate	Epileptiform EEG;EEG slowing;α peak frequency	NA	NA NA; NA	Presence of epileptiform EEG and EEG slowing associated with ↓response in SSRI and SNRI group. Presence of slow α peak associated with response to Sertraline only.

(Continued)

10.3389/fnhum.2022.940759

TABLE 1 Continued

rEEG measure	References	*n* (F)	EEG protocol (# of electrode; reference; electrode placement)	rEEG protocol (recording time; EO vs. EC; rEEG measure)	Recording period	Treatment type	Treatment name	Treatment protocol	Treatment length	Quality assessment	Outcome measure	Brain region	Change in measure following treatment	Association with response
iAPF														
	Bailey et al., 2019	42 (23)	30 electrodes; CPz reference; NA	3 min; EO and EC; iAPF calculated.	Baseline, After 1-week of treatment, Post-treatment	Brain stimulation therapies	rTMS	110% RMT, HF L-DLPFC or LF R-DLPFC or BL rTMS (CJ).	15 sessions	Low	iAPF	NA	NS	No
	Philip et al., 2019	83 (70)	2 electrodes; NA; 10–20 system	NA; NA; iAPF calculated.	Baseline	Brain stimulation therapies	sTMS or sham	sTMS ($n = 42$) or sham ($n = 41$)/	10 weeks	High	iAPF	NA	↑	Yes
Entropy														
	Jaworska et al., 2017	36 (21)	32 electrodes; Average mastoid reference; 10-10 system	3 min; EC and EO; MSE calculated.	Baseline	Antidepressant pharmacotherapies	Escitalopram (SSRI) or Bupropion (DRI) or combination	Escitalopram ($n = 11$) ∼30 mg. Bupropion ($n = 14$) ∼360 mg.	12 weeks	Moderate (without placebo controlled)	MSE	NA	↓ At fine temporal scales and ↑ at coarser temporal scales	Yes
Other														
	Arns et al., 2014	90 (49)	26 electrodes; Average mastoid reference; 10–20 system	2 min; EC and EO; LZC calculated.	Baseline	Brain stimulation therapies	rTMS + psychotherapy	110% MT, HF L-DLPFC or LF R-DLPFC rTMS.	21 sessions	Low	LZC	NA	↑	Yes

ACC, anterior cingulate cortex; ATR, antidepressant treatment response; BL, bilateral; CJ, treatment titrated according to clinical judgment; CR, central region; DLPFC, dorsolateral prefrontal cortex; DMPFC, dorsomedial prefrontal cortex; DRI, dopamine reuptake inhibitor; EC, eyes closed; ECT, electroconvulsive therapy; EO, eyes open; FR, frontal region; HF, high-frequency; iAPF, individualized α peak frequency; LF, low-frequency; LH, left-hemisphere; LZC, Lempel-Ziv Complexity; MAOI, monoamine oxidase inhibitor; MRF, midline and right frontal; MSE, multiscale entropy; MT, motor threshold; NRI, norepinephrine reuptake inhibitor; NS, non-significant; PF, pre-frontal; PR, parietal region; rACC, rostral anterior cingulate cortex; rAI, right anterior insula; RH, right-hemisphere; RMT, resting motor threshold; rTMS, repetitive transcranial magnetic stimulation; SCC, subgenual cingulate cortex; sgACC, subgenual anterior cingulate cortex; SGPFC, subgenual prefrontal cortex; SNRI, serotonin norepinephrine reuptake inhibitor; SSRI, selective serotonin reuptake inhibitor; sTMS, synchronized transcranial magnetic stimulation; tACS, transcranial altering current stimulation; TCA, tricyclic antidepressant; TRD, treatment-resistant depression; UL, unilateral.

10.3389/fnhum.2022.940759

TABLE 2 TMS-EEG outcomes for brain stimulation studies.

TMS-EEG measure	References	*n* (F)	EEG protocol (# of electrode; reference; electrode placement)	TMS-EEG protocol (stimulation intensity, TMS stimulation site)	Recording period	Treatment Type	Treatment name	Treatment protocol	Treatment length	Quality assessment	Outcome measure	Brain region	Change in measure following treatment	Association with response
TEP														
	Voineskos et al., 2021	30 (15)	64 electrodes; Common average reference; NA	120% RMT; Single-pulse TMS to DLPFC.	Baseline, post-treatment	Brain stimulation therapies	rTMS	120% RMT, BL rTMS (R-DLPFC 1 Hz + L-DLPFC 10 Hz) or UL rTMS (L-DLPFC 10 Hz) or sham	30 sessions	High	P60; N45; N100	GMFA	NS; ↓; ↓	No; No; Yes
	Eshel et al., 2020	33 (19)	64 electrodes; Common average reference; NA	120% RMT; Single-pulse TMS to left/right DLPFC, left VAN, left V1.	Baseline, post-treatment	Brain stimulation therapies	rTMS	120% RMT, L-DLPFC 10 Hz rRMS or sham	20 sessions	High	P30	Frontal and Parietal electrodes	↓	Yes
Power analysis														
	Hill et al., 2021	38 (19)	64 electrodes; Common average reference; 10–20 system	120% RMT; Single-pulse TMS to DLPFC, motor cortex.	Baseline, post-treatment	Brain stimulation therapies	MST or ECT	BL MST (F3 and F4) or BL ECT	∼1,420 sessions	Low	δ power; θ power; α power	MC; DLPFC	MST: ↓ over DLPFC; ↓ over DLPFC; ↓ over DLPFC ECT: ↓ over MC and DLPFC;↓ over MC and DLPFC; ↓ over DLPFC	MST: No; No; Yes ECT: No; No; Yes

(Continued)

10.3389/fnhum.2022.940759

TABLE 2 Continued

TMS-EEG measure	References	*n* (F)	EEG protocol (# of electrode; reference; electrode placement)	TMS-EEG protocol (stimulation intensity, TMS stimulation site)	Recording period	Treatment Type	Treatment name	Treatment protocol	Treatment length	Quality assessment	Outcome measure	Brain region	Change in measure following treatment	Association with response
Other														
	Hadas et al., 2019	26 (17)	64 electrodes; Common average reference; NA	NA; Single-pulse TMS to left DLPFC.	Baseline, post-treatment	Brain stimulation therapies	rTMS	120% RMT, BL 3–6 weeks rTMS (R-DLPFC 1 Hz + L-DLPFC 10 Hz) or UL rTMS (L-DLPFC 10 Hz) or sham		High	SCD; SCS	NA	NS; ↓	NA; Yes

BL, bilateral; ECT, electroconvulsive therapy; MC, motor cortex; MST, magnetic seizure therapy; RMT, resting motor threshold; rTMS, repetitive transcranial magnetic stimulation; SCD, significant current density; SCS, significant current scattering; TEP, TMS-evoked potential; UL, unilateral; DLPFC, dorsolateral prefrontal cortex.

10.3389/fnhum.2022.940759

2017). However, there were no significant results in patients randomized to SSRI, SNRI or placebo (Cook, 2002; Leuchter et al., 2002). One moderate quality rated study reported higher frontal alpha absolute power at baseline in SSRI, DRI or combination pharmacotherapy responders which decreased in the SSRI group after 1 week (Jaworska et al., 2014). Additionally, female SSRI responders and remitters showed greater baseline right-sided alpha power (Arns et al., 2016). In one low rated study in men only, both SSRI and placebo resulted in increased relative and absolute beta, but decreased alpha power after 6 weeks (Knott et al., 2002). Overall, alpha findings warrant more exploration, however, it remains unclear whether other frequency bands show promise due to the variability in these results.

Brain stimulation therapies

Two high-quality studies reported power analysis outcomes. Patients randomized to receive 10 Hz tACS for 5 sessions showed decreased frontal alpha power over the left hemisphere, which was not noted in patients who received 40 Hz or sham tACS (Alexander et al., 2019). In contrast, there were no changes in absolute or relative power bands following 6 weeks of sTMS (Cook et al., 2019). *One* moderately rated HF L-DLPFC rTMS study (Widge et al., 2013) reported no absolute or relative power differences between responders and non-responders at baseline. In low quality rated studies, no differences in alpha power appeared between responders and non-responders to HF L-DLPFC or LF R-DLPFC rTMS combined with psychotherapy (Arns et al., 2014). Further, there were no changes in theta or alpha power following 3 weeks of HF L-DLPFC, LF R-DLPFC, or combination rTMS (Bailey et al., 2019). To conclude, most brain stimulation studies did not find significant power analysis findings.

Other therapies

Two high-quality studies reported IV ketamine effects on power analysis (Cao et al., 2019; McMillan et al., 2020). Post-infusion, theta, high-beta, and gamma power increased, whereas delta, alpha, and low-beta power decreased. However, no relationship was found between any bands and antidepressant response (McMillan et al., 2020). In contrast, in an earlier study, decreases in relative theta and alpha power following IV ketamine infusion were associated with treatment response (Cao et al., 2019). One moderate quality rated study following 8 sessions of mindfulness-based cognitive therapy showed no change in frontal alpha power over either cortical hemisphere (Szumska et al., 2021). Two low-rated studies reported conflicting results. Absolute alpha power decreased following 1-year of pharmacotherapy alone, but not in patients receiving pharmacotherapy plus aerobic training (Deslandes et al., 2010). In contrast, there was no change in frontal alpha power following 16 sessions of behavioral activation therapy (Gollan et al., 2014). As such, decreased alpha power appears to consistently be associated with treatment response across diverse modalities of antidepressant intervention.

Cordance

Cordance is quantified by integrating absolute and relative EEG power measures, and is strongly associated with cerebral blood perfusion (Leuchter et al., 1994, 1999). Similar to functional neuroimaging, it is used to quantify abnormalities in brain activity, namely over dysregulated regions in MDD such as the frontal cortex (Hunter et al., 2007).

Antidepressant pharmacotherapies

Seven high quality rated studies reported cordance. Treatment response was associated with decreased prefrontal (PF) theta cordance after 48 h and 1 week of SSRI or SNRI treatment (Cook, 2002). Similar results in midline and right frontal regions emerged after 8 weeks of SSRIs or SNRIs (Cook et al., 2009; Hunter et al., 2010b). Interestingly, decreases in midline and right frontal theta cordance were also associated with medication-induced suicidal ideation (Hunter et al., 2010a). PF theta cordance decrease during placebo lead-in was also associated with greater response (Hunter et al., 2006), especially in female participants (Hunter et al., 2009), but the opposite trend was found for placebo responders (Leuchter et al., 2002). Two moderately rated studies examined theta cordance. One week after SNRI initiation, decreased PF theta cordance predicted greater response (AUC = 0.89) (Bares et al., 2015b). This relationship also appeared 1 week after initiation of SSRI, DRI, or combination, in both PF and midline and right frontal regions (de la Salle et al., 2020). Taken together, the above evidence demonstrates that decreased theta cordance after 1 week of pharmacotherapy may be a reliable measure of forthcoming antidepressant response.

Brain stimulation therapies

No high quality rated studies were found addressing cordance measures with regard to brain stimulation. *One* moderately rated study reported decreased PF theta cordance following high-frequency (HF) left dorsolateral prefrontal cortex (DLPFC) rTMS with placebo in treatment-resistant depression (TRD) (Bares et al., 2015b). Higher PF theta cordance at baseline was correlated with a greater reduction in symptoms following 4 weeks of rTMS, and PF theta cordance values decreased in responders 1 week post-treatment (Bares et al., 2015b). One low quality rated study following 3 weeks of HF L-DLPFC, LF R-DLPFC, or combination rTMS found no significant changes in theta cordance (Bailey et al., 2019). Despite this conflicting evidence, the moderately rated brain stimulation study is more in line with trends of decreased PF theta cordance that were noted with antidepressants.

Other studies

Only one study met criteria for this section, a high quality rated investigation which reported decreased theta cordance in responders after IV ketamine infusion (Cao et al., 2019). While singular, these findings echo the trend from pharmacotherapy and brain stimulation studies.

Current density

Current density quantifies rEEG activity, and is positively correlated with glucose metabolism (Pizzagalli et al., 2001). In MDD, abnormal metabolism levels in the rostral anterior cingulate cortex (rACC) and frontal regions have been related to symptom presentation (Martinot et al., 2011), and may be studied using current density.

Antidepressant pharmacotherapies

Four high quality rated studies reported theta current density. At baseline, responders showed higher rACC (SSRIs and SNRIs) and medial orbitofrontal cortex (mOFC) (SNRIs) (Korb et al., 2009; Hunter et al., 2013) theta current density, although another study did not replicate findings (Korb et al., 2011). Responders in both placebo and TCA groups showed elevated rACC at baseline and after 1 week of pharmacotherapy (Pizzagalli et al., 2018). Four moderate quality rated studies reported theta current density. In two, pharmacotherapy responders showed baseline elevated mOFC (NRIs and SSRIs) and rACC (NRIs) theta current density (Mulert et al., 2007a,b). DRI, but not SSRI responders, had higher baseline rACC theta current density. Responders showed increased rACC theta current density after 1 week of combination SSRI and DRI treatment (Jaworska et al., 2014). In contrast, at baseline and 8 weeks after SSRI or SNRI initiation, non-responders exhibited higher rACC and frontal theta current density, especially in non-responders with treatment resistant depression (Arns et al., 2015). Three low quality studies reported theta current density. One linked elevated baseline rACC theta current density with TCA response (Pizzagalli et al., 2001). Another, following 1 year of SSRIs, showed that patients exhibited lower alpha current density at each follow-up visit compared to healthy controls, despite some subjects reaching remission (Almeida Montes et al., 2015). In contrast, responders to SSRI, SNRI, or SSRI plus NDRI exhibited higher alpha current density at baseline compared to non-responders and healthy controls (Tenke et al., 2011). Given the above evidence, higher baseline theta current density shows clear promise in predicting pharmacotherapeutic response.

Brain stimulation therapies

One moderately rated randomized, sham-controlled HF L-DLPFC rTMS trial in patients with vascular depression recorded theta current density in the subgenual anterior cingulate cortex (sACC) and rACC (Narushima et al., 2010). At baseline, responders showed higher theta current density in sACC than non-responders, but no significant rACC findings were reported. No high or low quality rated studies were found in the literature review, but the single brain stimulation study reported findings consistent with antidepressant studies.

Other therapies

No studies reported on current density measures.

Antidepressant treatment response

The antidepressant treatment response (ATR) is a non-linear weighted combination of theta and alpha power, both relative and absolute, measured at baseline and 1 week after initiation (Leuchter et al., 2009a,b). However, it is unclear how the ATR directly reflects brain activity (Wade and Iosifescu, 2016).

Antidepressant pharmacotherapies

One high quality rated study reported higher ATR predicted both response and remission after 8 weeks of SSRIs (Hunter et al., 2011). Three moderately rated studies reported ATR levels following SSRI, DRI, or combination (Leuchter et al., 2009a,b; Cook et al., 2013). SSRI responders who underwent 7 weeks (Leuchter et al., 2009a,b) and 13 weeks (Cook et al., 2013) of treatment showed higher ATR values than non-responders, but findings were inconsistent for DRIs. Overall, higher ATR may predict response to some antidepressant pharmacotherapies.

Brain stimulation therapies

One moderately rated study reported no association between ATR and response following HF L-DLPFC rTMS (Widge et al., 2013).

Other therapies

No studies reported on the ATR measure.

Vigilance

EEG vigilance is a validated algorithm using rEEG frequency bands to quantify brain arousal into specific stages (Olbrich et al., 2009). Individuals with MDD typically show higher arousal patterns than healthy individuals (Hegerl et al., 2012).

Antidepressant pharmacotherapies

No high-quality rated studies were present in the literature review. One moderately rated study recorded vigilance as an index of central-nervous system arousal, and found decreased arousal in patients following 8-weeks of SSRIs, but not SNRI (Olbrich et al., 2016). Two low quality rated studies recorded vigilance following SSRIs, mirtazapine, SNRIs, or other medications (Schmidt et al., 2017; Ip et al., 2021). At baseline, responders had high vigilance in relaxed wakeful states and low vigilance in drowsy states, trends which were reversed after 4 weeks (Schmidt et al., 2017) and 8 weeks of treatment (Ip et al., 2021). Taken together, vigilance measures indicate that

responders to various pharmacotherapies show high arousal at baseline that may be reversed following treatment.

Brain stimulation therapies

No studies reported on vigilance measures.

Other therapies

One low quality rated study which calculated mean vigilance values (MVV) as a measure of average brain arousal following partial sleep deprivation therapy showed that responders were characterized by lower MVV compared to non-responders (Sander et al., 2018).

Normalization and abnormalities

Abnormal EEG activity is characterized by slowing, epileptiform or paroxysmal activity, and alpha peak frequencies (APF) (Noachtar et al., 1999; Niedermeyer, 2005). In contrast, normalization occurs when abnormalities disappear or return to stable recording.

Antidepressant pharmacotherapies

Three moderately rated studies reported EEG normalization or abnormalities. Following SSRIs or SNRIs, epileptiform activity or slowing was negatively correlated with response (Arns et al., 2017). Slow APF was associated with SSRI response only (Arns et al., 2017). EEG normalization was noted in SSRI but not SNRI responders (van der Vinne et al., 2019a). Higher right-sided alpha power at baseline and after 8 weeks of SSRI was a stable marker associated with response in females, but not SNRI response (van der Vinne et al., 2019b). No high or low quality rated studies were present in the literature review. While there were inconsistencies, EEG abnormalities and normalization and stability may predict SSRI response.

Brain stimulation therapies

No studies reported on EEG normalizations and abnormalities.

Other therapies

No studies reported on EEG normalizations and abnormalities.

Individual alpha peak frequency

Individualized alpha peak frequency (iAPF) is used to quantify the average alpha power across frontal electrodes in eyes open and eyes closed conditions (Doppelmayr et al., 1998). It has been used to capture inter- and intra-individual differences in alpha frequency (Haegens et al., 2014).

Antidepressant pharmacotherapies

No studies reported on the iAPF measure.

Brain stimulation therapies

One high quality study demonstrated that higher iAPF at baseline was associated with response to 10 weeks of sTMS, compared to sham (Philip et al., 2019). In contrast, iAPF did not appear to have association with response after multiple therapeutic rTMS paradigms (HF L-DLPFC, LF R-DLPFC rTMS or BL rTMS) in a low quality rated study (Bailey et al., 2019). Thus, the predictive value of iAPF may be different depending on the type of brain stimulation delivered.

Other therapies

No studies reported on the iAPF measure.

Entropy

Multiscale entropy (MSE) quantifies brain signal variability over fine or coarse time scales (Costa et al., 2005), and may be used to study global and local connectivity disturbances in MDD (Jaworska et al., 2017).

Antidepressant pharmacotherapies

Only one moderately rated study recorded MSE with SSRI, DRI or combination pharmacotherapy. Responders were characterized by decreased baseline MSE at fine and increased MSE at coarser temporal scales (Jaworska et al., 2017).

Brain stimulation therapies

No studies reported on entropy measures.

Other therapies

No studies reported on entropy measures.

Other algorithms

The Lempel-Ziv Complexity (LZC) value quantifies the complexity of the EEG signal (see Bravi et al., 2011), to understand whether non-linear measures can better characterize cortical temporal patterns in MDD.

Antidepressant pharmacotherapies

No studies reported on the LCZ value.

Brain stimulation therapies

Only one low quality rated study reported on this measure. In patients undergoing HF L-DLPFC or LF R-DLPFC rTMS combined with psychotherapy (Arns et al., 2014), LZC increased from minute 1 to 2 of the baseline EEG in responders and decreased in non-responders. Further examination of LZC may further clarify its value as an EEG marker of brain stimulation response.

Other therapies

No studies reported on the LCZ value.

TMS-EEG studies

No studies reported TMS-EEG outcome with antidepressant pharmacotherapies or other therapies. Four studies reported brain stimulation effects on TMS-EEG measures (Table 2). From the limited number of studies, TMS-EEG outcomes included TEP components (Eshel et al., 2020; Voineskos et al., 2021), power analysis (Hill et al., 2021), and other novel TMS-EEG algorithms (Hadas et al., 2019).

TMS-EEG studies mainly analyzed the effects of therapeutic rTMS, although the ECT and magnetic seizure therapy (MST) were also explored. Stimulation targets and duration/number of treatment sessions varied across studies. As well, diverse stimulation targets were applied in the investigatory TMS-EEG protocols. Due to the low number of studies, synthesis was limited.

TMS evoked potential components

TEPs over the motor cortex and DLPFC demonstrate replicable peaks (i.e., P30, N45, P60, N100) characterized by polarity and latency (Freeman and Quiroga, 2013). Several components have been linked to specific neurotransmitter receptor activity, including the P60 to glutamatergic receptor activity (Noda et al., 2017; Belardinelli et al., 2021), and N45 and N100 to gamma-aminobutyric acid (GABA) receptor activity (Farzan et al., 2013; Premoli et al., 2014; Rogasch et al., 2015).

Brain stimulation therapies

Two high quality rated investigations reported on the effects of a therapeutic course of rTMS on TEP components. Following 20 sessions of HF L-DLPFC rTMS, P30 amplitude decreased over the left frontal and parietal electrodes and was correlated with better clinical outcomes (Eshel et al., 2020). Similarly, the N45 and N100 amplitude decreased following 30 sessions of HF L-DLPFC or sequential bilateral rTMS (LF R-DLPFC rTMS followed by HF L-DLPFC rTMS), but there was no change to P60 (Voineskos et al., 2021). As well, the N100 decrease was related to improved depression symptoms post-treatment (Voineskos et al., 2021). Given the different components reported, high-quality replication studies are needed to elucidate the predictive ability of the P30, N45, and N100.

Power analysis

TMS-EEG power analysis is very similar to resting EEG power analysis, with frequency bands defined from alpha to theta.

Brain stimulation therapies

One low-quality rated study reported power analysis from TMS-EEG at baseline and after MST or ECT for TRD (Hill et al., 2021). Both treatments resulted in decreased delta and theta power over DLPFC (Hill et al., 2021). However, only ECT resulted in reduced alpha power over the DLPFC, and decreased delta and theta power over motor cortex (Hill et al., 2021). To this end, it is possible that MST effects were localized whereas ECT effects appear generalized over the cortex. As well, combined ECT and MST datasets showed a relationship between reduced alpha power and depression symptom improvements following treatment.

Novel TMS-EEG algorithms

Significant current density (SCD) and significant current scatter (SCS) are measures of subgenual cingulate cortex (SGC) excitability, and DLPFC-SGC effective connectivity, respectively (Hadas et al., 2019). Hyperactivity of the SGC and DLPFC-SGC connectivity have repeatedly been implicated in the pathophysiology of MDD (Mayberg et al., 1999).

Brain stimulation therapies

One high quality rated study examined SCS and SCD in patients with TRD. Here, the effects of HF L-DLPFC, sequential bilateral rTMS (LF R-DLPFC rTMS followed by HF L-DLPFC rTMS) or sham for 3–6 weeks were compared (Hadas et al., 2019). After active rTMS, SCS change and change in depression severity were positively correlated (Hadas et al., 2019). Further, after active rTMS, both P60 and P200 TEP component SCD decreased (Hadas et al., 2019). Given these results, TMS-EEG connectivity measures should be further explored in relation to treatment response.

Discussion

We have presented a synthesis of existing literature focused on EEG markers of treatment response in MDD. In studies focused on rEEG markers, both theta cordance and theta current density consistently show potential as predictors of response for multiple modalities of MDD treatment. Decreased prefrontal theta cordance 1-week post-treatment was robust in predicting pharmacotherapy response, regardless of antidepressant medication class. The same trend was seen in higher quality brain stimulation and other therapy studies. Thus, theta cordance appears to be a reliable measure, especially for pharmacotherapies, perhaps in part due to the larger volume of studies focused on this intervention. Additionally, higher baseline theta current density may also have predictive value in pharmacotherapy response, with less existing evidence for brain stimulation interventions. In antidepressant studies, these findings were noted in rACC (Pizzagalli et al., 2001; Mulert et al., 2007b; Korb et al., 2009; Hunter et al., 2013; Jaworska et al., 2014) and mOFC (Mulert et al., 2007b; Korb et al., 2009). In contrast, alpha current density showed inconsistent value (Tenke et al., 2011; Almeida Montes et al., 2015). To this end, the replication of theta current density across higher-rated quality studies reinforces its potential as a predictive measure. These

findings are encouraging given the biological implications of the theta band in MDD. Theta is usually most prominent in fronto-central regions, specifically the ACC and frontal cortex, both shown to be hypoactive in MDD (Asada et al., 1999). As theta is thought to represent drowsiness and low levels of cortical activation (Kropotov, 2016), it follows that this marker may hold high promise in our understanding of MDD. Thus, we encourage future biomarker guided clinical trials to verify theta markers of treatment response, specifically theta current density and theta cordance, as both show high potential to serve clinical utility in the treatment of MDD.

When examining power analysis, decreases in alpha power were the most consistently reported following treatment with SSRI (Knott et al., 2002; Jaworska et al., 2014; Leuchter et al., 2017), 10 Hz-tACS (Alexander et al., 2019), and IV Ketamine (Cao et al., 2019; McMillan et al., 2020). Thus, this measure may serve as a broad marker across treatment types, although further high-quality replication studies are needed. The remaining frequency bands (delta, theta, beta, and gamma) were reported in limited studies, with variable treatment types and inconsistent findings. Nevertheless, future focus on the alpha band is warranted given its ability to reflect inactivity of brain regions in MDD (Bruder et al., 1997). Previous research has linked the left frontal cortex to hypoactivity, reflected by high alpha power and reduced approach behavior (i.e., positive emotions) (Davidson, 1992). In contrast, the opposite trend is found over the right frontal cortex, reflected by low alpha power and increased withdrawal behavior (i.e., negative emotions). Taken together, the linkage between alpha power, cortical activity, and behavioral manifestations in MDD indicate the potential of this measure being extended to help guide treatment. Alpha band guided treatments have already proved useful in novel closed-loop neuromodulation techniques (Zrenner et al., 2016, 2020). Alpha oscillation-synchronized rTMS appears to improve treatment efficacy and may prove useful in personalizing therapeutic rTMS parameters (Zrenner et al., 2016, 2020). Phase synchronization has also been explored with the theta rhythm in healthy subjects, but requires replication in MDD populations undergoing therapeutic rTMS as a method for novel personalized treatments (Gordon et al., 2021). Additionally, sleep EEG power analysis may prove fruitful in identifying frequency band markers of MDD treatment response. Since the brain evidently behaves differently in wakeful and sleep states, especially for lower frequency bands, there is likely added value in exploring these markers in patients undergoing MDD interventions during sleep (Olbrich and Arns, 2013).

There were inconsistent findings across multiple treatment modalities with the remaining rEEG measures. First, higher ATR was replicated in responders or remitters to SSRIs (Leuchter et al., 2009a; Hunter et al., 2011), but was inconsistent for other medication classes such as DRIs (Leuchter et al., 2009b; Hunter et al., 2011), and in brain stimulation (Widge et al., 2013). Second, EEG abnormality measures were inconsistent, possibly due to high variability in selected outcome measures. SSRI response favored low EEG abnormalities and higher stability at baseline, but these were not predictive of SNRI response (Arns et al., 2017; van der Vinne et al., 2019a,b). Third, the different vigilance outcomes reported hindered the synthesis of results, but most studies reported that responders to various pharmacotherapies showed high brain arousal at baseline (Olbrich et al., 2016; Schmidt et al., 2017; Ip et al., 2021). Finally, very few studies reported iAPF (Bailey et al., 2019; Philip et al., 2019), entropy (Jaworska et al., 2017), and LCZ (Arns et al., 2014). While promise may remain within these measures, clear future directions cannot be gleaned from this synthesis of the literature.

In contrast, there were relatively few TMS-EEG studies to review, and all were focused on brain stimulation. Of the four studies included, three were high-quality, reflecting the high promise of TMS-EEG as a repository for neurophysiological biomarkers across brain stimulation modalities. rTMS appears to modulate DLPFC-SGC connectivity in parallel with improvements in MDD symptoms (Hadas et al., 2019). Additionally, better clinical outcomes were associated with decreased P30 amplitude (Eshel et al., 2020), and N100 amplitude (Voineskos et al., 2021) following active HF L-DLPFC and BL rTMS. While the biological association of the P30 is still unknown, the N100 seems to be linked to GABAergic receptor activity (Farzan et al., 2013; Premoli et al., 2014; Rogasch et al., 2015), a neurotransmitter highly implicated in the pathophysiology of MDD (Luscher et al., 2011). One low-quality study reported that decreased alpha power following MST or ECT was related to clinical response (Hill et al., 2021), adding to rEEG evidence of alpha band predictive power. There were three additional articles from our search that explored TMS-EEG effects following MST and ECT, however, they were deemed very *Low quality* and reported different outcomes, limiting synthesis (Casarotto et al., 2013; Miyauchi et al., 2019; Hadas et al., 2020). Overall, the high quality findings indicate that TMS-EEG measures may serve as MDD markers of response in the future.

There were some limitations to the literature reviewed. While non-linear rEEG quantitative algorithms (i.e., theta cordance, theta current density) show higher predictive value than traditional linear metrics, in part due to the non-linear behavior of brain function (Elbert et al., 1994), a recent meta-analysis calls the reliability of these indices into question, given the lack of direct replication studies and under-reporting of negative results (Widge et al., 2019). Further, evidence of biological linkages between rEEG measures and MDD symptomatology should also be verified using other modalities (i.e., imaging) or correlational studies before implementing these markers into clinical practice. A potential way of relieving these issues is by exploring novel computational and modeling approaches, which have gained traction. Cross-validated machine learning combining rEEG and mood

measures show promise in distinguishing rTMS responders (Bailey et al., 2019). As well, a recent machine learning rEEG study differentially predicted response to SSRIs vs. low-frequency rTMS (Wu et al., 2020), which has generated much discussion on generalizability (Michel and Pascual-Leone, 2020; Nilsonne and Harrell, 2021; Wu et al., 2021). As such, while traditional rEEG measures are well documented, future studies may benefit from focusing on more complex indices.

A potential future direction of TMS-EEG markers may be in predicting specific MDD symptom improvements, as was shown by TMS-EEG indicators of suicidal ideation remission following MST (Sun et al., 2016). As well, combining TMS-EEG measures with other predictors of treatment response, such as rEEG outcomes or symptom presentation, using machine learning is another promising avenue that may serve clinical utility (Wu et al., 2020). Theta-burst stimulation (TBS), a novel rTMS therapy that produces significant antidepressant effects in patients with TRD (Blumberger et al., 2018), provides a further field for marker exploration with TMS-EEG. Notably, TBS builds on the concept of theta-gamma coupling, first proposed in animal models (Larson et al., 1986), a potential method of neural communication between brain regions thought to underly the basis of learning and memory (Lisman and Jensen, 2013). Taken together, TMS-EEG time-frequency analysis may be used to examine this theory by measuring changes in frequency power markers before and after TBS. Overall, TMS-EEG offers a novel area for discovery, offering replicable indices of cortical reactivity and connectivity that should be explored by future studies.

This review calls for more placebo-controlled, high-powered, replication studies to identify response markers for MDD treatments. Future EEG studies focusing on brain stimulation and novel therapeutics may lead to further understanding of neurophysiological treatment effects. We suggest a focus on TMS-EEG, given its potential to specifically target brain regions relevant to MDD. Specifically, emphasis on automation of TMS-EEG techniques and outcomes may eliminate variability in results, which can allow for more widespread clinical use in the future. In addition, rEEG has been more extensively studied than other methods, but further work is needed and the highest yield results are likely to emerge from the theta and alpha frequency markers defined above. Given the minimal cost associated with EEG, the potential for recordings to be distilled to a few electrodes and performed in community labs, it allows for far reaching real world clinical utility if such a treatment marker is identified. Importantly, improving predictions of treatment response, has the potential to spare patients and our healthcare system the burden of undergoing ineffective therapies, which would be of great clinical and scientific benefit.

Data availability statement

The original contributions presented in the study are included in the article/supplementary material, further inquiries can be directed to the corresponding author.

Author contributions

RS and DV conceived and designed the study, carried out the search, screening, data extraction, quality assessment, and drafted the manuscript. DV checked the inclusion/exclusion criteria. DMB, RC, and TKR critically revised the manuscript for intellectual content and reviewed the drafted manuscript. All authors contributed to critical revisions of the manuscript and gave final approval of the version to be published.

Funding

RS was supported by an Ontario Graduate Scholarship. This work was also supported in part by an Academic Scholars Award from the Department of Psychiatry, University of Toronto, awarded to DV.

Conflict of interest

TKR has received research support from Brain Canada, Brain and Behavior Research Foundation, BrightFocus Foundation, Canada Foundation for Innovation, Canada Research Chair, Canadian Institutes of Health Research, Center for Aging and Brain Health Innovation, National Institutes of Health, Ontario Ministry of Health and Long-Term Care, Ontario Ministry of Research and Innovation, and the Weston Brain Institute. TKR also received for an investigator-initiated study in-kind equipment support from Newronika, and in-kind research online accounts from Scientific Brain Training Pro, and participated in 2021 in an advisory board for Biogen Canada Inc. DMB receives research support from CIHR, NIH, Brain Canada and the Temerty Family through the CAMH Foundation and the Campbell Research Institute. He received research support and in-kind equipment support for an investigator-initiated study from Brainsway Ltd., and he has been the site principal investigator for three sponsor-initiated studies for Brainsway Ltd. He also receives in-kind equipment support from Magventure for investigator-initiated studies. He received medication supplies for an investigator-initiated trial from Indivior. He has participated in Scientific Advisory Board for Welcony Inc. DV holds the Labatt Family Professorship in Depression Biology, a University Named Professorship at

the University of Toronto. She receives research support from CIHR, the Center for Addiction and Mental Health (CAMH) and the Department of Psychiatry at the University of Toronto. DV declares no biomedical interests or conflicts.

The remaining authors declare that the research was conducted in the absence of any commercial or financial relationships that could be construed as a potential conflict of interest.

Publisher's note

References

Abhang, P. A., Gawali, B. W., and Mehrotra, S. C. (2016). *Introduction to EEG-and Speech-Based Emotion Recognition*. Academic Press.

Aftanas, L. I., Varlamov, A. A., Pavlov, S. V., Makhnev, V. P., and Reva, N. V. (2002). Time-dependent cortical asymmetries induced by emotional arousal: EEG analysis of event-related synchronization and desynchronization in individually defined frequency bands. *Int. J. Psychophysiol.* 44, 67–82. doi: 10.1016/S0167-8760(01)00194-5

Aftanas, L. I., and Golocheikine, S. A. (2001). Human anterior and frontal midline theta and lower alpha reflect emotionally positive state and internalized attention: high-resolution EEG investigation of meditation. *Neurosci. Lett.* 310, 57–60. doi: 10.1016/S0304-3940(01)02094-8

Alexander, M. L., Alagapan, S., Lugo, C. E., Mellin, J. M., Lustenberger, C., Rubinow, D. R., et al. (2019). Double-blind, randomized pilot clinical trial targeting alpha oscillations with transcranial alternating current stimulation (tACS) for the treatment of major depressive disorder (MDD). *Transl. Psychiatry* 9, 1–12. doi: 10.1038/s41398-019-0439-0

Almeida Montes, L. G., Prado Alcántara, H., Portillo Cedeño, B. A., Hernández García, A. O., and Fuentes Rojas, P. E. (2015). Persistent decrease in alpha current density in fully remitted subjects with major depressive disorder treated with fluoxetine: a prospective electric tomography study. *Int. J. Psychophysiol.* 96, 191–200. doi: 10.1016/j.ijpsycho.2015.03.010

Amzica, F., and Steriade, M. (1998). Electrophysiological correlates of sleep delta waves. *Electroencephalogr. Clin. Neurophysiol.* 107, 69–83. doi: 10.1016/S0013-4694(98)00051-0

Arns, M., Bruder, G., Hegerl, U., Spooner, C., Palmer, D. M., Etkin, A., et al. (2016). EEG alpha asymmetry as a gender-specific predictor of outcome to acute treatment with different antidepressant medications in the randomized iSPOT-D study. *Clin. Neurophysiol.* 127, 509–519. doi: 10.1016/j.clinph.2015.05.032

Arns, M., Cerquera, A., Gutiérrez, R. M., Hasselman, F., and Freund, J. A. (2014). Non-linear EEG analyses predict non-response to rTMS treatment in major depressive disorder. *Clin. Neurophysiol.* 125, 1392–1399. doi: 10.1016/j.clinph.2013.11.022

Arns, M., Etkin, A., Hegerl, U., Williams, L. M., DeBattista, C., Palmer, D. M., et al. (2015). Frontal and rostral anterior cingulate (rACC) theta EEG in depression: implications for treatment outcome? *Eur. Neuropsychopharmacol.* 25, 1190–1200. doi: 10.1016/j.euroneuro.2015.03.007

Arns, M., Gordon, E., and Boutros, N. N. (2017). EEG abnormalities are associated with poorer depressive symptom outcomes with escitalopram and venlafaxine-XR, but not sertraline: results from the multicenter randomized iSPOT-D study. *Clin. EEG Neurosci.* 48, 33–40. doi: 10.1177/1550059415621435

Asada, H., Fukuda, Y., Tsunoda, S., Yamaguchi, M., and Tonoike, M. (1999). Frontal midline theta rhythms reflect alternative activation of prefrontal cortex and anterior cingulate cortex in humans. *Neurosci. Lett.* 4. doi: 10.1016/S0304-3940(99)00679-5

Bailey, N. W., Hoy, K. E., Rogasch, N. C., Thomson, R. H., McQueen, S., Elliot, D., et al. (2019). Differentiating responders and non-responders to rTMS treatment for depression after one week using resting EEG connectivity measures. *J. Affect. Disord.* 242, 68–79. doi: 10.1016/j.jad.2018.08.058

Bares, M., Brunovsky, M., Novak, T., Kopecek, M., Stopkova, P., Sos, P., et al. (2015a). QEEG Theta cordance in the prediction of treatment outcome to prefrontal repetitive transcranial magnetic stimulation or venlafaxine er in patients with major depressive disorder. *Clin. EEG Neurosci.* 46, 73–80. doi: 10.1177/1550059413520442

Bares, M., Novak, T., Kopecek, M., Brunovsky, M., Stopkova, P., and Höschl, C. (2015b). The effectiveness of prefrontal theta cordance and early reduction of depressive symptoms in the prediction of antidepressant treatment outcome in patients with resistant depression: analysis of naturalistic data. *Eur. Arch. Psychiatry Clin. Neurosci.* 265, 73–82. doi: 10.1007/s00406-014-0506-8

Barker, A. T., Jalinous, R., and Freeston, I. L. (1985). Non-invasive magnetic stimulation of human motor cortex. *Lancet* 325, 1106–1107. doi: 10.1016/S0140-6736(85)92413-4

Belardinelli, P., König, F., Liang, C., Premoli, I., Desideri, D., Müller-Dahlhaus, F., et al. (2021). TMS-EEG signatures of glutamatergic neurotransmission in human cortex. *Sci. Rep.* 11, 8159. doi: 10.1038/s41598-021-87533-z

Belmaker, R. H. (2008). Major depressive disorder. *New Engl. J. Med.* 14, 96. doi: 10.1056/NEJMra073096

Berger, H. (1929). On the EEG in humans. *Arch. Psychiatr. Nervenkr* 87, 527–570. doi: 10.1007/BF01797193

Blumberger, D. M., Vila-Rodriguez, F., Thorpe, K. E., Feffer, K., Noda, Y., Giacobbe, P., et al. (2018). Effectiveness of theta burst versus high-frequency repetitive transcranial magnetic stimulation in patients with depression (THREE-D): a randomised non-inferiority trial. *Lancet* 391, 1683–1692. doi: 10.1016/S0140-6736(18)30295-2

Bravi, A., Longtin, A., and Seely, A. J. (2011). Review and classification of variability analysis techniques with clinical applications. *Biomed. Eng. Online* 10, 1–27. doi: 10.1186/1475-925X-10-90

Bruder, G. E., Fong, R., Tenke, C. E., Leite, P., Towey, J. P., Stewart, J. E., et al. (1997). Regional brain asymmetries in major depression with or without an anxiety disorder: a quantitative electroencephalographic study. *Biol. Psychiatry* 41, 939–948. doi: 10.1016/S0006-3223(96)00260-0

Cao, Z., Lin, C.-T., Ding, W., Chen, M.-H., Li, C.-T., and Su, T.-P. (2019). Identifying ketamine responses in treatment-resistant depression using a wearable forehead EEG. *IEEE Trans. Biomed. Eng.* 66, 1668–1679. doi: 10.1109/TBME.2018.2877651

Casarotto, S., Canali, P., Rosanova, M., Pigorini, A., Fecchio, M., Mariotti, M., et al. (2013). Assessing the effects of electroconvulsive therapy on cortical excitability by means of transcranial magnetic stimulation and electroencephalography. *Brain Topogr.* 26, 326–337. doi: 10.1007/s10548-012-0256-8

Cook, I. (2002). Early changes in prefrontal activity characterize clinical responders to antidepressants. *Neuropsychopharmacology* 27, 120–131. doi: 10.1016/S0893-133X(02)00294-4

Cook, I. A., Hunter, A. M., Abrams, M., Siegman, B., and Leuchter, A. F. (2009). Midline and right frontal brain function as a physiologic biomarker of remission in major depression. *Psychiatry Res. Neuroimaging* 174, 152–157. doi: 10.1016/j.pscychresns.2009.04.011

Cook, I. A., Hunter, A. M., Gilmer, W. S., Iosifescu, D. V., Zisook, S., Burgoyne, K. S., et al. (2013). Quantitative electroencephalogram biomarkers for predicting likelihood and speed of achieving sustained remission in major depression: a report from the biomarkers for rapid identification of treatment effectiveness in major depression (BRITE-MD) trial. *J. Clin. Psychiatry* 74, 813. doi: 10.4088/JCP.10m06813

Cook, I. A., Wilson, A. C., Corlier, J., and Leuchter, A. F. (2019). Brain activity and clinical outcomes in adults with depression treated with synchronized transcranial magnetic stimulation: an exploratory study. *Neuromodul. Technol. Neural Interface* 22, 894–897. doi: 10.1111/ner.12914

Costa, M., Goldberger, A. L., and Peng, C.-K. (2005). Multiscale entropy analysis of biological signals. *Phys. Rev. E* 71, 021906. doi: 10.1103/PhysRevE.71.021906

Daskalakis, Z. J., Farzan, F., Radhu, N., and Fitzgerald, P. B. (2012). Combined transcranial magnetic stimulation and electroencephalography: its past, present and future. *Brain Res.* 1463, 93–107. doi: 10.1016/j.brainres.2012.04.045

Davidson, R. J. (1992). Anterior cerebral asymmetry and the nature of emotion. *Brain Cogn.* 20, 125–151. doi: 10.1016/0278-2626(92)90065-T

de la Salle, S., Jaworska, N., Blier, P., Smith, D., and Knott, V. (2020). Using prefrontal and midline right frontal EEG-derived theta cordance and depressive symptoms to predict the differential response or remission to antidepressant treatment in major depressive disorder. *Psychiatry Res. Neuroimag.* 302, 111109. doi: 10.1016/j.pscychresns.2020.111109

Deslandes, A. C., Moraes, H., Alves, H., Pompeu, F. A., Silveira, H., Mouta, R., et al. (2010). Effect of aerobic training on EEG alpha asymmetry and depressive symptoms in the elderly: a 1-year follow-up study. *Braz. J. Med. Biol. Res.* 43, 585–592. doi: 10.1590/S0100-879X2010007500041

Doppelmayr, M., Klimesch, W., Pachinger, T., and Ripper, B. (1998). Individual differences in brain dynamics: important implications for the calculation of event-related band power. *Biol. Cyber.* 79, 49–57. doi: 10.1007/s004220050457

Elbert, T., Ray, W. J., Kowalik, Z. J., Skinner, J. E., Graf, K. E., and Birbaumer, N. (1994). Chaos and physiology: deterministic chaos in excitable cell assemblies. *Physiol. Rev.* 74, 1–47. doi: 10.1152/physrev.1994.74.1.1

Eshel, N., Keller, C. J., Wu, W., Jiang, J., Mills-Finnerty, C., Huemer, J., et al. (2020). Global connectivity and local excitability changes underlie antidepressant effects of repetitive transcranial magnetic stimulation. *Neuropsychopharmacology* 45, 1018–1025. doi: 10.1038/s41386-020-0633-z

Farzan, F., Barr, M. S., Hoppenbrouwers, S. S., Fitzgerald, P. B., Chen, R., Pascual-Leone, A., et al. (2013). The EEG correlates of the TMS induced EMG silent period in humans. *Neuroimage* 83, 120–134. doi: 10.1016/j.neuroimage.2013.06.059

Farzan, F., Vernet, M., Shafi, M. M. D., Rotenberg, A., Daskalakis, Z. J., and Pascual-Leone, A. (2016). Characterizing and modulating brain circuitry through transcranial magnetic stimulation combined with electroencephalography. *Front. Neural Circuits* 10, 73. doi: 10.3389/fncir.2016.00073

Freeman, W. J., and Quiroga, R. Q. (2013). *Imaging Brain Function With EEG: Advanced Temporal and Spatial Analysis of Electroencephalographic Signals [WWW Document]*. Available online at: https://books-scholarsportal-info.myaccess.library.utoronto.ca/en/read?id=/ebooks/ebooks3/springer/2016-05-20/1/9781461449843#page=18 (accessed November 15, 2020).

Friedrich, M. J. (2017). Depression is the leading cause of disability around the world. *JAMA* 317, 1517–1517. doi: 10.1001/jama.2017.3826

Gollan, J. K., Hoxha, D., Chihade, D., Pflieger, M. E., Rosebrock, L., and Cacioppo, J. (2014). Frontal alpha EEG asymmetry before and after behavioral activation treatment for depression. *Biol. Psychol.* 99, 198–208. doi: 10.1016/j.biopsycho.2014.03.003

Gordon, P. C., Dörre, S., Belardinelli, P., Stenroos, M., Zrenner, B., Ziemann, U., et al. (2021). Prefrontal theta-phase synchronized brain stimulation with real-time EEG-triggered TMS. *Front. Hum. Neurosci.* 15, 1821. doi: 10.3389/fnhum.2021.691821

Hadas, I., Sun, Y., Lioumis, P., Zomorrodi, R., Jones, B., Voineskos, D., et al. (2019). Association of repetitive transcranial magnetic stimulation treatment with subgenual cingulate hyperactivity in patients with major depressive disorder. *JAMA Netw Open.* 2, 5578. doi: 10.1001/jamanetworkopen.2019.5578

Hadas, I., Zomorrodi, R., Hill, A. T., Sun, Y., Fitzgerald, P. B., Blumberger, D. M., et al. (2020). Subgenual cingulate connectivity and hippocampal activation are related to MST therapeutic and adverse effects. *Transl. Psychiatry* 10, 1–8. doi: 10.1038/s41398-020-01042-7

Haegens, S., Cousijn, H., Wallis, G., Harrison, P. J., and Nobre, A. C. (2014). Inter- and intra-individual variability in alpha peak frequency. *Neuroimage* 92, 46–55. doi: 10.1016/j.neuroimage.2014.01.049

Hegerl, U., Wilk, K., Olbrich, S., Schoenknecht, P., and Sander, C. (2012). Hyperstable regulation of vigilance in patients with major depressive disorder. *World J. Biol. Psychiatry* 13, 436–446. doi: 10.3109/15622975.2011.579164

Hill, A. T., Hadas, I., Zomorrodi, R., Voineskos, D., Fitzgerald, P. B., Blumberger, D. M., et al. (2021). Characterizing cortical oscillatory responses in major depressive disorder before and after convulsive therapy: a TMS-EEG study. *J. Affect. Disord.* 287, 78–88. doi: 10.1016/j.jad.2021.03.010

Hunter, A. M., Cook, I. A., Greenwald, S., Tran, M. L., Miyamoto, K. N., and Leuchter, A. F. (2011). The antidepressant treatment response (ATR) index and treatment outcomes in a placebo-controlled trial of fluoxetine. *J. Clin. Neurophysiol.* 28, 478–482. doi: 10.1097/WNP.0b013e318230da8a

Hunter, A. M., Cook, I. A., and Leuchter, A. F. (2007). The promise of the quantitative electroencephalogram as a predictor of antidepressant treatment outcomes in major depressive disorder. *Psychiatr. Clin. North Am.* 30, 105–124. doi: 10.1016/j.psc.2006.12.002

Hunter, A. M., Korb, A. S., Cook, I. A., and Leuchter, A. F. (2013). Rostral anterior cingulate activity in major depressive disorder: state or trait marker of responsiveness to medication? *J, Neuropsychiatry Clin. Neurosci.* 8, 330. doi: 10.1176/appi.neuropsych.11110330

Hunter, A. M., Leuchter, A. F., Cook, I. A., and Abrams, M. (2010a). Brain functional changes (QEEG cordance) and worsening suicidal ideation and mood symptoms during antidepressant treatment: QEEG cordance and worsening symptoms. *Acta Psychiatr. Scand.* 122, 461–469. doi: 10.1111/j.1600-0447.2010.01560.x

Hunter, A. M., Leuchter, A. F., Morgan, M. L., and Cook, I. A. (2006). Changes in brain function (quantitative EEG Cordance) during placebo lead-in and treatment outcomes in clinical trials for major depression. *Am. J. Psychiatry* 7, 1426. doi: 10.1176/ajp.2006.163.8.1426

Hunter, A. M., Muthén, B. O., Cook, I. A., and Leuchter, A. F. (2010b). Antidepressant response trajectories and quantitative electroencephalography (QEEG) biomarkers in major depressive disorder. *J. Psychiatr. Res.* 44, 90–98. doi: 10.1016/j.jpsychires.2009.06.006

Hunter, A. M., Ravikumar, S., Cook, I. A., and Leuchter, A. F. (2009). Brain functional changes during placebo lead-in and changes in specific symptoms during pharmacotherapy for major depression. *Acta Psychiatr. Scand.* 119, 266–273. doi: 10.1111/j.1600-0447.2008.01305.x

Ip, C.-T., Ganz, M., Dam, V. H., Ozenne, B., Rüesch, A., Köhler-Forsberg, K., et al. (2021). NeuroPharm study: EEG wakefulness regulation as a biomarker in MDD. *J. Psychiatr. Res.* 141, 57–65. doi: 10.1016/j.jpsychires.2021.06.021

Jasper, H. H. (1958). The ten-twenty electrode system of the International Federation. *Electroencephalogr. Clin. Neurophysiol.* 10, 370–375.

Jaworska, N., Blondeau, C., Tessier, P., Norris, S., Fusee, W., Blier, P., et al. (2014). Examining relations between alpha power as well as anterior cingulate cortex-localized theta activity and response to single or dual antidepressant pharmacotherapies. *J. Psychopharmacol.* 28, 587–595. doi: 10.1177/0269881114523862

Jaworska, N., Wang, H., Smith, D. M., Blier, P., Knott, V., and Protzner, A. B. (2017). Pre-treatment EEG signal variability is associated with treatment success in depression. *Neuroimage Clin.* 17, 368–377. doi: 10.1016/j.nicl.2017.10.035

Knott, V., Mahoney, C., Kennedy, S., and Evans, K. (2002). EEG correlates of acute and chronic paroxetine treatment in depression. *J. Affect. Disord.* 69, 241–249. doi: 10.1016/S0165-0327(01)00308-1

Kobayashi, M., and Pascual-Leone, A. (2003). Transcranial magnetic stimulation in neurology. *Lancet Neurol.* 2, 145–156. doi: 10.1016/S1474-4422(03)00321-1

Korb, A. S., Hunter, A. M., Cook, I. A., and Leuchter, A. F. (2009). Rostral anterior cingulate cortex theta current density and response to antidepressants and placebo in major depression. *Clin. Neurophysiol.* 120, 1313–1319. doi: 10.1016/j.clinph.2009.05.008

Korb, A. S., Hunter, A. M., Cook, I. A., and Leuchter, A. F. (2011). Rostral anterior cingulate cortex activity and early symptom improvement during treatment for major depressive disorder. *Psychiatry Res.* 192, 188–194. doi: 10.1016/j.pscychresns.2010.12.007

Kropotov, J. (2016). *Functional Neuromarkers for Psychiatry: Applications for Diagnosis and Treatment*. Academic Press.

Kupfer, D. J., Frank, E., and Phillips, M. L. (2012). Major depressive disorder: new clinical, neurobiological, and treatment perspectives. *Lancet* 379, 1045–1055. doi: 10.1016/S0140-6736(11)60602-8

Larson, J., Wong, D., and Lynch, G. (1986). Patterned stimulation at the theta frequency is optimal for the induction of hippocampal long-term potentiation. *Brain Res.* 368, 347–350. doi: 10.1016/0006-8993(86)90579-2

Leuchter, A. F., Cook, I. A., Gilmer, W. S., Marangell, L. B., Burgoyne, K. S., Howland, R. H., et al. (2009a). Effectiveness of a quantitative electroencephalographic biomarker for predicting differential response or remission with escitalopram and bupropion in major depressive disorder. *Psychiatry Res.* 169, 132–138. doi: 10.1016/j.psychres.2009.04.004

Leuchter, A. F., Cook, I. A., Lufkin, R. B., Dunkin, J., Newton, T. F., Cummings, J. L., et al. (1994). Cordance: a new method for assessment of cerebral perfusion and metabolism using quantitative electroencephalography. *Neuroimage* 1, 208–219. doi: 10.1006/nimg.1994.1006

Leuchter, A. F., Cook, I. A., Marangell, L. B., Gilmer, W. S., Burgoyne, K. S., Howland, R. H., et al. (2009b). Comparative effectiveness of biomarkers and clinical indicators for predicting outcomes of SSRI treatment in major depressive disorder: results of the BRITE-MD study. *Psychiatry Res.* 169, 124–131. doi: 10.1016/j.psychres.2009.06.004

Leuchter, A. F., Cook, I. A., Witte, E. A., Morgan, M., and Abrams, M. (2002). Changes in brain function of depressed subjects during treatment with placebo. *Am. J. Psychiatry* 159, 122–129. doi: 10.1176/appi.ajp.159.1.122

Leuchter, A. F., Hunter, A. M., Jain, F. A., Tartter, M., Crump, C., and Cook, I. A. (2017). Escitalopram but not placebo modulates brain rhythmic oscillatory activity in the first week of treatment of Major Depressive Disorder. *J. Psychiatr. Res.* 84, 174–183. doi: 10.1016/j.jpsychires.2016.10.002

Leuchter, A. F., Uijtdehaage, S. H., Cook, I. A., O'Hara, R., and Mandelkern, M. (1999). Relationship between brain electrical activity and cortical perfusion in normal subjects. *Psychiatry Res. Neuroimag.* 90, 125–140. doi: 10.1016/S0925-4927(99)00006-2

Lisman, J. E., and Jensen, O. (2013). The theta-gamma neural code. *Neuron* 77, 1002–1016. doi: 10.1016/j.neuron.2013.03.007

Luscher, B., Shen, Q., and Sahir, N. (2011). The GABAergic deficit hypothesis of major depressive disorder. *Mol. Psychiatry* 16, 383–406. doi: 10.1038/mp.2010.120

Martinot, M.-L. P., Martinot, J.-L., Ringuenet, D., Galinowski, A., Gallarda, T., Bellivier, F., et al. (2011). Baseline brain metabolism in resistant depression and response to transcranial magnetic stimulation. *Neuropsychopharmacol* 36, 2710–2719. doi: 10.1038/npp.2011.161

Mayberg, H. S., Liotti, M., Brannan, S. K., McGinnis, S., Mahurin, R. K., Jerabek, P. A., et al. (1999). Reciprocal limbic-cortical function and negative mood: converging pet findings in depression and normal sadness. *AJP* 156, 675–682.

McMillan, R., Sumner, R., Forsyth, A., Campbell, D., Malpas, G., Maxwell, E., et al. (2020). Simultaneous EEG/fMRI recorded during ketamine infusion in patients with major depressive disorder. *Prog. Neuro Psychopharmacol. Biol. Psychiatry* 99, 109838. doi: 10.1016/j.pnpbp.2019.109838

Michel, C. M., and Pascual-Leone, A. (2020). Predicting antidepressant response by electroencephalography. *Nat. Biotechnol.* 38, 417–419. doi: 10.1038/s41587-020-0476-5

Miyauchi, E., Ide, M., Tachikawa, H., Nemoto, K., Arai, T., and Kawasaki, M. (2019). A novel approach for assessing neuromodulation using phase-locked information measured with TMS-EEG. *Sci. Rep.* 9, 428. doi: 10.1038/s41598-018-36317-z

Mulert, C., Juckel, G., Brunnmeier, M., Karch, S., Leicht, G., Mergl, R., et al. (2007a). Prediction of treatment response in major depression: integration of concepts. *J. Affect. Disord.* 98, 215–225. doi: 10.1016/j.jad.2006.07.021

Mulert, C., Juckel, G., Brunnmeier, M., Karch, S., Leicht, G., Mergl, R., et al. (2007b). Rostral anterior cingulate cortex activity in the theta band predicts response to antidepressive medication. *Clin. EEG Neurosci.* 38, 78–81. doi: 10.1177/155005940703800209

Narushima, K., McCormick, L., Yamada, T., Thatcher, R., and Robinson, R. G. (2010). Subgenual cingulate theta activity predicts treatment response of repetitive transcranial magnetic stimulation in participants with vascular depression. *J. Neuropsychiatry Clin. Neurosci.* 22, 75–84. doi: 10.1176/jnp.2010.22.1.75

Niedermeyer, E. (1999). The normal EEG of the waking adult. *Electroencephalogr. Basic Princip. Clin. Appl. Relat. Fields* 20, 149–173.

Niedermeyer, E. (2005). Abnormal EEG patterns: Epileptic and paroxysmal. *Electroencephalogr. Basic Princip. Clin. Appl. Related Fields*. 5th edition. 255–280.

Nilsonne, G., and Harrell, F. E. (2021). EEG-based model and antidepressant response. *Nat. Biotechnol.* 39, 27–27. doi: 10.1038/s41587-020-00768-5

Noachtar, S., Binnie, C., Ebersole, J., Mauguière, F., Sakamoto, A., and Westmoreland, B. (1999). A glossary of terms most commonly used by clinical electroencephalographers and proposal for the report form for the eeg findings. The international federation of clinical neurophysiology, *Electroencephalography and Clinical Neurophysiology. Supplement.* 52, 21-Ü41.

Noda, Y., Zomorrodi, R., Cash, R. F. H., Barr, M. S., Farzan, F., Rajji, T. K., et al. (2017). Characterization of the influence of age on GABAA and glutamatergic mediated functions in the dorsolateral prefrontal cortex using paired-pulse TMS-EEG. *Aging* 9, 556–567. doi: 10.18632/aging.101178

Olbrich, S., and Arns, M. (2013). EEG biomarkers in major depressive disorder: Discriminative power and prediction of treatment response. *Int. Rev. Psychiatry* 25, 604–618. doi: 10.3109/09540261.2013.816269

Olbrich, S., Mulert, C., Karch, S., Trenner, M., Leicht, G., Pogarell, O., et al. (2009). EEG-vigilance and BOLD effect during simultaneous EEG/fMRI measurement. *Neuroimage* 45, 319–332. doi: 10.1016/j.neuroimage.2008.11.014

Olbrich, S., Tränkner, A., Surova, G., Gevirtz, R., Gordon, E., Hegerl, U., et al. (2016). CNS- and ANS-arousal predict response to antidepressant medication: findings from the randomized iSPOT-D study. *J. Psychiatr. Res.* 73, 108–115. doi: 10.1016/j.jpsychires.2015.12.001

Philip, N. S., Leuchter, A. F., Cook, I. A., Massaro, J., Goethe, J. W., and Carpenter, L. L. (2019). Predictors of response to synchronized transcranial magnetic stimulation for major depressive disorder. *Depress Anxiety* 36, 278–285. doi: 10.1002/da.22862

Pizzagalli, D., Pascual-Marqui, R. D., Nitschke, J. B., Oakes, T. R., Larson, C. L., Abercrombie, H. C., et al. (2001). Anterior cingulate activity as a predictor of degree of treatment response in major depression: evidence from brain electrical tomography analysis. *AJP* 158, 405–415. doi: 10.1176/appi.ajp.158.3.405

Pizzagalli, D. A., Webb, C. A., Dillon, D. G., Tenke, C. E., Kayser, J., Goer, F., et al. (2018). Pretreatment rostral anterior cingulate cortex theta activity in relation to symptom improvement in depression: a randomized clinical trial. *JAMA Psychiatry* 75, 547. doi: 10.1001/jamapsychiatry.2018.0252

Premoli, I., Castellanos, N., Rivolta, D., Belardinelli, P., Bajo, R., Zipser, C., et al. (2014). TMS-EEG signatures of GABAergic neurotransmission in the human cortex. *J. Neurosci.* 34, 5603–5612. doi: 10.1523/JNEUROSCI.5089-13.2014

Rogasch, N. C., Daskalakis, Z. J., and Fitzgerald, P. B. (2015). Cortical inhibition of distinct mechanisms in the dorsolateral prefrontal cortex is related to working memory performance: a TMS–EEG study. *Cortex* 64, 68–77. doi: 10.1016/j.cortex.2014.10.003

Sander, C., Schmidt, J. M., Mergl, R., Schmidt, F. M., and Hegerl, U. (2018). Changes in brain arousal (EEG-vigilance) after therapeutic sleep deprivation in depressive patients and healthy controls. *Sci. Rep.* 8, 15087. doi: 10.1038/s41598-018-33228-x

Schmidt, F. M., Sander, C., Dietz, M.-E., Nowak, C., Schröder, T., Mergl, R., et al. (2017). Brain arousal regulation as response predictor for antidepressant therapy in major depression. *Sci. Rep.* 7, 45187. doi: 10.1038/srep45187

Schünemann, H. J., Schünemann, A. H. J., Oxman, A. D., Brozek, J., Glasziou, P., Jaeschke, R., Vist, G. E., e al. (2008). Grading quality of evidence and strength of recommendations for diagnostic tests and strategies. *BMJ* 336, 1106–1110. doi: 10.1136/bmj.39500.677199.AE

Spellman, T., and Liston, C. (2020). Toward circuit mechanisms of pathophysiology in depression. *Am. J. Psychiatry* 177, 381–390. doi: 10.1176/appi.ajp.2020.20030280

Sun, Y., Farzan, F., Mulsant, B. H., Rajji, T. K., Fitzgerald, P. B., Barr, M. S., et al. (2016). Indicators for remission of suicidal ideation following magnetic seizure therapy in patients with treatment-resistant depression. *JAMA Psychiatry* 73, 337–345. doi: 10.1001/jamapsychiatry.2015.3097

Szumska, I., Gola, M., Rusanowska, M., Krajewska, M., Zygierewicz, J., Krejtz, I., et al. (2021). Mindfulness-based cognitive therapy reduces clinical symptoms, but do not change frontal alpha asymmetry in people with major depression disorder. *Int. J. Neurosci.* 131, 453–461. doi: 10.1080/00207454.2020.1748621

Tenke, C. E., Kayser, J., Manna, C. G., Fekri, S., Kroppmann, C. J., Schaller, J. D., et al. (2011). Current source density measures of EEG alpha predict antidepressant treatment response. *Biol. Psychiatry* 70, 388–394. doi: 10.1016/j.biopsych.2011.02.016

van der Vinne, N., Vollebregt, M. A., Boutros, N. N., Fallahpour, K., van Putten, M. J. A. M., and Arns, M. (2019a). Normalization of EEG in depression after antidepressant treatment with sertraline? A preliminary report. *J. Affect. Disord.* 259, 67–72. doi: 10.1016/j.jad.2019.08.016

van der Vinne, N., Vollebregt, M. A., van Putten, M. J. A. M., and Arns, M. (2019b). Stability of frontal alpha asymmetry in depressed patients during antidepressant treatment. *Neuroimage Clin.* 24, 2056. doi: 10.1016/j.nicl.2019.102056

Voineskos, D., Blumberger, D. M., Rogasch, N. C., Zomorrodi, R., Farzan, F., Foussias, G., et al. (2021). Neurophysiological effects of repetitive transcranial magnetic stimulation (rTMS) in treatment resistant depression. *Clin. Neurophysiol.* S1388245721005927. doi: 10.1016/j.clinph.2021.05.008

Voineskos, D., Daskalakis, Z. J., and Blumberger, D. M. (2020). Management of treatment-resistant depression: challenges and strategies. *Neuropsychiatr. Dis. Treat.* 16, 221–234. doi: 10.2147/NDT.S198774

Wade, E. C., and Iosifescu, D. V. (2016). Using electroencephalography for treatment guidance in major depressive disorder. *Biol. Psychiatry Cogn. Neurosci. Neuroimaging* 1, 411–422. doi: 10.1016/j.bpsc.2016.06.002

Widge, A. S., Avery, D. H., and Zarkowski, P. (2013). Baseline and treatment-emergent EEG biomarkers of antidepressant medication response do not predict response to repetitive transcranial magnetic stimulation. *Brain Stimul.* 6, 929–931. doi: 10.1016/j.brs.2013.05.001

Widge, A. S., Bilge, M. T., Montana, R., Chang, W., Rodriguez, C. I., Deckersbach, T., et al. (2019). Electroencephalographic biomarkers for treatment response prediction in major depressive illness: a meta-analysis. *Am. J. Psychiatry* 176, 44–56. doi: 10.1176/appi.ajp.2018.17121358

Wu, W., Pizzagall, D. A., Trivedi, M. H., and Etkin, A. (2021). Reply to: EEG-based model and antidepressant response. *Nat. Biotechnol.* 39, 28–29. doi: 10.1038/s41587-020-0738-2

Wu, W., Zhang, Y., Jiang, J., Lucas, M. V., Fonzo, G. A., Rolle, C. E., et al. (2020). An electroencephalographic signature predicts antidepressant response in major depression. *Nat. Biotechnol.* 38, 439–447. doi: 10.1038/s41587-019-0397-3

Zrenner, B., Zrenner, C., Gordon, P. C., Belardinelli, P., McDermott, E. J., Soekadar, S. R., et al. (2020). Brain oscillation-synchronized stimulation of the left dorsolateral prefrontal cortex in depression using real-time EEG-triggered TMS. *Brain Stimul.* 13, 197–205. doi: 10.1016/j.brs.2019.10.007

Zrenner, C., Belardinelli, P., Müller-Dahlhaus, F., and Ziemann, U. (2016). Closed-loop neuroscience and non-invasive brain stimulation: a tale of two loops. *Front. Cell Neurosci.* 10, 92. doi: 10.3389/fncel.2016.00092

Appendix

Appendix 1. PubMed Search Strategy ("Depressive Disorder, Major/therapy"[Mesh]) OR ("Depression/therapy"[MAJR]) OR ("Antidepressive Agents/therapeutic use"[MAJR])) AND ((EEG) OR (electroencephalography) OR (TMS-EEG) OR (TMS)) Filters: English, Human Date range: 2000-2021.

Appendix 2. EMBASE Search Strategy (major depressive disorder) AND (antidepressant agent OR ECT OR transcranial magnetic stimulation OR repetitive transcranial magnetic stimulation) AND (electroencephalography) Filters: English, Human Date range: 2000-2021.

frontiers | Frontiers in Human Neuroscience

TYPE Original Research
PUBLISHED 07 October 2022
DOI 10.3389/fnhum.2022.962231

OPEN ACCESS

EDITED BY
Felipe Fregni,
Harvard Medical School, United States

REVIEWED BY
Nayara de Lima Froio,
Hospital Alemão Oswaldo Cruz, Brazil
Muzhen Guan,
Fourth Military Medical University, China

*CORRESPONDENCE
Wei-Wei Song
zhuzhen625@163.com

†These authors have contributed equally to this work

SPECIALTY SECTION
This article was submitted to Brain Imaging and Stimulation, a section of the journal Frontiers in Human Neuroscience

RECEIVED 14 June 2022
ACCEPTED 23 August 2022
PUBLISHED 07 October 2022

CITATION
Zhu Z, Zhu H-X, Jing S-W, Li X-Z, Yang X-Y, Luo T-N, Ye S, Ouyang X-C and Song W-W (2022) Effect of transcranial magnetic stimulation in combination with citalopram on patients with post-stroke depression. *Front. Hum. Neurosci.* 16:962231. doi: 10.3389/fnhum.2022.962231

Effect of transcranial magnetic stimulation in combination with citalopram on patients with post-stroke depression

Zhen Zhu[1†], Hao-Xuan Zhu[2†], Shao-Wei Jing[2], Xia-Zhen Li[1], Xiao-Yan Yang[2], Tu-Nan Luo[2], Shuai Ye[3], Xiao-Chun Ouyang[2] and Wei-Wei Song[1*]

[1]Rehabilitation Medicine Department, The 908th Hospital of Chinese People's Liberation Army Joint Logistic Support Force, Nanchang, China, [2]Department of Neurology, The 908th Hospital of Chinese People's Liberation Army Joint Logistic Support Force, Nanchang, China, [3]Department of Neurology, Fuzong Clinical Medical College of Fujian Medical University (900 Hospital of the Joint Logistics Team), Fuzhou, China

Background: Amelioration of depression in patients with post-stroke depression (PSD) remains challenging.

Objective: The primary vision was to explore the effect of transcranial magnetic stimulation (TMS) in combination with citalopram on patients with PSD.

Methods: One hundred eligible patients who were diagnosed with PSD were recruited and randomly assigned to the control group ($n = 50$) or the TMS group ($n = 50$). The controls were given citalopram (10 mg/d for consecutive 8 weeks), while, in addition to citalopram, patients in the TMS group were also given TMS at 5 Hz once a workday for 8 weeks. The primary outcome was patient depression status as reflected by 17-item Hamilton Rating Scale for Depression (HAMD-17) score, and the secondary outcome was patient neuropsychological score determined by Mini-Mental State Examination (MMSE) and Wisconsin Card Sorting Test (WCST).

Results: Patients treated with TMS in combination with citalopram had a drastic decrease in HAMD-17 score during treatment. Bigger changes in HAMD-17 score between baseline and 2 weeks as well as between baseline and 8 weeks in the TMS group were observed ($P < 0.01$). Patients in both groups had increased MMSE scores after treatment. Data of WCST revealed patients with TMS treatment completed more categories ($P < 0.01$) and had a lower RPP in comparison to patients in the control group ($P < 0.0001$). Additionally, TMS in combination with citalopram strikingly improved patients' MMSE scores when compared with those taking citalopram alone. Last, there was no striking difference in side effects between the two groups ($P > 0.05$).

Conclusion: Our study found TMS in combination with citalopram is conducive to improving depression status and neuropsychological function, which holds great promise for treating PSD.

KEYWORDS

transcranial magnetic stimulation, citalopram, post-stroke depression, cognitive function, neuropsychological score

Introduction

Stroke is the most frequent serious neurological disease, leading to a great number of deaths and disabilities, particularly in adults between 50 and 60 years old (Robinson and Jorge, 2016). Previous progress in diagnosis and neurosurgical treatment of stroke have strikingly diminished the mortality rate, leaving an elevated prevalence of stroke survivors (Ekker et al., 2018). Despite the elusive mechanism, previous studies have consistently shown a strong association between stroke and mental diseases (Cumming et al., 2016; Robinson and Jorge, 2016). Among those, post-stroke depression (PSD) is proven to be the most frequent condition in acute settings or rehabilitation units, with a prevalence of 33% (Hackett and Pickles, 2014). Not only does PSD cause depression, loss of interest, sleep disturbances, and cognitive and executive function impairment, but it could also delay rehabilitation and even increase the risk of suicide, which creates a heavy burden on patients and society (Mijajlovic et al., 2017). Moreover, PSD is likely to be most severe at an early stage; it is of great importance to palliate depressive symptoms as soon as possible when patients begin to seek help (Starkstein and Hayhow, 2019). Thus, enhancing the early diagnostic and therapeutic efficacy of PSD is highly imperative.

The current strategy to improve PSD mainly depends on several antidepressants, including the most commonly prescribed, paroxetine and citalopram (Villa et al., 2018). Although several small-size studies have indicated that citalopram exerted a remission of PSD, with an effectiveness of 47% (Starkstein and Hayhow, 2019), there is still a long way to go to find highly effective treatment to relieve depressive behaviors in PSD patients, especially for those who are at an early stage. As a non-invasive treatment, transcranial magnetic stimulation (TMS) has been widely used in rehabilitation units for the improvement of paralysis (Jo and Perez, 2020). It has also been recently proposed as a promising strategy for major depression (George et al., 2010). Patients with major depression find relief without adverse effects after being treated with TMS in combination with citalopram (Huang et al., 2012). In addition, TMS is also suggested to improve synaptic plasticity and neuropsychological functions in animal models and humans (Kaster et al., 2018; Pang and Shi, 2021), highlighting the therapeutic potential of TMS in the central nervous system. Previously, some researchers found some beneficial effects of TMS on patients with PSD, hastening the efficacy of antidepressants, however, it was limited in antidepressant-resident or late-stage patients. Larger scale studies are needed to determine the safety and efficacy of TMS based on antidepressants in PSD patients.

In the present study, we enrolled 100 PSD patients to determine the effect of TMS in combination with citalopram on patients with PSD. We found TMS in combination with citalopram significantly improved depression status and cognitive function in patients with PSD with no obvious adverse effects.

Methods

Subjects

A total of 100 first-episode PSD patients, from February 2021 to March 2022, were consecutively recruited. All patients were treated in the rehabilitation- and neurology departments of the 908th Hospital of the Chinese People's Liberation Army Joint Logistic Support Force. Patients were randomly assigned into two groups, the control group ($n = 50$) and the TMS group ($n = 50$). Notably, all patients in both groups received treatment of citalopram (10 mg per day for consecutive 8 weeks). We have obtained the consent for clinical information collection from patients, and this study was approved by the Institutional Review Board of the 908th Hospital of the Chinese People's Liberation Army Joint Logistic Support Force (reference number: 2022YYLL113).

Inclusion and exclusion criteria

Patients with PSD were included if they complied with the following principles: (1) age over 18 years old; (2) clinical symptoms and imaging evidence showing they first suffered from ischemic stroke and PSD; (3) onset time < 7 day; (4) 17-item Hamilton Rating Scale for Depression (HAMD-17) between 7 and 24; (5) the National Institute of Health Stroke Scale (NIHSS) score was 1–15 when admitted; (6) patient's family signed the informed consent. Contrarily, patients were excluded if they met either of the following principles: (1) age below 18 years old; (2) patients didn't meet the diagnosis of PSD; (3) intellectual, language, or expression dysfunction; (4) a history of depression or anxiety.

Treatment

Conventional treatments including hyperbaric oxygen treatment, blood pressure control, neurotrophic support treatment, and symptomatic treatment supplemented by acupuncture, massage, and rehabilitation training, were applied to all patients. As mentioned above, patients in the control group were given oral citalopram (Xian-Janssen Pharmaceutical Ltd, China) 10 mg per day for consecutive 8 weeks. Apart from this, patients in the TMS group also received repetitive TMS once a day for 5 workdays a week for 8 weeks. The experimental setting of TMS was according to the treatment recommendations of TMS for major depressive disorder

(Perera et al., 2016). Briefly, the stimulation site was selected as the left dorsolateral prefrontal cortex (LDLPFC) at a magnetic stimulation frequency of 5 Hz, matching specifications of a prior study (Li et al., 2022). Before the probe test, an individual's level of movement threshold (MT) needed to be determined, which was defined as when the contralateral thumb abductor motor evoked potential exceeds 50 μV for at least 5 times in ten stimulations, the minimum stimulus intensity is MT. During probe treatment, patients were placed in a sitting or supine position. The magnetic stimulation intensity was 60% MT, and the interval was 56 s for every 4 s stimulation, and the total stimulation period was 20 min. Notably, 800 magnetic pulse stimulation was given every day.

NIHSS

The NIHSS comprises 15 items of a neurologic examination stroke scale for evaluating patient status after acute cerebral infarction. The details regarding the 15 items are presented in previous literature (Kwah and Diong, 2014). A well-trained neurosurgeon was responsible for rating patient ability to answer and perform.

HAMD-17

A HAMD-17 assessment was conducted according to a previous study (Zimmerman et al., 2013). In brief, the scale encompasses seventeen aspects, including sleep disorder, cognitive impairment, tardiness, and sense of hopelessness. The higher the total score is, the more severe the degree of depression is. According to the scores, depression severity is segmented into three statuses: mild depression (8–17), moderate depression (17–24), and severe depression (≥24). All patients received the HAMD-17 assessment at 0-, 2-, 4-, 6-, and 8-weeks after stroke.

Mini-mental state examination

The Chinese version of Mini-Mental State Examination (MMSE) was performed to assess the cognitive function, which encompasses tests of attention, orientation, memory, language, visual-spatial skills, etc. The total score of MMSE is 30, and the cognitive function is reflected by the score.

Wisconsin card sorting test

The Wisconsin Card Sorting Test (WCST) was used for the neuropsychological function of patients according to a previous method (Huang et al., 2012). Subjects were required to sort 48 cards presented on the computer, which are categorized into three conditions: color, shape, and number. Patients were required to change one sorting to another one if they had consecutively completed six correct tasks. The end of WCST was defined as the correct completion of all six categories using 48 cards. Several parameters, including the total number of errors, total trials, correct trials, etc., were recorded and assessed blindly.

Statistical analysis

All data in the present study were analyzed by SPSS 26.0 and graphed by Graphed Prism. Except for those especially noted, data were presented as mean ± SD. An independent *t*-test was used to determine differences between the two groups if the data complied with the normality examined by Kolmogorov–Smirnov test. Otherwise, the Mann-Whitney U test was applied. Comparisons between two categorical groups were performed by a chi-square test. A paired *t*-test was conducted to determine the difference between before and after treatment in the same group. Differences between the two groups at different time points were determined by repetitive measuring tests. The sample size was calculated using an online model (http://www.powerandsamplesize.com/). A $P < 0.05$ was considered statistically significant.

Results

Patient characteristics

As is shown in Table 1, a total of 100 patients with PSD were enrolled in our study, the control group ($n = 50$) and the TMS group ($n = 50$). There was no significant difference in age, gender, BMI, the incidence of hypertension, or rate of diabetes between the two groups ($P > 0.05$). Also, the onset time of PSD did not differ in the two groups and neither did education level ($P > 0.05$). Notably, cognitive function, as reflected by MMSE, also didn't differ between the two groups ($P > 0.05$). Additionally, patients in the control group bore a close resemblance to the TMS group in depression severity indicated by HAMD-17 ($P > 0.05$).

Effect of TMS in combination with citalopram on depression status

To interrogate the effect of TMS in combination with citalopram on depression severity (primary outcome), we conducted HAMD-17 assessment at 0-, 2-, 4-, 6-, and 8-weeks for all patients with PSD. As mentioned above, there was no striking difference in HAMD-17 between groups at admission. In general, we found a more dramatic decrease in HAMD-17 score in the TMS group than in the control group during

TABLE 1 Demographic characteristics.

Variable	Control group	TMS group	Statistics	*P*-value
No. of patients	50	50		
Age (years)	48.13 ± 13.42	48.25 ± 12.82	$t = 0.0457$	0.964
Male/female	24 (26)	27 (23)	$\chi^2 = 0.360$	0.5485
Onset time of PSD	4.23 ± 2.25	4.15 ± 1.82	$t = 0.196$	0.845
BMI (kg/m^2)	23.11 ± 2.41	23.28 ± 1.34	$t = 0.436$	0.664
Education level (years)	11.34 ± 3.25	11.84 ± 2.97	$t = 0.803$	0.424
Hypertension (%)	10 (20)	9 (22.5)	$\chi^2 = 0.0650$	0.799
Diabetes (%)	5 (10)	6 (12)	$\chi^2 = 0.102$	0.749
MMSE (at admission)	25.34 ± 3.21	25.49 ± 2.29	$t = 0.270$	0.789
HAMD-17 (at admission)	24.54 ± 2.27	24.40 ± 3.01	$t = 0.793$	0.782

BMI, body mass index; Control group, citalopram + sham TMS; TMS group, citalopram + TMS.

the 8-week treatment ($P < 0.0001$, Figure 1A). Indeed, the sub-analysis showed that changes in HAMD-17 score between baseline and 2 weeks in the TMS group were much higher than that in the control group ($P < 0.01$, Figure 1B). In addition, we also found patients in the control group had a higher HAMD-17 score than that of the TMS group ($P < 0.01$, Figure 1C), indicating a severe depression status, whereas changes in HAMD-17 score between baseline and 8 weeks in TMS group was higher than that in the control group ($P < 0.01$).

Effect of TMS in combination with citalopram on neuropsychological score

We also performed an MMSE assessment and WCST to investigate the neuropsychological status (second outcome). The data showed MMSE scores in both the control and TMS group were increased after treatment ($P < 0.05$ for the control group; $P < 0.001$ for the TMS group; Figures 2A,B), whereas there was no remarkable difference in MMSE scores between the two groups ($P > 0.05$, Figure 2C). Additionally, in the WSCT task, patients in two groups had improvements in CC, RFPP, and RPP. Moreover, patients with TMS treatment completed more categories ($P < 0.01$, Table 2) and had a lower RPP in comparison with patients in the control group ($P < 0.0001$, Table 2). Lastly, we also found TMS in combination with citalopram strikingly improved the NIHSS and MMSE scores in comparison with citalopram alone (Table 3).

The impact of TMS in combination with citalopram on the occurrence of side effects

Despite a high incidence of headache, nausea, and dizziness in both groups, there was no striking difference in those side effects between the two groups ($P > 0.05$, Table 4). We reasoned the high incidence of headache, nausea, and dizziness resulted from the stroke itself.

Discussion

In the present study, we investigated the safety and efficacy of TMS in combination with citalopram in patients with PSD, with merely citalopram administration as a control. Dramatically, we found TMS in combination with citalopram significantly improved depression status in patients with PSD with no obvious adverse effects. In addition, our study also revealed TMS in combination with citalopram could exert an improving function in neuropsychological tests, including MMSE and WCST.

PSD has been proven to pose a high risk to individuals who survive stroke for causing depression, loss of interest, and delaying rehabilitation, even elevating the possibility of suicide, which creates a grave burden for families and society (Robinson and Jorge, 2016). Disease-mortifying treatment, such as citalopram, has been widely utilized to alleviate symptoms of PSD without dissatisfying outcomes, indicating a single treatment might not be enough to obtain positive outcomes. Enhancing the efficacy of disease-mortifying treatment is the goal for doctors to pursue. TMS has been widely utilized to promote recovery of motor functions after spinal cord injury (Jo and Perez, 2020). Recently, TMS has also been proposed as a promising strategy for improving depression status (Huang et al., 2012). A recent study on patients with major depression revealed that TMS in combination with citalopram bore an improving function in relieving depression symptoms (Huang et al., 2012). The primary purpose was to investigate the effect of TMS in combination with citalopram on PSD patients. Dramatically, we found a remarkable improvement in depression status after treatment of TMS in combination with citalopram, as reflected by HAMD-17 scores. As mentioned in

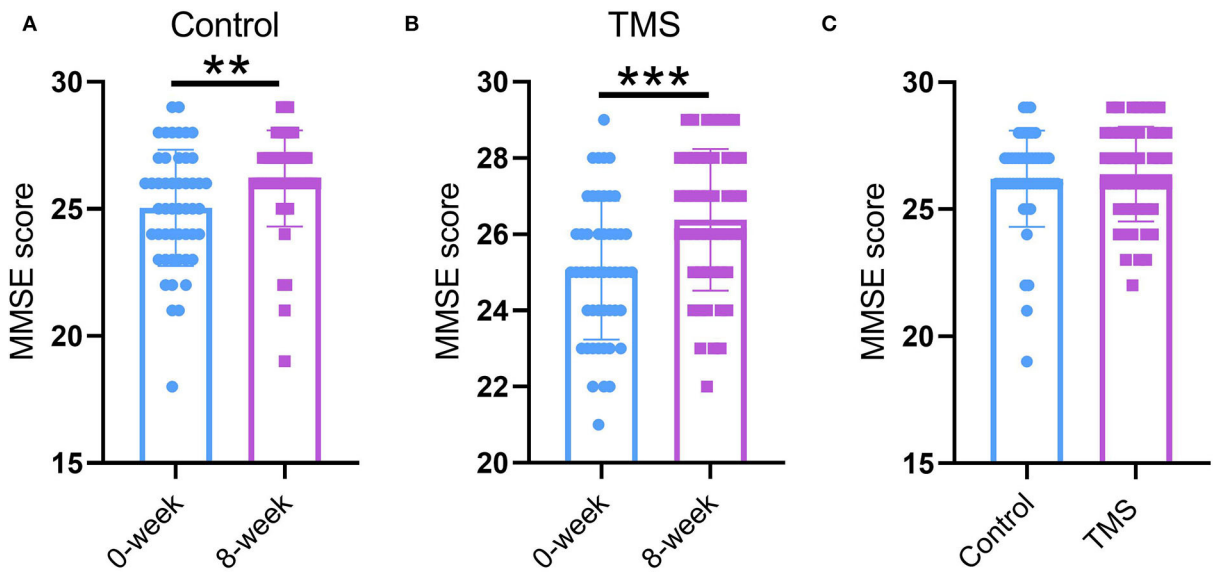

FIGURE 1
Effect of TMS in combination with citalopram on depression status. **(A)** HAMD-17 score from baseline throughout 8 weeks of treatment. **(B)** Changes of HAMD-17 score between baseline and 2 weeks. **(C)** Changes of HAMD-17 score between baseline and 8 weeks. ** $P < 0.01$, *** $P < 0.001$. $N = 50$ per group. The error bars present the SD.

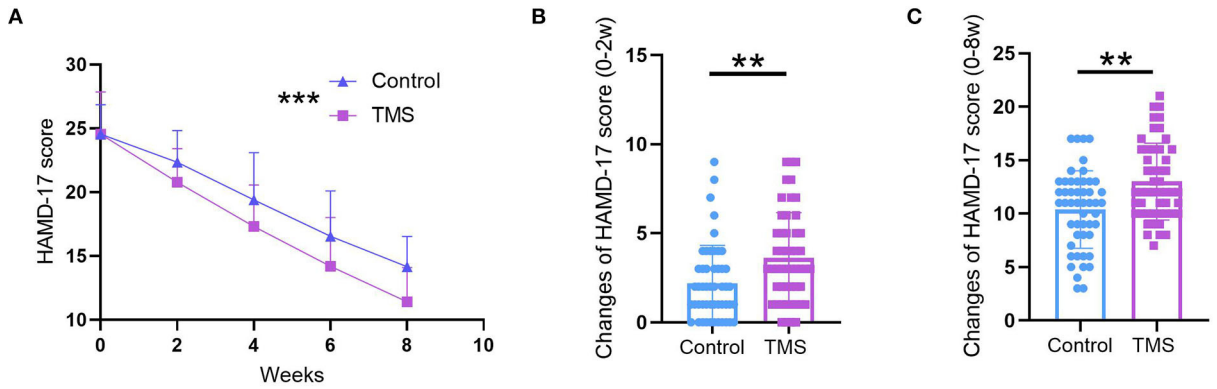

FIGURE 2
Effect of TMS in combination with citalopram on MMSE score. **(A)** Comparison of MMSE scores between 0-weeks and 8-weeks in the control group. **(B)** Comparison of MMSE score between 0-weeks and 8-weeks in TMS group. **(C)** Comparison of MMSE score between the control group and TMS group at 8-weeks. ** $P < 0.01$, *** $P < 0.001$. $N = 50$ per group. The error bars present the SD.

TABLE 2 Results of WCST.

Variable	Control group		TMS group	
	Baseline	Week 8	Baseline	Week 8
CC	2.41 ± 0.72	$2.92 \pm 0.78^{*}$	2.43 ± 0.91	3.46 ± 1.12^{yz}
RFPP	0.33 ± 0.22	0.48 ± 0.12^{y}	0.34 ± 0.11	0.53 ± 0.34^{y}
RPP	0.53 ± 0.11	0.31 ± 0.10^{y}	0.55 ± 0.12	$0.21 \pm 0.07^{y\S}$

Control group, citalopram + sham TMS; TMS group, citalopram + TMS. CC, categories completed; RFPP, percent conceptual level responses percentage; PRP, perseverative responses percentage. vs. baseline, $^{*}P < 0.01$; vs. baseline, $^{y}P < 0.001$; vs. week 8, $^{z}P < 0.01$; vs. week, $^{\S}P < 0.0001$.

TABLE 3 Results of MMSE and NIHSS score.

Variable	Control group		TMS group	
	Baseline	Week 8	Baseline	Week 8
MMSE	25.34 ± 3.11	26.33 ± 1.05*	25.25 ± 3.22	28.25 ± 1.23^{y§}
NIHSS	10.31 ± 2.22	4.48 ± 1.12^{y}	10.28 ± 2.11	3.23 ± 1.34^{yz}

Control group, citalopram + sham TMS; TMS group, citalopram + TMS. MMSE, Mini-mental State Examination; NIHSS, National Institute of Health Stroke Scale (NIHSS). vs. baseline, *$P < 0.01$; vs. baseline, $^{y}P < 0.001$; vs. week 8, $^{z}P < 0.001$; vs. week 8, $^{\S}P < 0.0001$.

TABLE 4 Occurrence of side effects during treatment.

Variable	Control group	TMS group	Statistics	*P*-value
Headache (%)	40 (80)	42 (84)	$\chi^2 = 0.271$	0.603
Nausea (%)	11 (22)	10 (20)	$\chi^2 = 0.219$	0.640
Dizziness (%)	35 (70)	39 (78)	$\chi^2 = 1.372$	0.242

Control group, citalopram + sham TMS; TMS group, citalopram + TMS.

the introduction, relieving symptoms at an early stage of PSD holds great importance during treatment as a whole (Mijajlovic et al., 2017). Sub-analysis found that TMS enhanced symptom improvement in the first 2 weeks when regularly treated in an early period of PSD, indicating TMS in combination with citalopram improved PSD at an early stage. Although we found that patients have some discomforts, such as headache, nausea, and dizziness, those discomforts might derive from the stroke itself. Taken together, our findings are consistent with previous studies that repetitive TMS is an effective and safe treatment for PSD (Li et al., 2022; Shen et al., 2022).

The brain dysfunction of depressive patients is mainly related to the abnormal interaction between the cortex and subcortical nuclei (Villa et al., 2018). LDLPFC is involved in positive emotion regulation, while the right DLPFC (RDLPFC) is involved in negative emotion regulation. In general, DLPFC usually presents a weakened function in depressive patients, while the right DLPFC function was significantly enhanced (Fitzgerald et al., 2006). Thus, it is theoretically beneficial to alleviate the symptoms of patients with depression by adjusting the function of DLPFC on both sides of the patient's brain. In the present study, we selected LDLPFC as the stimulation site for TMS that intensified the brain function and added the evidence that this action site indeed is a therapeutic target for attenuating PSD. Another critical concern that should also be noted is that the frequency of TMS was 5 Hz in our study. High frequent stimulation of TMS for LDLPFC and low frequency for RDLPFC are preferred. Previously a systematic review from China found that 10 Hz could evoke the left-brain function and palliate the PSD (Shao et al., 2021). Our study found that 5 Hz was enough to obtain those protective effects, which is also supported by another study (Li et al., 2022).

This leaves the question of how does TMS in combination with citalopram improve the symptoms of PSD. Previous analysis revealed that PSD is related to the disrupted neurotransmitter metabolism, particularly for decreased 5-HT and norepinephrine (NE) neurotransmitter contents in lesioned regions (Liu et al., 2022). Citalopram is a kind of 5-HT reuptake inhibitor that reduces 5-HT reuptake by neurons, thereby producing antidepressant effects. Dopamine (DA) is one of the most important neurotransmitters in the NE system. DA contents in the brain were proved to be decreased after stroke, as confirmed by animal and clinical research (Grace, 2016; Liu et al., 2022). Considering the provoking effects of TMS in the cortex, we speculate that TMS might activate the cingulate gyrus, putamen, hippocampus, and thalamus through the frontal to subcortical nucleus neural circuits, and activate the contralateral region through the corpus callosum to enhance the dopamine (DA) release of the striatum and mesolimbic system (Fitzgerald et al., 2006). This notion is also supported by a recent study that TMS effectively promotes the synthesis and release of DA in patients with PSD (Liu et al., 2022). In those regards, TMS in combination with citalopram holds more therapeutic value for treating PSD in comparison with only citalopram administration.

In addition, we also conducted the neuropsychological assessment, including MMSE and WSCT, to explore the cognitive function and working memory. A previous study has revealed that PSD was always companied by disrupted cognitive function and working memory (Price and Duman, 2020). Our findings uncovered that TMS in combination with citalopram improved those disruptions, which might result from improved depression status or the recovery of stroke.

There are some limitations in our study. First, we don't provide the direct evidence to prove the beneficial role of TMS in ameliorating the depressive symptoms of PSD. Second, other confounders, such as placebo effect or other medications, might also bring the additive outcomes. Last, we only included the

HAMD-17 scale to evaluate the primary outcome, which might not fully reflect the depressive status.

Conclusion

Our study found TMS in combination with citalopram is conducive to improving depression status and neuropsychological function, which holds great promise for treating PSD.

Data availability statement

The original contributions presented in the study are included in the article/supplementary material, further inquiries can be directed to the corresponding author.

Ethics statement

The studies involving human participants were reviewed and approved by the Institutional Review Board of the 908th Hospital of the Chinese People's Liberation Army Joint Logistic Support Force. The patients/participants provided their written informed consent to participate in this study.

Author contributions

ZZ, W-WS, and X-CO conceived and designed the project. ZZ, SY, and H-XZ collected the data. ZZ, H-XZ, S-WJ, X-ZL, X-YY, and T-NL analyzed data. ZZ and W-WS wrote the manuscript. All authors contributed to the article and approved the submitted version.

Funding

This study was supported by the 908th Hospital of the Chinese People's Liberation Army Joint Logistic Support Force (Funding is to W-WS). The funding had no role in the present study.

Conflict of interest

The authors declare that the research was conducted in the absence of any commercial or financial relationships that could be construed as a potential conflict of interest.

Publisher's note

All claims expressed in this article are solely those of the authors and do not necessarily represent those of their affiliated organizations, or those of the publisher, the editors and the reviewers. Any product that may be evaluated in this article, or claim that may be made by its manufacturer, is not guaranteed or endorsed by the publisher.

References

Cumming, T. B., Packer, M., Kramer, S. F., and English, C. (2016). The prevalence of fatigue after stroke: a systematic review and meta-analysis. *Int. J. Stroke*. 11, 968–977. doi: 10.1177/1747493016669861

Ekker, M. S., Boot, E. M., Singhal, A. B., Tan, K. S., Debette, S., Tuladhar, A. M., et al. (2018). Epidemiology, aetiology, and management of ischaemic stroke in young adults. *Lancet Neurol*. 17, 790–801. doi: 10.1016/S1474-4422(18)30233-3

Fitzgerald, *P*. B., Oxley, T. J., Laird, A. R., Kulkarni, J., Egan, G. F., Daskalakis, Z. J., et al. (2006). An analysis of functional neuroimaging studies of dorsolateral prefrontal cortical activity in depression. *Psychiatry Res*. 148, 33–45. doi: 10.1016/j.pscychresns.2006.04.006

George, M. S., Lisanby, S. H., Avery, D., McDonald, W. M., Durkalski, V., Pavlicova, M., et al. (2010). Daily left prefrontal transcranial magnetic stimulation therapy for major depressive disorder: a sham-controlled randomized trial. *Arch. Gen. Psychiatry*. 67, 507–516. doi: 10.1001/archgenpsychiatry.2010.46

Grace, A. A. (2016). Dysregulation of the dopamine system in the pathophysiology of schizophrenia and depression. *Nat. Rev. Neurosci*. 17, 524–532. doi: 10.1038/nrn.2016.57

Hackett, M. L., and Pickles, K. (2014). Part I: frequency of depression after stroke: an updated systematic review and meta-analysis of observational studies. *Int. J. Stroke*. 9, 1017–1025. doi: 10.1111/ijs.12357

Huang, M. L., Luo, B. Y., Hu, J. B., Wang, S. S., Zhou, W. H., Wei, N., et al. (2012). Repetitive transcranial magnetic stimulation in combination with citalopram in young patients with first-episode major depressive disorder: a double-blind, randomized, sham-controlled trial. *Aust. NZ J. Psychiatry*. 46, 257–264. doi: 10.1177/0004867411433216

Jo, H. J., and Perez, M. A. (2020). Corticospinal-motor neuronal plasticity promotes exercise-mediated recovery in humans with spinal cord injury. *Brain*. 143, 1368–1382. doi: 10.1093/brain/awaa052

Kaster, T. S., Daskalakis, Z. J., Noda, Y., Knyahnytska, Y., Downar, J., Rajji, T. K., et al. (2018). Efficacy, tolerability, and cognitive effects of deep transcranial magnetic stimulation for late-life depression: a prospective randomized controlled trial. *Neuropsychopharmacology*. 43, 2231–2238. doi: 10.1038/s41386-018-0121-x

Kwah, L. K., and Diong, J. (2014). National Institutes of Health Stroke Scale (NIHSS). *J. Physiother*. 60, 61. doi: 10.1016/j.jphys.2013.12.012

Li, Y., Li, K., Feng, R., Li, Y., Li, Y., Luo, H., et al. (2022). Mechanisms of repetitive transcranial magnetic stimulation on post-stroke depression: a resting-state functional magnetic resonance imaging study. *Brain Topogr*. 35, 363–374. doi: 10.1007/s10548-022-00894-0

Liu, S., Wang, X., Yu, R., and Sun, Y. (2022). Effect of transcranial magnetic stimulation on treatment effect and immune function. *Saudi J. Biol. Sci*. 29, 379–384. doi: 10.1016/j.sjbs.2021.08.104

Mijajlovic, M. D., Pavlovic, A., Brainin, M., Heiss, W. D., Quinn, T. J., Ihle-Hansen, H. B., et al. (2017). Post-stroke dementia—a comprehensive review. *BMC Med*. 15:11. doi: 10.1186/s12916-017-0779-7

Pang, Y., and Shi, M. (2021). Repetitive transcranial magnetic stimulation improves mild cognitive impairment associated with Alzheimer's disease in mice

by modulating the miR-567/NEUROD2/PSD95 axis. *Neuropsychiatr. Dis. Treat.* 17, 2151–2161. doi: 10.2147/NDT.S311183

Perera, T., George, M. S., Grammer, G., Janicak, *P.* G., Pascual-Leone, A., Wirecki, T. S., et al. (2016). The clinical TMS society consensus review and treatment recommendations for TMS therapy for major depressive disorder. *Brain Stimul.* 9, 336–346. doi: 10.1016/j.brs.2016.03.010

Price, R. B., and Duman, R. (2020). Neuroplasticity in cognitive and psychological mechanisms of depression: an integrative model. *Mol. Psychiatry.* 25, 530–543. doi: 10.1038/s41380-019-0615-x

Robinson, R. G., and Jorge, R. E. (2016). Post-stroke depression: a review. *Am. J. Psychiatry.* 173, 221–231. doi: 10.1176/appi.ajp.2015.15030363

Shao, D., Zhao, Z. N., Zhang, Y. Q., Zhou, X. Y., Zhao, L. B., Dong, M., et al. (2021). Efficacy of repetitive transcranial magnetic stimulation for post-stroke depression: a systematic review and meta-analysis of randomized clinical trials. *Braz. J. Med. Biol. Res.* 54, e10010-e. doi: 10.1590/1414-431x202010010

Shen, Y., Cai, Z., Liu, F., Zhang, Z., and Ni, G. (2022). Repetitive transcranial magnetic stimulation and transcranial direct current stimulation as treatment of poststroke depression: a systematic review and meta-analysis. *Neurologist.* 27, 177–182. doi: 10.1097/NRL.0000000000000416

Starkstein, S. E., and Hayhow, B. D. (2019). Treatment of post-stroke depression. *Curr. Treat. Options Neurol.* 21, 31. doi: 10.1007/s11940-019-0570-5

Villa, R. F., Ferrari, F., and Moretti, A. (2018). Post-stroke depression: mechanisms and pharmacological treatment. *Pharmacol. Ther.* 184, 131–144. doi: 10.1016/j.pharmthera.2017.11.005

Zimmerman, M., Martinez, J. H., Young, D., Chelminski, I., and Dalrymple, K. (2013). Severity classification on the Hamilton Depression Rating Scale. *J. Affect. Disord.* 150, 384–388. doi: 10.1016/j.jad.2013.04.028

frontiers | Frontiers in Human Neuroscience

TYPE Original Research
PUBLISHED 12 October 2022
DOI 10.3389/fnhum.2022.973298

OPEN ACCESS

EDITED BY
Jiaojian Wang,
Kunming University of Science and Technology, China

REVIEWED BY
Yating Lv,
Hangzhou Normal University, China
Rong Li,
University of Electronic Science and Technology of China, China

*CORRESPONDENCE
Gong-jun Ji
jigongjun@163.com
Kai Wang
wangkai1964@126.com

†These authors have contributed equally to this work

SPECIALTY SECTION
This article was submitted to Brain Imaging and Stimulation, a section of the journal Frontiers in Human Neuroscience

RECEIVED 20 June 2022
ACCEPTED 24 August 2022
PUBLISHED 12 October 2022

CITATION
Hua Q, Zhang Y, Li Q, Gao X, Du R, Wang Y, Zhou Q, Zhang T, Sun J, Zhang L, Ji G-j and Wang K (2022) Efficacy of twice-daily high-frequency repetitive transcranial magnetic stimulation on associative memory. *Front. Hum. Neurosci.* 16:973298. doi: 10.3389/fnhum.2022.973298

Efficacy of twice-daily high-frequency repetitive transcranial magnetic stimulation on associative memory

Qiang Hua[1,2,3,4†], Yuanyuan Zhang[2,3,4†], Qianqian Li[3,4,5†], Xiaoran Gao[2,3,4], Rongrong Du[2,3,4], Yingru Wang[2,3,4], Qian Zhou[1,3,4], Ting Zhang[1,3,4], Jinmei Sun[1,3,4], Lei Zhang[1,2,3,4], Gong-jun Ji[2,3,4,6*] and Kai Wang[1,2,3,4,6,7*]

[1]Department of Neurology, The First Affiliated Hospital of Anhui Medical University, Anhui Medical University, Hefei, China, [2]School of Mental Health and Psychological Sciences, Anhui Medical University, Hefei, China, [3]Anhui Province Key Laboratory of Cognition and Neuropsychiatric Disorders, Hefei, China, [4]Collaborative Innovation Centre of Neuropsychiatric Disorder and Mental Health, Hefei, China, [5]Department of Psychiatry, The First Affiliated Hospital of Anhui Medical University, Hefei, China, [6]Hefei Comprehensive National Science Center, Institute of Artificial Intelligence, Hefei, China, [7]Anhui Institute of Translational Medicine, Hefei, China

Objectives: Several studies have examined the effects of repetitive transcranial magnetic stimulation (rTMS) on associative memory (AM) but findings were inconsistent. Here, we aimed to test whether twice-daily rTMS could significantly improve AM.

Methods: In this single-blind, sham-controlled experiment, 40 participants were randomized to receive twice-daily sham or real rTMS sessions for five consecutive days (a total of 16,000 pulses). The stimulation target in left inferior parietal lobule (IPL) exhibiting peak functional connectivity to the left hippocampus was individually defined for each participant. Participants completed both a picture-cued word association task and Stroop test at baseline and 1 day after the final real or sham rTMS session. Effects of twice-daily rTMS on AM and Stroop test performance were compared using two-way repeated measures analysis of variance with main factors Group (real vs. sham) and Time (baseline vs. post-rTMS).

Results: There was a significant Group × Time interaction effect. AM score was significantly enhanced in the twice-daily real group after rTMS, but this difference could not survive the *post hoc* analysis after multiple comparison correction. Further, AM improvement in the twice-daily real group was not superior to a previously reported once-daily rTMS group receiving 8,000 pulses. Then, we combined the twice- and once-daily real groups, and found a significant Group × Time interaction effect. *Post hoc* analysis indicated that the AM score was significantly enhanced in the real group after multiple comparisons correction.

Conclusion: Our prospective experiment did not show significant rTMS effect on AM, but this effect may become significant if more participants could be recruited as revealed by our retrospective analysis.

KEYWORDS

associative memory, hippocampal-cortical network, inferior parietal lobule, stimulation dose, transcranial magnetic stimulation

Introduction

Transcranial magnetic stimulation (TMS) is a non-invasive technique for modulating brain network connectivity with demonstrated therapeutic efficacy against neurological and neuropsychiatric illnesses (Fox et al., 2012). Wang et al. (2014) reported that once-daily repetitive TMS (rTMS) to the inferior parietal lobule (IPL), a region strongly connected to the hippocampus, significantly improved associative memory (AM) in healthy participants, suggesting possible utility for treatment of disorders characterized by AM deficits, such as stroke, age-related cognitive decline, neurotrauma, and various neuropsychiatric and neurodegenerative conditions.

However, the physiological response to non-invasive brain stimulation is known to be highly variable among individuals (López-Alonso et al., 2014), and several subsequent TMS studies found no significant AM improvement. For instance, a survey of research groups found that approximately 50% were not able to reproduce rTMS effects from original publications and a recent investigation by Héroux et al. (2015) reported significant changes in functional connectivity (FC) following multi-day rTMS of the parietal cortex but no AM enhancement (Hendrikse et al., 2020). Similarly, we found no significant difference in AM following once-daily rTMS sessions for 5 days compared to a sham group (Gao et al., 2021). Collectively, these inconsistencies suggest that rTMS efficacy for improving AM is highly dependent on stimulus protocol (e.g., stimulus intensity, duration), target, study design, and (or) treatment group characteristics.

Increasing the stimulation dose (total number of impulses) is one potential method to achieve a more robust effect on AM (Nettekoven et al., 2014). A recent study found that a high-dose rTMS protocol is safe and produces more reliable remission from depression (Cole et al., 2020). In addition to stimulation dose, the experimental design may influence outcome. The seminal study by Wang et al. (2014) and most subsequent studies reproducing AM improvement (Freedberg et al., 2019; Hermiller et al., 2019; Hendrikse et al., 2020; Gao et al., 2021) used a within-subject crossover design with an approximately 2-week delay (washout period) between real and control (sham) stimulation. However, the AM improvement from baseline was still significant 2-weeks after real rTMS, suggesting that a longer interval is needed for crossover studies (Wang and Voss, 2015; Gao et al., 2021). Nonetheless, no study has specifically examined the optimal interval for comparison of control (sham) stimulation to real stimulation.

In the present study, we aimed to investigated whether a higher rTMS dose could produce significantly greater AM improvement, beyond the sham rTMS. To this end, we modified the paradigm of our previous study (Gao et al., 2021) in two points: (1) using a parallel rather than crossover design; (2) doubling the 20-Hz rTMS dose (twice-daily sessions for 5 days, total 16,000 pulses).

Materials and methods

Participants

Forty healthy subjects (24 females and 16 males) with no history of rTMS, transcranial electric stimulation, neuropsychological disorders, or psychoactive drug use were recruited for this study. All participants met the safety criteria for MRI and rTMS (Rossi et al., 2009) and provided written informed consent. Each was remunerated for their participation after study completion. Experiments were conducted in accordance with the Declaration of Helsinki (2008 revised edition) and were approved by the local ethics committee.

Experimental design

This was a randomized, single-blind, sham-controlled, parallel design study consisting of two arms, real 20-Hz rTMS over the IPL (experimental) and sham rTMS (control). Forty subjects were included based on our previous work using single daily rTMS sessions. Subjects were assigned to the real or sham group according to random number selection while ensuring 20 per group. All subjects were unaware of the stimulation protocols until the end of the study (single-blind).

Each participant received twice-daily rTMS sessions over five consecutive days, for a total of ten sessions and 16,000 pulses. A face-cued word recall task was using to test AM

and the Stroop test to assess non-associative memory cognitive processing. Tasks were performed both 1 day prior to the first real or sham stimulation session (baseline assessment) and 1 day after the final session (post-rTMS assessment). Structural MRI and rs-fMRI were conducted on each subject prior to baseline testing to identify the IPL target site (**Figure 1A**). After each session, subjects self-reported TMS adverse events on a numeric rating scale from 0 (no side effects) to 5 (unbearable side effects).

Magnetic resonance images acquisition

Magnetic resonance images (MRI) were collected at the University of Science and Technology of China (Hefei, Anhui Province) using a 3.0 T scanner (Discovery 750; GE Healthcare, Milwaukee, WI, United States). Functional and structural images were acquired using the same parameters as in our previous studies (Ji et al., 2019a,b, 2021). Briefly, high spatial resolution T1-weighted anatomic images were acquired in the sagittal orientation using a three-dimensional brain-volume sequence (repetition/echo time, 8.16/3.18 ms; flip angle, 12°; field of view, 256 × 256 mm^2; 256 × 256 matrix; section thickness, 1 mm, without intersection gap; voxel size, 1 × 1 × 1 mm^3; 188 sections). Following structural MRI scanning, functional images (217 volumes) were acquired using a single-shot gradient-recalled echo planar imaging sequence (repetition/echo time, 2,400/30 ms; flip angle, 90°). Images of 46 transverse sections (field of view, 192 mm × 192 mm; 64 × 64 in-plane matrix; section thickness without intersection gap, 3 mm) were acquired parallel to the anteroposterior commissure line. Foam fillers and earplugs were used to minimize head motion and scanner noise during image acquisition. All participants were asked to keep their eyes close and rest without falling asleep during scanning. Scanning was performed prior to AM and Stroop testing to exclude potential carry-over effects.

Identification of stimulation locations

Cortical stimulation locations over the IPL were identified from individual resting-state functional connectivity maps with the left hippocampus as the seed region (Wang et al., 2014; Hendrikse et al., 2020; Gao et al., 2021). The hippocampal seed was set at [−24, −18, −18] in Montreal Neurological Institute (MNI) coordinates according to Wang et al. (2014). The stimulation target for each participant was defined as the strongest connectivity site within the spherical mask of the left IPL (MNI coordinates [−47, −68, 36], radius 15 mm).

Preprocessing consisted of seven steps: (1) deleting the first five functional volumes; (2) slice timing correction and realignment; (3) co-registration of structural and functional images; (4) normalization of functional images by the matrix computed in structural segmentation and normalization; (5) smoothing of functional images using a 4-mm full-width at half-maximum isotropic Gaussian kernel; (6) temporal band-pass filtering (0.01–0.1 Hz); (7) regressing out 27 nuisance signals (average white matter, cerebrospinal fluid, and whole-brain signals as well as 24 head motion parameters). All processing steps were performed using Statistical Parametric Mapping (SPM) 12 and in-house software TMStarget.[1,2]

Transcranial magnetic stimulation parameters

Transcranial magnetic stimulation was delivered to the IPC using a Magstim Rapid^2 stimulator (Magstim Company, Whitland, United Kingdom) through a 70-mm air-cooled figure-of-eight coil under the guidance of a frameless stereotactic optical tracking neuronavigation system (Brainsight; Rogue Research, Montreal, QC, Canada) (Gao et al., 2021). Individual stimulus intensity was set according to the resting motor threshold (RMT), defined as the minimum stimulator output necessary to evoke a potential with peak-to-peak amplitude ≥50 mV from the right first dorsal interosseous (FDI) muscle in at least 5 out of 10 consecutive trials (Ji et al., 2017). For the real stimulation group, rTMS was applied with 100% of RMT at 20-Hz (2 s on, 28 s off) for 20 min (1,600 pulses/session) over the individual IPL target. A total of 10 rTMS sessions were performed over a 5-day period with 2 sessions per day (16,000 pulses in total) separated by at least 1 h.

For the sham stimulation condition, participants received the same rTMS protocol using a sham coil (Magstim Company, Whitland, United Kingdom) with the same appearance as the real coil to avoid participants identifying rTMS group allocation. This sham coil generated only sound and sensations on the scalp similar to the real coil but no current (Chen et al., 2019).

Associative memory test

We employed the computerized Chinese face-cued word recall task described by Gao et al. (2021) to assess AM. Each subject studied 15 photographs of Chinese faces presented individually on a computer screen while a common word was read aloud in standard Mandarin. Each face corresponded to a unique word and was shown for 4 s. There were four alternative versions of the test, each using a different set of faces and words, and each participant was randomly assigned two, one to complete at baseline and the other following sham or real rTMS. All the face photos were presented at

1 https://www.fil.ion.ucl.ac.uk/spm/

2 https://github.com/jigongjun/Neuroimaging-and-Neuromodulation

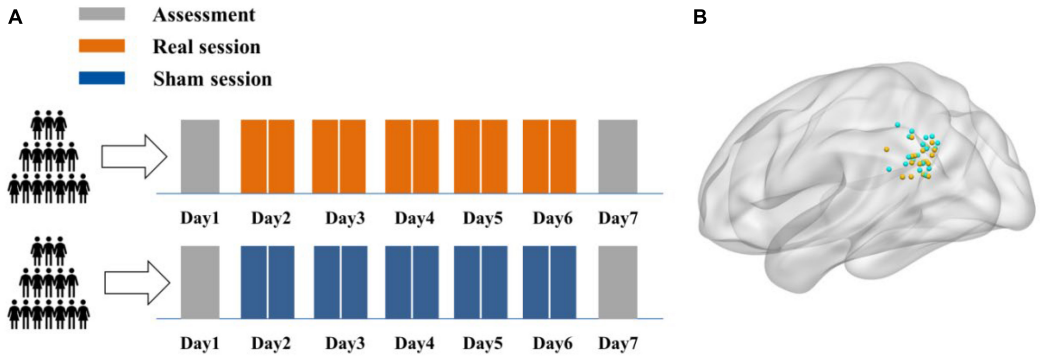

FIGURE 1
Experimental design. **(A)** Each participant received ten real or sham rTMS sessions delivered two per day for five consecutive days. A face-cued recall (associative memory) task and non-associative Stroop task were completed 1 day prior to the first stimulation session (baseline) and 1 day after the final session. **(B)** The individual stimulation sites in the left IPL were identified by rs-fMRI maps of hippocampal functional connectivity. The stimulation sites for all subjects in real and sham groups are demarcated by green and yellow spheres, respectively, in standard MNI space.

4,800 × 6,000 pixels per inch in greyscale and all words were nouns of two Chinese characters taken from the Chinese Corpus Word list, with written frequency between 500 and 3,000 (Chinese Language and Writing Network).[3] Subjects were instructed to pay attention and try to remember the face-word associations. After the learning phase, subjects were given a rest of approximately 1 min, followed by face ire-presentation in a different and random order. Subjects were instructed to recall the word that accompanied each face during the learning phase, and each word response was scored as correct or incorrect (with no errors relating to pronunciation). Participants received no prompts or feedback on the correctness of their answers. The number of correctly recalled face–word pairs was recorded as the AM score. To account for inter-subject differences in baseline AM performance, the individual improvement in AM following rTMS was expressed as a percentage change relative to baseline [AM score percentage change = *(post correct – baseline correct)/baseline correct* × *100%*] (Wang et al., 2014).

Stroop test

To prevent the participants from easily guessing the purpose of the study and to assess general non-associative cognitive processing capacity, a Stroop Color Word Test (Victoria version) adapted to local Chinese was also conducted (Lee and Chan, 2000; Lee et al., 2002; Yu and Lee, 2018). The test stimuli included images of colored dots (Part A), words unrelated to color presented in colored font (Part B), and color names presented in font colors different from the word (Part C) (e.g., the word "red" in green font). Each image consisted of 24 items in red, green, blue, or yellow presented in a 4-by-6 matrix. Each color was used six times per image, and the four colors were arranged once per row in a pseudo-random order. The participants were asked to name the colors of stimuli (font) from left to right and from top to bottom while ignoring semantic content (i.e., the correct answer for the example above is "green"). For each condition, the naming completion time (response time) and number of errors were recorded. The interference value was defined as the response time for Part B minus Part A (low interference condition), and Part C minus Part A (high interference condition).

Methodological similarities and differences from Gao et al. (2021)

Gao et al. (2021) used a within-subjects design to examine the effect of rTMS on AM. Participants received real rTMS on IPL and sham rTMS on pre-SMA targets, separated by at least 2 weeks. For each condition, a total of 5 rTMS sessions were performed over 5 consecutive days with one session per day. The rTMS involving 1,600 total pulses in one session was delivered at 100% of RMT at 20 Hz (2 s followed by 28 s of vacancy). The experimental design of the current study was modified according to Gao et al. (2021). The same rTMS parameters and face-cued word recall task were used in both studies. In contrast to Gao et al. (2021), the current study added a second session to double the rTMS dose (for a total of 16,000 pulses rather than 8,000). Additionally, we used a between-subjects design and sham stimulation was performed at 100% RMT over IPL with a sham coil in the current study.

Statistical analysis

Continuous baseline variables were compared between groups by independent samples *t*-test and categorical

3 http://www.china-language.edu.cn/

TABLE 1 Characteristics of participants from twice-daily data.

	Twice-daily(R) (*N* = 20)	*Twice-daily(S)* (*N* = 19)	Statistics/p
Demographic			
Age (years)	22.25 (0.55)	21.11 (0.48)	0.14[a]
Gender (female/male)	13/7	10/9	0.52[b]
RMT (%)	60.80 (1.23)	63.53 (1.27)	1.54/0.20[c]
Test delay (h)[d]	21.22 (0.82)	21.49 (0.93)	0.21/0.83[c]
Tests			
AM test (Baseline)	4.55 (0.45)	5.16 (0.62)	0.80/0.43[c]
Stroop test (Baseline)			
low interference (s)	1.50 (0.28)	0.75 (0.28)	1.88/0.07[c]
high interference (s)	7.62 (0.90)	7.50 (0.66)	0.11/0.91[c]

Data from Twice-daily(R) and Twice-daily(S) groups are represented as mean (SEM). [a]Mann–Whitney test; [b]Fisher's exact test; [c]Two-sample t-test; [d]Test delay depicts the interval between the end of final stimulation session and the post-rTMS tests.

baseline variables by χ^2 test. Differences in AM and Stroop test performance were compared by two-way repeated measures analysis of variance (RT-ANOVA) with main factors Group (sham vs. real rTMS) and Time (baseline vs. post-rTMS), followed by *post hoc* Sidak's multiple comparison tests. AM score percentage change was compared between groups using the independent samples *t*-test. Outliers were identified by non-linear regression using GraphPad Prism and removed from subsequent analysis.

Three separate analyses were performed using two-way ANOVA. The primary analysis included only the current data from participants receiving sham rTMS and participants receiving real rTMS (termed the *Twice-daily dataset* including *Twice-daily(R)* and *Twice-daily(S)* groups). The second analysis tested if the higher rTMS dose produced more prominent effects on AM by comparing the *Twice-daily(R)* group to the *Once-daily(R)* group. This *Once-daily(R)* group included 16 subjects from Gao et al. (2021). In the third analysis, we combined *Twice-daily(R) and Once-daily(R)* groups to produce a *Combined(R)* group and investigated the effects on AM compared to the *Twice-daily(S)* group.

Results

Primary analysis of the current experimental cohort

Characteristics of participants

Forty subjects were initially recruited to receive twice-daily sham or real rTMS (*Twice-daily dataset*) but one participant randomized to the sham group [*Twice-daily(S)*] dropped out for personal reasons. Thus, data from 39 subjects (23 females/16 males, mean age = 21.69, SEM = 0.37, range 18–29 years) were included in the primary analyzes. *Twice-daily(R) and Twice-daily(S)* groups did not differ significantly in age, gender ratio, RMT, test delay (time between the final stimulation session and post-rTMS test), baseline AM score, or baseline Stroop test score (Table 1). The averaged side effect scores are presented in Table 1, and no significant difference (p = 0.12) between the *Twice-daily(R)* and *Twice-daily(S)* groups. In general, both sham and real rTMS were well tolerated, with only slight discomfort reported by some participants. But this effect disappeared after the stimulation ended. The average (± SEM) MNI coordinate of IPL stimulation was x = −45.4 (0.92), y = −72.0 (0.83), z = 33.1 (1.01) (Figure 1B).

Associative memory performance

The AM scores for the *Twice-daily(R)* and *Twice-daily(S)* groups are presented in Table 2. Two-way RT-ANOVA revealed a significant Group [*Twice-daily(R)* vs. *Twice-daily(S)*] × Time (baseline vs. post-rTMS) interaction ($F_{1,37}$ = 5.99, p = 0.019), but no main effect of Time ($F_{1,37}$ = 0.51, p = 0.48) or Group ($F_{1,37}$ = 0.16, p = 0.70). *Post hoc* analyses using Sidak's multiple comparison test indicated that AM score was not increased significantly after real stimulation (t = 2.26, p = 0.06; Figure 2A) or sham stimulation (t = 1.21, p = 0.41; Figure 2A) compared to baseline. Further, AM score change normalized to baseline (percentage change) did not differ between *Twice-daily(R)* and *Twice-daily(S)* groups [34.7% (SEM = 15.2) vs. 3.0% (SEM = 14.8); P = 0.16].

Stroop test performance

Two measures of Stroop test performance, response time and error rate, are presented in Supplementary Table 1. ANOVA indicated no significant main effects of Group [*Twice-daily(R)* vs. *Twice-daily(S)*] and Time, and no significant Group [*Twice-daily(R)* vs. *Twice-daily(S)*] × Time (baseline vs. post-rTMS) interaction (see details in the Supplementary material).

Twice-daily versus once-daily repetitive transcranial magnetic stimulation

Characteristics of participants

There were no significant differences in age, gender ratio, RMT, AM scores, and Stroop tests between *Twice-daily(R)* and *Once-daily(R)* groups, while test delay was slightly but significantly lower in the *Twice-daily(R)* group (Table 3).

Associative memory performance

Analysis of variance revealed no significant Group [*Twice-daily(R)* and *Once-daily(R)*] × Time (baseline and post-rTMS)

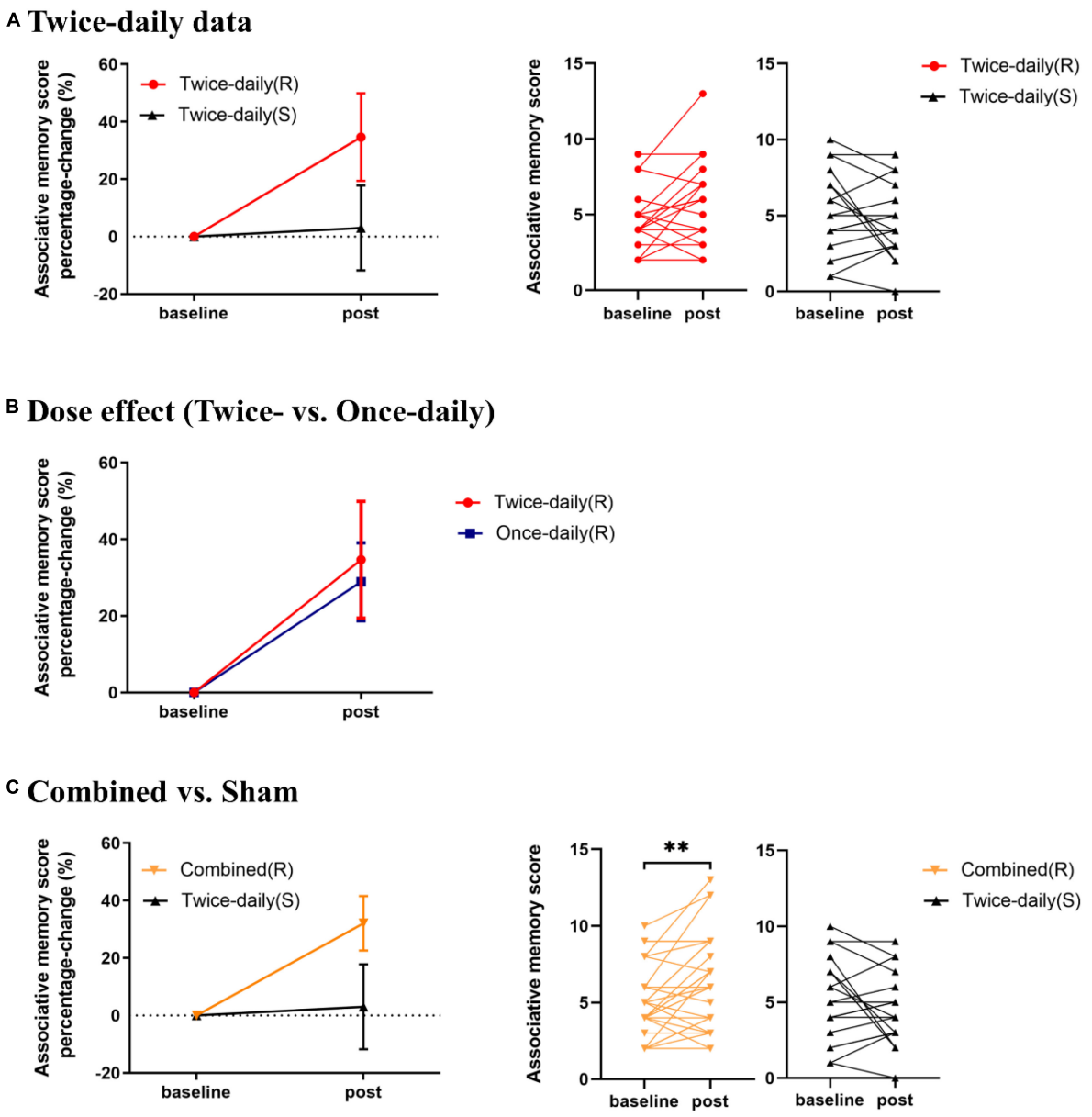

FIGURE 2
Effects of rTMS on associative memory performance. **(A)** Mean percentage change in AM score from baseline for *Twice-daily(R)* and *Twice-daily(S)* groups. The interaction effect was significant, but *post hoc* analyses indicated no significant increase following real or sham stimulation. **(B)** Mean percentage change in AM score from baseline for *Twice-daily(R)* and *Once-daily(R)* groups. There was no significant Group × Time interaction. **(C)** Mean percentage change in AM score for *Combined(R)* and *Twice-daily(S)* groups. A significant Group × Time interaction was found, and *post hoc* analyses indicated that real rTMS but not sham rTMS significantly improved AM score compared to baseline. AM score Percentage-change = *(post correct − baseline correct)/baseline correct* × *100%*. Error bars indicate SEM, $^{**}P < 0.01$.

interaction ($F_{1,34}$ = 0.02, p = 0.89) (Table 2) suggesting no difference in effect stability between *Twice-daily(R)* and *Once-daily(R)* rTMS. There was a significant main effect of Time ($F_{1,34}$ = 11.96, p = 0.002) but not Group ($F_{1,34}$ = 0.05, p = 0.82). Average percentage change in AM score did not differ significantly between *Twice-daily(R)* and *Once-daily(R)* groups [34.7% (SEM = 15.2) vs. 28.9% (SEM = 10.2); p = 0.80] (Figure 2B).

Stroop test performance

The response times and error rates for the Stroop tests from *Once-daily(R)* and *Twice-daily(R)* groups are presented in Supplementary Table 1. ANOVA revealed no significant interaction of Group [*Twice-daily(R)* vs. *Once-daily(R)*] × Time (baseline vs. post-rTMS). See details in the Supplementary material.

TABLE 2 Associative memory performance.

	AM scores	
	Baseline	**Post-rTMS**
Twice-daily(R) group	4.55 (0.45)	5.70 (0.63)
Twice-daily(S) group	5.16 (0.62)	4.53 (0.53)
Once-daily(R) group	4.69 (0.62)	5.94 (0.84)
Combined(R) group	4.61 (0.37)	5.81 (0.51)

AM performance provided as mean raw scores (numbers of words correctly recalled). Data are represented as mean (SEM).

TABLE 3 Characteristics of participants from *Twice-daily(R)* and *Once-daily(R)*.

	***Twice-daily(R)* (*N* = 20)**	***Once-daily(R)* (*N* = 16)**	**Statistics/p**
Demographic			
Age (years)	22.25 (0.55)	21.13 (0.48)	0.25[a]
Gender (female/male)	13/7	9/7	0.31[b]
RMT (%)	60.80 (1.23)	59.50 (2.15)	0.55/059[c]
Test delay (h)[d]	21.22 (0.82)	23.28 (0.17)	2.21/0.03[c]
Tests			
AM test (Baseline)	4.55 (0.45)	4.69 (0.62)	0.18/0.86[c]
Stroop test (Baseline)			
low interference (s)	1.50 (0.28)	1.06 (0.59)	0.08[b]
high interference (s)	7.62 (0.90)	7.38 (1.24)	0.16/0.88[c]

Data from Twice-daily(R) and Once-daily(R) are represented as mean (SEM). [a]Mann–Whitney test; [b]Fisher's exact test; [c]Two-sample t-test; [d]Test delay depicts the interval between the end of final stimulation session and the post-rTMS tests.

Combined analysis of once-daily and twice-daily repetitive transcranial magnetic stimulation

Characteristics of participants

There were no significant differences in any of the aforementioned baseline characteristics between *Combined(R)* and *Twice-daily(S)* groups (**Table 4**).

Associative memory performance

Associative memory scores for the *Combined(R)* and *Twice-daily(S)* groups are presented in **Table 2**. ANOVA revealed a significant Group [*Combined(R)* vs. *Twice-daily(S)*] × Time (baseline vs. post-rTMS) interaction effect on AM change ($F_{1,53} = 9.08$, $p = 0.004$) but no main effect of Time ($F_{1,53} = 0.86$, $p = 0.36$) or Group ($F_{1,53} = 0.29$, $p = 0.59$). Further, *post hoc* analyses using Sidak's multiple comparison tests indicated that real stimulation significantly enhanced AM score compared to baseline ($t = 3.35$, $p = 0.003$) (**Figure 2C**) while sham stimulation did not ($t = 1.29$, $p = 0.37$) (**Figure 2C**). In addition, the average percentage change in AM score was not significantly higher in the *Combined(R)* group than the *Twice-daily(S)* group [32.11% (SEM = 9.49) vs. 3.0% (SEM = 14.8); $p = 0.09$] (**Figure 2C**).

TABLE 4 Characteristics of participants from *Combined(R)* and *Twice-daily(S)*.

	***Combined(R)* (*N* = 36)**	***Twice-daily(S)* (*N* = 19)**	**Statistics/*p***
Demographic			
Age (years)	21.75 (0.38)	21.11 (0.48)	0.35[a]
Gender (female/male)	20/16	10/9	>0.9999[b]
RMT (%)	60.22 (1.16)	63.53 (1.27)	1.79/0.08[c]
Test delay (h)[d]	22.14 (0.49)	21.42 (0.92)	0.68/0.50[c]
Tests			
AM test (Baseline)	4.61 (0.37)	5.16 (0.62)	0.81/0.42[c]
Stroop test (Baseline)			
low interference (s)	1.31 (0.30)	0.75 (0.28)	1.23/0.22[c]
high interference (s)	7.51 (0.74)	7.50 (0.66)	0.01/0.99[c]

Data from Combined(R) and Twice-daily(S) groups are represented as mean (SEM). [a]Mann–Whitney test; [b]Fisher's exact test; [c]Two-sample t-test; [d]Test delay depicts the interval between the end of final stimulation session and the post-rTMS tests.

Stroop test performance

The Stroop test response times and error rates for *Combined(R)* and *Twice-daily(S)* groups are presented in **Supplementary Table 1**. ANOVA indicated no significant Group [*Combined(R)* vs. *Twice-daily(S)*] × Time (baseline vs. post-rTMS) interaction. See details in the **Supplementary material**.

Discussion

In the present study, we found that the twice-daily rTMS enhanced AM significantly better than the placebo effect. However, the improvement in the twice-daily real stimulation group was not significant after multiple comparisons correction. Furthermore, the twice-daily protocol was not superior to the once-daily sessions previously reported by Gao et al. (2021). When combining the twice- and once-daily rTMS data to enlarge sample size, the group by time interaction effect showed better AM improvement in the real than sham group, and the *post hoc* analysis in real group survived the multiple comparisons correction.

Wang et al. (2014) first reported that once-daily rTMS session targeting the hippocampal-cortical network can significantly improve AM, but several subsequent studies yielded inconsistent findings. We speculated that doubling the number of stimuli by delivery twice-daily rTMS sessions could induce significant AM improvement as has been shown for other clinical effects of rTMS, including relief of depressive symptoms (Cole et al., 2020). Twice-daily rTMS sessions did enhance AM task performance to a greater extent than sham rTMS (34.7 vs. 3.0%). But the difference from baseline was not significant by *post hoc* multiple comparison tests for the twice-daily real stimulation group. As small sample size reduces statistical power (Button et al., 2013), we combined

the *Twice-daily dataset* and *Once-daily dataset* from our previous experiment (Gao et al., 2021) to enlarge the sample size (N = 36), and *post hoc* multiple comparison test analyses showed significant AM improvement. An insufficient sample size could contribute to variability and affect the reliability of non-invasive brain stimulation studies (Guerra et al., 2020a,b). Thus, the required sample size should be calculated with great care in future TMS studies. We recommend that future studies examining multi-day rTMS-induced effects on memory include more participants in the real rTMS group.

Increasing the number of rTMS sessions per day and number of pulses per day has been reported to have superior antidepressant and altering cortical excitability efficacy (Nettekoven et al., 2014; Cole et al., 2020). Thus, increasing the session number was expected to enhance AM improvement from rTMS on the IPL. However, improvements twice-daily and once-daily rTMS were roughly equal (34.7 vs. 28.9%). An alternative strategy to increase rTMS dose is to use multiple targets, as several studies have demonstrated that other cortical nodes in the hippocampal-cortical network, such as dorsolateral prefrontal cortex (DLPFC), contribute to AM (Blumenfeld and Ranganath, 2006; Bilek et al., 2013). Future studies should consider combined DLPFC- and IPL-targeted rTMS.

This study has several limitations, most notably the small sample size. Although combining datasets yielded significant AM improvement, the two studies differed in several respects (e.g., experimental design, stimulus doses). Future large-sample prospective studies are warranted to document the reliability and duration of this AM-enhancing effect. Second, the RMT was measured only once rather than prior to each session, and a previous study reported that RMT varied significantly across days among subjects receiving rTMS (Cotovio et al., 2021).

Conclusion

Possibly due to the small sample size, our prospective experiment did not find significant rTMS effect on memory. But this effect may become significant if more participants could be recruited as revealed by our retrospective analysis.

Data availability statement

The raw data supporting the conclusions of this article will be made available by the authors, without undue reservation.

Ethics statement

The studies involving human participants were reviewed and approved by the Anhui Medical University. The patients/participants provided their written informed consent to participate in this study.

Author contributions

QH, G-JJ, and KW: conceptualization. QH, YZ, QL, XG, RD, YW, QZ, TZ, LZ, and JS: data acquisition. QH and G-JJ: methodology and formal analysis. QH: writing – original draft. G-JJ and KW: writing – review and editing and funding acquisition. All authors had full access to all the data in the study and take responsibility for the integrity of the data and the accuracy of the data analysis.

Funding

This study was funded by the National Natural Science Foundation of China, Grant/Award Numbers: 31970979, 82090034, 81971689, 32071054, and 82001429; the Scientific Research Fund of Anhui Medical University: 2019xkj199; and the Collaborative Innovation Center of Neuropsychiatric Disorders and Mental Health of Anhui Province: 2020xkjT057.

Acknowledgments

We thank the participants for taking part in this study. We also thank the Information Science Laboratory Center of USTC for measurement services.

Conflict of interest

The authors declare that the research was conducted in the absence of any commercial or financial relationships that could be construed as a potential conflict of interest.

Publisher's note

Supplementary material

The Supplementary Material for this article can be found online at: https://www.frontiersin.org/articles/10.3389/fnhum.2022.973298/full#supplementary-material

References

Bilek, E., Schäfer, A., Ochs, E., Esslinger, C., Zangl, M., Plichta, M. M., et al. (2013). Application of high-frequency repetitive transcranial magnetic stimulation to the DLPFC alters human prefrontal-hippocampal functional interaction. *J. Neurosci.* 33, 7050–7056. doi: 10.1523/JNEUROSCI.3081-12.2013

Blumenfeld, R. S., and Ranganath, C. (2006). Dorsolateral prefrontal cortex promotes long-term memory formation through its role in working memory organization. *J. Neurosci.* 26, 916–925. doi: 10.1523/JNEUROSCI.2353-05.2006

Button, K. S., Ioannidis, J. P., Mokrysz, C., Nosek, B. A., Flint, J., Robinson, E. S., et al. (2013). Power failure: Why small sample size undermines the reliability of neuroscience. *Nat. Rev. Neurosci.* 14, 365–376. doi: 10.1038/nrn3475

Chen, X., Ji, G. J., Zhu, C., Bai, X., Wang, L., He, K., et al. (2019). Neural correlates of auditory verbal hallucinations in schizophrenia and the therapeutic response to theta-burst transcranial magnetic stimulation. *Schizophr. Bull.* 45, 474–483. doi: 10.1093/schbul/sby054

Cole, E. J., Stimpson, K. H., Bentzley, B. S., Gulser, M., Cherian, K., Tischler, C., et al. (2020). Stanford accelerated intelligent neuromodulation therapy for treatment-resistant depression. *Am. J. Psychiatry* 177, 716–726. doi: 10.1176/appi.ajp.2019.19070720

Cotovio, G., Oliveira-Maia, A. J., Paul, C., Faro Viana, F., Rodrigues, da Silva, D., et al. (2021). Day-to-day variability in motor threshold during rTMS treatment for depression: Clinical implications. *Brain Stimul.* 14, 1118–1125. doi: 10.1016/j.brs.2021.07.013

Fox, M. D., Halko, M. A., Eldaief, M. C., and Pascual-Leone, A. (2012). Measuring and manipulating brain connectivity with resting state functional connectivity magnetic resonance imaging (fcMRI) and transcranial magnetic stimulation (TMS). *Neuroimage* 62, 2232–2243. doi: 10.1016/j.neuroimage.2012.03.035

Freedberg, M., Reeves, J. A., Toader, A. C., Hermiller, M. S., Voss, J. L., and Wassermann, E. M. (2019). Persistent enhancement of hippocampal network connectivity by parietal rTMS is reproducible. *eNeuro* 6. doi: 10.1523/ENEURO.0129-19.2019

Gao, X., Hua, Q., Du, R., Sun, J., Hu, T., Yang, J., et al. (2021). Associative memory improvement after 5 days of magnetic stimulation: A replication experiment with active controls. *Brain Res.* 1765:147510. doi: 10.1016/j.brainres.2021.147510

Guerra, A., López-Alonso, V., Cheeran, B., and Suppa, A. (2020a). Solutions for managing variability in non-invasive brain stimulation studies. *Neurosci. Lett.* 719:133332. doi: 10.1016/j.neulet.2017.12.060

Guerra, A., López-Alonso, V., Cheeran, B., and Suppa, A. (2020b). Variability in non-invasive brain stimulation studies: Reasons and results. *Neurosci. Lett.* 719:133330. doi: 10.1016/j.neulet.2017.12.058

Hendrikse, J., Coxon, J. P., Thompson, S., Suo, C., Fornito, A., Yücel, M., et al. (2020). Multi-day rTMS exerts site-specific effects on functional connectivity but does not influence associative memory performance. *Cortex* 132, 423–440. doi: 10.1016/j.cortex.2020.08.028

Hermiller, M. S., Karp, E., Nilakantan, A. S., and Voss, J. L. (2019). Episodic memory improvements due to noninvasive stimulation targeting the cortical-hippocampal network: A replication and extension experiment. *Brain Behav.* 9:e01393. doi: 10.1002/brb3.1393

Héroux, M. E., Taylor, J. L., and Gandevia, S. C. (2015). The use and abuse of transcranial magnetic stimulation to modulate corticospinal excitability in humans. *PLoS One* 10:e0144151. doi: 10.1371/journal.pone.0144151

Ji, G. J., Liu, T., Li, Y., Liu, P., Sun, J., Chen, X., et al. (2021). Structural correlates underlying accelerated magnetic stimulation in Parkinson's disease. *Hum. Brain Mapp.* 42, 1670–1681. doi: 10.1002/hbm.25319

Ji, G. J., Ren, C., Li, Y., Sun, J., Liu, T., Gao, Y., et al. (2019a). Regional and network properties of white matter function in Parkinson's disease. *Hum. Brain Mapp.* 40, 1253–1263. doi: 10.1002/hbm.24444

Ji, G. J., Wei, J. J., Liu, T., Li, D., Zhu, C., Yu, F., et al. (2019b). Aftereffect and reproducibility of three excitatory repetitive tms protocols for a response inhibition task. *Front. Neurosci.* 13:1155. doi: 10.3389/fnins.2019.01155

Ji, G. J., Yu, F., Liao, W., and Wang, K. (2017). Dynamic aftereffects in supplementary motor network following inhibitory transcranial magnetic stimulation protocols. *Neuroimage* 149, 285–294. doi: 10.1016/j.neuroimage.2017.01.035

Lee, T., Yuen, K., and Chan, C. (2002). Normative data for neuropsychological measures of fluency, attention, and memory measures for Hong Kong Chinese. *J. Clin. Exp. Neuropsychol.* 24, 615–632. doi: 10.1076/jcen.24.5.615.1001

Lee, T. M., and Chan, C. C. (2000). Stroop interference in Chinese and English. *J. Clin. Exp. Neuropsychol.* 22, 465–471. doi: 10.1076/1380-3395(200008)22:4;1-0;FT465

López-Alonso, V., Cheeran, B., Río-Rodríguez, D., and Fernández-Del-Olmo, M. (2014). Inter-individual variability in response to non-invasive brain stimulation paradigms. *Brain Stimul.* 7, 372–380. doi: 10.1016/j.brs.2014.02.004

Nettekoven, C., Volz, L. J., Kutscha, M., Pool, E. M., Rehme, A. K., Eickhoff, S. B., et al. (2014). Dose-dependent effects of theta burst rTMS on cortical excitability and resting-state connectivity of the human motor system. *J. Neurosci.* 34, 6849–6859. doi: 10.1523/JNEUROSCI.4993-13.2014

Rossi, S., Hallett, M., Rossini, P. M., and Pascual-Leone, A. (2009). Safety, ethical considerations, and application guidelines for the use of transcranial magnetic stimulation in clinical practice and research. *Clin. Neurophysiol.* 120, 2008–2039. doi: 10.1016/j.clinph.2009.08.016

Wang, J. X., Rogers, L. M., Gross, E. Z., Ryals, A. J., Dokucu, M. E., Brandstatt, K. L., et al. (2014). Targeted enhancement of cortical-hippocampal brain networks and associative memory. *Science* 345, 1054–1057. doi: 10.1126/science.1252900

Wang, J. X., and Voss, J. L. (2015). Long-lasting enhancements of memory and hippocampal-cortical functional connectivity following multiple-day targeted noninvasive stimulation. *Hippocampus* 25, 877–883. doi: 10.1002/hipo.22416

Yu, J., and Lee, T. M. C. (2018). Profiles of cognitive impairments in an older age community sample: A latent class analysis. *Neuropsychology* 32, 102–109. doi: 10.1037/neu0000391

Frontiers in
Human Neuroscience

Bridges neuroscience and psychology to understand the human brain

The second most-cited journal in the field of psychology, that bridges research in psychology and neuroscience to advance our understanding of the human brain in both healthy and diseased states.

Discover the latest Research Topics

See more →

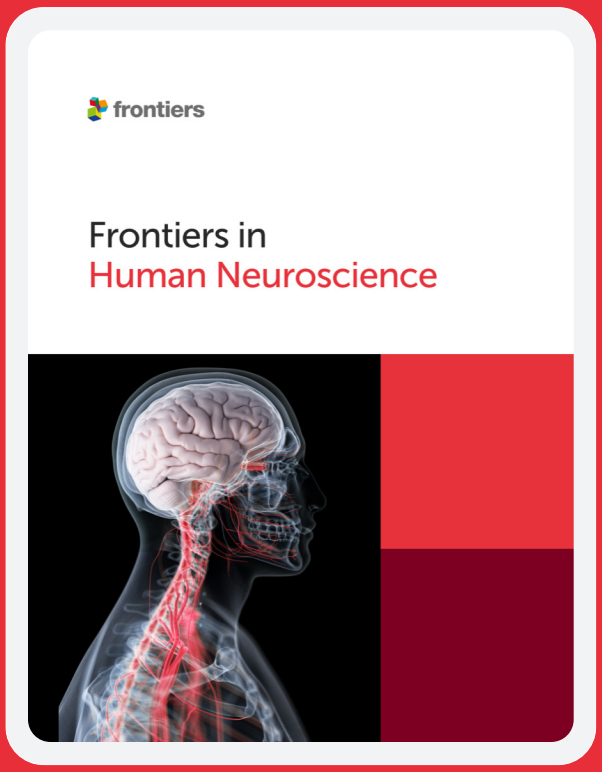

Frontiers

Avenue du Tribunal-Fédéral 34
1005 Lausanne, Switzerland
frontiersin.org

Contact us

+41 (0)21 510 17 00
frontiersin.org/about/contact